

Use of Linear Motor as Active Heave Compensator

Tor-Anders Rusvik

Supervisor

Hamid Reza Karimi (UiA)

Narve Kristiansen (NOV)

This master's thesis is carried out as a part of the education at the University of Agder and is therefore approved as a part of this education. However, this does not imply that the University answers for the methods that are used or the conclusions that are drawn.

Preface

This thesis was written as part of the University of Agder's (UiA) Master of Science program in Mechatronics. In this thesis a LinMot® linear motor has been examined to determine if it is suitable as an active heave compensator in conjunction with a scale model CMC. The system is a very good example of a mechatronic system, combining fields such as mechanics, hydraulics, pneumatics, electronics, instrumentation and control, though some areas were more prominent than others. The thesis was somewhat plagued by equipment that did not work and so changes had to be made underway in order to compensate. The thesis would also have benefitted from more time to test and improve the system further, as it took a long time for the linear motor to arrive.

The author wishes to thank his thesis supervisor at UiA, professor Hamid Reza Karimi for guidance over Skype during the project, thanks also goes out to Kjell Gunnar Robbersmyr at UiA for acting as a co-supervisor. I would also like to thank my supervisor at National Oilwell Varco (NOV), Narve Kristiansen. In addition I want to thank Arve Johnsen at NOV for help with setting up the drive system, and also Jan Terje HÅekedal at NOV for organizing the transport of the scale model CMC. For help with fabrication of parts and practical issues such as hoisting the model onto the Stewart platform thanks goes out to the staff at the UiA machine laboratory, and in particular to Jan Andreas Holm for transporting the scale model CMC to UiA and for help with trying to get the model running.

Grimstad, the 30th of May 2015.

Tor-Anders Rusvik

Abstract

This thesis investigates the possibility of using a linear motor as an active heave compensator in conjunction with a 1:7 scale model of a passive crown mounted compensator (CMC). A linear motor was selected and used with the scale model as an active heave compensator. The system was placed on a Stewart platform and subjected to simulated wave induced heave motion with a load suspended from the system. By reducing the effect of the heave motion on the drill string, the compensator system increases the drilling performance, in addition should the linear motor fail it will not introduce a very high friction in the system compared to earlier solutions.

The linear motor used was selected based on simulation models of the scale model, in addition, parts for connecting the motor to the scale model had to be procured or constructed and then assembled on the scale model. A control system was designed for use with the linear motor and the existing instrumentation on the scale model. The control system was implemented on a PLC, which together with a drive system controls the linear motor.

Unfortunately it was discovered late in the thesis that the scale model CMC was not usable due to one of its hydraulic cylinders being stuck. It could therefore not be used in the testing. Investigating the linear motor as an active heave compensator by itself then became the primary goal. Even though it was never tested the work done on the CMC and linear motor system is still relevant and could serve as foundation for future testing.

Contents

Preface	ii
Abstract	iii
1 Introduction	1
2 Crown Mounted Compensator	4
2.1 The Crown Mounted Compensator Type E	4
2.1.1 CMC Passive System	6
2.1.1.1 Hydraulic/Pneumatic System	6
2.1.1.2 Equalizing System	6
2.1.2 CMC Active System	6
2.2 The Scaled CMC	9
2.2.1 Defining Waves	9
2.2.2 Scaled CMC response	12
3 Hardware and Software	13
3.1 Instrumentation of the Scaled CMC	13
3.2 Sensors and Wire Encoder	14
3.3 Motion Reference Unit and Stewart Platform	15
3.4 Programmable Logic Controller	15
3.5 Siemens Drive System	16
3.6 Software	16
4 Linear Motor	17
4.1 Electric Linear Motors	17
4.2 Choosing the Linear Motor(s)	17
4.2.1 Motor Requirements	17
4.2.2 Choosing a Supplier and Motor	19
4.2.2.1 LinMot-Designer	19
4.2.2.2 Looking at different motors	20
4.2.3 Electric Linear Motor	21
4.2.4 Order Information	23
4.3 Linear Motor Testing	24
4.3.1 Friction	24
4.3.2 Force Ripple	24
4.3.3 Test Results	25
5 System Models	28
5.1 Modelling the Compensator	28
5.1.1 SimulationX Model #1	28
5.1.2 SimulationX Model #2	29
5.1.3 Matlab/Simulink Model	29

5.1.4	Linear Motor Model	30
6	Control System	32
6.1	Control Strategy	32
6.1.1	The System to be Controlled	33
6.1.2	Force PI controller with Hookload feedback	33
6.1.3	Force PI controller with Position Feedback	33
6.1.4	Cascade Structure Controller	33
6.2	Feed Forward Compensation	34
6.2.1	Friction in CMC	34
6.2.2	Friction in Linear Motor	37
6.2.3	Force Ripple in Linear Motor	37
6.3	Control Simulation and Tuning	37
6.3.1	Choosing a Model	37
6.3.2	Tuning Strategies	38
6.3.3	Force PI Controller with Friction Feed Forward	39
6.3.4	Cascade Structure Controller	41
6.4	Chosen Control Strategy	42
7	System Implementation	43
7.1	Incorporating the Linear Motor Into the CMC	43
7.2	Stator Mounting	46
7.2.1	Finite Element Analysis of the Bracket	48
7.2.2	Fabricating the Bracket	51
7.3	Transportation of CMC and Initial Setup	51
7.3.1	Linear Motor Assembly	52
7.3.2	Siemens S120 Drive System and Control Cabinet	52
7.4	Mounting of Equipment on CMC and Placement on Stewart Platform	55
7.5	PLC Programming and HMI - CMC with Linear Motor	60
7.6	Linear Motor Active Heave Compensator System	63
7.7	PLC Programming and HMI - Linear Motor AHC	65
8	Testing	68
8.1	Testing Scenarios	68
8.2	Initial Testing	68
8.3	New Testing Scenarios	69
8.4	Performing Tests	70
8.5	Test Results	72
8.5.1	Initial Results	72
8.5.2	Final Results	74
8.5.2.1	Wave Two	74
8.5.2.2	Wave Four	76
8.5.3	Test Conclusions	78
9	Conclusion	82
	Bibliography	84
	List of Figures	86
	List of Tables	88

A	Test Results	89
A.1	Wave One	89
A.1.1	No Load	89
A.1.2	Load	90
A.2	Wave Two	92
A.2.1	No Load	92
A.2.2	Load	93
A.3	Wave Three	94
A.3.1	No Load	94
A.3.2	Load	96
A.4	Wave Four	97
A.4.1	No Load	97
A.4.2	Load	98
B	PLC Program - Linear Motor AHC	100
C	Drive Controller Structure	129
C.1	Drive System	129
C.2	Drive Velocity Setpoint	129
C.3	Drive Velocity Filter	130
C.4	Drive Velocity Controller	130
C.5	Drive Force Setpoint	131
C.6	Drive Force Limit	131
C.7	Drive Current Controller	132
C.8	Drive Current Filter	132
C.9	Drive Power Unit	133
C.10	Drive Encoder	133
D	SimulationX Model	134
E	CAD Drawings	164

Chapter 1

Introduction

When drilling a well the weight on the drill bit (WOB) has a big impact on the drilling performance. When drilling from a ship or a floating platform the heave motion of the vessel induced by waves makes it difficult to control the WOB. Passive heave compensation (PHC) systems such as compensators have been in use since the 1970s and are still widely used. The system basically functions as a hydro-pneumatic spring which absorbs the forces created by the heave motion of the vessel relative to the drill string [1].

However in order to more precisely control the WOB an Active heave compensation (AHC) system have to be used. By using both a passive and an active compensator the system will continue to operate if the active system fails. However if the active system should fail it is vital that it does not lock the movement of the crown block so that the passive system is still able to function. Normally a hydraulic actuator driven by a hydraulic power unit is used for the AHC system. The actuator on top of the derrick is connected to the power unit by two hydraulic lines which run up the derrick. Due to the long hydraulic lines the actuator will suffer from some inherent delay, made worse if there is air in the oil, and the oil flow will also cause a pressure drop which is a loss of power [2].

National Oilwell Varco (NOV) has requested a master project where the scope is to investigate the pros and cons of using an electric linear motor as the AHC component. The reason for using an electric linear motor is because it does not lock in place when power to the motor is lost, which means the passive system still can function when the linear motor is not. This is in contrast to most electric linear actuators based on for example lead or ball screws. An electric linear motor also have other desirable characteristics such as the absence of mechanical power transmission systems which results in higher efficiency, better dynamic performance and improved reliability [3]. However without auxiliary systems, linear motors are affected by friction force, force ripple and external load disturbance in a drive system [4].

The master thesis will be done as a collaboration between National Oilwell Varco (NOV) and the University of Agder (UIA). NOV will supply a scale model of the Crown Mounted Compensator (CMC), an electrical Siemens drive for operating the linear motor and a control unit with software for controlling the model. UIA will supply a Stewart Platform, on which the scale model will be mounted, to simulate wave motion. The type and size etc. of the Electric Linear Motor will be chosen and then mounted on the scale model. Currently the AHC system on the scale model consist of a rack and pinion system which was developed by Atle Aalerud and Tomas Klevmo in a master project in 2013.

The primary goals for the project are:

1. Find a linear motor suited for this application.
2. Mechanically implementing the linear motor concept into the CMC structure.
3. Modifying the control system (PLC and drive) to be able to control the linear motor.
4. Check performance of the system and compare with the previous rack and pinion system.

For this project Ex Zone or weather requirements will not be taken into consideration.

Equipment that will be used in the project: **Provided by NOV:**

- 1:7 scale model of a passive CMCe
- Electric drive for operating linear motor.
- Electric linear motor.
- MRU for measuring wave reference.
- Siemens PLC for control system including some already made software.
- Instrumentation for measuring forces, positions, pressure etc.

Provided by UiA:

- Stewart Table

In addition to the equipment NOV would also assist in setting up the drive system for the linear motor due to its complexity.

The first priority of the thesis when starting the work was to investigate the requirements for the linear motor, then find a suitable motor and order it as soon as possible as it would take some time before it was delivered. After the linear motor was ordered work began on creating a control system, simulating the system and designing parts for mechanically implementing the linear motor into the scale model CMC. After the linear motor and scale model had arrived at the lab work began getting the motor working with the drive system, programming the PLC and assembly of the system. When the system was ready it was lifted onto the stewart platform and testing could begin. When beginning to test the system it was immediately discovered that the scale model alone was not performing satisfactory as there was very much friction in the system, after some investigation it was discovered that one of the main hydraulic cylinders was more or less stuck and was barely able to move. As it was at this time only two weeks left until delivery of the thesis it was decided to drop the scale model from the project instead of trying to repair it. Instead the linear motor would have to be used as an active heave compensator by itself, which required disassembling the scale model system and creating and mounting the linear motor system on the stewart platform, in addition some of the PLC program had to be changed. In the report the system with the CMC is referred to as the CMC with linear motor system, while the linear motor by itself is referred to as the linear motor AHC system. As it did not become clear that the scale model CMC could not be used until two weeks before delivery of the thesis, a large part of the report focuses on the CMC with linear motor system.

Also the motion reference unit (MRU) refused to work, so with so little time left it was decided to just use a simulated wave from the PLC instead and not use the stewart platform for testing the performance. While it did serve the same purpose during testing, it was not as visually intuitive.

The structure of the report is very much representative of the projects work flow, though some chapters were done in parallel or had to be filled in as new information became available, a good example of

this is testing of the linear motor which appears at the end of chapter 4 but in reality was performed as a part of chapter 8.

Chapter 2 focuses on describing and understanding the Crown Mounted Compensator and its active and passive systems in both full size and scaled down form. Chapter 3 looks at the hardware and software used in the project such as the instrumentation on the scaled CMC and control cabinet. Chapter 4 is devoted to the linear motor, the process of selecting a motor, specifications and testing. Models of the system was made in chapter 5 in order to determine which motor to use and for developing the control system, which is then explored further in chapter 6. The process of implementing the linear motor in the passive CMC scale model, including mounting it to the structure and programming of the PLC and drive system, as well as the setup for running the linear motor by itself, is described in chapter 7. Chapter 8 covers the testing setup and actual testing of both the scale model and the linear motor, and chapter 9 provides the conclusions to the thesis.

Chapter 2

Crown Mounted Compensator

2.1 The Crown Mounted Compensator Type E

The National Oilwell Varco Crown Mounted Compensator type E (CMC-E), referred hereafter to as CMC, is a passive heave motion compensator, "crown mounted" means it is mounted at the crown on top of the drilling derrick. Its task is to compensate for the vertical movements (heave) of the drilling vessel so that the movement of the top drive in relation to the seabed is minimized. In order to achieve this, near constant tension has to be applied to the drill string so that the weight on bit (WOB) remains correct.

To achieve this the CMC converts the moving force of the crown block into hydraulic pressure which then is converted to pneumatic pressure in an air reservoir by use of an accumulator. The air reservoir consists of several air pressure vessels (APVs or CAPVs) with a precisely calculated volume according to the parameters of the rest of the system. This means the CMC-basically acts as a large pneumatic spring. The passive CMC and its location on top of the derrick of the Cerrado drillship can be seen in figures 2.1 2.2.



Figure 2.1: The passive CMC



Figure 2.2: CMC location on top of the derrick of the Cerrado drillship

2.1.1 CMC Passive System

The CMC consists of two main systems:

1. The hydraulic/pneumatic system for converting hydraulic pressure into pneumatic pressure ,acting like a spring.
2. The equalizing system which is responsible for minimizing the fluctuation of the lifting force caused by the variation of pressure in the main cylinders when they are moving.

2.1.1.1 Hydraulic/Pneumatic System

The hydraulic/pneumatic system consist of two vertically mounted hydraulic lifting plunger cylinders which are responsible for converting the moving force of the crown block into hydraulic pressure, and can also locked in any position by use of the hydraulic isolation valve, which also closes in case of sudden load changes, the cylinders are equipped with low friction seals to make them more efficient. The travelling block is connected to the lifting cylinder by use of two tie rods on each cylinder and moves along guide structures mounted on the cylinders by use of roller assemblies to keep it fixed.

The hydraulic lifting cylinders is then hard piped to an air/fluid accumulator which converts the hydraulic pressure to pneumatic pressure by use of a free floating steel piston inside the accumulator that separates the air from the hydraulic fluid, the displacement of the piston due to the hydraulic pressure compresses the air in the APVs. The Accumulator is mounted between the main air valve and the hydraulic isolation valve. The accumulator is also equipped with low friction seals and are hard piped to the APVs, each APV has its own shut off valve so that the volume of the system can be changed. The APVs also has an air fill and drain valve so the pressure in the system can also be changed in order to keep the lifting cylinders moving around the mid-stroke point.

The hydraulic isolation valve between the hydraulic lifting cylinders and the accumulator is under normal operation fully open, but will close if sudden crown block load drop is detected. If closing of the valve is not necessary it will open again when the load induced pressure increases, it can also be closed remotely in order to lock the crown block in place.

2.1.1.2 Equalizing System

The equalizing system consists of two equalizing cylinders each connected by a lifting chain to an eccentric hub connected together with another eccentric hub, which is connected to the travelling block by a set of lifting chains. The equalizing cylinders are fed the same pressure as in the main cylinders and converts the pressure into torque in the first eccentric hub causing it to rotate by use of the lifting chain. As the eccentric hubs rotate, the torque in the first hub is transferred to the second hub which then converts the torque into lifting force on the crown block by use of the second lifting chain. The eccentric hubs and their orientation relative to each other is carefully chosen to give the desired lifting characteristic. The equalizing system always contributes lifting force in the same direction as the main cylinders. It is configured to the main cylinder volume and the APVs volume so that the lifting force will balance out any fluctuation in the system pressure as the main cylinders moves in and out. The equalizing system is passive, i.e. it does not require any control or power to be able to function.

2.1.2 CMC Active System

PHC systems alone are less costly compared with AHC systems and perform well during contact-operations [1]. However when the ship heave is less than about 2 meters PHC systems have about 40% heave reduction efficiency, compared to about 85% efficiency when the heave is larger than about 4 meters [6]. The reason for this is the friction in the system and the finite volume of the APVs, the equalizing system reduces the pressure induced fluctuations,however at the cost of increased friction. Therefore PHC are commonly used in combination with AHC, by combining the two a heave reduction efficiency of 90-95% is possible [2].

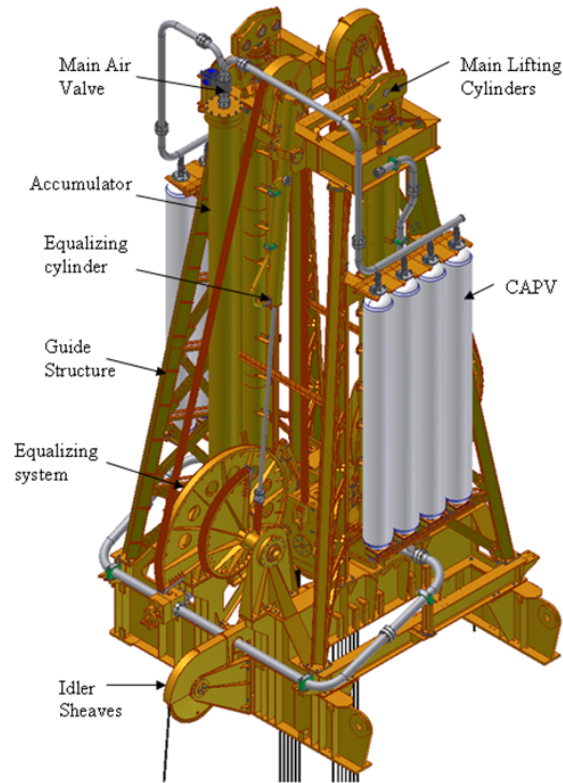


Figure 2.3: Model of the CMC with platforms removed

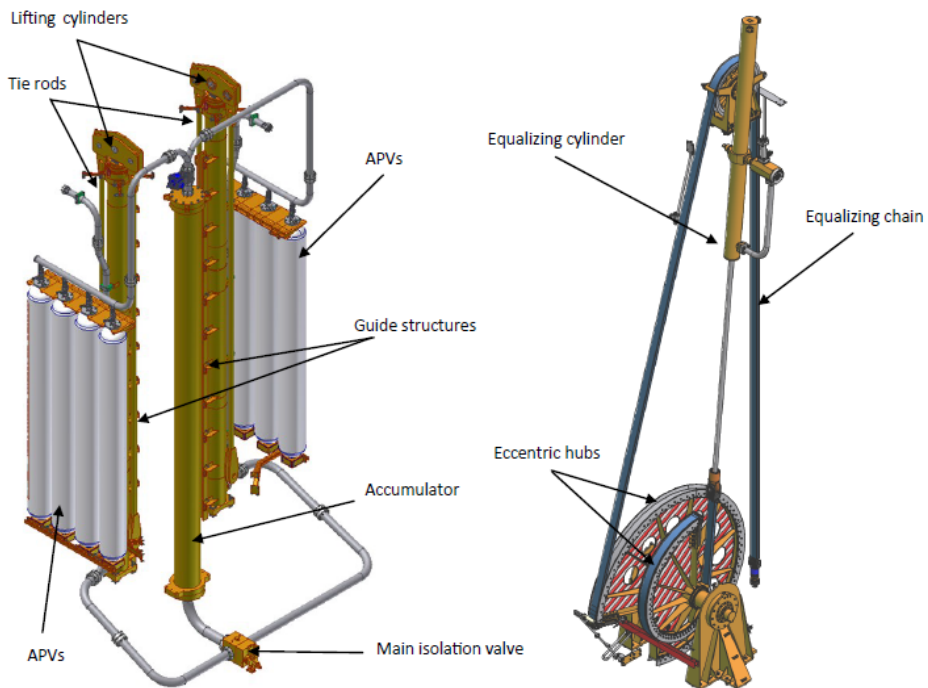


Figure 2.4: Closer look at the main CMC systems [5]

For this compensator the optional AHC system consists primarily of an active compensator unit along with control, control panels, sensors and an hydraulic power unit. The active compensator unit consist of a hydraulically actuated cylinder and a hydraulic valve block. The cylinder is designed as a three-chamber type with two-chamber area balanced, providing equal displacement and force in both working directions it is also equipped with low friction seals [7]. The cylinder, seen in figure 2.5 is mounted on top of the CMC, the bracket on the piston rod is fixed to the crown block.

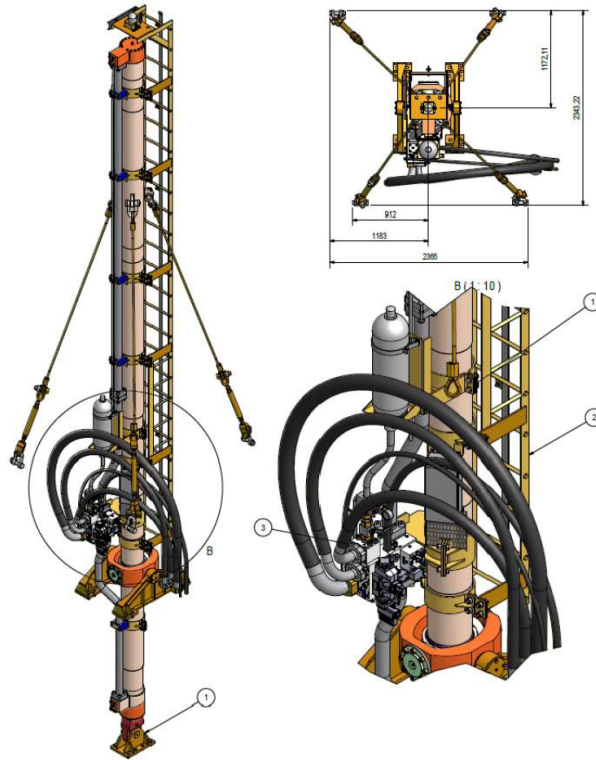


Figure 2.5: The AHC system

2.2 The Scaled CMC

The scale model of the CMC is an almost exact 1:7 scale replica of the real CMC.

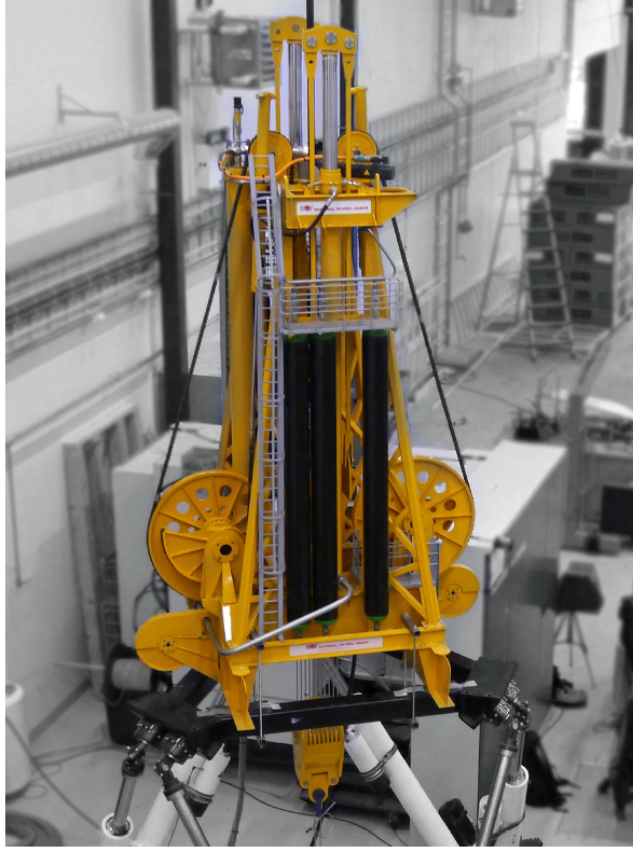


Figure 2.6: The scaled CMC on top of a Stewart platform with a rack and pinion AHC system

Work was done by Aalerud and Klevmo [5] to verify the scaled dimensions, including finding functions for the radii of the eccentric hubs which could be used in the simulation models, see equations 2.1-2.2.

$$r_1(\theta) = 0.0003 \cdot \theta^2 - 0.137 \cdot \theta + 0.3143 \quad (2.1)$$

$$r_2(\theta) = -0.0003\theta^5 + 0.0036 \cdot \theta^4 - 0.017 \cdot \theta^3 + 0.0362 \cdot \theta^2 + 0.0131 \cdot \theta + 0.0673 \quad (2.2)$$

$$(2.3)$$

Where $r_1(\theta)$ is the large hub and $r_2(\theta)$ is the small hub, θ is in radians. They were verified as being sufficiently accurate for their project and therefore also for this project.

The scale model was initially not fitted with an AHC system, but a rack and pinion system driven by a servo motor was added by Aalerud and Klevmo.

2.2.1 Defining Waves

As the CMC is scaled down, the wave signal for testing also had to be scaled down. In order to use the data from [5] and for easy comparison the same waves were chosen. The relevant waves for this type of equipment are ocean waves with a heave motion from 0.2 to 2 meters, with periods of 5 to 15 seconds [2]. According to [8] the nominal maximum operating condition, which the dynamic performance of the CMC is specified, is a 12 foot peak-to-peak heave with 12 second period, approximately equal to an amplitude of 1.83 meters and a frequency of 0.0833 hertz. From this information 3 different waves were created by Aalerud and Klevmo [5] which are seen in equations 2.4 to 2.6 and figure 2.7.

$$z_{wave1} = 0.1 \cdot \sin(0.1 \cdot 2\pi t) \quad (2.4)$$

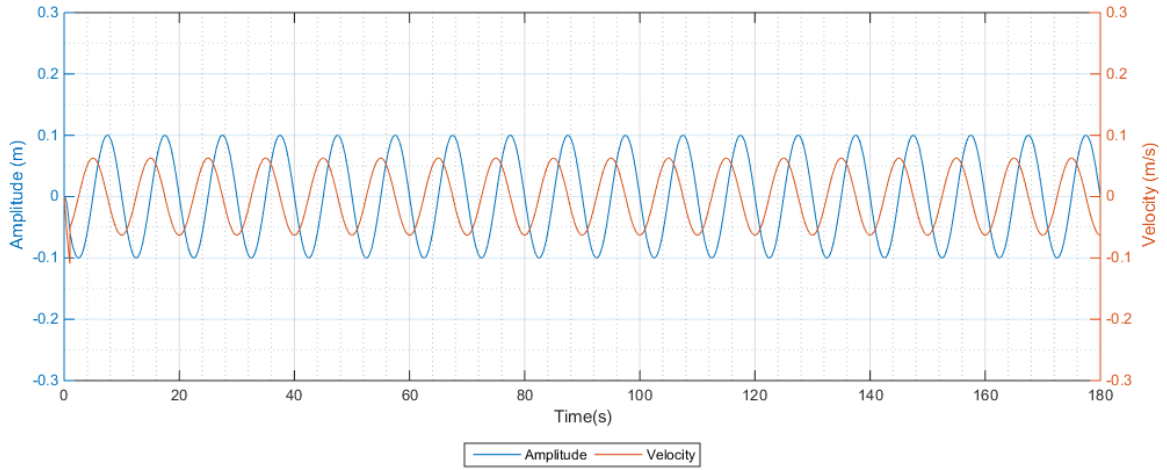
The first wave with amplitude of 0.1 meters and frequency of 0.1 hertz, equal to a full size wave with amplitude of 0.7 meters and period of 10 seconds.

$$z_{wave2} = 0.26 \cdot \sin(0.08 \cdot 2\pi t) \quad (2.5)$$

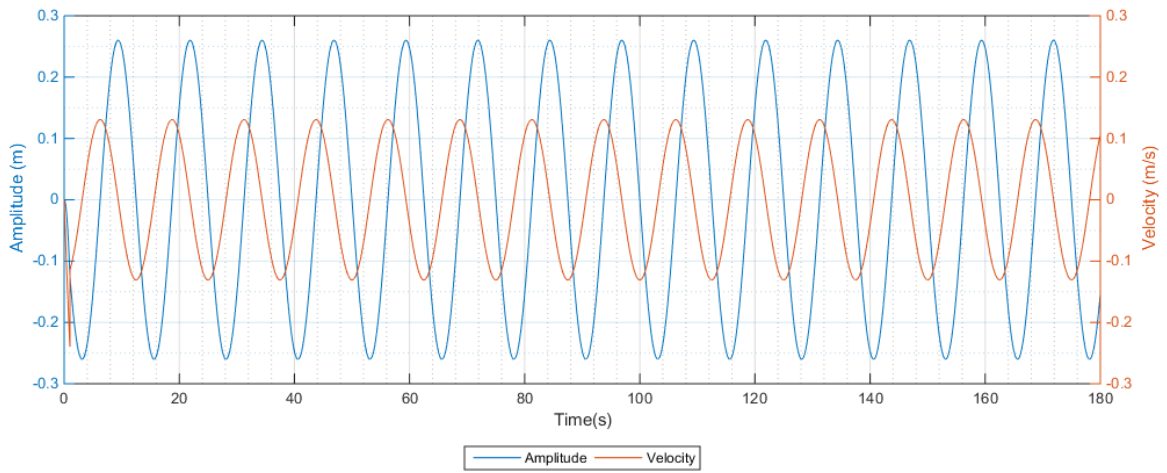
The second wave with amplitude of 0.26 meters and frequency of 0.08 hertz, equal to a full size wave with amplitude of 1.82 meters and period of 12.5 seconds.

$$z_{wave3} = \sin\left(\frac{1}{600} \cdot 2\pi t\right) \cdot (0.15 \cdot \sin(0.08 \cdot 2\pi t) + 0.1 \cdot \sin(0.11 \cdot 2\pi t)) \quad (2.6)$$

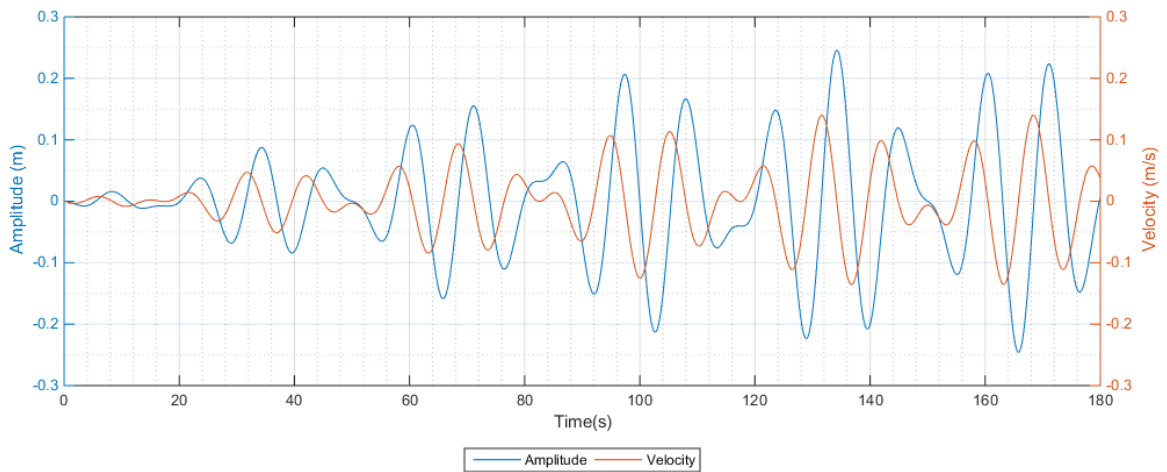
The third wave is a combination of waves where the maximum amplitude is 0.25 meters which equals to 1.75 meters amplitude in full size. The wave also includes sections where the wave velocity reaches zero and then continues in the same direction.



(a) Wave #1



(b) Wave #2



(c) Wave #3

Figure 2.7: The three different waves defined for the project

2.2.2 Scaled CMC response

As seen in figure 2.8 the hook load changes very rapidly when encountering wave peaks and troughs, when the wave is at its highest and lowest point, which is also the point where the wave velocity crosses zero. The reason for this is largely dependant on the friction in the system, even though all the cylinders and the accumulator is fitted with low friction seals. When the wave changes direction the velocity changes direction which means the friction changes direction. The fluctuations in hook load induced by fluctuations in the pressure is reduced by the equalizing systems at the cost of increased friction in the system from the equalizing cylinders and the hubs [9]

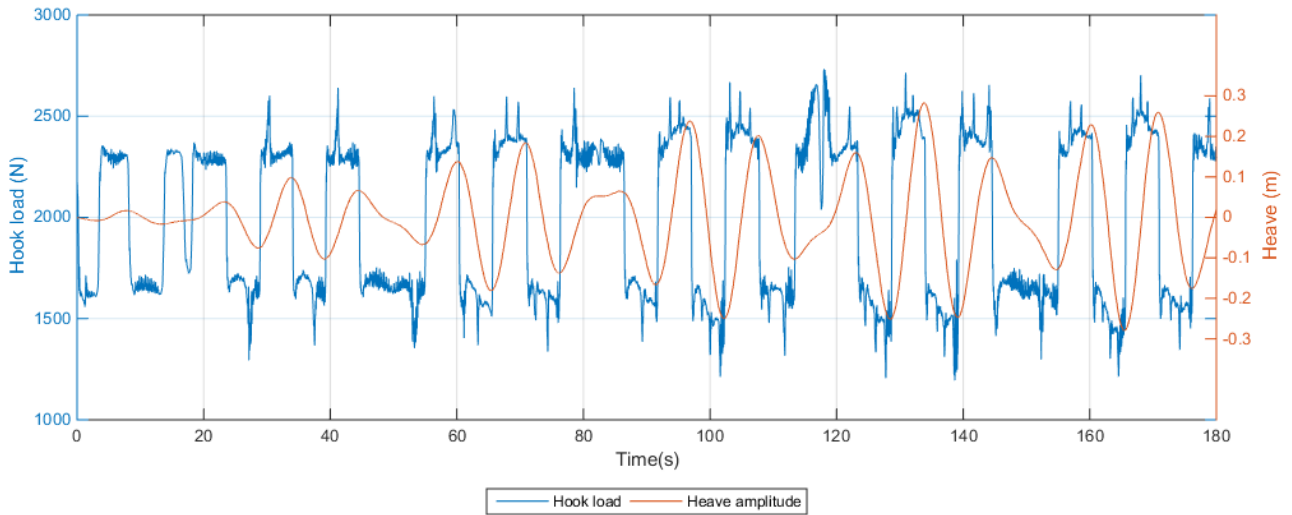


Figure 2.8: The response of the CMC with respect to hook load while subjected to wave #3 at 6 bar

Chapter 3

Hardware and Software

3.1 Instrumentation of the Scaled CMC

A thorough job of instrumenting the scaled CMC was done by Aalerud and Klevmo [5]. The full scale CMC has an array of redundant sensors and actuators, measuring position of crown block, valve positions and air and hydraulic pressure to name some, to ensure efficient and safe operation. The parameters are monitored by the PLC which serves as the interface between the operator and the CMC. A Motion Reference Unit (MRU) measuring the heave, pitch and roll of the vessel is also included.

For the scaled CMC however the focus of the instrumentation was to monitor the essential parameters in order to create a control system, it should also be able to capture the defining features of the model such as friction, pressure, position of the crown block and the force exerted by the AHC system. An overview of the instrumentation is shown in figure 3.1.

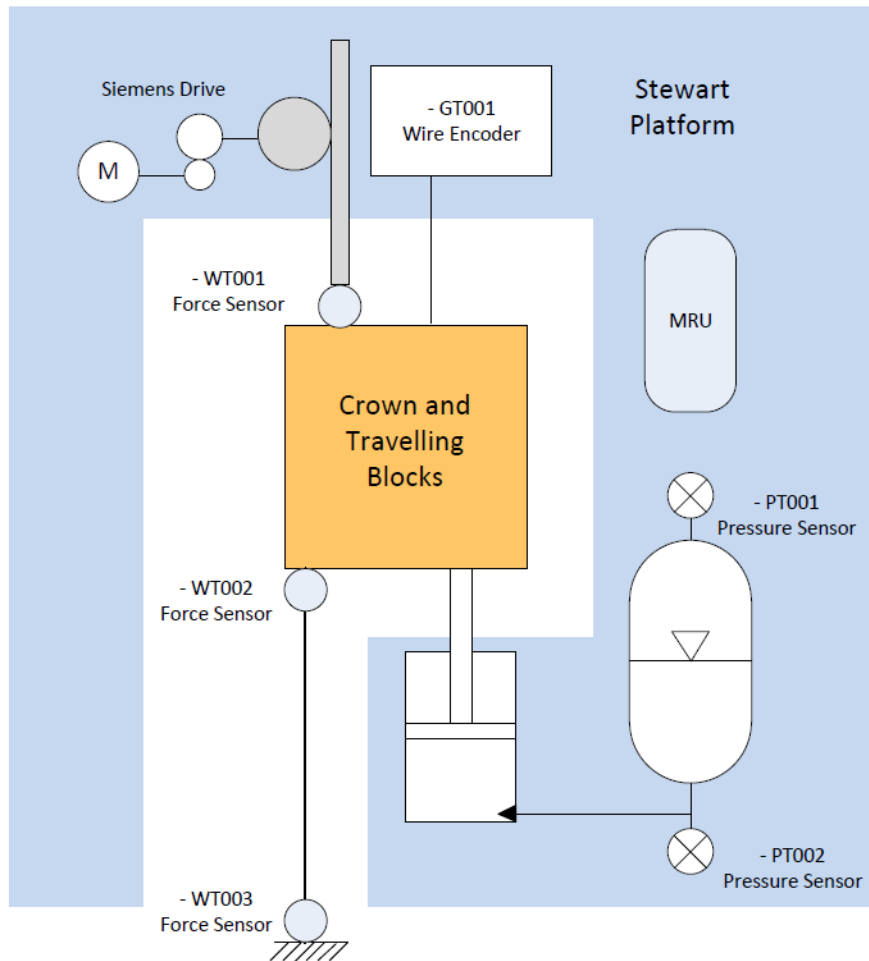


Figure 3.1: Illustrated overview of the instrumentation for the scaled CMC with the rack and pinion system [5]

When the model was transported to UiA it was revealed that some of the sensors had gone missing since the last time the model was used. The next sections will therefore describe the equipment that was available.

3.2 Sensors and Wire Encoder

There were one force sensor, one pressure sensor and a draw wire encoder on available with the scale model CMC.

The force sensor are the Tecsia F23011350002. It has a nominal load of 5 kN and an accuracy of $\leq \pm 0.2\%$ [10]. The sensor consists of thin film strain gauges connected to a Wheatstone Bridge and an integrated amplifier giving an analog output of 4-20 mA through two-wire transmission. The location of the three sensors were, ref. figure 3.1. It was originally located between the rack and the crown block to measure the force exerted on the crown block by the AHC system. This was not needed with the linear motor as the force it delivers could be read from the drive system. It was planned to use this sensor as a replacement for the WT002 sensor in figure 3.1, however as the scale model CMC ended up not being used there was no need for this sensor.

The pressure sensor are the Aplisens PCE2812000AAC with a measurement range of 25 bar and an accuracy of 0.2%, thermal error is max 0.3% per 10°C [11]. It is located on the top of the accumulator,

measuring the air pressure in the system.

A draw wire encoder is fitted to the top frame of the scaled model and the end of the wire is fastened to the travelling block. The encoder measure the motion of the travelling block relative to the scale model CMC, which equals the stroke of the linear motor and main cylinders. In the linear motor AHC system it was used to measure the position of the linear motor slider. The draw wire encoder consists of the rope length transmitter FSG SL 3005 - D9 GS 130 F and the Hengstler EX Heavy Duty Absolute encoder, model AX65/1213EL.72SGA. The rope length transmitter has a patented drum mechanism which ensures the wire is unwound constantly side by side with constant distance, the revolutions of the drum will then be transmitted to a suitable transmitter system [12]. The transmitter system in this case the Hengstler encoder. The wire is 5 meters long and the mechanics of the rope length transmitter has a repeatability of 0.1%.

The Hengstler Heavy Duty Absolute encoder is a very robust encoder suitable for offshore applications. It communicates with the PLC over a 25 bit Synchronous Serial Interface (SSI), the measured value has a resolution of 12 bit. The encoder has an absolute accuracy of $\pm 1^\circ$ and a repeatability of $\pm 0.2^\circ$ [13].

3.3 Motion Reference Unit and Stewart Platform

The motion reference unit (MRU) is the Kongsberg Seatex MRU H. It has a dynamic accuracy for heave motion of 5 cm or 5% whichever is highest.

The Stewart platform is the Bosch Rexroth EMotion-1500 which has a capacity of 1500 kg. The maximum heave motion is 0.829 meters peak to peak, with a maximum velocity of ± 0.6 m/s and a maximum acceleration of ± 0.6 g.

As the MRU was not working properly both items ended up not being used in the project, though the Stewart platform was used as mounting for the system.

3.4 Programmable Logic Controller

The Siemens Programmable Logic Controller (PLC) used in this project consists of a Siemens 319-3 PN/DP CPU which is located in slot 2, FIGURE. The CPU is the unit containing the software and is responsible for executing it. It has ethernet ports for connecting to a computer and to the drive system, two white cables for computers and a blue cable for the drive system.

In addition to the CPU the PLC contains several modules for communicating with the instrumentation and controls. A CP 341-RS232C RS232 card for interfacing with the MRU is located in slot 4. Slot 5 contains a digital input card, DI16xDC24V, and slot 6 a digital output card, DO16xRel AC120V/230V. These cards are used for the buttons and joystick on the control panel for controlling the motor manually. In slot 7 is the A18x14Bit analog input card which handles all the analog measurements, like the force and pressure sensors and the analog joystick input. The last slot, number 8, contains a counter card for the wire encoder, SM 338 POS-INPUT.

On the left in the cabinet is a terminal block which connects the electrical equipment to the PLC modules. The PLC and all its modules along with the terminal block was installed by AÅlerud and Klevmo in their thesis [5].

3.5 Siemens Drive System

The drive system is the Siemens SINAMICS S120, with a CU320 controller and an SMC20 encoder module. Configuring the drive system is a very difficult and time consuming task for someone who is not familiar with it, NOV will therefore assist with configuring the drive system to the linear motor. When configuring the drive system some of the components, the CU320 controller and the S120 motor module, had to be changed to a newer version in order to be able to install new firmware required for the linear motor. In addition the motor module was upgraded from a 3 ampere unit to a 9 ampere unit so it would be capable of driving the linear motor. In addition the SMC20 encoder module was later upgraded from a "version A" to a "version G".

3.6 Software

The PLC will be programmed using Siemens SIMATIC STEP 7 software.

The drive system will be programmed using Siemens Starter.

SIMATIC WinCC will be used to create a Human Machine Interface (HMI) so that the system can be operated and system parameters monitored from a laptop.

Logging of data from the PLC, including the performance of the system and relevant parameters, will be done using PlcLog32.

Chapter 4

Linear Motor

4.1 Electric Linear Motors

A permanent magnet linear synchronous motor (PMLSM) is to be used for the active heave compensation (AHC) system. Using an electric linear actuator like a lead or ball screw for example is not desirable as it would introduce considerable resistance to or potentially hinder the passive heave compensation (PHC) system when not in operation. Also an electric motor is a more simple construction mechanically, basically consisting of just two parts, a stator and a slider. The electric linear motors mode of operation is similar to a brushless rotary motor, except with different configuration and arrangement of the magnets which results in a linear motion, and a slider in place of a rotor. The characteristics of an electric linear motors is high force and high precision combined with high speeds and accelerations [14].

PMLSM motors are sensitive to change of temperature, overtop temperature lowers the motors load capacity [15]. Proper cooling of the motor will therefore increase its performance greatly.

4.2 Choosing the Linear Motor(s)

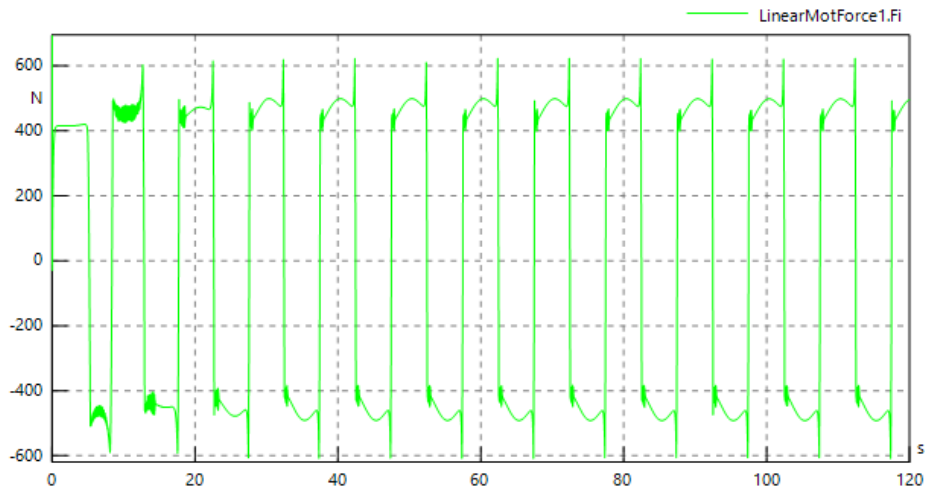
Before choosing which electric linear motor to use for this thesis a number of requirements for the motor had to be established.

4.2.1 Motor Requirements

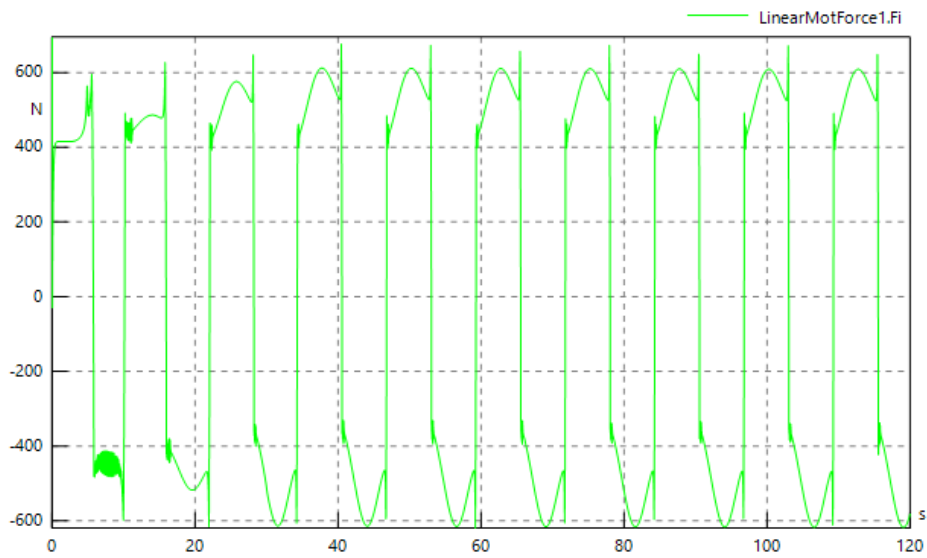
The motor had to be able to use the same Siemens drive that had been used on the scale model before, meaning it had to be compatible with the Siemens drive and be able to run on 3x400VAC supply. The motion required of the motor is equal to the motion of the waves defined in the master thesis by Atle A.Alerud and Tomas Klevmo [5], seen in equations 2.4 to 2.6 and figure 2.7, in chapter ??

The force that the linear motor(s) has to deliver was found by creating a very simple version of a linear motor in SimulationX and connecting it to the CMC-E model, see section 5.1.1.

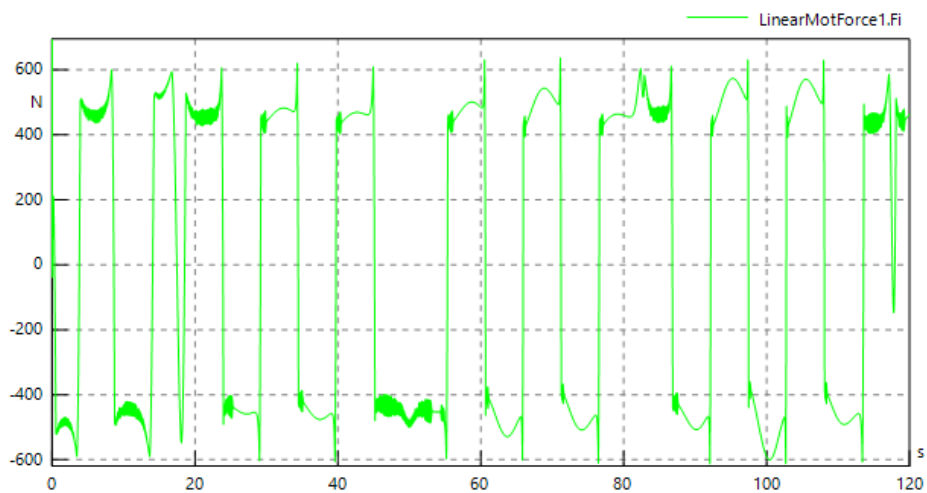
A simple control system, consisting of a P controller that stabilizes the hookload, was then implemented in the SimulationX so that the contributing force of the linear motor could be plotted as seen in figure 4.1. The controller was set quite aggressive so that there is very small variation in the hookload. To compensate for the weight of the slider in the linear motor, so that the positive and negative force required by the linear motor is approximately the same, the setpoint for the hookload force can be increased depending on the weight of the slider. For the simulation with the chosen motor 2660N was used as hookload setpoint, and the pressure was set to 7.07 bar.



(a) Wave #1



(b) Wave #2



(c) Wave #3

Figure 4.1: The force required by the linear motor(s) for the three waves in SimulationX

4.2.2 Choosing a Supplier and Motor

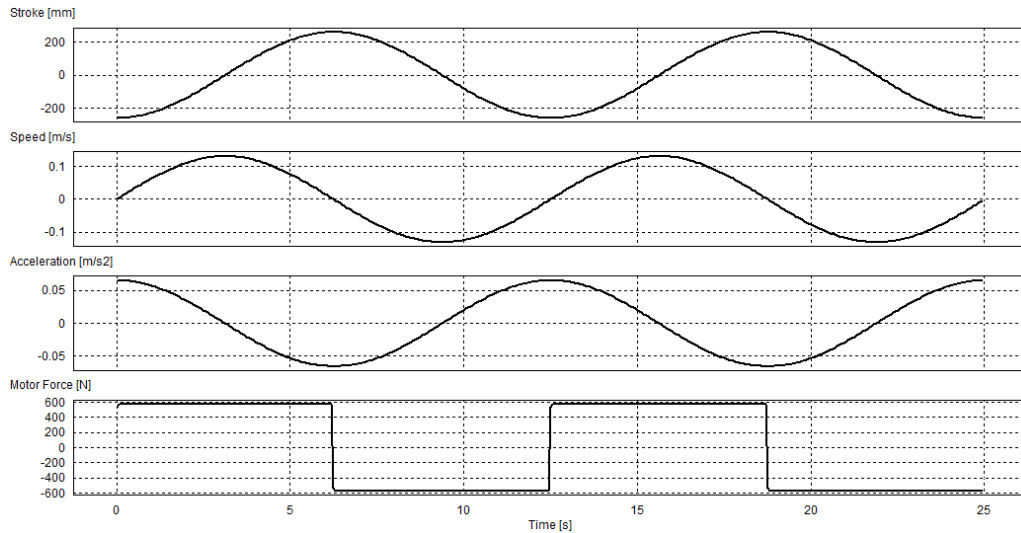
NTI AG was chosen as a potential motor supplier after suggestion from Narve Kristiansen at NOV. They have a brand of tubular electric linear motors called LinMot®, which have a series of motors which run on 3x400VAC and support third-party drives, like the Siemens SINAMICS S120 with the SMC20 encoder. The motors are tubular linear motors which by addition of a flange simplifies the mounting of the motor. Their motors also had longer possible stroke lengths than others that were looked at combined with a compact size and different options for cooling. In addition a program called LinMot® designer was available which simplified the calculations for the motors.

4.2.2.1 LinMot-Designer

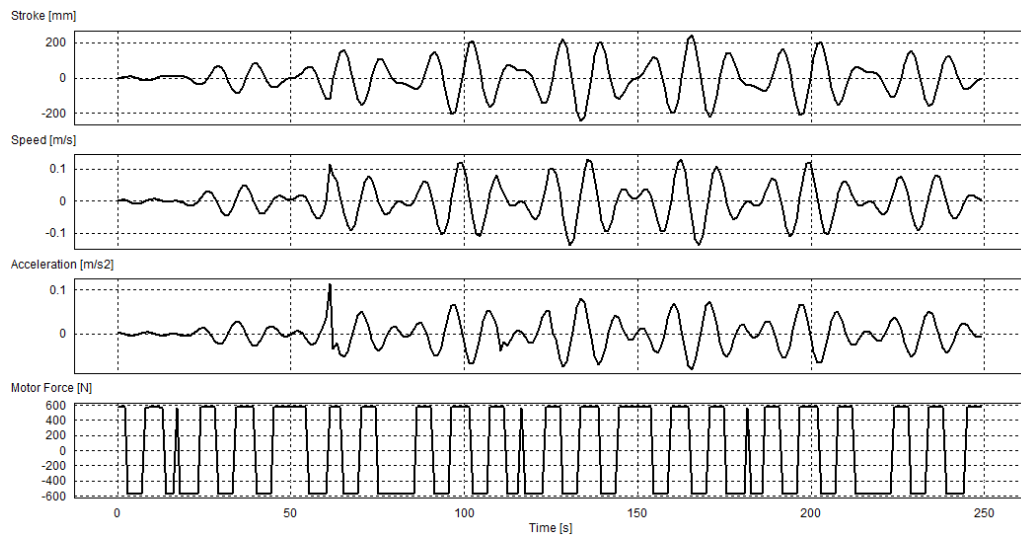
LinMot® Designer is a sizing tool for the LinMot® motor system that simulates the behaviour of the LinMot® linear motors under static and dynamic load conditions. By defining the motion and forces required from the linear motor the program can simulate how the chosen motor will perform under the given conditions. The following criteria are then checked and the programs gives a warning if any of them are violated:

- Stroke - If the motion required exceeds the motors stroke limit.
- Force - If the force required exceeds the motors force limit.
- Short Time Overload - If the short time overload protection limit is exceeded.
- Thermal Load - If the thermal load limit of the motor is exceeded.
- Acceleration Reserve - If the ratio of the motor peak force and the moving mass is less than 10N/kg.

Using a design program significantly simplifies the process of choosing which linear motor to use. Not only by reducing the amount and time of calculations, but also making it easy to explore other options or configurations without having to redo all the calculations [16]. Figure 4.2 shows two of the three waves in LinMot® Designer



(a) Wave #2



(b) Wave #3

Figure 4.2: Waves #2 and #3 in LinMot designer

4.2.2.2 Looking at different motors

Since the motors had to be of the $3 \times 400\text{VAC}$ type and support third party drives only the motors of type P10-70 was suitable. It quickly became apparent that the heat generated by the motors was a major design factor due to the constant movement and continuous force required by the motor. The second most powerful motor from LinMot®, the P10-70x320U [17], could handle the forces and motion required. If liquid cooling was not to be used, an alternative would be to use two air-cooled motors instead. The motors would still have to be fairly large, only one step down from the one-motor solution (P10-70x320U [17]), then it would be sufficient with air-cooling. However this seemed impractical due to the cost of two motors, the need for another drive for the second motor and the synchronization and mounting of two motors on the scale model. It was decided that the advantages of using one instead of two far outweighed the disadvantage of using fluid-cooling compared to air-cooling, and therefore the LinMot® P10-70x320U was chosen as the motor to use in this thesis. The stroke length of the motor should be equal to, or preferably longer than the stroke of the cylinders, which is 1270mm. Therefore a 1790mm long slider was chosen which, in combination with the chosen stator, gives a stroke length of 1330mm. For the motor and encoder cables a length of 8m was chosen.

4.2.3 Electric Linear Motor

The LinMot® P10-70x320U/1330 is a tubular permanent magnet linear synchronous servo motor (PMLSM), it consists of only two parts: the stator P10-70x320U and the slider PL10-28x1790/1740. The stator is made of nickel plated iron contains the motor windings, bearings for the slider, position capture sensors, overload protection and a microprocessor for monitoring the motor. The slider is made of neodymium magnets mounted in a high-precision stainless steel tube, all designed for use in harsh industrial environments. The front end of the slider is equipped with an M10 threaded hole and the rear end with an M8 threaded hole for mounting the load. The internal position sensor monitors the current position of the linear motor not only when it is stopped, but also during the motion, deviations are detected immediately and reported to the controller. There are no mechanical linkages for power transmission that causes wear which means there is very low friction and gives the motor a long operational life. The connectors for the power and signal cables are IP67 classified and are both rotatable to provide easy cable management. [18] [14] [17]

The linear motor will be cooled by the liquid cooling flange PF10-70x350-FC. The flange is clamped around the stator and also provides bolt holes for mounting the motor.

The mechanical and electrical properties of the motor with the liquid cooling flange attached, is shown in table 4.2. As seen, the velocity and particularly the acceleration the motor is capable of is many times what is required for the active heave compensation. The peak force of the motor is also much higher than what is required, but since the motor is only capable of delivering peak force over short periods of time, and the AHC requires a force almost constantly with small variations, the continuous stall force is therefore much more relevant. By looking at figure 4.1 it can be seen that the force required by the motor is almost always lower than the continuous stall force except for some peaks where the AHC have to overcome the friction of the PHC.

Table 4.1: Linear motor P10-70X320U/1330 [17]

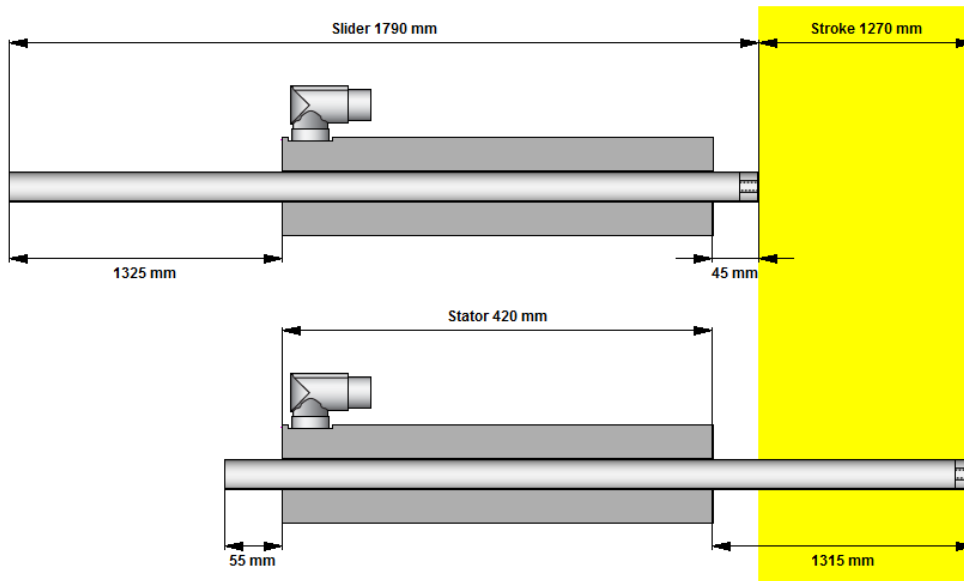
Description	Value	unit
Mechanical specification		
Maximum stroke	1330	mm
Peak force	2162	N
Continuous stall force	673	N
Peak velocity	5.9	m/s
Peak acceleration	939	m/s ²
Stator length	420	mm
Stator diameter	70	mm
Stator mass	6.9	kg
Slider length	1790	mm
Slider diameter	28	mm
Slider mass	8.41	kg
Magnetic period (el.cycle)	40	mm
Electrical specification		
DC-Link voltage (Nominal/Max)	560/750	V
Peak Current	34	A
Peak Current RMS	24	A
Continuous stall current	7.8	A
Force Constant @ 25°C	89.9	N/A
Resistance (ph-ph) @ 25°C	5.4	Ohm
Resistance (ph-ph) @ 100°C	6.98	Ohm
Thermal Specification		
Maximum winding temperature	90	°C
Maximum duration with peak current	4.6	s
Maximum Power dissipation	611	W

Table 4.2: Linear motor P10-70X320U/1330 power supply

Description	Wave #1	Wave #2	Wave #3	unit
Peak supply power	410	470	480	W
Mean supply power	400	440	420	W
Maximum Power dissipation	611	611	611	W

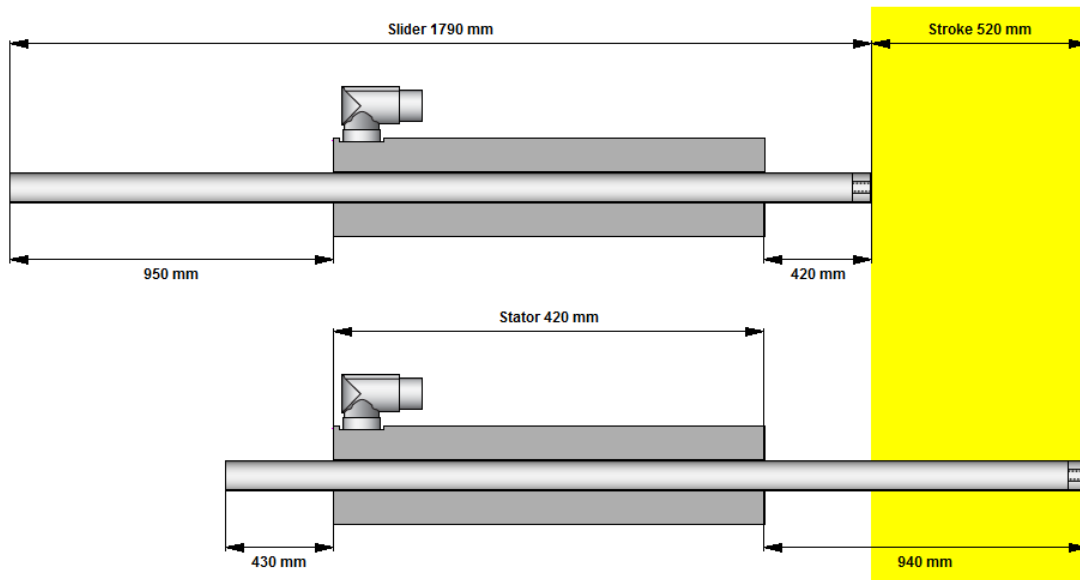
The motor is protected from overheating by three internal thermistors embedded in the motor windings which are monitored by the motors electronics. 4.3

P10-70x320U/1330



(a) Stroke in wave #2

P10-70x320U/1330



(b) Maximum stroke of the CMC

Figure 4.3: Stroke of the motor

4.2.4 Order Information

The complete order information, with all the parts required for the linear motor is shown in table 4.3

Table 4.3: Linear motor order information

Type	Ordering Number	Description
PS-10x320U-BL-QJ-D02	0150-2343	Stator 3x400V for 3rd party drive
PL10-28x1790/940	0150-2207	Standard slider for 1330mm stroke
PF10-70x350-FC	0150-2294	Motor Flange w/Fluid Cooling
KPS15-04L/Q-8	0150-2276	Motor power cable 10m 3rd party
KSS05-02/08-D15/J-8	0150-2277	Signal cable 10m 3rd party
LU02-08	0150-1953	Lubricant for linear motors 8g

4.3 Linear Motor Testing

Since some parameters of the PMLSM that have impact on the performance of the controller and the system is not known, it is desirable to estimate these parameters by running tests on the motor. The two main parameters in question that can impact the control aspect is the friction in the motor and the force ripple. By estimating these parameters some kind of compensation for them can be created.

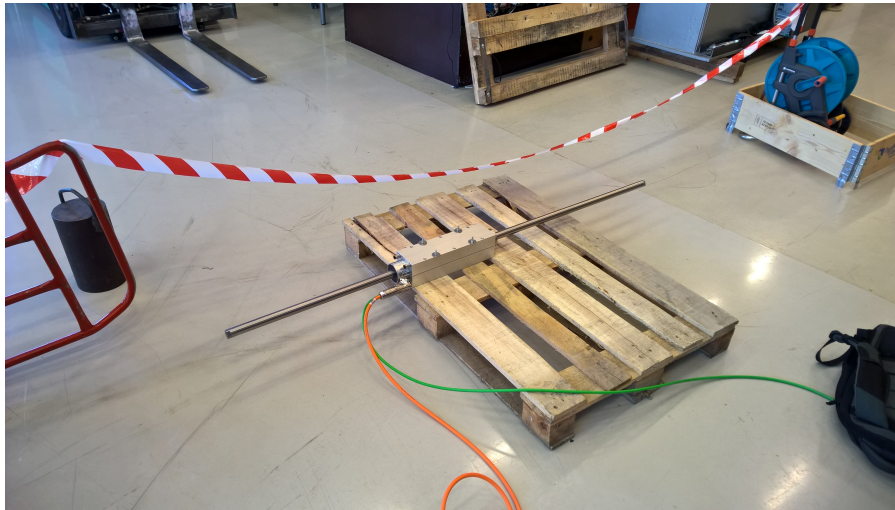


Figure 4.4: Testing the linear motor

4.3.1 Friction

The friction in the PMLSM is probably very low compared with the rest of the system, however it is still desirable information to have when creating the control system. Measuring the friction in the motor can be done in several different ways. One method is to fix the motor in place and then connecting the slider to a force transducer and applying force until the slider starts to move and then keeping the speed of the slider constant. By logging the force in the force transducer the static friction, the coulomb friction and the viscous friction can be estimated, from the resulting friction curve. Another method is to run the motor at constant speed using the drive system and then log the force directly from the drive.

4.3.2 Force Ripple

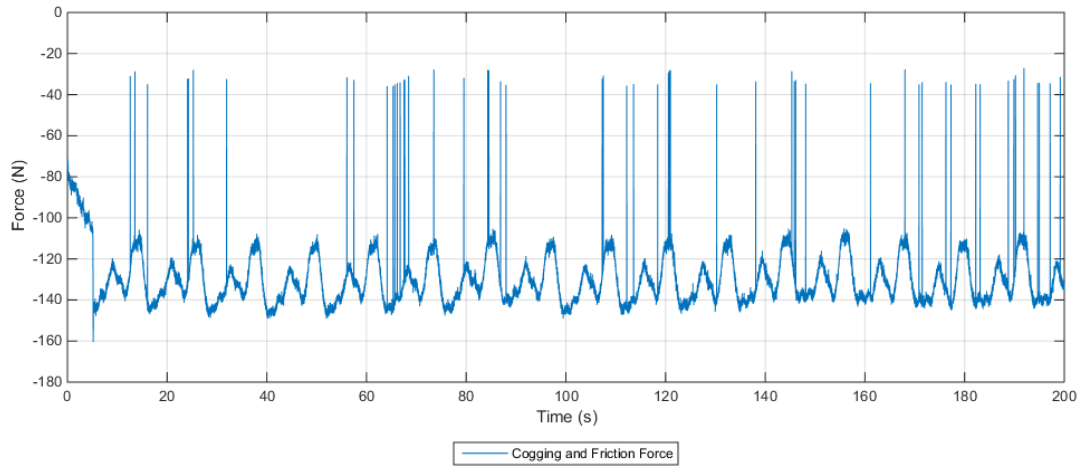
The force ripple in the motor is one of the significant drawbacks of a PMLSM [19] [20]. Force ripples is the result of flux linkage harmonics, reluctance harmonics, cogging harmonics and time harmonics and change periodically as the mover advances during its motion, with cogging force being the main contributor [19]. The cogging force is generated when the permanent magnets in the slider interacts with the ferromagnetic core of the stator, and is dependent on the position of the slider, it is preferable

to minimize the cogging force at the motor design stage [21]. However no matter how good the design of the motor is, it will still experience some cogging force.

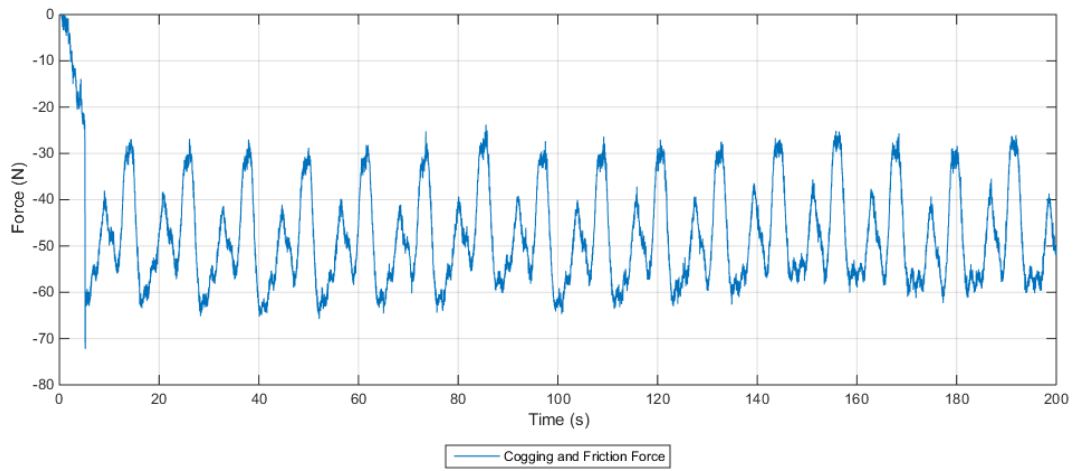
Cogging forces can be extracted by Finite Element Method, however a precise model of the motor would have to be made and the necessary data was not available. A different approach to measure the cogging forces experimentally is described in [22]. The method consist of fixing the stator in place and then blocking the slider inside the stator and measure the blocking force with zero input voltage using a force transducer. The measurement is then repeated for various positions with a defined incremental distance. For performing the experiment in the lab the stator will be fastened to its bracket and fixed in place, the force transducer will be connected to the end of the slider using a thread reducer. For adjusting the position of the slider inside the stator a turnbuckle and threaded rods will be used between the force transducer and a fixed point. The method decided upon was to use the drive system to drive the slider in the same manner as estimating friction. The force can then be logged from the drive system and used to estimate the cogging force, however the friction force will also have an effect on the output.

4.3.3 Test Results

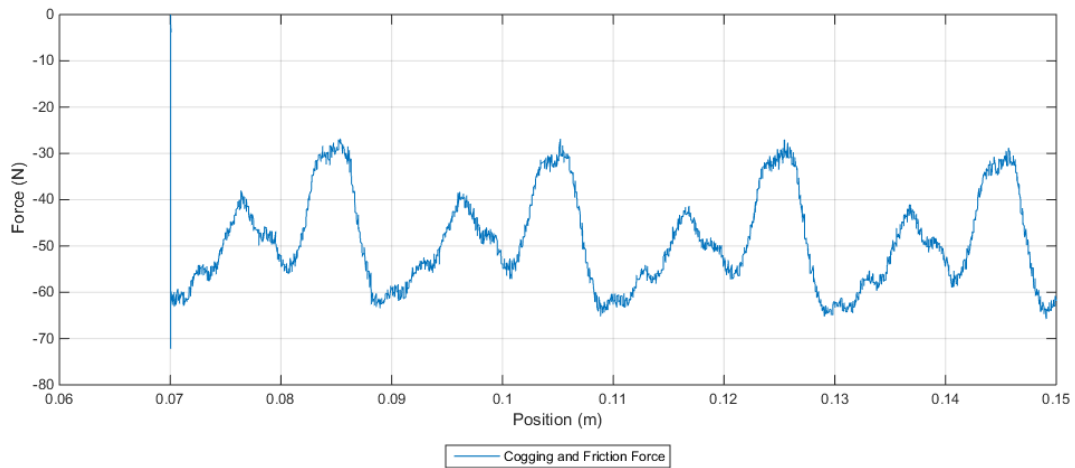
As mentioned above when testing the motor in this way it is not possible to test for just friction or just cogging force as both always will be present, some assumptions will therefore have to be made when estimating the forces. The friction and cogging force therefore had to be extracted from the same force curve when running the motor at a constant speed through its full range of motion. The motor was mounted vertically during testing with its positive axis downwards as this is how it will be operated, also when lying down the moment created by the unsupported slider generates increased friction as it moves past its center point. For testing the motor was set to run at 0.1 m/min in an upwards direction as this gave more stable results then when going downwards. The measured friction and cogging forces post processed in MATLAB, subtracting the weight of the slider and applying a median filter to remove spikes from the signal. The test results can be seen in figure 4.5.



(a) Friction and cogging forces before correction and filtering



(b) Friction and cogging forces after correction and filtering



(c) Close up of the friction and cogging forces plotted as a function of the slider position

Figure 4.5: Friction and cogging forces in the motor

As the motor is running at a constant velocity it can be concluded from the results that the cogging force is position dependant. Which is also true, as it arises from interaction between the magnets in the slider [22] [19]. In figure 4.5c the friction and cogging force has been plotted as a function of the slider position which also confirms that the cogging force is position dependant. From the figure it can be seen that the cogging force pattern repeats every 20 mm which corresponds to the motors pole pair width of 40 mm.

Looking at figure 4.5b it can be seen that the breakaway force when the motor starts moving, at approximately 5 seconds into the test, is approximately 72 N, however the cogging force also has to be taken into account. The acceleration is so low that the forces related to it can be neglected. From 4.5c by studying cogging force pattern it can be deduced that the cogging force plus the Coulomb friction at the start of the test is approximately 60 N which gives a Stribeck friction of approximately 12N. Supported by the test results it is assumed that the friction force does not change with the slider position. Estimation of the Coulomb friction is more uncertain but is approximately 49 N, giving a stiction of $49 + 12 = 61$ N. The cogging force can then be estimated by removing the friction from the data and doing a curve fitting as seen in figure 4.6. The fitted curve is a sum of sine curve consisting of three sine functions shown in equation 4.1 which was considered suitable to describe the cogging force.

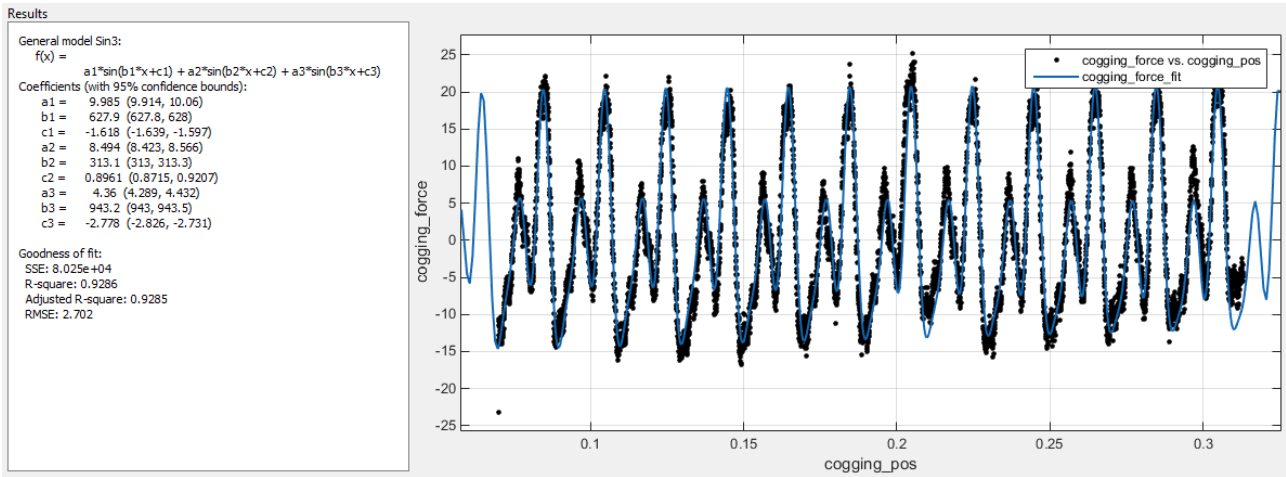


Figure 4.6: Curve fitting the cogging force

$$F_{cog}(x) = 9.985 \sin(627.9x - 1.618) + 8.494 \sin(313.1x + 0.8961) + 4.36 \sin(943.2x - 2.778) \quad (4.1)$$

where x is the slider position.

As the results were not going to be used for the control system due to the unforeseen events during testing and limited time available for testing and estimating this is only a rough estimate of the friction and cogging force in the linear motor.

Chapter 5

System Models

5.1 Modelling the Compensator

Aalerud and Klevmo had created models of the scaled CMC in their master thesis which could be reused for this project, among those a SimulationX model and a set of differential equations which describe the dynamics of the system [5]. Along with the models of the system was also PLC logs from their tests with the scale model which were used as reference.

5.1.1 SimulationX Model #1

The SimulationX model was created from the information in the report by Aalerud and Klevmo [5]. This model is a simplified and scaled down version of the model for the full scale CMC provided by NOV. The model was simplified by replacing pipe dimensions with volumes, combining orifices into equivalent orifices, combining APV volumes into one volume and removing all movement of the vessel except heave in order to reduce the computation time while minimizing the response change [5]. The model is based on fastening a short drill string from the hook and fixing it to the floor so that the crownblock stays in the same position and the force on the hook can be measured.

Once the model was created and verified by comparing it to the logs from the scale model, a simple model of a linear motor was added as shown in figure 5.1.

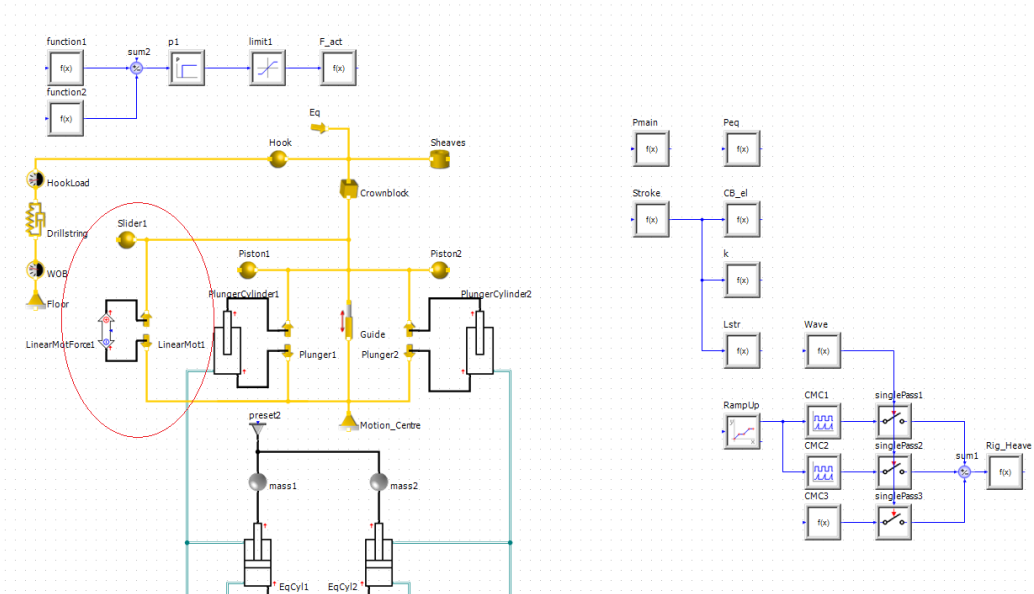


Figure 5.1: Simple linear motor in SimulationX

The model served well for discovering the force required by the linear motor. However it was unsuitable

for use in designing a control system as by simply using a p controller with very high gain (~ 1000) would give a very good result, which seemed unlikely for the real system. The model was therefore exported as an S-function for use with Matlab/Simulink where its response was quite similar to the data from the real model. This model was therefore used for testing the control system.

5.1.2 SimulationX Model #2

The model was modified so that instead of the hook being fixed to the floor a load was fastened to it so that the system could be controlled by using the position of the crownblock as feedback. This became the model used for creating the control system, and is shown in appendix D.

5.1.3 Matlab/Simulink Model

The Simulink model was made as a Matlab function by use of equations 5.1 to 5.13 created by Aalerud and Klevmo [5]. The LuGre friction model from [23] is used to model the friction in the system. This model is also based on the hook being connected to the floor by use of a drill string, it was decided not to create a model for where a load is fastened to the hook instead, as it had been decided to use the SimulationX model for the creation of the control system.

$$r_1(\theta) = 0.0003 \cdot \theta^2 - 0.137 \cdot \theta + 0.3143 \quad (5.1)$$

$$r_2(\theta) = -0.0003\theta^5 + 0.0036 \cdot \theta^4 - 0.017 \cdot \theta^3 + 0.0362 \cdot \theta^2 + 0.0131 \cdot \theta + 0.0673 \quad (5.2)$$

$$Q = k_0 \cdot \sqrt{|p_2 - p_1|} \cdot \text{sign} p_2 - p_1 \quad (5.3)$$

$$\dot{p}_1 = \frac{\beta \cdot Q \cdot n \cdot p_1}{\frac{p_0}{p_1} \cdot \beta + V_{10} \cdot n \cdot p_1} \quad (5.4)$$

$$\dot{\theta} = \frac{V_{cb} - V_{sp}}{r_1(\theta)} \quad (5.5)$$

$$\dot{x}_{eq} = r_2 \cdot \dot{\theta} \quad (5.6)$$

$$\dot{p}_2 = \frac{\beta \cdot (-Q - (V_{cb} - V_{sp}) \cdot A_1 - \dot{x}_{eq} \cdot A_2)}{V_{20} + (x_{cb} - x_{sp}) \cdot A_1 + x_{eq} \cdot A_2} \quad (5.7)$$

$$g(v) = \frac{F_c}{\sigma_0} + \frac{F_s - F_c}{\sigma_0} \cdot e^{-\frac{|v_{cb} - v_{sp}|}{v_s}} + k_v \cdot (v_{cb} - v_{sp}) \quad (5.8)$$

$$\dot{z} = (v_{cb} - V_{sp}) - \frac{|v_{cb} - v_{sp}| \cdot z}{g(v)} \quad (5.9)$$

$$\dot{x}_{cb} = v_{cb} \quad (5.10)$$

$$F_{hook} = (x_{cb} - x_0) \cdot k_s + v_{cb} \cdot k_d \quad (5.11)$$

$$F_{fric} = \sigma_0 \cdot z + \sigma_1 \cdot \dot{z} + \sigma_2 \cdot (v_{cb} - V_{sp}) \quad (5.12)$$

$$\dot{v}_{cb} = \frac{p_2 \cdot A_1 + p_2 \cdot A_2 \cdot \frac{r_2(\theta)}{r_1(\theta)} + F_{act} - F_{fric} - F_{hook} - m \cdot g}{m} \quad (5.13)$$

$$(5.14)$$

Where:

$r_1(\theta)$	=	radius of the first eccentric hub
$r_2(\theta)$	=	radius of the second eccentric hub
θ	=	angle of rotation for the hubs
Q	=	flow through the Olmsted valve
k_0	=	orifice constant for Olmsted valve
p_0	=	initial air pressure in APVs
p_1	=	hydraulic pressure in accumulator
p_2	=	hydraulic pressure in cylinders
β	=	bulk modulus of hydraulic oil
n	=	polytropic index
V_0	=	initial APV volume
V_{10}	=	initial fluid volume in accumulator
V_{20}	=	initial fluid volume in plunger and equalizing cylinders
v_{cb}	=	velocity of the crownblock
v_{sp}	=	velocity of the vessel
x_{cb}	=	displacement of the crownblock
x_{sp}	=	displacement of the vessel
x_{eq}	=	position of equalizing cylinders
A_1	=	Area of the two plunger cylinders
A_2	=	Area of the two equalizing cylinders
$g(v)$	=	arbitrary function to express the Stribeck effect
z	=	bristle micro displacement
F_c	=	Coulomb friction
F_s	=	maximum static friction force
σ_0	=	elastic bristle stiffness
σ_1	=	micro damping
σ_2	=	viscous friction coefficient
v_s	=	Stribeck velocity
m	=	mass of the suspended load
k_s	=	Stiffness of drill string
k_d	=	Damping constant of drill string

5.1.4 Linear Motor Model

The electromagnetic force produced by the linear can be found by using the equation for electromagnetic torque in a permanent magnet synchronous motor (PMSM) seen in figure 5.15 [24].

$$\tau_e = \frac{3n_p}{2K^2} \psi_R i_q \quad (5.15)$$

As the only parameter that varies is i_q and everything else is constants this can be written as:

$$\tau_e = K_t i_q \quad (5.16)$$

Where k_T is the torque constant of the motor in Nm/A.

For the permanent magnet linear synchronous motor (PMLSM) it simply becomes:

$$F_e = k_F i_q \quad (5.17)$$

Where k_F is the force constant of the motor in N/A.

The simple dynamic model of a PMLSM can therefore be assumed to be [4] [25]:

$$Ma = k_F i_q - F_d \quad (5.18)$$

Where F_d is the disturbance force composed of the load force, the friction force and the force ripple. The load force is the force the motor needs to produce, the friction and the force ripple in the linear motor is unknown but is possible to estimate during testing. The friction in the PMLSM is fairly low and can be described in the same manner as for a hydraulic cylinder, by the stribek effect. In [26] the friction in the smallest LinMot ® motor was measured which gave a stiction force $f_s = 2\text{N}$, and Coulomb friction $f_c = 1.7\text{N}$, however simply scaling this up is not feasible.

The model for the linear motor in simulink is therefore simply created as shown in figure 5.2 with a force reference as input and the same force as output until the friction and ripple forces could be measured and implemented. After the testing was finished however it was decided not to go back to work on and update the simulation models and instead focus on the physical system.

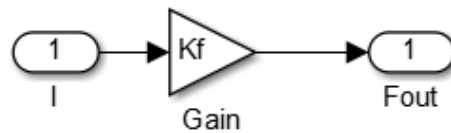


Figure 5.2: Simple linear motor in Simulink

The weight of the slider in the linear motor is taken account for in the SimulationX model and in the Matlab function and is therefore not added to the linear motor model.

Chapter 6

Control System

6.1 Control Strategy

Usually electric linear motors are used in applications where high speed and precise position control is desired, however in this project control of the force generated by the motor could be desirable.

Several methods for controlling PMLSMs have been proposed. Since the PMLSM is not using conventional gears or ball screws uncertainties such as parameter variations, load disturbance, friction force and unknown dynamics in the drive system greatly affects performance. A controller that solves these problems is very beneficial [25]. While waiting for the motor to be delivered a model of the motor was made in simulink and used to simulate the control system in combination with the models created of the scaled down CMC system. As no data could be found about the friction forces and force ripple in the motor it was decided to simulate the control system without and then add compensation for it later when the forces could be measured. In addition the method of testing the scale model, either by fixing the crownblock to the floor by a drill string or by hanging a load from the hook, had not been decided upon. Therefore control strategies for both situations were explored and simulated as in theory it should not matter much which method is used.

Initially it was unclear how the linear motor could be controlled by the Siemens drive system with respect to the reference input to the drive, whether it would be position, speed or force. Since this would not be determined until the drive system was set up with the linear motor, control strategies using either output was looked at.

Different methods were looked at for controlling the active heave compensation system. There were two main control strategies that were looked at:

- Controlling the force of the linear motor by using the weight on bit (WOB) or position of the crownblock as feedback.
- Controlling the position and speed of the linear motor by using the position and speed of the crownblock as feedback, and the wave amplitude and velocity measured by the MRU as setpoints.
- Controlling the force of the linear motor by using the position and speed of the crownblock as feedback, and the wave amplitude and velocity measured by the MRU as setpoints.

For both these main strategies the primary goal of the active heave compensation (AHC) is to overcome to the friction in the system and assist the passive heave compensation (PHC) system in negating the effects of heave motion on the load. For this reason it would be an advantage to control the force reference of the linear motor as this would simplify adding compensation for friction etc. There are many proposed methods for these strategies, all achieving good results with varying degrees of complexity. For simplicity the first control strategy looked at was the method used by Aalerud and Klevmo in their thesis.

6.1.1 The System to be Controlled

6.1.2 Force PI controller with Hookload feedback

This method used by Aalerud and Klevmo in their thesis [5] for controlling the torque output of their servo motor, using the hookload as feedback when a drill string is bolted to the floor. With some modification it should also be suitable for controlling the force output of the linear motor. The controller is a simple PI controller trying to stabilize the hookload by increasing or decreasing the force exerted by the linear motor. The control structure is shown in figure ??.

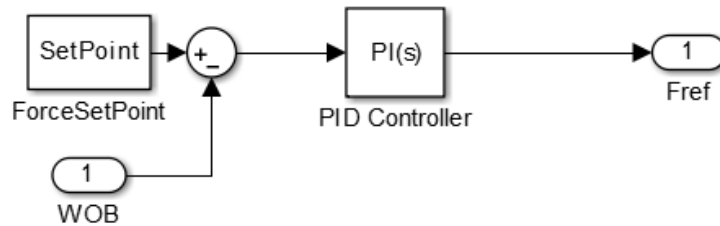


Figure 6.1: Force PI controller with force feedback

6.1.3 Force PI controller with Position Feedback

Using the same setup as in the previous section, except instead of bolting the travelling block to the floor, a weight will be hung from it. Instead of comparing the hookload to a setpoint, the position of the crownblock, measured by the GT001 wire encoder, will be used as feedback and compared to the inverse wave amplitude, measured by the MRU. When using position feedback either the wire encode have to be reset when the load is rest at with zero waves, so its value is zero. The control structure is shown in figure 6.2.

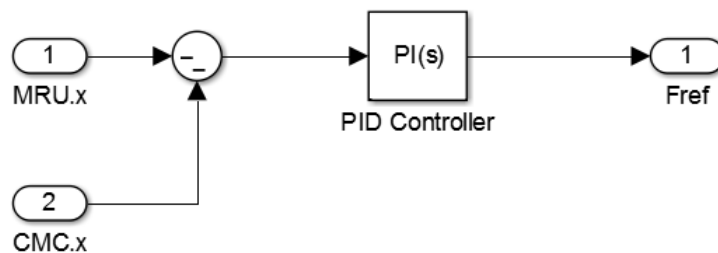


Figure 6.2: Force PI controller with position feedback

6.1.4 Cascade Structure Controller

A cascade structure controller has the advantage that two PID controllers can be used together to give better performance. In a cascade controller the first PID controller in the outer loop controls the primary parameter which is then used as set point of the second controller. In this case the first controller is a P controller which controls the position using the inverted wave measured by the MRU as a setpoint and the measured position of the crownblock as feedback. The inverted wave velocity is then added as a feed forward and the result is a velocity reference for the linear motor. The second controller is of the PI type and controls the velocity, using the velocity reference as setpoint and the actual velocity of the crownblock as feedback, the output can be either motor velocity or motor force.

By using force as the output a feed forward friction estimator and force ripple compensator can also be easily implemented. The control structure is shown in figure 6.3.

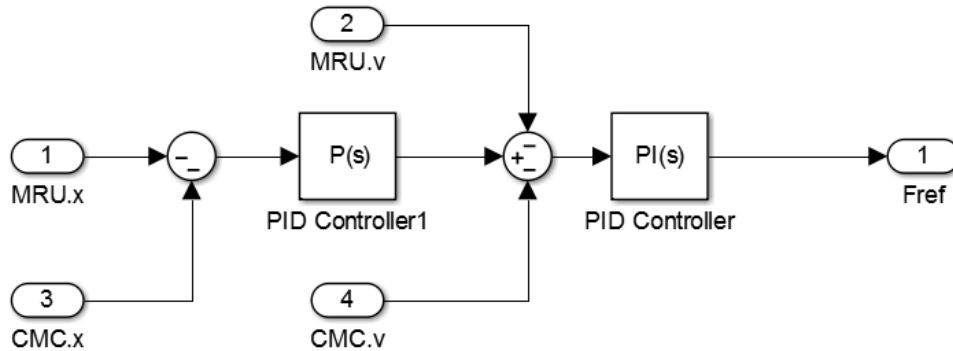


Figure 6.3: The cascade structure controller

6.2 Feed Forward Compensation

6.2.1 Friction in CMC

Sine the primary obstacle to overcome from a controlling perspective is the friction in the system, a feed forward loop consisting only of the wave velocity will therefore in itself have little effect on the variation in the WOB as seen in figure 6.5a. It does lower the average deviation from the mean value but it does nothing to decrease the force peaks and it is not very effective at low velocity. However by using the wave velocity to predict the friction in the system, figure 6.4, and then using the estimated friction as a feed forward yields much better results, figure 6.5a and ???. The friction estimator is created by the equations used in the Matlab function in section 5.1.3 seen in equations 6.2 - 6.4. In addition a pressure dependent friction part was added.

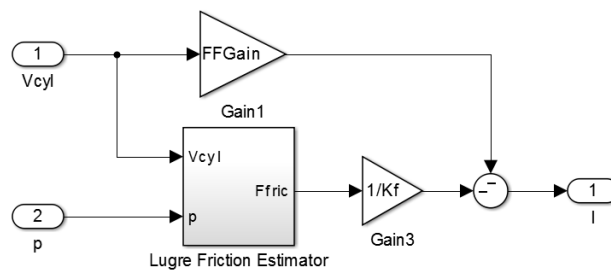


Figure 6.4: Velocity and friction feed forward without PI controller

$$\dot{z} = (v_{cb} - V_{sp}) - \frac{|v_{cb} - v_{sp}| \cdot z}{g(v)} \quad (6.1)$$

$$g(v) = \frac{F_c}{\sigma_0} + \frac{F_s - F_c}{\sigma_0} \cdot e^{-\frac{|V_{cb} - V_{sp}|}{v_s}} \quad (6.2)$$

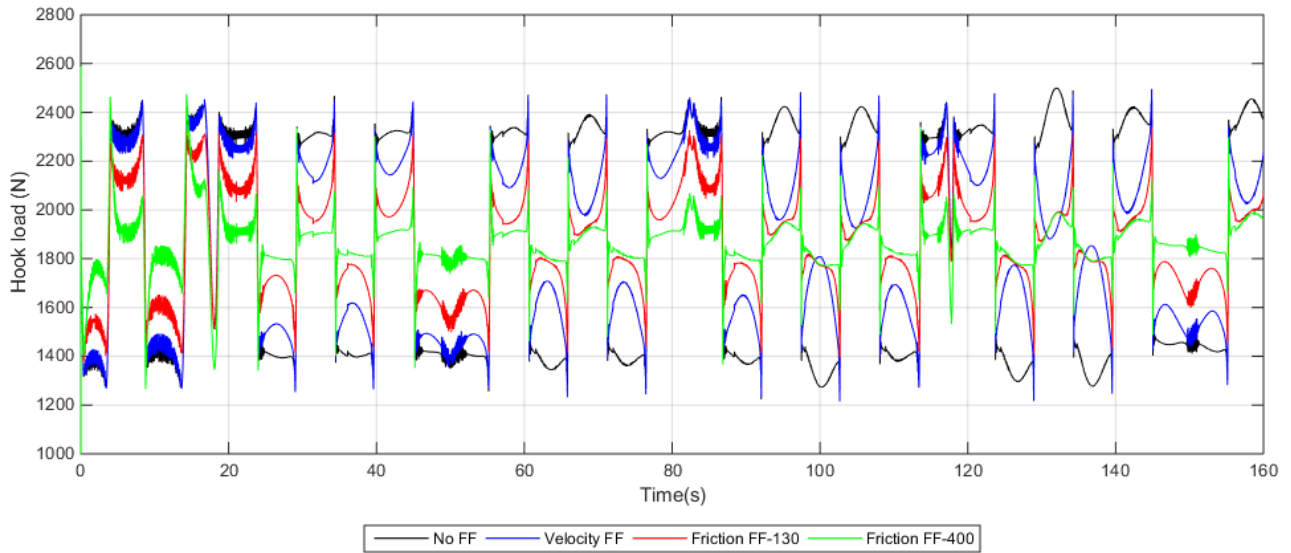
$$F_{fric} = \sigma_0 \cdot z + \sigma_1 \cdot \dot{z} + \sigma_2 \cdot (v_{cb} - v_{sp}) + k_p \cdot p \quad (6.3)$$

$$(6.4)$$

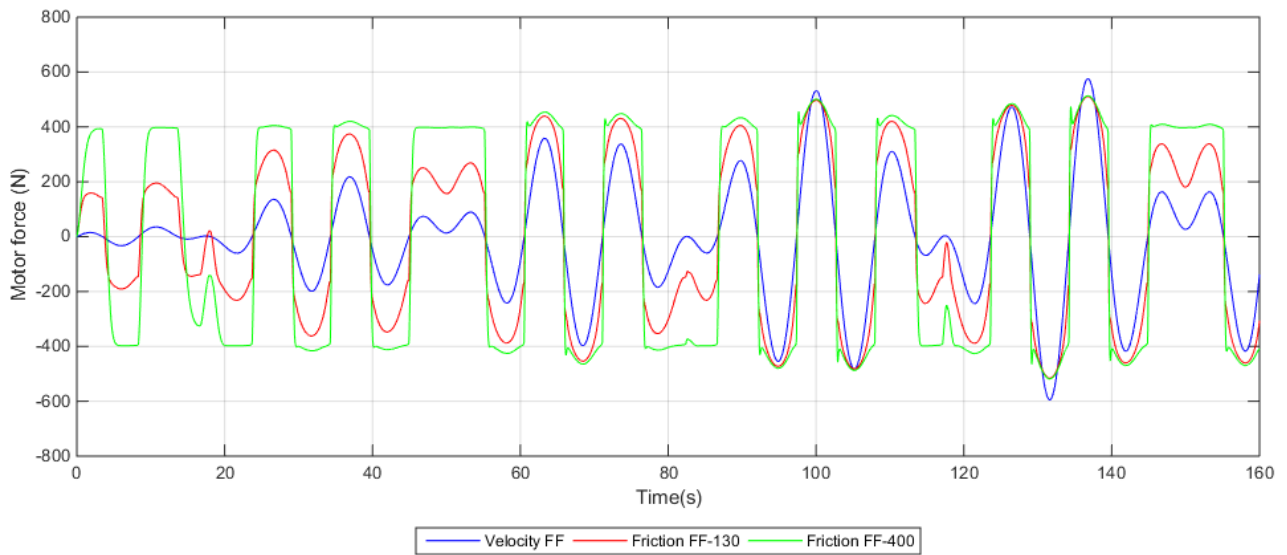
Where:

$g(v)$	=	arbitrary function to express the Stribeck effect
z	=	bristle micro displacement
F_c	=	Coulomb friction
F_s	=	maximum static friction force
σ_0	=	elastic bristle stiffness
σ_1	=	micro damping
σ_2	=	viscous friction coefficient
v_s	=	Stribeck velocity
k_p	=	pressure friction constant
p	=	Pressure in cylinders

In figure 6.5a its effect can be seen with two different values for the static friction factor F_s , 130 and 400, and in figure 6.6 with F_s at 400. These simulations were done with the model where the drill string is connected to the floor and with the simple model for the PMLSM (no friction and force ripple). However the results for the feed forward part is just as relevant for the scenario with a load hanging from the hook. As the friction in the linear motor also can be described by the Stribeck effect [27], this estimator should give just as good results for the system with the PMLSM connected by simply adjusting the parameters. In addition the friction in the linear motor is low compared to the friction in the passive compensator which means the controller should be able to compensate for the increased friction by itself.



(a) Effect on the hook load from different feed forward strategies



(b) The force output from the linear motor for different feed forward strategies

Figure 6.5: Different feed forward strategies

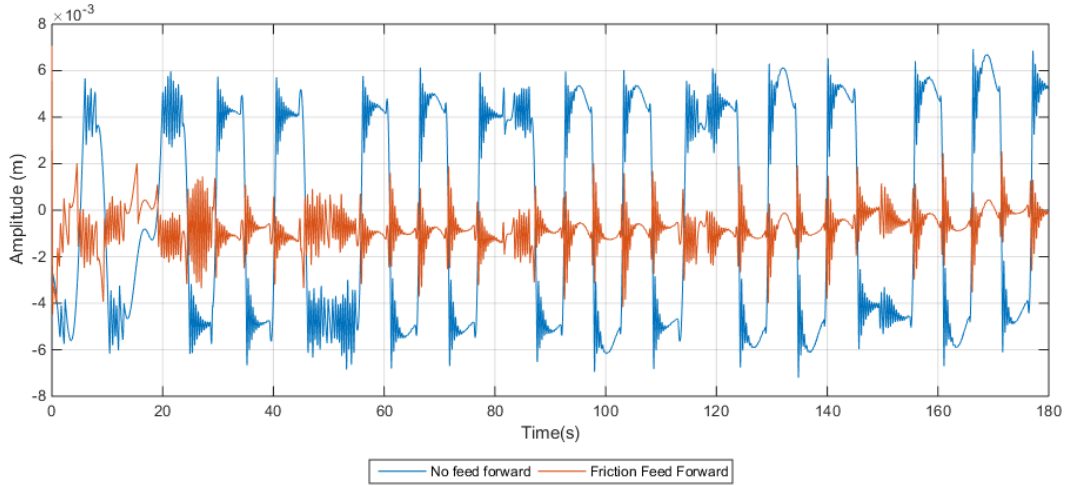


Figure 6.6: Effect of friction feed forward on position PI controller

Figure 6.7 shows an example of a PI controller with friction feed forward.

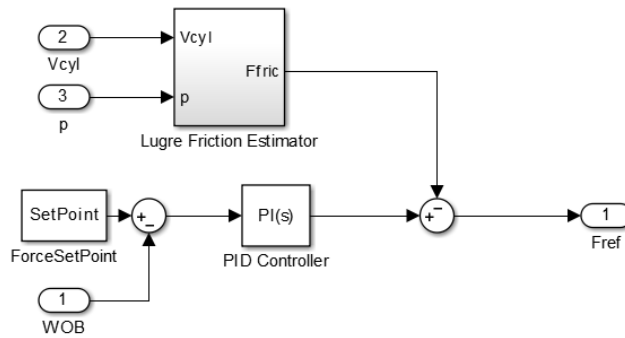


Figure 6.7: PI controller with friction feed forward structure in Simulink

6.2.2 Friction in Linear Motor

6.2.3 Force Ripple in Linear Motor

6.3 Control Simulation and Tuning

6.3.1 Choosing a Model

Both models are simplifications of the real world, but the SimulationX models was chosen when simulating the control system. The reasons for using the SimulationX models in the form of a S-function in Simulink instead of the Matlab function with differential equations is because the SimulationX models were deemed the most similar to the real system and because the friction estimator feed forward is created from the same equations as the Matlab function. A comparison between the SimulationXs model #1 and the real system with wave #3 as heave input is shown in figure 6.8.

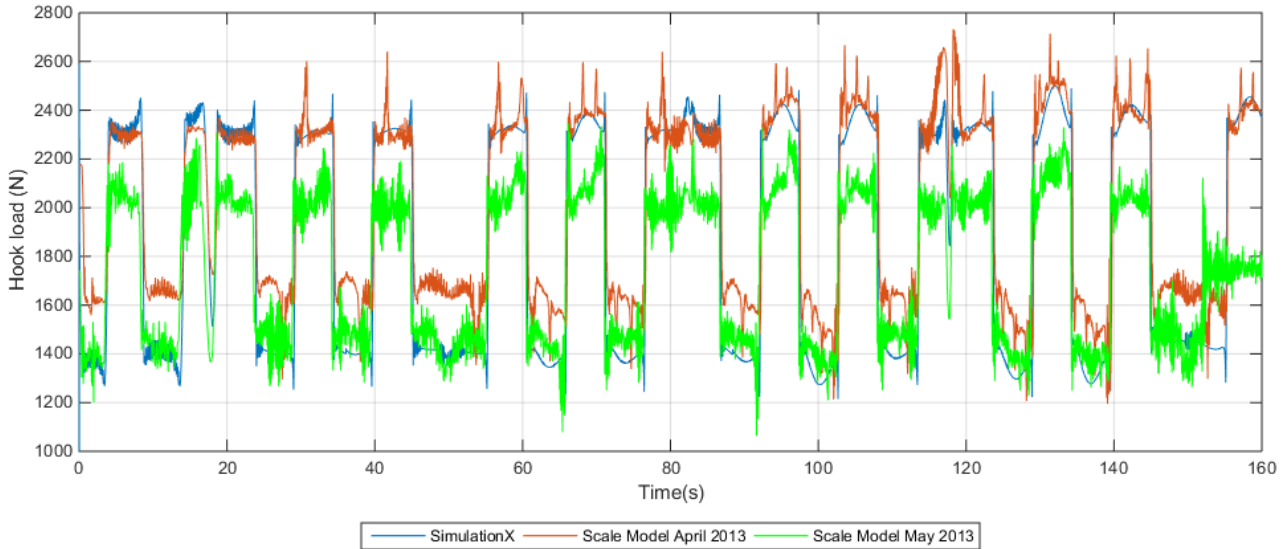


Figure 6.8: Comparison of the SimulationX s-function and data from the real model

As discovered by Aalerud and Klevmo [5] the characteristics of the system can change over time depending on the recent use of the model. As seen in figure 6.8 the friction in the system is lower in may of 2013, after a month of testing, than of april of 2013 when the system had not been run for several days. As the general shape of the curve is more or less the same except for the reduced friction, and the scale model has been sitting in a warehouse for a long time, it was decided not to change the SimulationX model for simulating the control system. However this fact is important to take into consideration when running tests on the scale model so the parameters of the control system, particularly the feed forward friction estimator, can be changed.

6.3.2 Tuning Strategies

Lots of different tuning strategies exist. One well-known example is the Ziegler-Nichols method, this involves setting the integral gain to zero and increasing the proportional gain until the system oscillates with constant amplitude, which takes the system to the edge of stability. This might be suitable for a system model, but it's not desirable to take a large system to the limit of its stability. Skogestads Method has been used to great effect for tuning of PID controllers in other projects, however it is a model-based method that depends on a linear model of the system. The same goes for Matlabs PID tuning toolbox. The models of the system are not linear and as discovered in [5] the friction elements were not suitable for linearization, and since the primary goal of the control system is to overcome this friction this is not suitable.

The Good Gain method is a simple, experimental method which can be used on a real process without any knowledge about the process to be controlled, or a simulated model [28]. Compared to the Ziegler-Nichols method the Good Gain method should give better stability and does not require the control loop to get into oscillations during the tuning [28]. The method works by setting the integral (and derivative) gain to zero and then increasing the proportional gain K_p until an overshoot and very small undershoot is achieved during a step input with the proportional gain K_{pGG} . The integral time can then be set as follows:

$$T_i = 1.5 \cdot T_{ou} \quad (6.5)$$

where T_{ou} is the time between the overshoot and the undershoot of the step response.

Since an integral term has been introduced K_p can be reduced to maintain stability, e.q. 80% of the original value:

$$K_p = 0.8 \cdot K_{pGG} \tag{6.6}$$

6.3.3 Force PI Controller with Friction Feed Forward

The proportional gain was initially set to 1 and the Integral gain to 40, using the parallel form in equation 6.7

$$P + I \frac{1}{s} \tag{6.7}$$

The gains was then gradually increased, the proportional gain by 0.5 and the integral gain by 20 for each step until the best response was found. The friction feed forward was left at the following values:

Table 6.1: Friction feed forward parameters

Parameter	Value	Unit
F_s	400	N
F_c	350	N
σ_0	$2.35 \cdot 10^5$	N/m
σ_0	$2.7 \cdot 10^4$	Ns/m
σ_0	$1.2 \cdot 10^3$	Ns/m
v_s	0.029	m/s
k_p	10	N/bar

The best response was found with the proportional gain at 6.5 and the integral gain at 260.

When using the Good Gain method the time T_{ou} between the overshoot and undershoot was very low (~ 0.0003 s) which resulted in a very low integral time (~ 0.00045 s), which translates into a very high integral gain (~ 2222.22 s). The proportional gain K_p was equal to 5.6. When simulating the system with these values the performance was worse compared with using the values that was found by manual tuning, as seen in figure ??, this is due to the very large integral gain which causes instability.

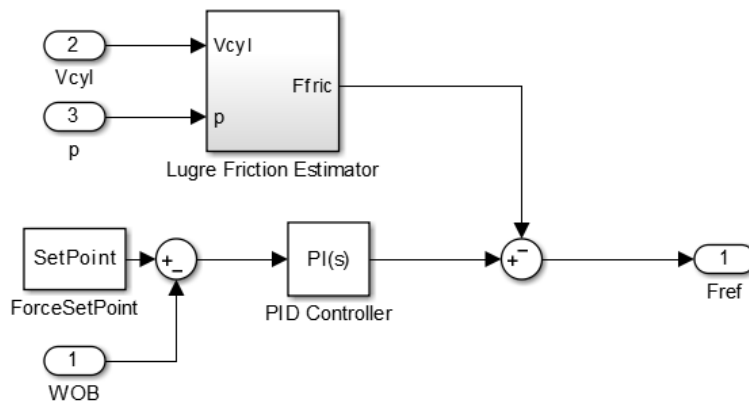


Figure 6.9: The PI controller with hookload feedback and friction estimator feed forward

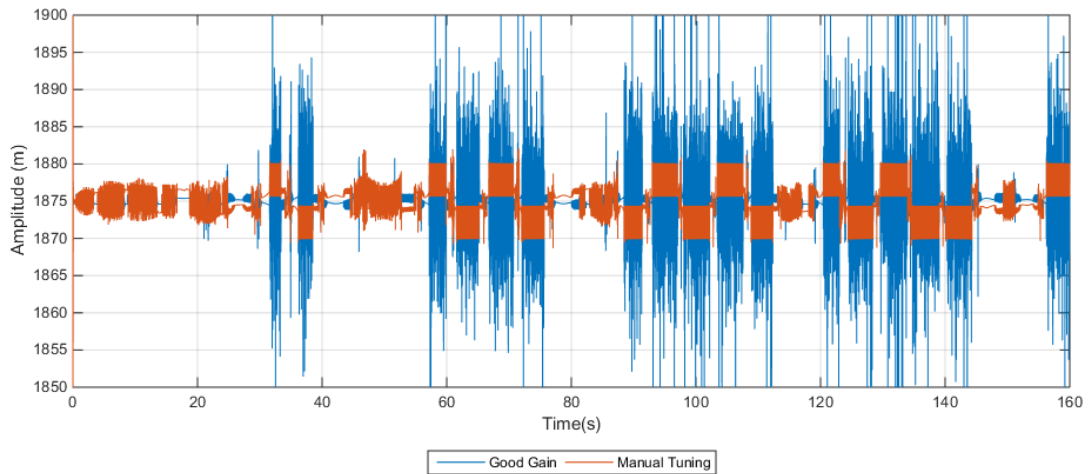


Figure 6.10: Hookload deviation using the PI controller with hookload feedback and friction estimator feed forward

When using the position only as feedback the best response found manually was with the proportional gain at 120000 and integral gain at 145 while the good gain method gave a proportional gain of 47000 and integral gain of 14.5. The comparison measured in the crownblocks deviation from control point.

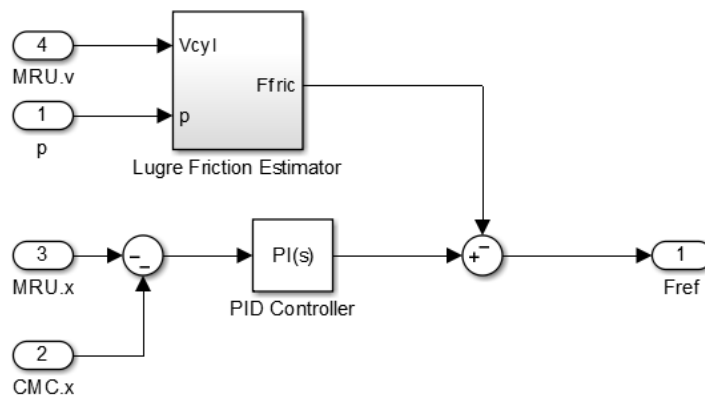


Figure 6.11: The PI controller with position feedback and friction estimator feed forward

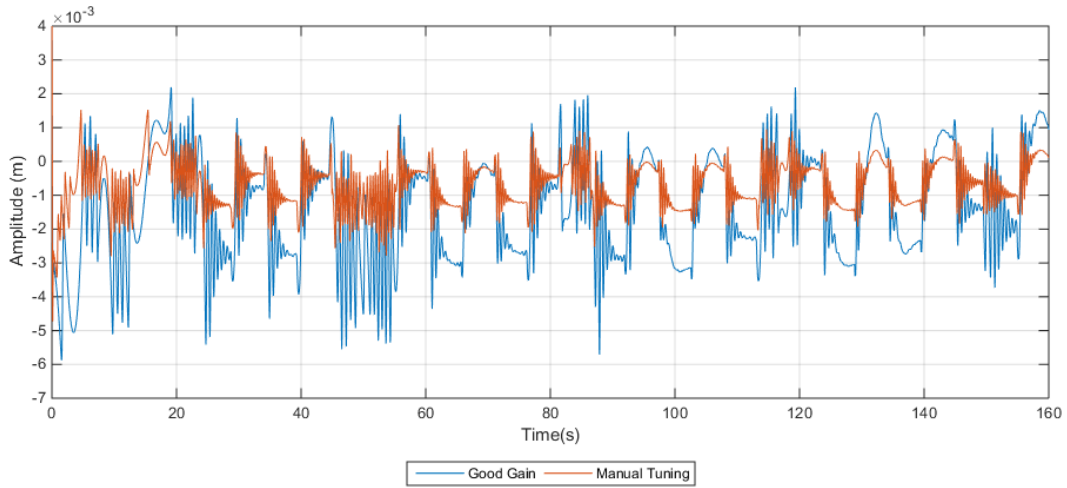


Figure 6.12: Crownblock deviation using the PI controller with position feedback and friction estimator feed forward

6.3.4 Cascade Structure Controller

After a while tuning the different controllers and gaining knowledge about the system, initial guesses for the controller gains became better and better and so less and less tuning of the control system became necessary. For the initial gains for the cascade controller with the friction estimator feed forward, see figure 6.13 crownblock position deviation of less than 0.5 mm was achieved, see figure 6.14. The proportional gain was set to 10 and 100000 for the first and second controller respectively and the integral gain of the second controller was set to. It was decided not to fine tune the model but instead focus on the practical part of the thesis, getting the motor and scale model up and running.

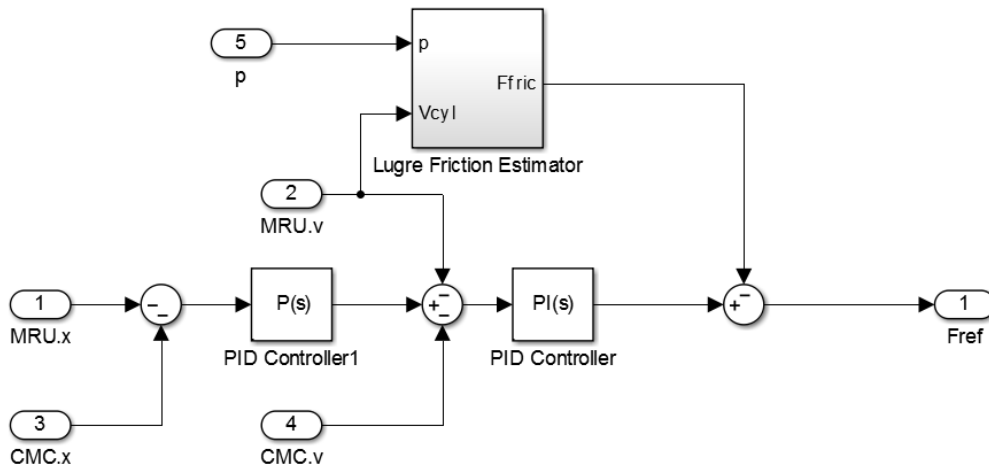


Figure 6.13: The cascade structure controller with friction estimator feed forward

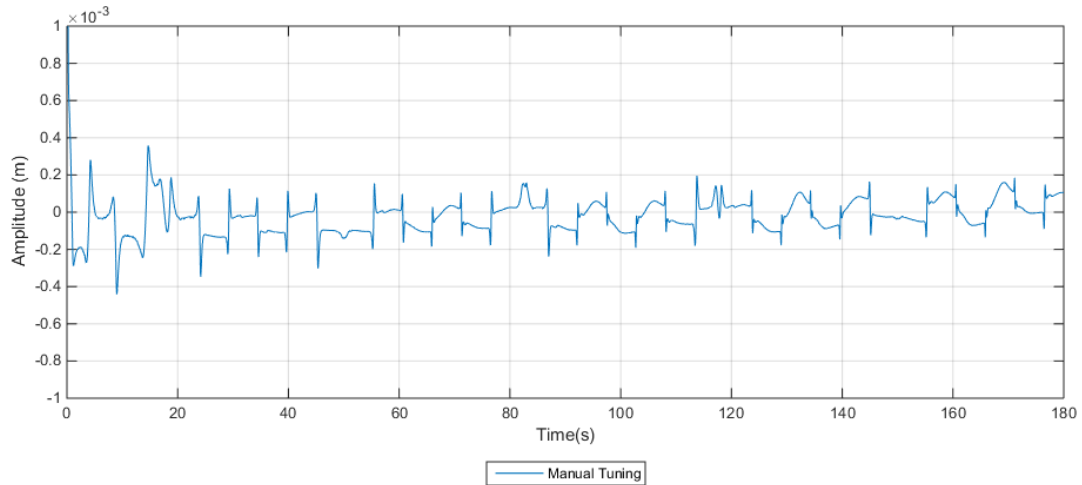


Figure 6.14: Crownblock deviation using the cascade structure controller with friction estimator feed forward

6.4 Chosen Control Strategy

When looking at the results from the simulations the choice of controller was obvious, the cascade controller clearly gave the best results combined with the friction feed forward. Since an accurate model of the linear motor is not included in the model it might behave slightly differently in real life than in the simulations, however it was felt that it gave a good indication of its performance. All the measurements in the simulations like wave amplitude and velocity and crownblock position and velocity are perfect, however this is not the case in real life as both the MRU which measure the waves and the wire encoder which measures crownblock position have a certain margin of error which will impact the performance of the controller.

Chapter 7

System Implementation

This chapter describes the processes required, including mechanical, electrical and control aspects, for using the LinMot ®P10 linear motor with the NOV Crown Mounted Compensator scale model. Near the end of the project it became clear that the CMC scale model was not working properly during the testing phase and the system had to be changed to running the linear motor by itself. This chapter is therefore split into two parts, the first part covers the CMC with linear motor system and the second part covers adaptations which had to be made to the system in order to run the linear motor alone.

7.1 Incorporating the Linear Motor Into the CMC

There are two principal ways of mounting the linear motor and both of the different methods can be executed in different ways

1. Fixed stator and moving slider.

- The stator part of the motor is mounted to the top of the structure of the Crown Mounted Compensator (CMC), directly above the center of the crown block, using the mounting points of the motor flange and constructing a bracket for fastening it to the CMC. The end of the slider is fastened to the crown block by use of the M10 threaded hole in the slider. This method is similar to how the hydraulic Active Heave Compensation (AHC) system is mounted.
- Mounting the motor on the side of the CMC structure and connecting the ends of the slider to the top and bottom of the crown block using wires and sheaves.

2. Fixed slider and moving stator.

- The slider of the motor is mounted at both ends to the structure of the CMC using a kit from the LinMot® catalogue and constructing the necessary brackets. The flange of the stator is fastened to the crown block by constructing another bracket.

The fixed slider and moving stator principle imposes some challenges:

- The cables for power and sensors connected to the stator along with the hose for cooling connected to the flange will be moving, which means a system for keeping the cables and hoses in place has to be added.
- Difficult to fasten the slider at both ends to a structure that was not designed for it.
- Lack of space for the stator to move up and down.

The fixed slider and moving stator principle was therefore rejected for use in this project due to the complexity and lack of available space. However it might be a viable option for the full scale CMC, though certain modifications would probably have to be done to the existing structure.

The fixed stator and moving slider principle is therefore the one that will be used on the scale model. Since this project is about investigating the possibility of using an electric linear motor as an AHC, the simplest method of mounting it to the scaled CMC was chosen, which is to mount it on top of the CMC structure with the slider connected to the crown block. The other methods was deemed to complex and time consuming and would required modifications to the scaled CMC. By using this method the bracket and force transducer assembly fitted by Aalerud and Klevmo [5] can be reused in this thesis, see figure 7.1.

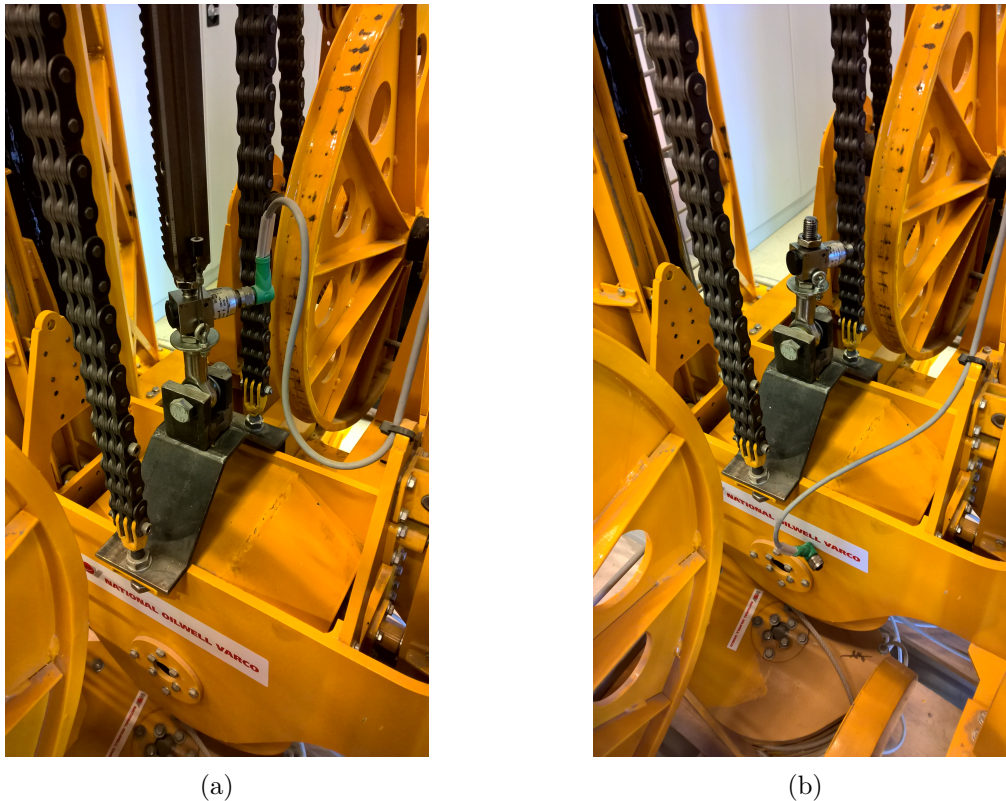


Figure 7.1: The bracket and force transducer assembly with rack and pinion system in place (a) and removed (b)

Initially it was desirable to be able to place the stator between the crown block and the top frame in order to minimize the length of the slider, however when the crown block is in the uppermost position there is not enough space for the stator. The ideal solution would therefore be to place the stator in the center gap in the top frame of the structure, see figure 7.2, however the flange of the motor is too large to fit in the space on the scale model. This would be the best solution for the scale model as the slider could be fastened directly to the crown block, without the need for a link in between, it would also reduce the total height of the CMC both wi This is could also be a viable solution for the full scale CMC provided the top frame of the structure was modified to accommodate the electric linear motor(s).

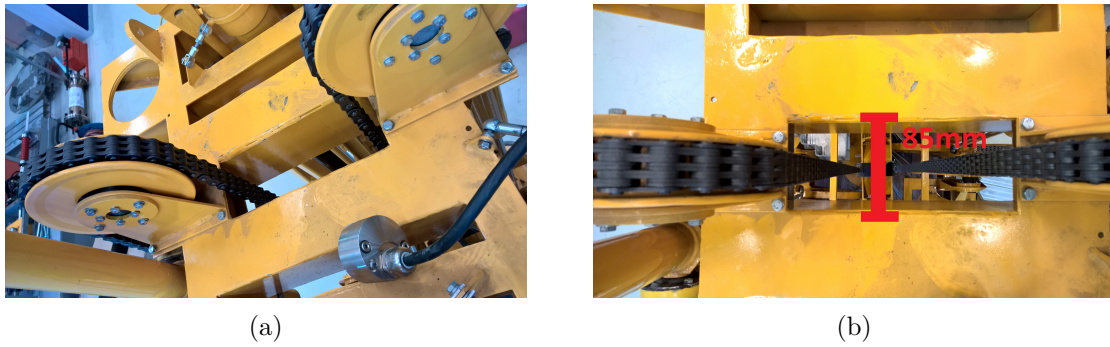


Figure 7.2: The top frame of the CMC with the rack and pinion system removed

On the scale model it was therefore decided to mount the stator on top of the structure by use of a bracket. Because of the distance between the crown block in its bottommost position and the top of the stator is larger than the length of the slider a link between the crown block bracket and the slider has to be created so that the top of the slider is always at least 25 mm above the top of the stator 7.3. Although the length of this link is made shorter by the bracket, swivel joint and force transducer that will be reused it is not enough to fasten the slider directly to the force transducer. The length of bracket, swivel joint and force transducer is approximately 220 mm. By looking at figure 7.4 it can be seen that when the top of the slider is 25 mm above the top of the stator then the distance between the bottom of the slider and the top of the force transducer is approximately 48 mm, which is the minimum length between the slider and transducer. (Measurements of parts etc etc!) Since the Tectis F2301 force transducer is fitted with male M12 thread an M12 coupling can be fitted which can be connected to an M12 threaded rod which is then connected to the slider through a M12 female to M10 male thread reducer. Since the stroke of the motor is 60 mm more than the calculated stroke of the CMC lifting cylinders, the precise length of the connection is not critical.

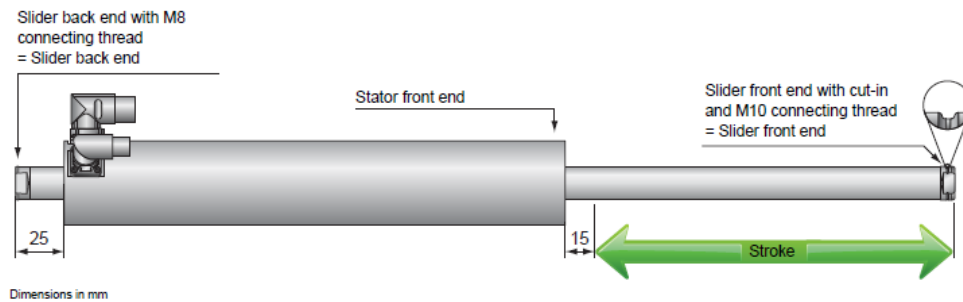


Figure 7.3: Stroke and slider connections

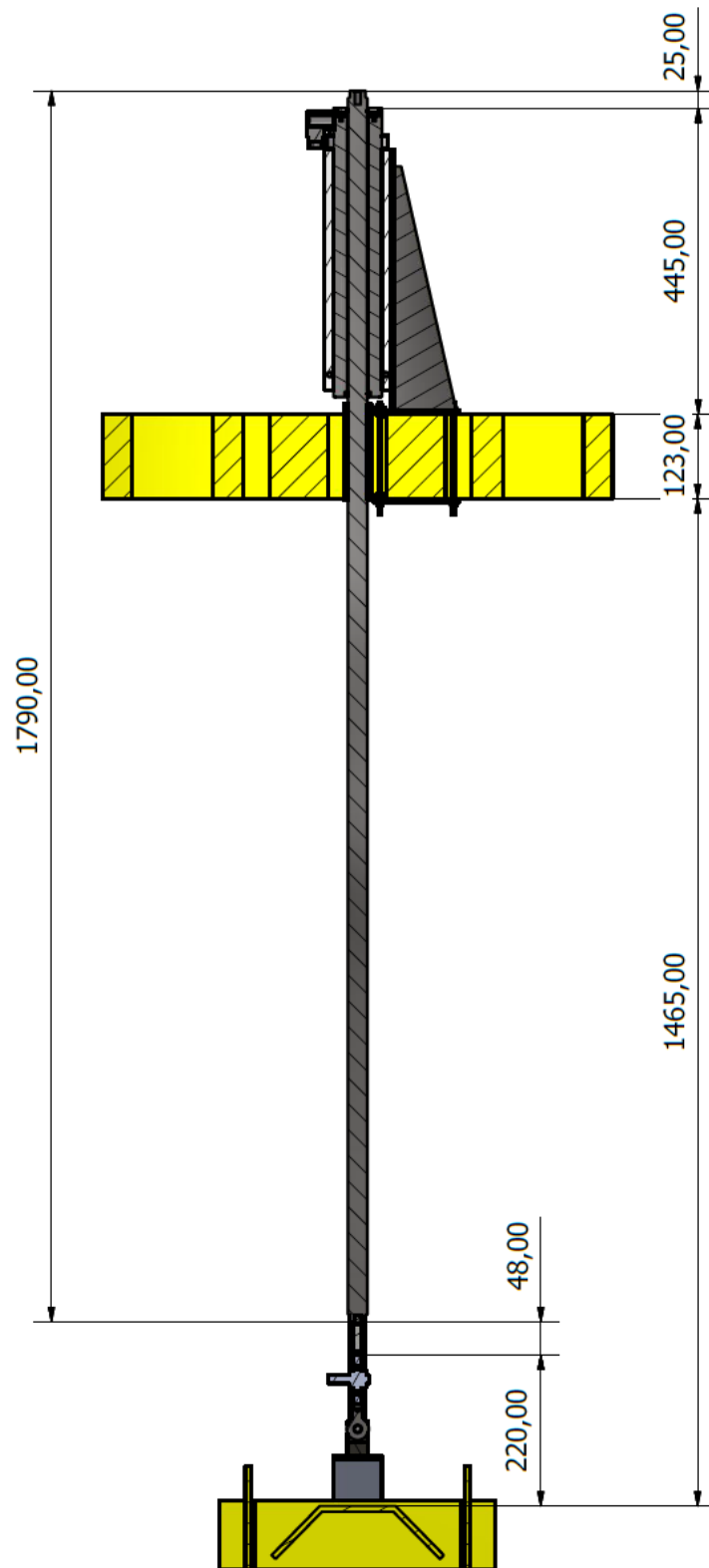


Figure 7.4: Dimensions of the system with lifting cylinders retracted and slider in its lowest position

7.2 Stator Mounting

The stator needs to be precisely mounted with regards to orientation in order to avoid unwanted forces in the slider which can cause wear on the stator [29]. In order to avoid modifying the CMC structure itself a type of bracket that will be clamped to the top of the CMC structure will be designed and constructed, bolt holes will be drilled in the bracket so that the flange can be fastened to it. Three

suggestions for the bracket are shown in 7.12a

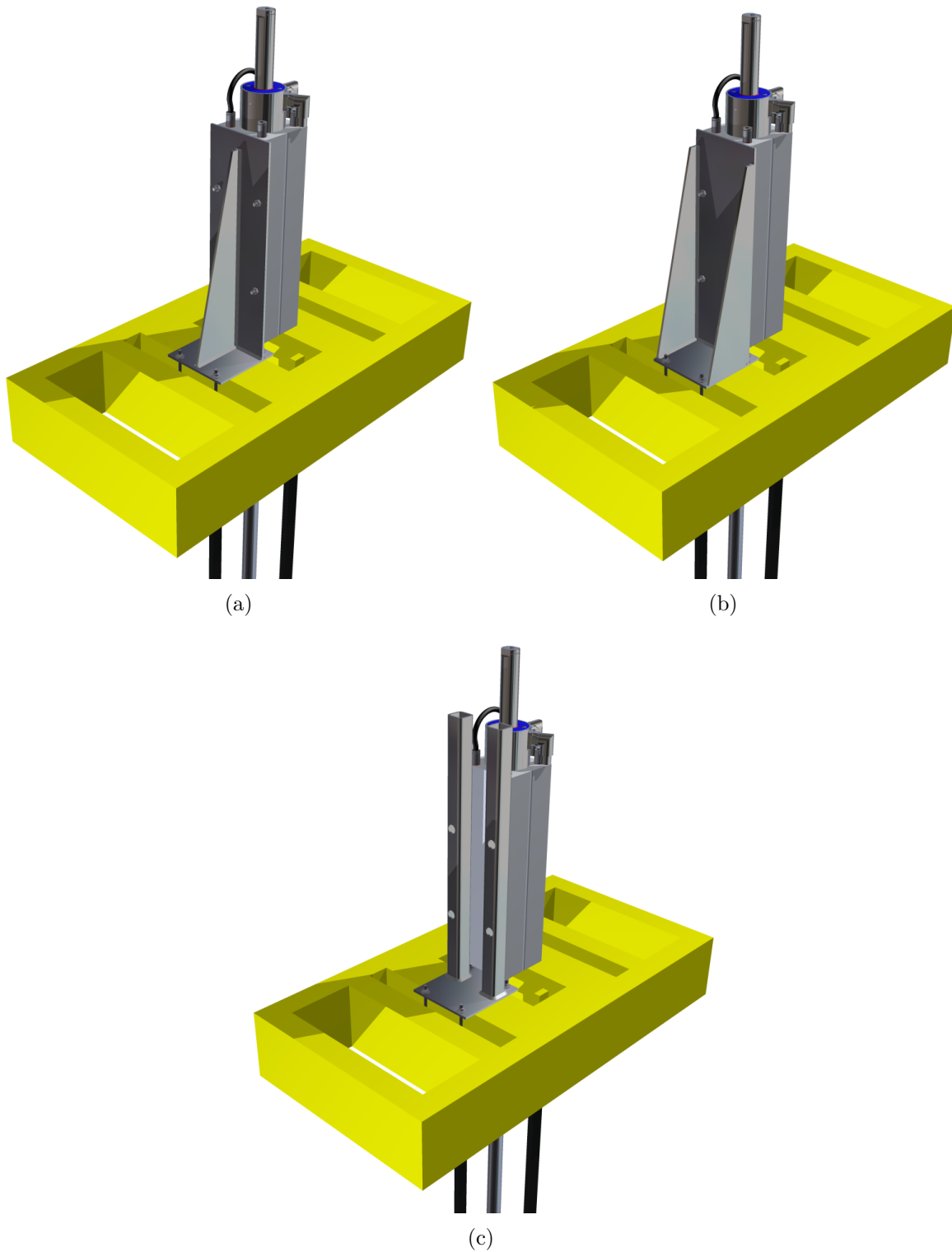


Figure 7.5: Suggestions for fastening the stator

It was decided that the bracket showed in 7.6 would be used because of its stiffness and ease of manufacturing. It will be clamped on the top frame by use of flat plates and 4 threaded rods. In addition to avoid modifying the CMC when fixing the linear motor it also makes it easy to properly position the linear motor in relation to the travelling block which is important to avoid wear and unwanted friction in the stator.

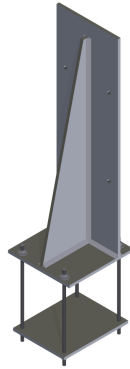


Figure 7.6: The chosen bracket

7.2.1 Finite Element Analysis of the Bracket

A simple Finite Element Analysis (FEA) was done of the bracket to make sure it could handle the force from the linear motor without too much deformation, which would be undesirable for the motor. The FEM analysis was done in ABAQUS/CAE 6.13. As the force from the motor originates from the center of the slider it will in addition to forces in z-direction also impose a torque on the bracket, see figure 7.7. The Inventor model of the bracket was exported as a surface model and imported into ABAQUS with plate thickness defined at 5 mm. Boundary conditions was applied at the bolt holes in the bottom plate, in reality the bracket also rests against the top frame of the CMC and washers will distribute the bolt forces more evenly, which means the stress at the bolt holes will not be realistic. The motor itself and the flange was not included in the simulation and the load from it was instead added directly to the bolt holes were it is fastened to the bracket, this is also a simplification as in reality the face of the motor flange rests against the bracket when regarding the torque imposed. The simulation was run twice, once when the motor is pulling up and once when it is pushing down. (WHY PLATE MODEL!)

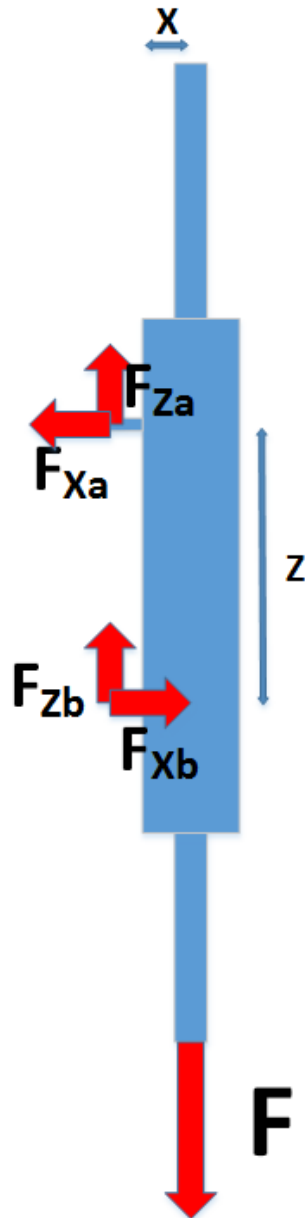


Figure 7.7: Forces in the motor and bracket

When the motor is pulling up, the force used in the simulation is equal to the maximum peak force the motor can deliver, with a safety factor of 1.5:

$$F = 1.5F_{max} = 1.5 \cdot -2162 = -3243\text{N} \quad (7.1)$$

The force is divided over four bolt holes, giving -811 N in each. The force from the torque imposed by the motor was calculated as follows:

$$F_{X_B} = \frac{F_{max} \cdot X}{Z} = \frac{3243 \cdot 0.05}{0.150} = 1081\text{N} \quad (7.2)$$

$$F_{X_A} = -F_{X_B} = -1081\text{N} \quad (7.3)$$

Where:

X = distance from center of slider to bracket

Z = distance from A to B

Divided by two bolt holes the force becomes 540.5 N and -540.5 N respectively.

When the motor is pushing downwards the direction of forces is changed however the magnitude is the same.

The resulting stress in the bracket can be seen in figure 7.8 and the deformation in figure 7.9.

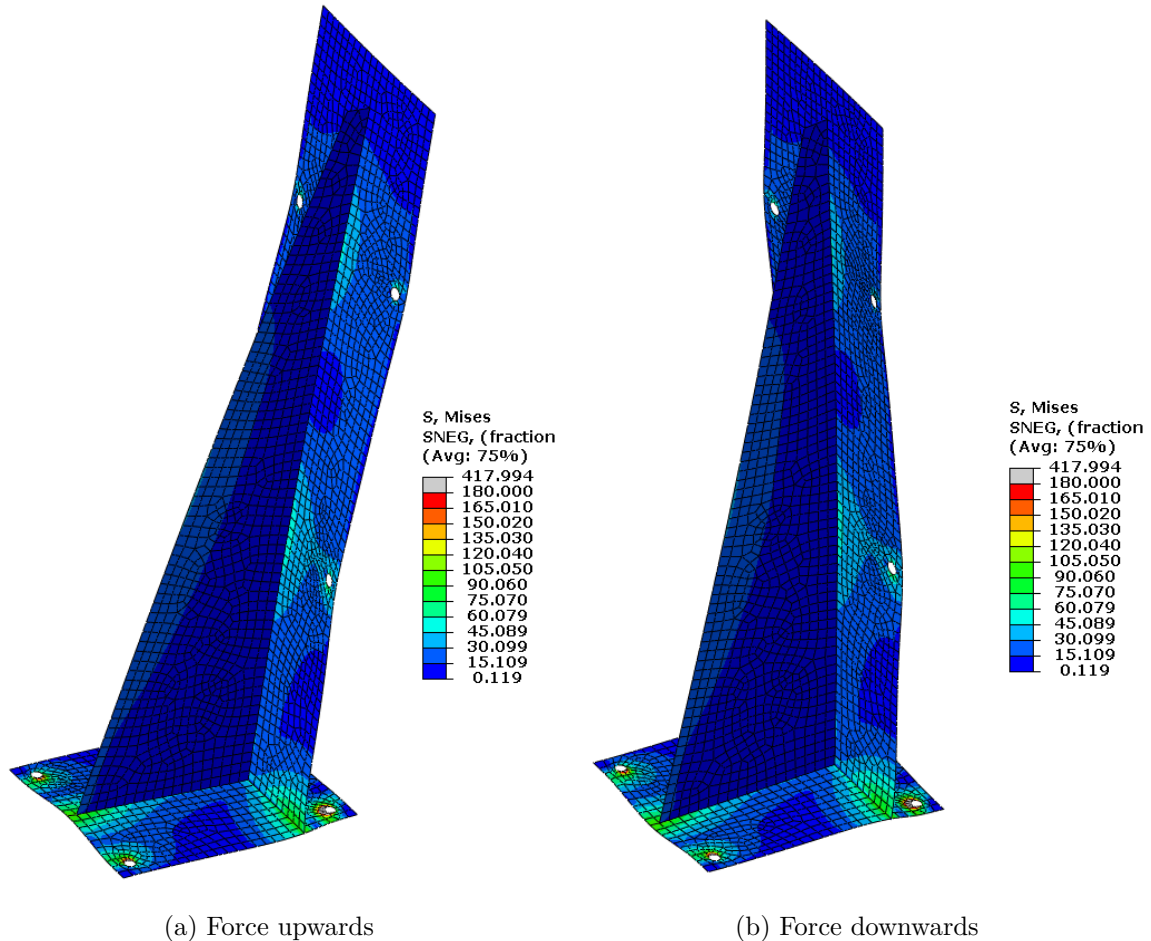


Figure 7.8: Stress in the bracket

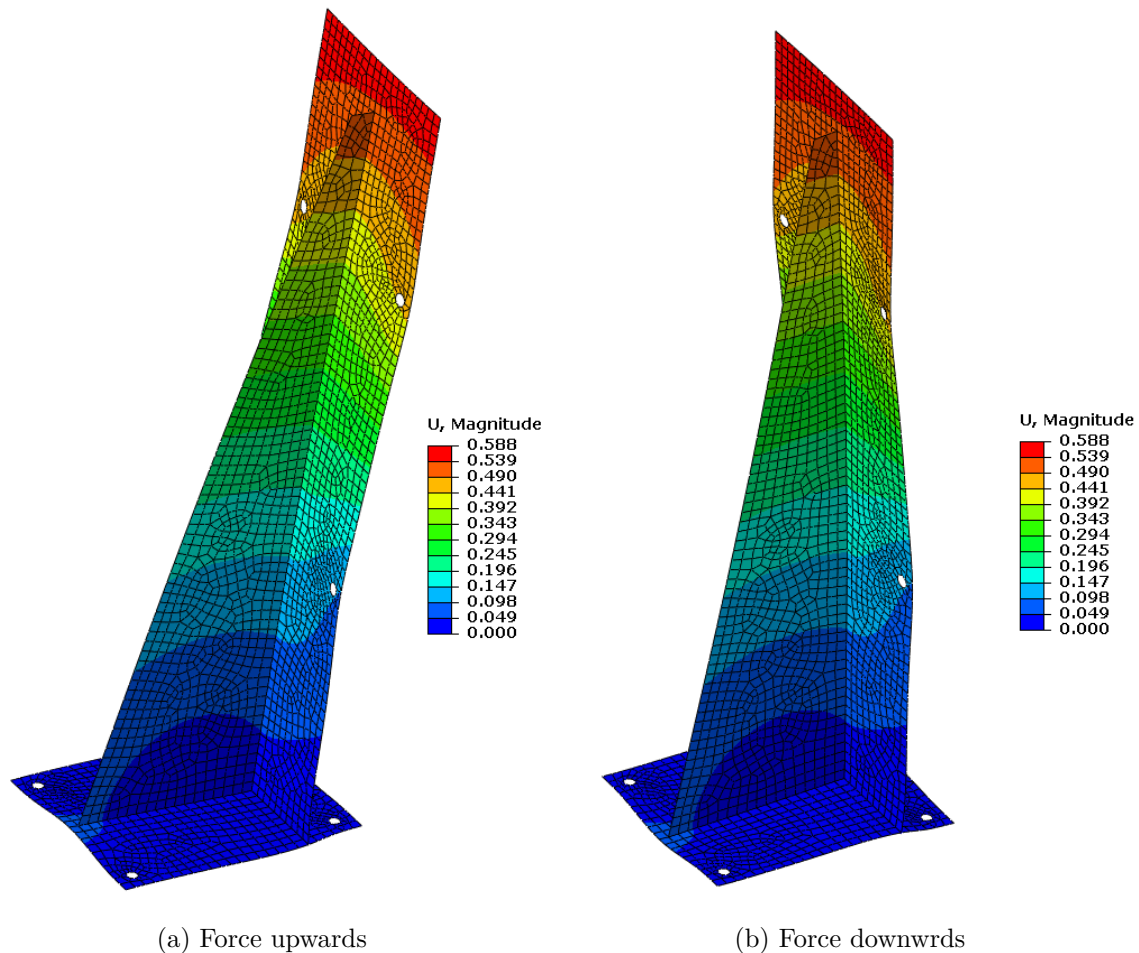


Figure 7.9: Deformation of the bracket

The FEA done here is a very simple analysis and not designed to give absolutely realistic results as some simplifications has been made, like the boundary conditions and removal of the motor and flange and adding the forces at the bolt holes. However it gives a good indication about the stress and deformation in the structure of the bracket. The deformation in the bracket is small and will likely be much smaller in reality due to the simplifications made in the simulation. Also the motor will most likely never be run at its peak force output, however the peak force could be relevant for future applications or tests, it also ensures that the bracket is not damaged if something goes wrong, it was therefore decided to design the bracket with the peak force in mind.

7.2.2 Fabricating the Bracket

Fabrication drawings were created of the parts and bracket assembly, see appendix E. The plates were cut out of a 5 mm steel plate using a cnc plasma cutter and then welded together, only so much welding cut be applied to avoid warping of the bracket. The finished bracket can be seen in figure ??

7.3 Transportation of CMC and Initial Setup

The scaled CMC model was currently residing in a warehouse in Vennessla where it had been since it was last used in 2013. Jan Andreas Holm offered to transport the model to the university, and after talking with Jan Terje Håkedal a date for transporting the model was set. 21st of April was the chosen date, our contact person at the warehouse had readied the model for transportation by wrapping it in plastic and helped loading it onto a car trailer. Jan Andreas Holm then drove it to the university

where it was unloaded using a forklift.

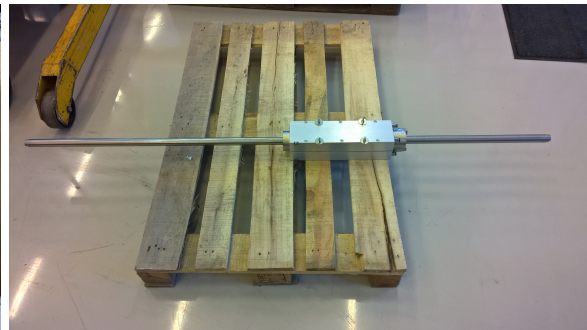
The scale model was not placed on the stewart platform right away as removal and fitting of equipment to the model would be easier with the model standing on the floor. In order to prepare the scale model for fitting of the linear motor the existing AHC system consisting of a servo motor and a rack and pinion had to be removed. In addition the wire encoder had to be removed to make room for the linear motor and would be refitted when the motor was in place.

7.3.1 Linear Motor Assembly

The stator, flange and cables for the motor was delivered to the lab at UiA on the 24th of April, the slider on the 27 of April. When receiving the packages its contents was inspected, ensuring no parts for the motor was missing or damaged during transit. The flange was fastened around the stator and the bolts tightened to the required torque. Holes were drilled in a pallet for use as temporary mounting for the motor during run-in and testing, the flange was then bolted to the pallet using threaded rods, washers and nuts, as no bolts were long enough. The slider was then cleaned, lubricated and inserted into the stator.



(a) The stator, flange and cables arrived in the lab



(b) The linear motor mounted to a pallet

7.3.2 Siemens S120 Drive System and Control Cabinet

Narve Kristiansen and Arve Johnsen from NOV arrived on the 29th of April to help configure the Siemens SINAMICS S120 drive system. It was decided to upgrade the CU320 controller to a newer version so that the newest firmware could be installed. When installing the new firmware it was discovered that the motor module was too old to receive the new firmware, and because it could only deliver 3 ampere continuous current it was decided to upgrade it to a newer 9 ampere version so the motor could be run to its full potential. After making some calls Narve Kristiansen was able to acquire a new controller and motor module for the next day. Although LinMot [®]advertises that The p10 motor "can be controlled by third-party servo drives without any difficulties" [14], the reality was a little more complex, as little to no information about the using the LinMot with the Siemens drive system exist, the only information available was a guide written in German. After the second day of working on the drive system the motor was moving, but not in the way we wanted. It was discovered that there was a lot of noise in the signal coming from the motor encoders and the result was that the motor would only move a short distance before an error message was received saying there was too large difference between the speed set-point and the actual speed of the motor. Eventually this was solved by experimenting with the zero mark distance parameter in the drive, increasing it gradually from 40mm to 1000mm solved the problem. The motor was then running fine when giving it a velocity set-point either in the drive or from the joystick on the control cabinet, however the actual velocity of the motor had a slight deviation from the velocity set-point. The next week the SMC20 encoder module was upgraded from a version A module to a version G module procured by Arve Johnsen in hope of reducing the noise on the encoder signal and generally improving the running of the motor. After the new module was installed there was slightly less noise on the encoder signal, but most important the zero mark distance could be reduced to its original value of 40mm which improved the

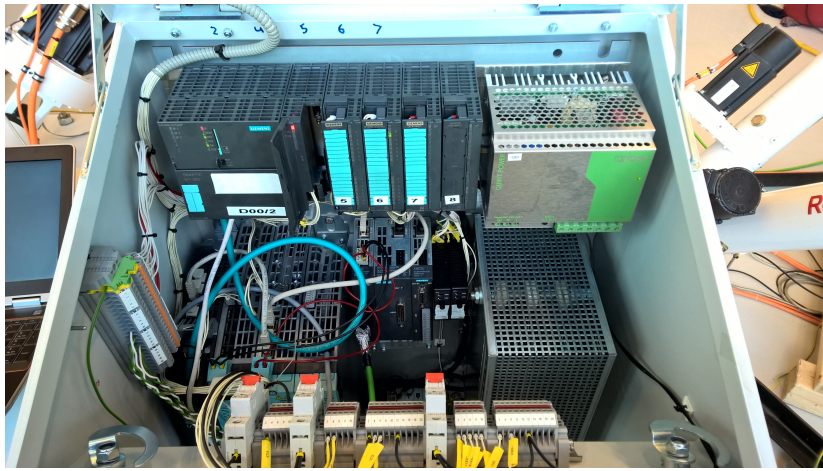
motors performance when running with a velocity input.

Although the encoders in the motor is supposed to be able to monitor the position of the linear motor, no solution for this was found when setting it up with the Siemens drive system and it was decided not to spend precious time trying to figure it out, and there was too much noise on the velocity signal to use it to calculate a position. The motor itself also contains hall sensors for measuring position but they were not supported by the drive. An external encoder will therefore have to be used if the position of the linear motor is to be measured and used for control.

An overview of the drive controller structure can be seen in appendix C.

The linear motor was now ready to be tested and mounted on the scaled CMC model.

Except for the swapped out modules no further changes were needed to the control cabinet which can be seen in figure 7.11a and 7.11b. The PLC and the power supply can be seen in the top of the cabinet, and the drive system components in the middle. The terminal blocks are for connecting the various sensors and wire encoder. The drive component to the far left is the CU320 controller, next is the smart line module responsible for supplying power to the motor module to its right. To the right of the motor module is a braking module which was not used in this project, to its right are the SMC20 encoder seen with the green encoder cable plugged into it. To the far right is a braking resistor which also was not used in this project.



(a)

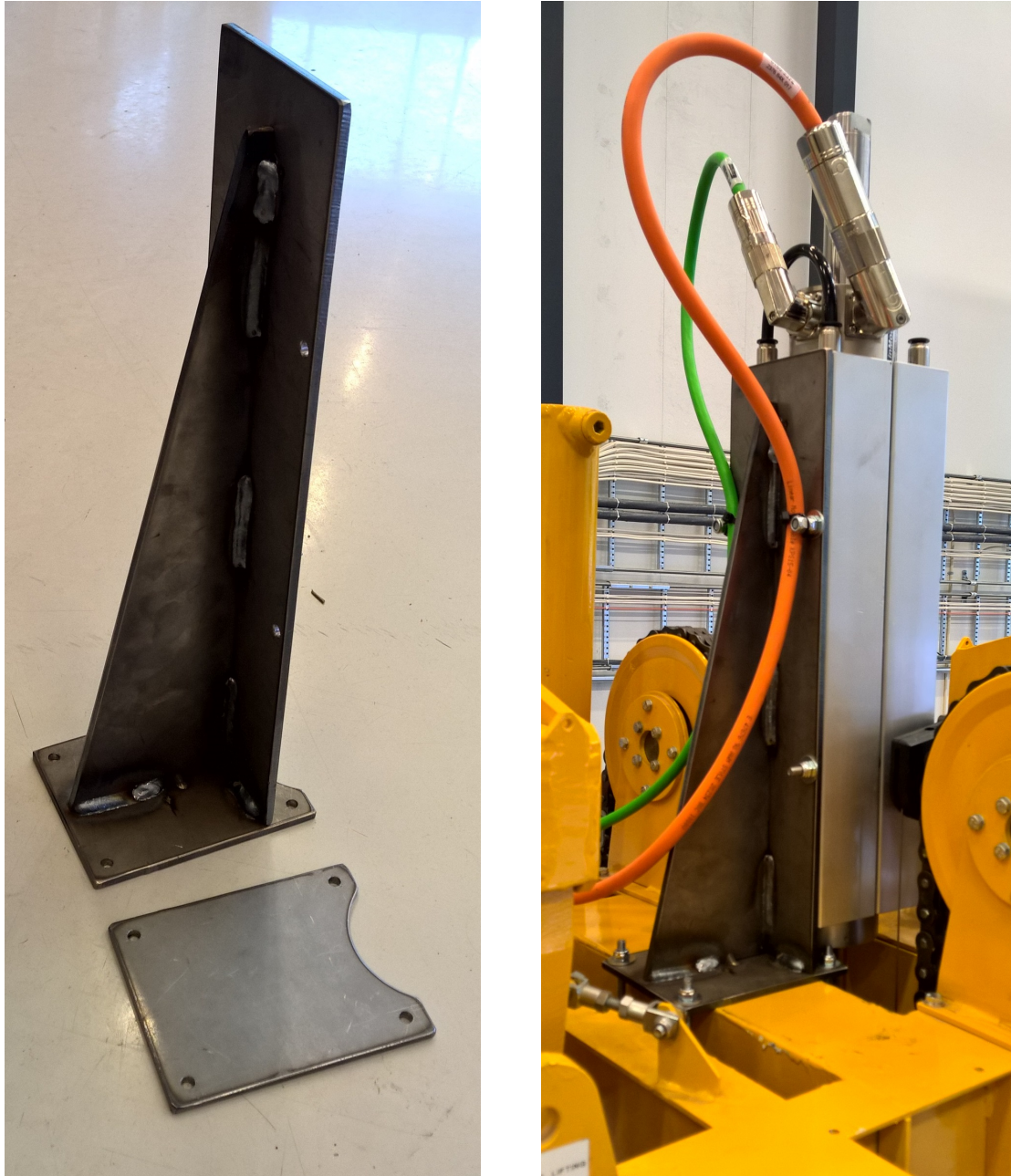


(b)

Figure 7.11: The control cabinet

7.4 Mounting of Equipment on CMC and Placement on Stewart Platform

The stator of the linear motor was bolted to the bracket and the bracket was then bolted to the top frame of the scaled CMC. A fabricated M10 to M12 thread adapter along with a 120mm threaded rod was used to attach the slider to the existing swivel joint on the crown block.



(a) The fabricated parts

(b) Attached to the CMC

Figure 7.12: The fabricated linear motor bracket

The draw wire encoder was placed to the side opposite the linear motor with the point where the wire exits close to the middle of the linear motor slider. The bolt that holds the swivel bracket was swapped for a longer one and the end of the wire was fastened to it so that it was completely parallel to the slider. The arrangement can be seen in figures 7.13a and 7.13b.



(a) Wire encoder on top of the CMC



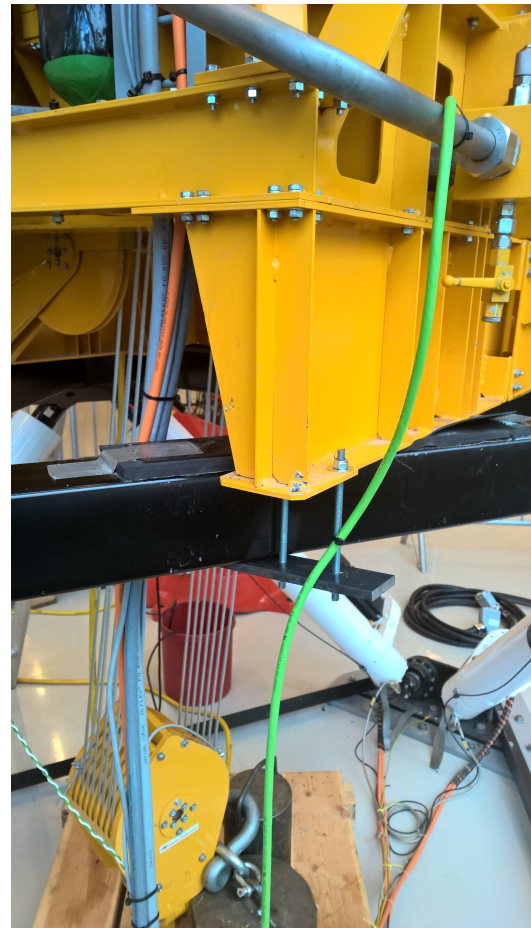
(b) Wire end fastened to crown block

Figure 7.13: Draw wire encoder

The fully assembled scale model CMC system was lifted onto the Stewart platform by Eivind Johansen using the overhead crane in the lab. The markers used for the model two years ago was still attached to the Stewart platform, it was measured that they were still in the right place, which they were. The model was then lined up with the markers and fastened down with pieces of flat steel and threaded rods, seen in figure 7.14a and 7.14b, note the green encoder cable being routed far from the orange power cable to try and minimize the encoder noise.



(a)



(b)

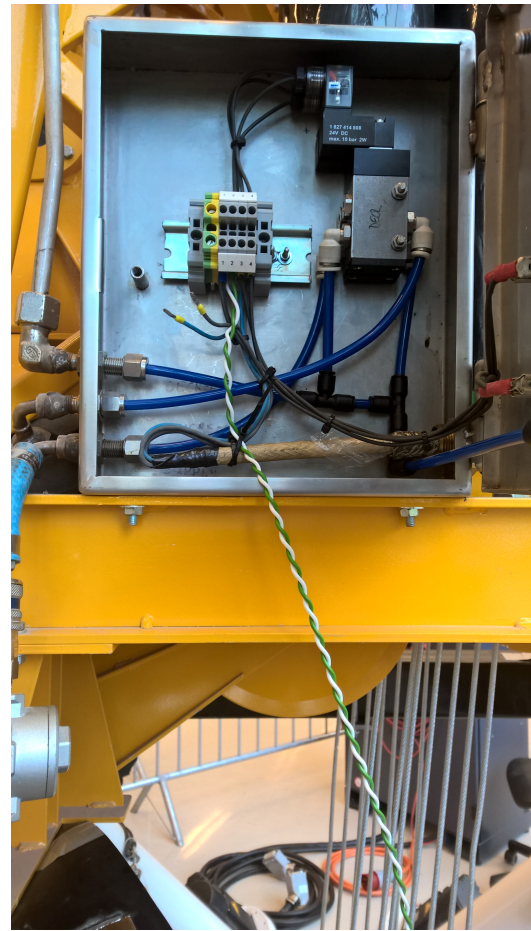
Figure 7.14: Scale model CMC fastened to the Stewart platform

The Motion Reference Unit (MRU) had to be mounted on either the CMC or the Stewart platform in order to measure the wave motion the CMC is subjected to. It was chosen to fasten it to the Stewart platform directly as this seemed to be the easiest solution, however there was no bracket for the MRU available. For fastening the MRU to the Stewart platform a plate was therefore manufactured to which the MRU was bolted, the plate was then bolted to existing holes on the top of the Stewart platform, see figure 7.15a. The location of the MRU is not important as the Stewart platform is only exhibiting heave motion.

The electrical cables from the CMC, which includes electrical wires from the sensors, wire encoder and air cabinet were connected to the terminal block in control cabinet. When trying to fill the APV's for the first time the valves who let air in and out was not working, it was discovered that they were not getting power from the control cabinet so a new wire was installed in a temporary fashion as seen in figure 7.15b.



(a) Fastening of MRU to the Stewart platform



(b) The CMC air valve cabinet

Figure 7.15

Water for cooling the linear motor was supplied from a tap nearby through a garden hose with a connection to a 5mm tube which connects to the fittings on the linear motor flange. The return tube goes to a drain close to the Stewart platform. Both tubes were fastened along the side of the scale model CMC structure.

The final system with everything fitted and ready for testing can be seen in figure 7.16

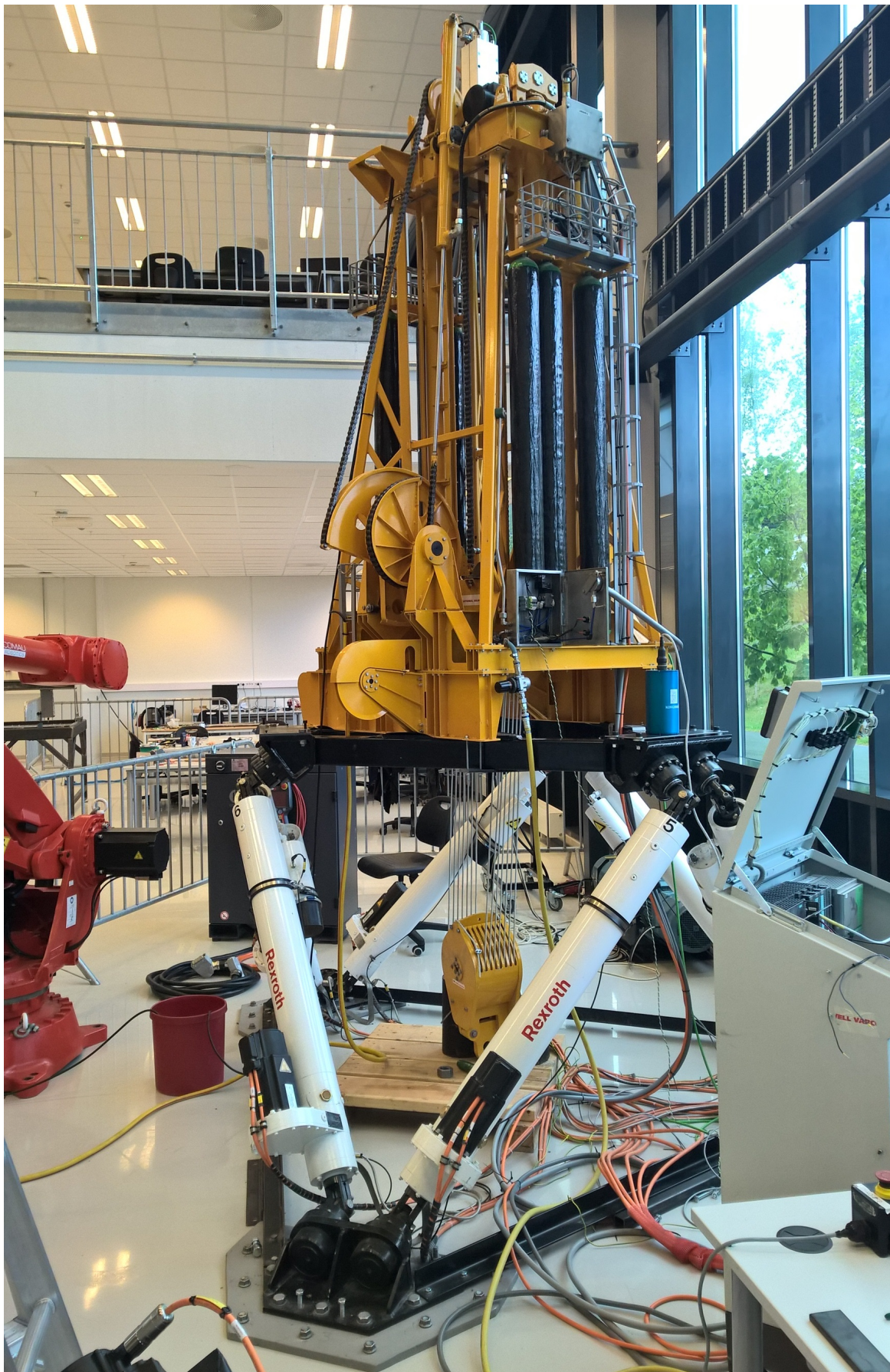


Figure 7.16: The scale model CMC on the Stewart platform ready for testing

7.5 PLC Programming and HMI - CMC with Linear Motor

Programming the Siemens PLC system is done using the Siemens SIMATIC Step 7 software. The PLC program code is commonly housed in different blocks which each has a specific function, and are then combined in a structured manner to perform the desired task. The blocks can be split into different categories [30]:

- Organization Block (OB) - Blocks that manage the control system and acts as interface between the program and the operating system. Numbered after their function, with the operating system calling OB1 cyclically and with this call starts cyclic execution of the user program, the other OBs being e.g. interrupt or event controlled.
- Function Call (FC) - A logic block "without memory", which means all calculation that happens within the block will be erased between each cycle. Typically used to return a function value to the calling block, e.g a math function, or to execute a technological function, e.g. a single control function.
- Function Block (FB) - Has basically the same properties as the the FC block, but "with memory" so data can be stored from one program cycle to the next by saving it in an instance data block. Used to program frequently occurring complex functions that are always executed when the FB is called.
- Data Block (DB) - Blocks that are used to store data. Two types:
 - Instance DB - Assigned to certain FBs, if an FB is called three times there are three instances of this DB.
 - Shared DB - Can be accessed by all other blocks.
- System function blocks(SFB) and system functions (SFC) - Blocks that are integrated in the CPU and allows access to important system functions.

An illustration of the PLC block hierarchy can be seen in figure 7.17.

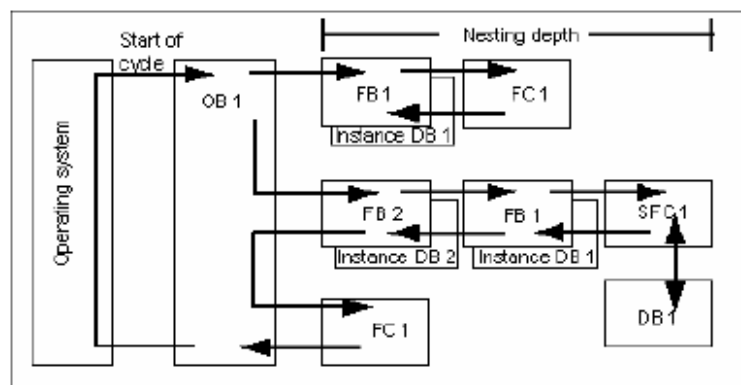


Figure 7.17: Illustration of the PLC block hierarchy [30]

It was decided to use the existing PLC program which was provided by NOV and modified by Aalerud and Klevmo in their thesis [5]. The program was initially written for a guide line winch and was modified to use with a servo motor and rack and pinion. Since this is quite a different setup compared to the linear motor quite a lot of modifications had to be carried out in order to make it function as desired.

The blocks in the 300x range was made by Aalerud and Klevmo and consists of:

- FB3001 - Measurement function block which contains the data interface for the MRU, wire encoder and sensors. It is made up of standard block which acquires and estimates the data from the various sensors.
- FB3002 - Luge friction force estimator function block which estimates the friction in the system.
- FB3003 - CMC Control function block which contains the feedback control and sets a torque setpoint for the motor based on the feedback control and the FB3002 feed forward friction estimator block, which is housed in this block.

The blocks are housed in the FC3 fast cycle function block inside the OB34 organization block, the structure of the program can be seen in 7.18 In addition the FB1000 block is used to log the data from the system.

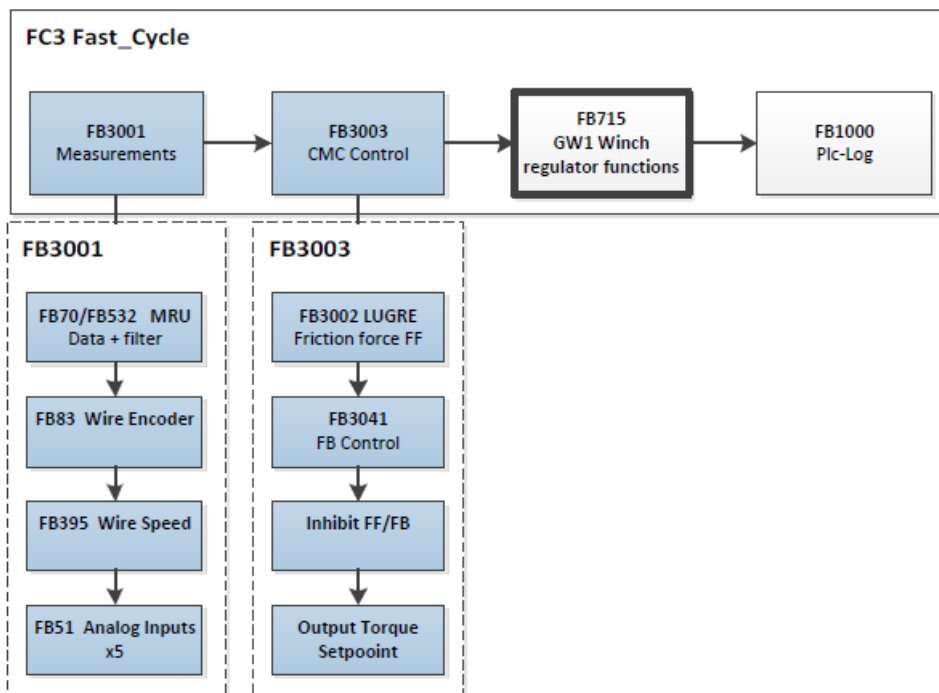


Figure 7.18: Structure of the PLC program before any modifications were made [5]

The measurement function block was kept as it was except for disabling the sensors that were not present on the model. The Luge friction force estimator function block was also kept as it was. The CMC control function block had to be extensively modified in order to control the linear motor instead of a servo motor with a rack and pinion. The old heave compensation control system was removed and replaced with the chosen cascade structure controller from the control system section 6.1.4. The position part of the controller consists of the measured wave from the MRU which is inverted and compared to the position of the crownblock measured by the GT001 wire encoder, the resulting deviation is then multiplied by the position gain. The inverted wave velocity is then added as a feed forward, yielding a velocity reference for the linear motor. It was decided to not use a controller block for this part as it was simpler to just use a multiplier block. However for controlling the force output of the linear motor a CONT_C PID controller block from Siemens standard library was used. The setpoint is the velocity reference from the position controller and feedforward, the feedback is the velocity of the crownblock measured by the GT001 wire encoder. The resulting force reference is then sent to the Siemens drive system. Logic was added so it was possible to switch the drive to force mode, receiving a force setpoint instead of a velocity setpoint, when the heave compensation controller was active.

In order for the system to compensate around its stabilizing point without having to reset the GT001 wire encoder value, a function was added which saves the current GT001 value as a starting point and subtracts it from the GT001 value during operation which then equals the position feedback sent to the controller.

A motor with gearbox and rack and pinion is principally quite similar to a motor driven winch with a drum and wire, however the linear motor has little in common with either of them. Therefore changes had to be made in other areas of the program as well. To get the different modes to run certain conditions that were not longer relevant was removed and calculations dealing with gear friction and wire tension etc. was removed or bypassed in order to use the existing setup for sending values to the drive system.

The PLC program includes two modes for controlling the linear motor:

- Normal Mode - The system is active and the linear motor can be controlled by sending a velocity setpoint using the joystick mounted on the control cabinet.
- Heave Compensation Mode - The joystick is deactivated, the linear motor switches to force mode and the controller described earlier becomes active and assists the CMC in compensating for wave motion.

As the joystick still sends a velocity setpoint to the drive when it is not in use, which will be 0 meters per minute (m/min), this causes the linear motor to try and hold the slider in place, resisting any movement of the slider by applying force in the opposite direction. This is highly undesirable as it will ruin the performance of the passive CMC if waves are present when the linear motor is in normal mode. The solution was to always keep the drive in force mode and instead add logic which switches it to velocity mode only when the joystick is being used. However caution has to be taken in order not to use the joystick when in normal mode and the passive CMC is working. There is no risk of physical damage if this was done as the force the linear motor can deliver is limited but it would severely impair the performance of the passive CMC.

The existing FB1000 block which was used to log data from the PLC will also be used in this project to log the performance of the system.

A human machine interface (HMI) was created in WinCC in order to operate the system, to keep track of important system parameters and to check the performance. The program was based on earlier work by Aalerud and Klevmo which in turn was based on a winch test program [5]. A screenshot of the screen used can be seen in figure 7.19

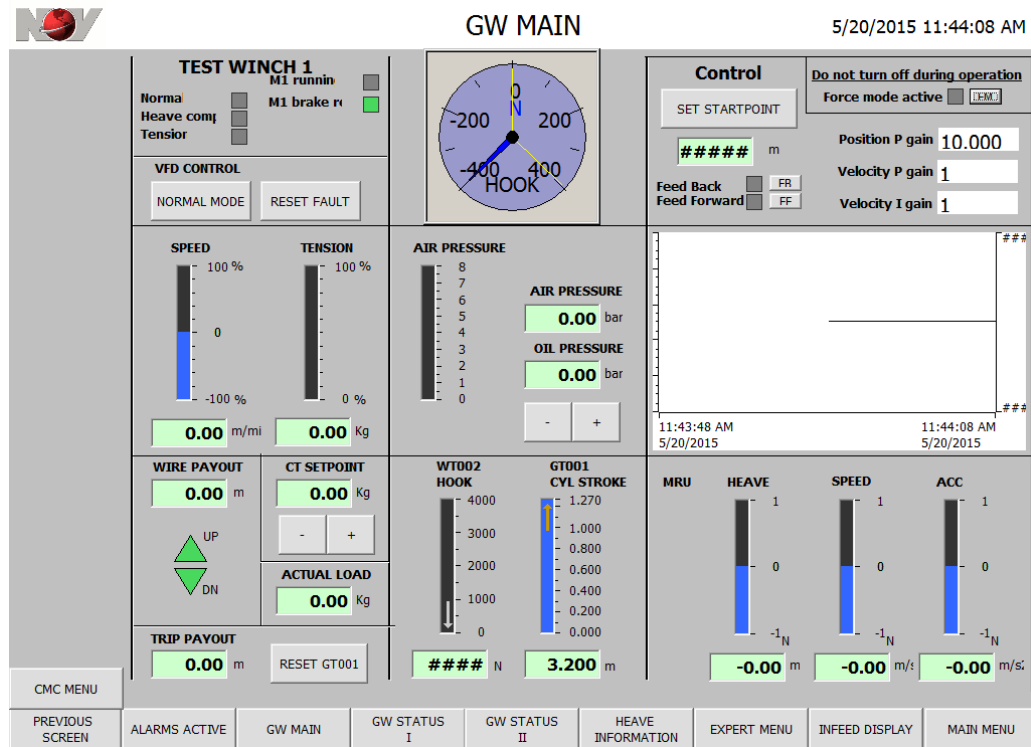


Figure 7.19: Screenshot of the HMI screen for the CMC and linear motor system

Had the scale model CMC been used further in the thesis there would certainly have been changes to both the PLC program and the HMI as testing went on, however as it was decided not to use the scale model CMC further in the thesis at this point, the development ended here. The programs were however modified and used for the linear motor alone.

The main section of the PLC program with the measurement and control blocks for the CMC with linear motor can be seen in appendix ??

7.6 Linear Motor Active Heave Compensator System

When during the start of the testing phase it was discovered that the scale model CMC was not working properly, 8.2, it was decided to use the linear motor as an AHC by itself. This however required several modifications to the system. The MRU would still be used to measure the heave motion of the stewart platform while the draw wire encoder would measure the position and speed of the load hanging from the end of the linear motor slider.

First of all scale model CMC had to be lifted off the stewart platform, in order to do this all electrical connections, tubes for water cooling etc. had to be disconnected. The CMC model was then lifted of the stewart platform and onto a pallet. The linear motor was then removed from the model along with the draw wire encoder, this included disconnecting the encoder wires from the junction box on the CMC model. Longer wires were then soldered to the existing wires so it could be connected directly to the terminal block in the control cabinet.

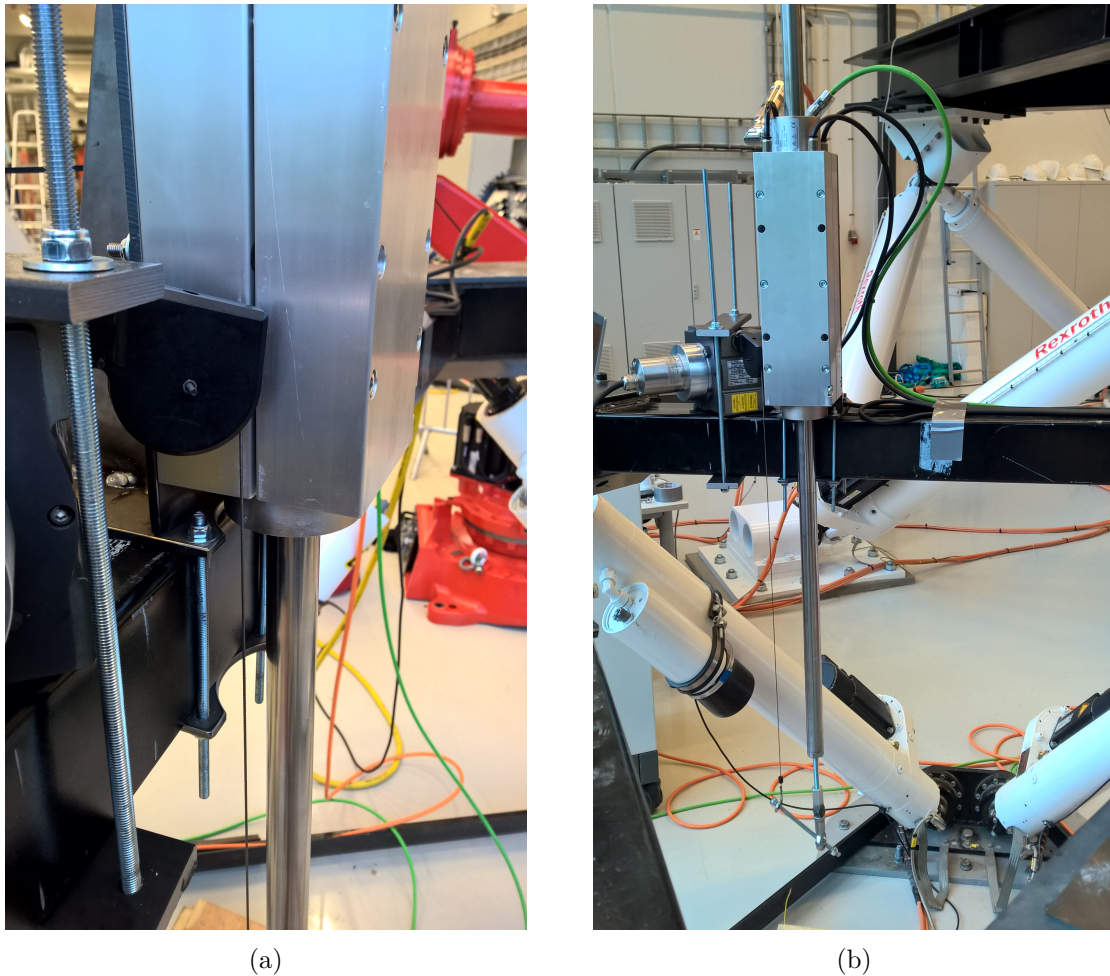
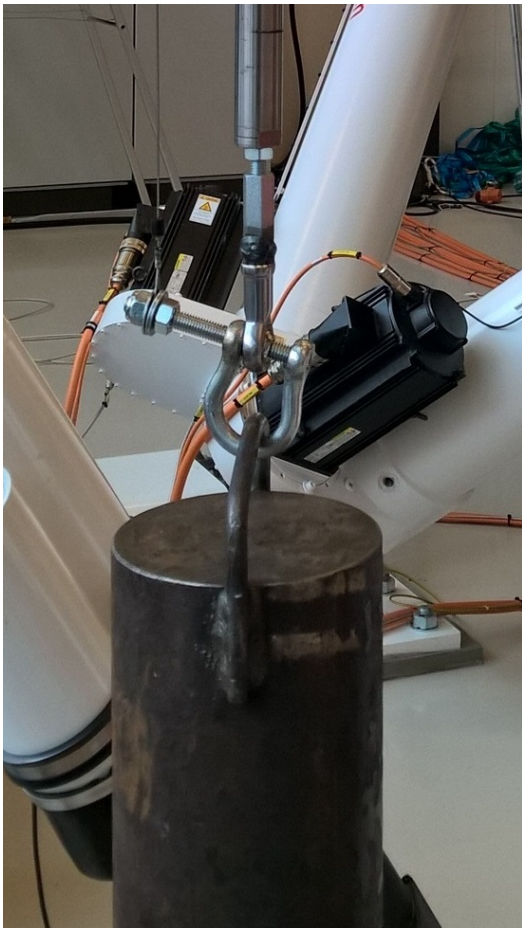
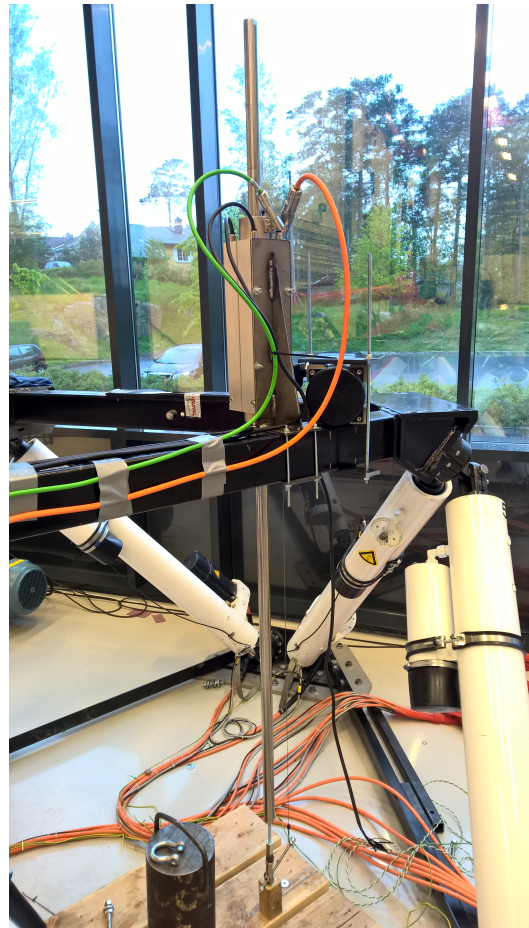


Figure 7.20: The GT001 wire encoder measuring the position of the slider

Fortunately the bracket for the linear motor just barely fitted around the one of the beams on the Stewart platform, it could therefore be mounted without any modifications. The draw wire encoder was placed beside it seen in figure 7.20, angled so that the wire could run parallel to the linear motor slider, it was held in place by the pieces of flat steel and threaded rods earlier used to fasten the scale model CMC to the Stewart platform. In order to hang a load from the slider the swivel bracket from the scale model CMC along with the M10 to M12 thread adapter and a short M10 threaded rod was used as shown in figure 7.21, the load could then be fastened by a threaded shackle. All the electrical connections were made, the water cooling was connected and then the system was ready to run.



(a) Adapter for attaching the load



(b) The linear motor AHC system ready for testing

Figure 7.21

7.7 PLC Programming and HMI - Linear Motor AHC

The most important part when modifying the PLC program for running the linear motor as an AHC by itself is the linear motor's mode of operation. While having the linear motor hold the slider in place when it is not heave compensating was very undesirable when it was used with the passive CMC, it is now required in order for the system to work. The program was therefore changed so that the linear motor always operates in velocity mode instead of force mode so that when there is no input to the motor it will hold the slider in place at 0 m/min. This means the output of the controller has to be a velocity setpoint instead of a force setpoint, which means adjusting the controller output from m/s, which is the unit used by the wire encoder and MRU, to m/min and multiplying with a factor so the velocity value in the PLC matches the velocity value in the drive. If the controller is turned off the velocity setpoint is set to 0 m/min so that the slider is held in place. As the motor is to be run in velocity mode there is no way of compensating for the friction and cogging forces directly in the PLC. The drive will regulate the force needed to maintain its velocity setpoint by itself and therefore it is not really necessary either.

The cascade controller was later swapped out for a PI position controller, though it still exists in the program. The PI position controller uses the inverse wave heave amplitude as setpoint and the slider stroke measured by the GT001 wire encoder as feedback.

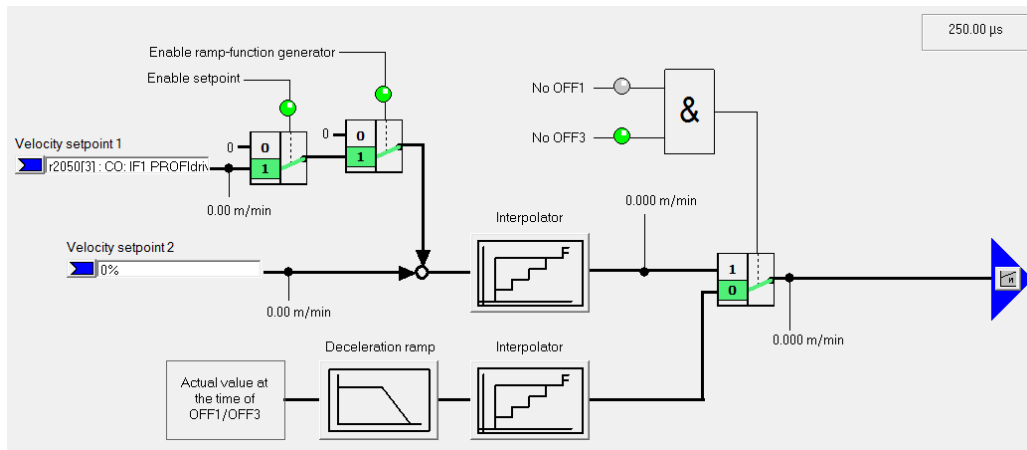


Figure 7.22: The controller in the drive responsible for regulating the force required

It was decided to add a limiting function to limit the value of the velocity setpoint to an adjustable value. Limiting the velocity can also be done in the drive setup, however it was more appropriate to implement it in the PLC program so the limit could be adjusted easily from the HMI. The limit was set close to the maximum velocity of the waves the system would encounter. This was done so that when the controller is activated when the end of the slider is far away from its setpoint, i.e. the wave is at its peak and the slider is at its starting position, the motor will make a controlled move to the right position and start heave compensating. However, the integral part of the controller which improves its performance will cause the system to become unstable in this situation. A function was therefore made which only activates the integral part of the controller when the deviation from setpoint is less than three millimeters. Though this value was suitable for this system it might have to be changed if used with the scale model CMC for example.

It was discovered when starting testing that the MRU was not working, with limited time left it was decided not to use it in the thesis and instead use a MRU simulator which was included in the PLC program. Variables were therefore created so that the simulator could be controlled from the HMI.

The HMI was also modified for the linear motor AHC, though in retrospect this is probably how the screen for the scale model CMC and linear motor would have ended up also, with some minor differences, if work on that had continued. Screenshot of the HMI screen can be seen in figure 7.23. It includes buttons for toggling the MRU simulator and heave compensation controller, setting the starting point and resetting the GT001 wire encoder. In addition there are interfaces for the controller gains, the parameters of the simulated wave and the velocity limit, while also showing the velocity setpoint and actual velocity of the linear motor. The most prominent feature of the HMI however is the trending graph window in the center in which the simulated wave, the slider stroke and also the deviation between the two are plotted continuously. These values as well as the two velocity variables is updated every 100 ms compared to every 500 ms for all other variables.

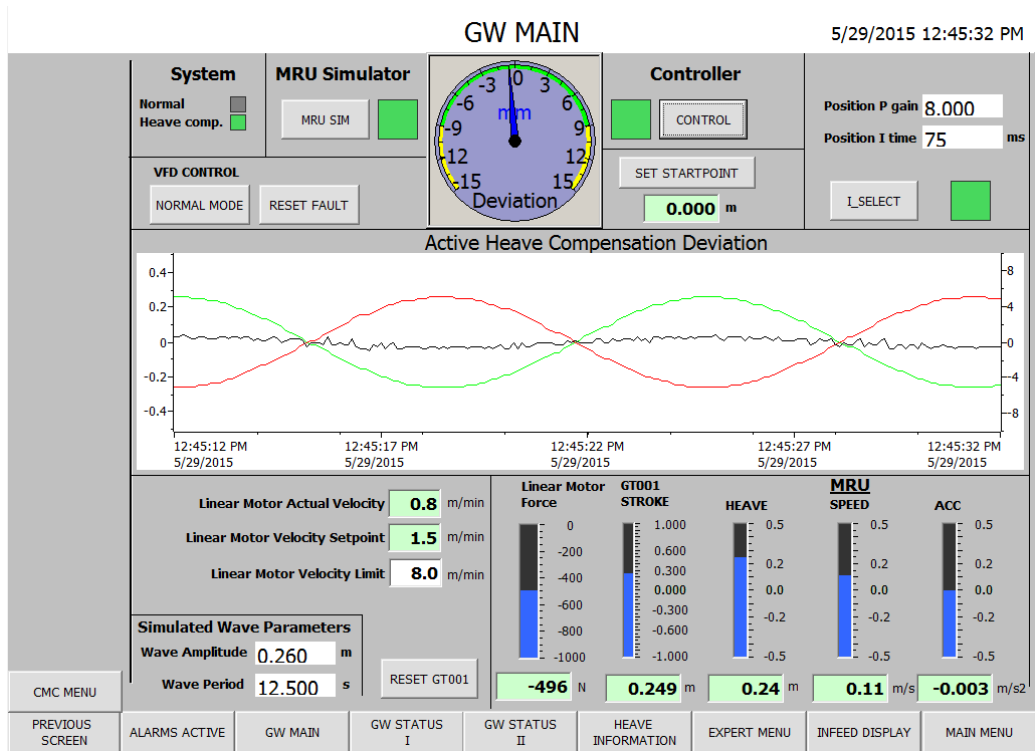


Figure 7.23: Screenshot of the HMI screen for the linear motor system AHC system

The main section of the PLC program with the measurement and control blocks for the linear motor AHC can be seen in appendix B

Chapter 8

Testing

8.1 Testing Scenarios

For simulating a drill string hanging from the compensator two main scenarios were initially looked at:

- Fastening a drill string made to the hook of the scaled CMC and bolting it to the concrete floor in the lab using an expansion bolt. This method would virtually lock the crownblock in place when the CMC is subjected to heave motion, whether or not the active system is turned on, the only movement coming from the deformation of the drill string, which is dependant on the material and structure of the drill string. The advantages of this solution is that it is easier to measure the WOB, disadvantage is that it requires a fabrication and instrumentation of a drill string and drilling of a hole under the stewart platform.
- Hanging a load from the hook of the scaled CMC in the form of a weight of a certain magnitude. The magnitude would be decided based on the pressure in the hydraulic system in the CMC, or vice versa. Initial simulations suggested a pressure of 6.1 bar when the load was 200 kg. The advantage is that it is simple and will visually show the performance of the system, disadvantage is that a heavy load hanging from wires is moving around when the active system is off.

However as the control system is based on measuring the position of the crownblock the second method is the that will be used, the performance will then be defined as the position of the crownblock compared to the wave amplitude and the resulting deviation.

The stewart platform will be configured to create heave motion similar to the waves used in the simulation, testing will be done with both the passive system alone and the passive and active system together in order to clearly show the effect of the AHC.

8.2 Initial Testing

When running the system for the first time no load was attached to the hook and the air pressure was slowly increased in order to move the main lifting cylinders out until the system stabilizes at the cylinders approximate mid-point. As the pressure increased it became clear that there was a lot of friction in the cylinders, at around 6.5 bars the friction was finally overcome. However as the pressure was much higher than what was required to stabilize the system the cylinders simply moved to their fully extended position. Air was released to relieve the pressure until it reached 1 bar and the cylinders still had not retracted. In order to try and retract the cylinders a ~ 120 kg load was attached to the hook and in addition the linear motor was used to push the crownblock down with a force of 750N, this then caused the cylinders to retract. The load was kept attached and by help of the linear motor and increasing and decreasing pressure when extending and retracting respectively the cylinders performance increased somewhat after a while but nowhere near enough to be able to do realistic tests of the system. From visual inspection of the cylinder movement and the movement

of the crownblock it suggested that only one of the cylinders was sticking. To test the cylinders the tie rods connecting the pistons rods to the crownblock was disconnected and pressure in the APV's increased until movement was detected in the cylinders. The first cylinder extended at around 2 bar, while the second cylinder had yet to extend at around 4.5 bar. By applying some external force to the second cylinder it was possible to move it approximately 15 cm before getting stuck again. The conclusion was that scale model CMC was not suitable for testing with the linear motor due to the second cylinder not working properly.

Since the linear motor is the important part of the thesis it was decided to use it as an AHC by itself, this required modification of the equipment and software and is described in 7.6.

Initial testing also revealed that no data was being received from the MRU, as this MRU had been used before in this setup in theory it should work by simply connecting it to the PLC however this was not the case. After some time trying to get it to work it was decided to not use too much time on diagnosing the fault as time was running out, and instead use the MRU simulator included in the PLC program. Another alternative would be to send values from the stewart platform to the PLC, however this was deemed to time consuming to set up. A third option could be to procure a second draw wire encoder and fix the wire to the ground so it would measure the heave motion of the stewart platform. A second encoder was not available although some testing was done with the GT001 encoder fixed to the ground and simply using the wire speed as a setpoint. This showed promise, however with no feedback on the slider position the error was about 5% of the wave amplitude, which is impressive considering there was no position feedback. The wire encoder connected to ground scenario is shown in figure 8.2b

The initial testing of the linear motor AHC system consisted of verifying that the control system was working as intended, to reveal any potential problems that needed addressing and some rough tuning. One example that needed addressing is the need to limit the velocity of the motor close to the wave velocity, as the motor with load attached would not always have enough force to stop if the velocity was too high and would go into error and shut down, which caused the load to drop to the ground. Programming some parts of the PLC program as well as creating much of the HMI was therefore done in parallel with testing the linear motor AHC system as problems and solutions was discovered along the way.

8.3 New Testing Scenarios

As the system has changed quite a lot since the testing phase was planned an update of the testing scenarios was required. Since the stewart platform will not be used the waves will be generated by the MRU simulator on the PLC, however it can only generate sine waves. The system will be tested both with and without external load and the performance criteria will be the deviation from setpoint. The deviation is defined as the wave amplitude minus the linear motor stroke measured by the GT001 wire encoder. The load used will be a steel weight of approximately 45 kg fastened to the swivel bracket by a threaded shackle. The weight is a little heavier than what was desired, however it was the only alternative in order to test the system close to or at its maximum. The linear motor had no problem with it however the drive system struggled a bit. Data from the system will be logged from the PLC using PlcLog version 3.3 which allowed exporting the logs as comma separated value files (.CSV) which then could be processed in MATLAB. The test setup is shown in figure 8.2a



(a) The linear motor AHC test setup

(b) GT001 wire encoder fastened to ground

Figure 8.1

Four waves were used for testing:

1. 0.110 meters amplitude and 10.0 second period.
2. 0.260 meters amplitude and 12.5 second period.
3. 0.420 meters amplitude and 24.0 second period.
4. 0.500 meters amplitude and 32.0 second period.

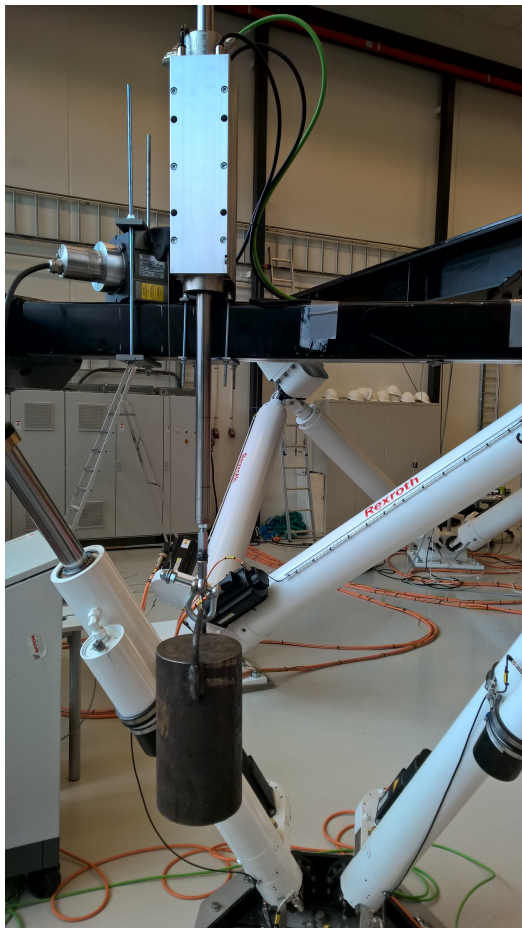
The two first waves were defined at the start of the project for the scale model CMC, while the two last waves were created just for the linear motor.

8.4 Performing Tests

The procedure for performing the testing of the linear motor were as follows:

1. Optionally: The 45kg steel weight was attached to the swivel bracket.
2. The system is started by pressing the normal mode button on the control cabinet which causes the drive to activate and the motor can be controlled by the joystick.
3. The slider was moved into its starting position to avoid hitting the ground when moving, the GT001 wire encoder was reset and the starting point was set using the HMI.

4. The MRU simulator and control system is activated in the HMI, the linear motor will not start moving until the heave compensation is activated however.
5. The AHC button is pressed which starts a countdown until the system switches to heave compensation mode, the process was started at random in relation to the MRU simulator which seemed the most realistic and ensured the motor had to catch up with or meet the wave before starting compensating.
6. The system was then left compensating for a time to get measurements of the performance, near the end the control system was sometimes deactivated and reactivated with a small delay to make sure the motor could catch up with the wave.
7. Stopping the system consist of switching the system back into normal mode, using either the normal mode button or emergency normal mode button, with the latter being the quickest option. The slider is then moved back into its resting position and the system is turned off by pressing the normal mode button. The MRU simulator and control system is turned off, this can be done before or after going into normal mode and at any slider position.



(a) Testing with 50kg steel weight applied



(b) Control cabinet and HMI during testing

Figure 8.2

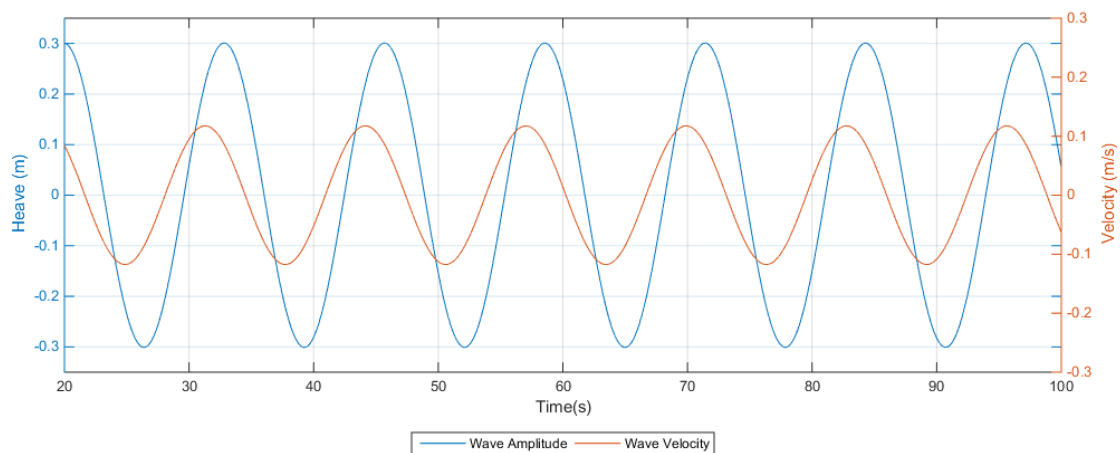
The emergency stop button was more or less useless as it would deactivate the drive which would cause the load to fall to the ground. If something went wrong the emergency normal mode button would have to be pressed which switches that the system switches to normal mode so the drive will try to hold the slider in place.

8.5 Test Results

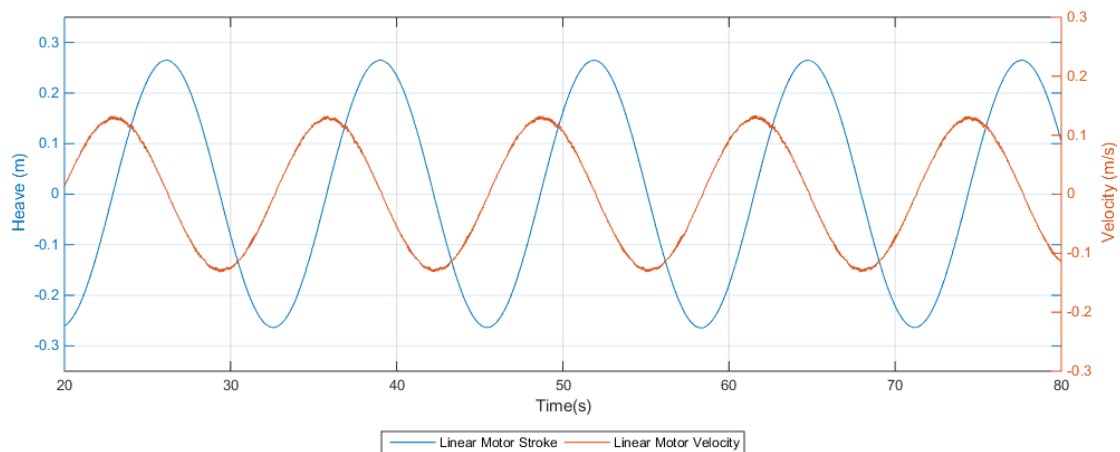
Since the MRU was not used in the testing the only possible physical source of error that remains is the potential error of the GT001 wire encoder, however since it is both responsible for the feedback and for measuring the performance this potential error will cancel itself out.

8.5.1 Initial Results

After Running initial tests with the cascade controller in the different waves and observing the results it was discovered that the wave velocity is not correct in relation to the wave amplitude, seen in 8.3a. The velocity is not zero at the top and bottom of the waves, compared to the stroke and velocity of the linear motor in figure 8.3b which has the correct relationship. In addition the logged heave was larger than the heave specified in the simulator. The output from the MRU simulator is wave heave and acceleration, these values then go through a filter to obtain the estimated heave, velocity and acceleration which are used for the control.



(a) Wave amplitude and velocity wave two



(b) Motor stroke and velocity wave two

Figure 8.3

As the wave velocity is used for feed forward in the control system it is possible this actually damages the performance of the system instead of enhancing. It was decided to plot the wave velocity plus

the linear motor, as these in perfect compensation should cancel each other out and give zero, versus the deviation. This plot can be seen in figure 8.4 and a clear correlation between the two curves can be seen, which means that the block estimating the wave velocity might actually worsen the performance of the system. This might have been different if the real MRU was used instead of the MRU simulator and filter in the PLC program. The maximum deviation during this test was ~ 5.4 mm which corresponds to $\sim 2.08\%$ of the wave amplitude.

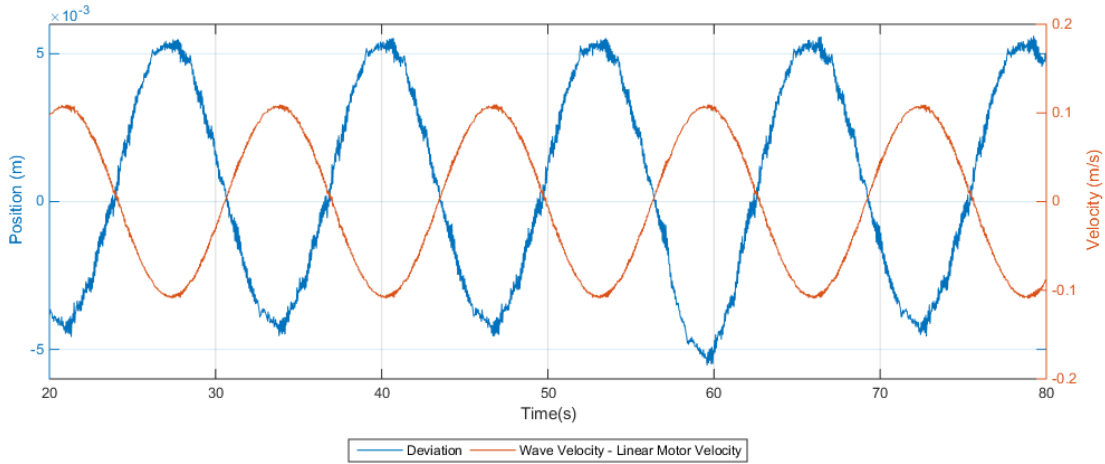


Figure 8.4: Deviations plotted versus the combined wave and motor velocity

To improve the performance it was decided not to use the MRU filter and use the heave amplitude directly from the simulator in the control, this meant the wave velocity was not available. The performance of the controller without the wave velocity was lacking and in addition was difficult to tune properly. As time was running out it was decided to replace the controller with a PI position controller using the inverse wave heave amplitude as setpoint and the slider stroke measured by the GT001 wire encoder as feedback. The tests were then done again with the new controller. Unfortunately a slight oversight when creating the controller caused the deviation to be calculated incorrectly when the controller was off as this also turned off the feedback inversion. This caused the deviation when the controller is off to sometimes be much higher than it actually was, however the correct value is shown as soon as the controller is turned back on. Another slight oversight caused the function for turning off the integral part when far away from setpoint to only be active when the deviation is positive, it was fixed but there was no time to run the tests again so some instability is present. Though at least it can be used to show the effect of the function.

The different gains for the PI position controller are shown in table 8.1, they were worked out by trial and error to save time, in order to optimize the system further more time could be spent fine tuning the system however it was not a priority at this time as the performance was satisfactory.

The force limit for the linear motor was set at $+80$ N and -700 N. The positive direction is downwards, and this limit makes sure the motor does not accidentally press against the ground with large forces. In order for the motor to overcome its own friction when moving downwards with no load the limit was set to 80 N. The continuous stall force of the motor is 673 N, the maximum upwards force was set a bit higher at 700 N as the load is a little heavier than desired. The reason for not setting the limit higher, which the motor can handle with no problem, is then the drive would go into power overload after a short while and would stop the compensation and keep the load still.

Table 8.1: Controller gains

Description	Without load	With 45 kg load	unit
Position P gain	25	8	-
Position I time	75	75	ms

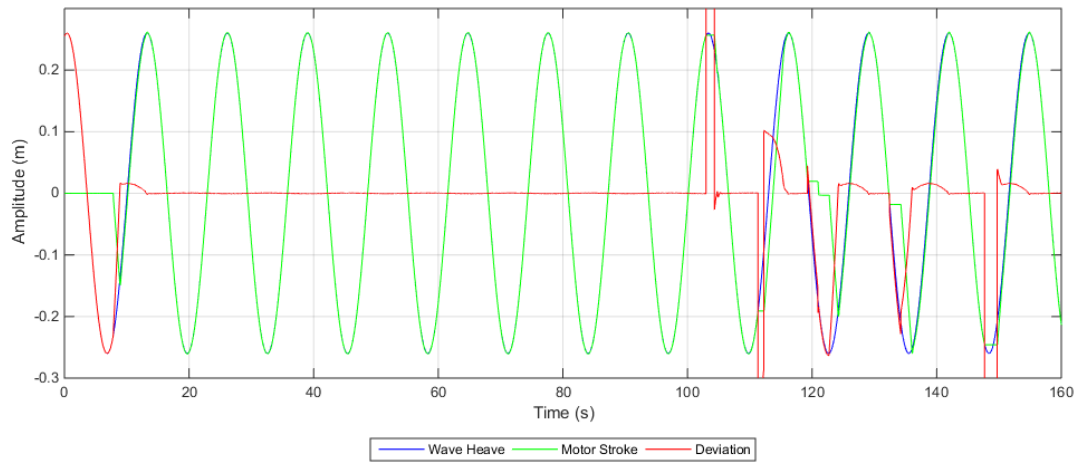
8.5.2 Final Results

After reviewing the test results it was decided to focus the in depth analysis in this section on wave two and four as those two described the system best.

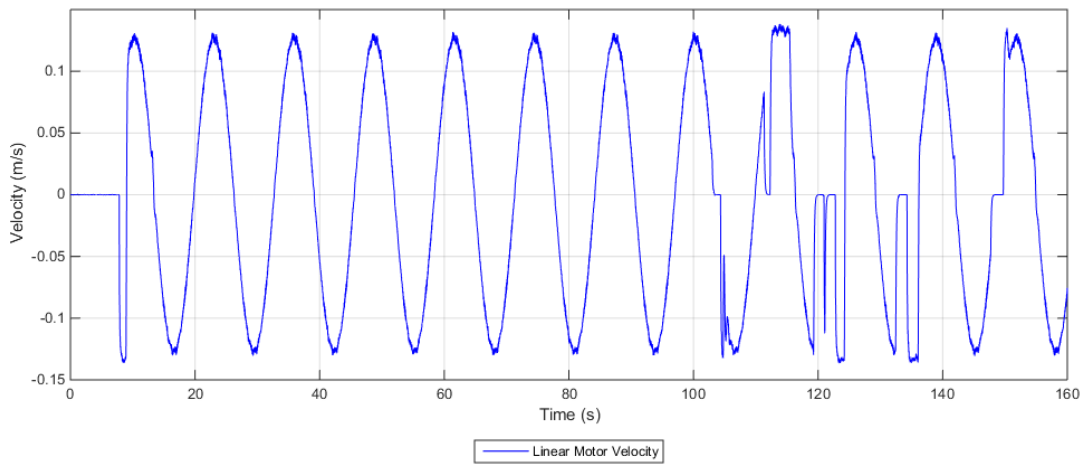
8.5.2.1 Wave Two

The results for the second wave with the load applied is shown in figure ??, this wave was chosen because it is the wave with the fastest wave velocity combined with a medium amplitude.

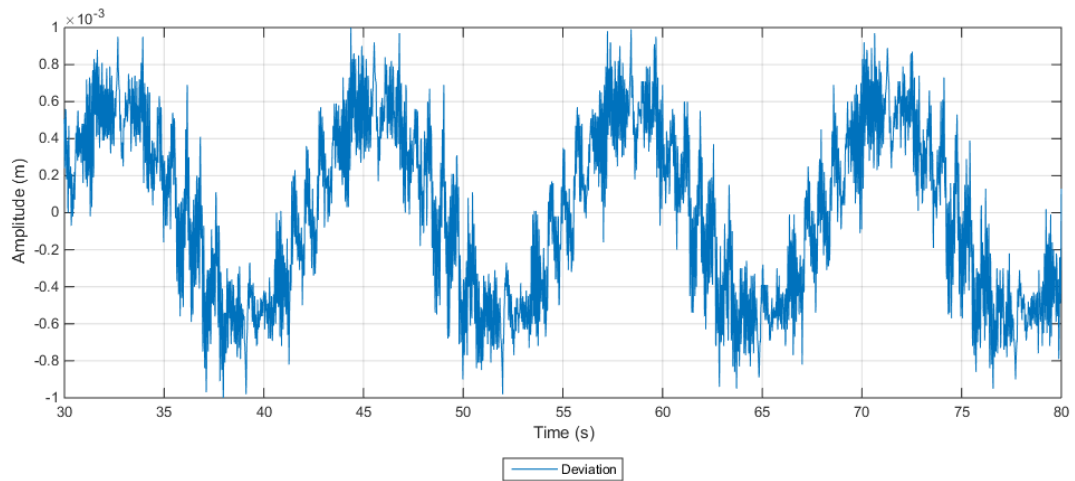
Figure 8.5a shows the wave heave and slider stroke which for perfect compensation should cancel each other out, the deviation is therefore the summation of the two, and perfect compensation yields a deviation of zero. Some interesting things are occurring at approximately 10 seconds when the heave compensation is activated, and at approximately 100 to 15 seconds where the controller is stopped and started again. When the heave compensation is activated the motor moves the load at the maximum speed allowed by the limit to intercept the wave and then starting heave compensating. The same occurs when the controller is switched off and on again, the motor uses its maximum allowed speed to catch up with the wave and then continues compensating. This effect can also be observed in figure 8.5b which shows the motor velocity.



(a) Wave heave, slider stroke and deviation between the two



(b) Linear motor velocity



(c) Close up of the deviation showing the performance

Figure 8.5: Test results for wave three

In figure 8.5c a close up of the deviation from setpoint can be seen. The maximum deviation is ~ 0.9

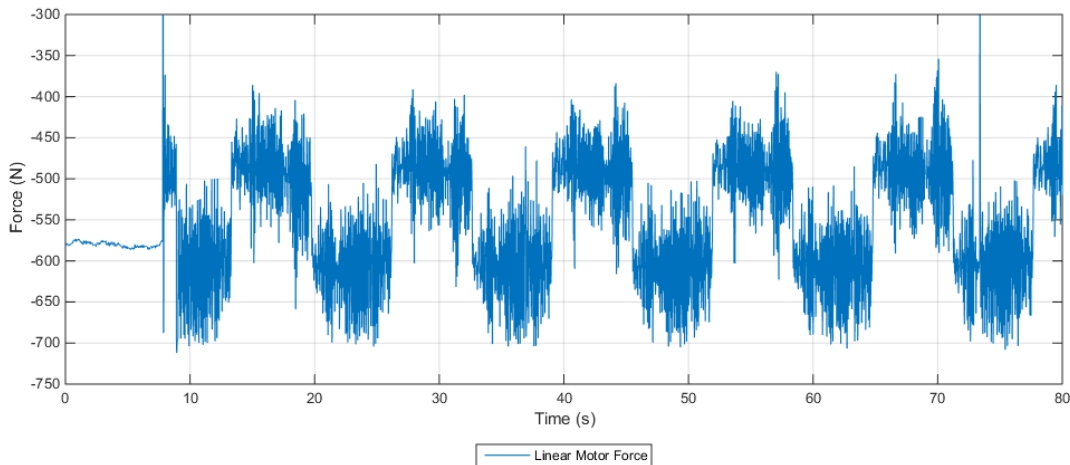


Figure 8.6: Force delivered by the linear motor heave compensation during wave three

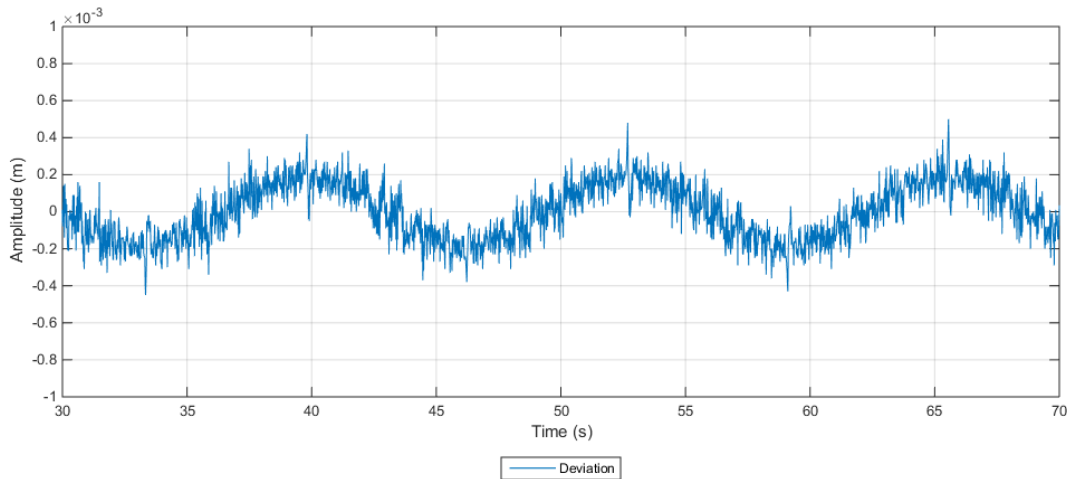


Figure 8.7: Close up of the deviation showing the performance when no load is applied

mm which corresponds to $\sim 0.35\%$ of the wave amplitude 8.1.

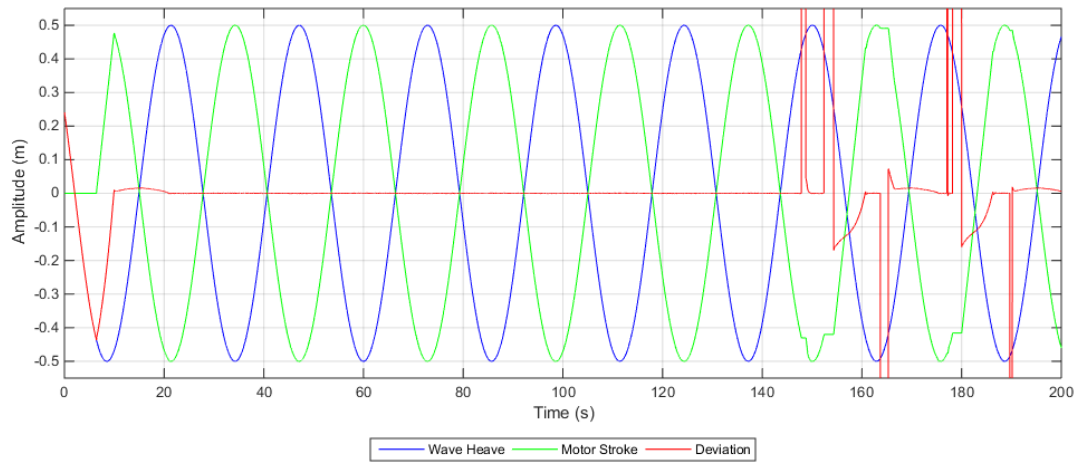
$$\text{Deviation \%} = 100 \cdot \frac{\text{Deviation}}{\text{Amplitude}} = 100 \cdot \frac{5.4}{260} = 2.08\% \tag{8.1}$$

The force delivered by the linear motor when compensating is shown in figure 8.6. It can be seen that the motor occasionally goes into force limitation which indicates the load is a little too heavy for the drive system, however the limit is only reached during very short peaks in the force which indicate it should not affect the performance too much.

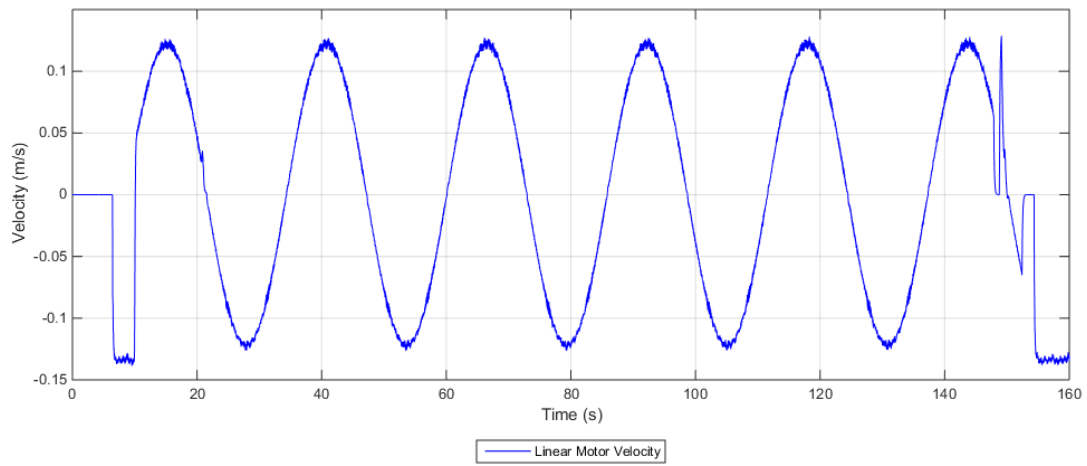
Figure 8.7 shows the deviation when there is no load applied in the same wave, the maximum deviation here is ~ 0.3 mm which corresponds to $\sim 0.12\%$ of the wave amplitude

8.5.2.2 Wave Four

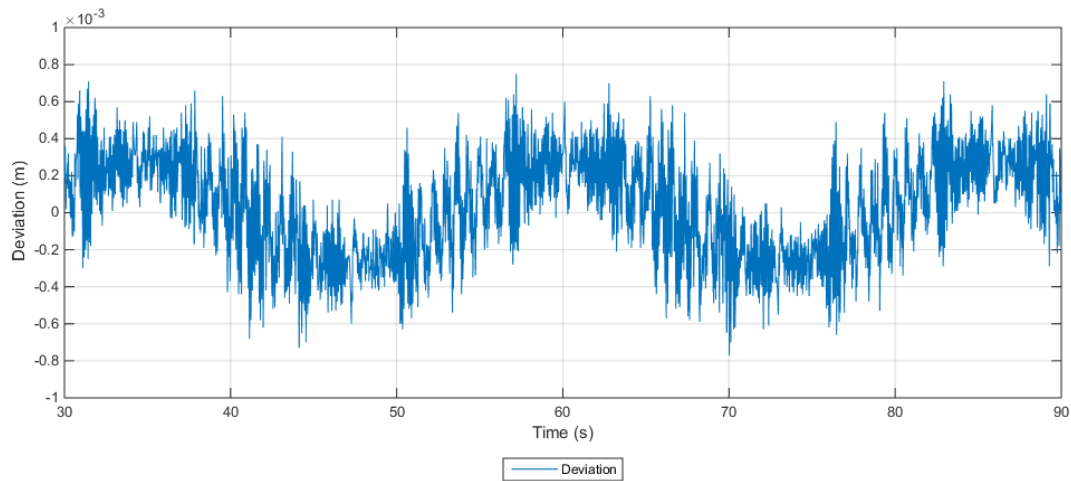
The results for the fourth wave with the load applied is shown in figure 8.8, this wave was chosen because it is the wave with the highest wave amplitude and its velocity is nearly as high as the second wave but its acceleration is lower.



(a) Wave heave, slider stroke and deviation between the two



(b) Linear motor velocity



(c) Close up of the deviation showing the performance

Figure 8.8: Test results for wave four

Again it can be seen that the motor intercept the wave at approximately 10 seconds when the heave

compensation is activated, and at between approximately 100 and 110 seconds when the controller is stopped and started again. This effect can also be observed in figure 8.8b which shows the motor velocity.

In figure 8.8c a close up of the deviation from setpoint can be seen. The maximum deviation is ~ 0.7 mm which corresponds to $\sim 0.14\%$ of the wave amplitude 8.2.

$$\%Deviation = 100 \cdot \frac{5.4}{260} = 2.08\% \quad (8.2)$$

The force delivered by the linear motor when compensating is shown in figure 8.9

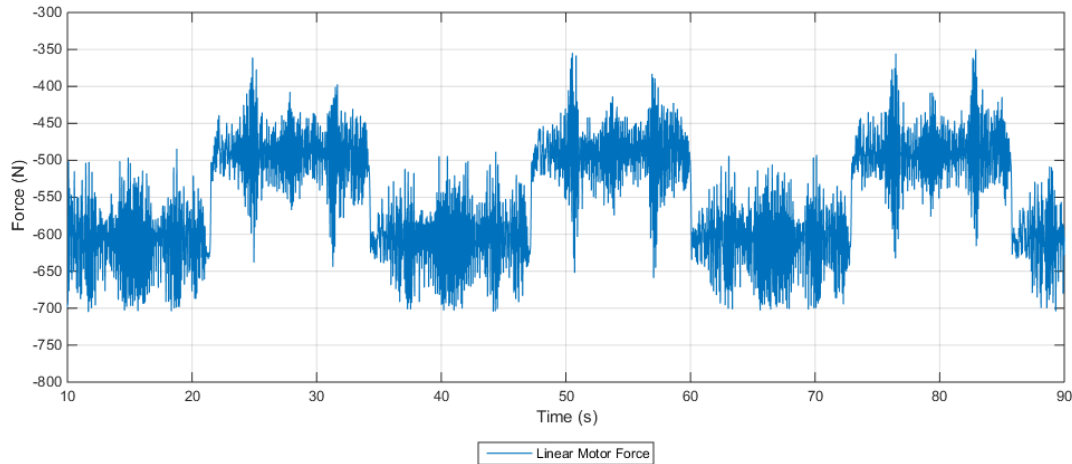


Figure 8.9: Force delivered by the linear motor heave compensation during wave three

Figure 8.10 shows the deviation when there is no load applied in the same wave, the maximum deviation here is ~ 0.3 mm which corresponds to $\sim 0.06\%$ of the wave amplitude

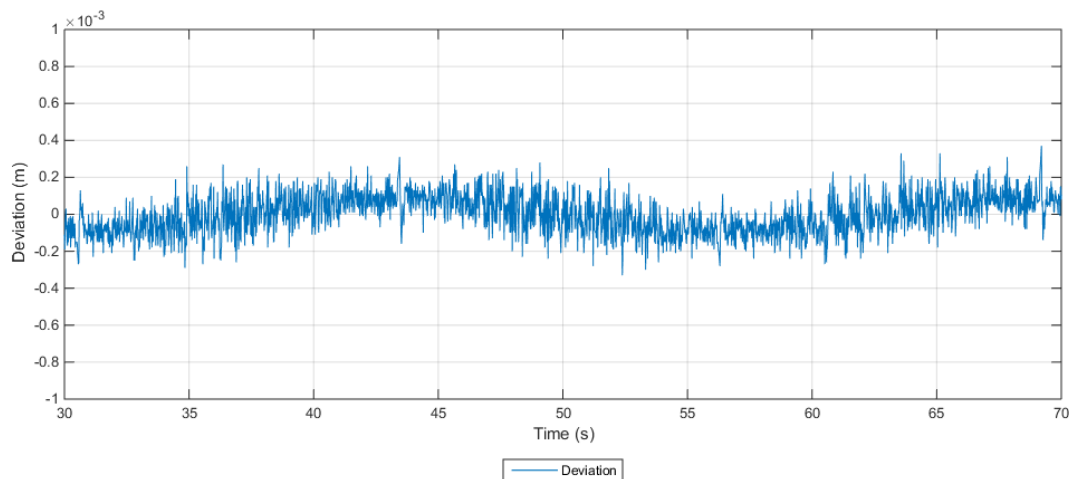


Figure 8.10: Close up of the deviation showing the performance when no load is applied

8.5.3 Test Conclusions

Table 8.2 shows the linear motors deviation during testing in the four different waves. When the linear motor is heave compensating without any external load the deviations in millimeters are basically the

same for all the waves. However when load is applied there are some differences in the performance in the different waves.

When looking at the close up plots of the deviation in figure 8.5c and zooming it in 8.11, oscillations of up to ± 0.4 mm can be seen with periods of ~ 0.6 second (1.67 Hz) and oscillations of up to ± 0.3 mm with ~ 0.05 second periods (20 Hz). The high frequency oscillations might originate from noise in the encoder signal or vibration in the wire as they can not be detected in the motor slider itself, however the lower frequency oscillations are present in the slider.

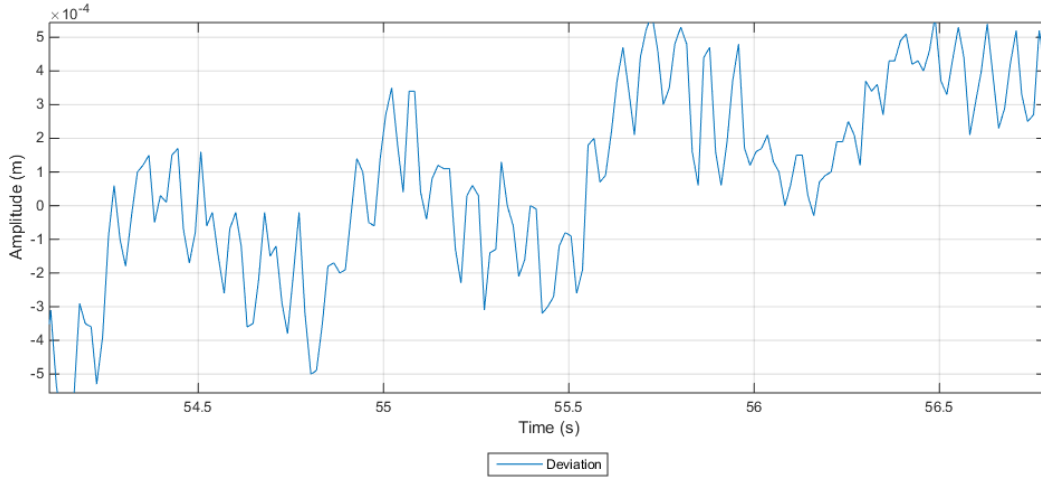


Figure 8.11: Oscillations in the deviation

Table 8.2: Linear motor deviation in mm (percent of wave amplitude)

Description	Without load	With 45 kg load	Maximum motor velocity
Wave One	0.3(0.27%)	0.6(0.55%)	0.068
Wave Two	0.3(0.12%)	0.9(0.35%)	0.128
Wave Three	0.3(0.07%)	0.8(0.19%)	0.104
Wave Four	0.3(0.06%)	0.7(0.14%)	0.124

Trying to find which parameter the deviation from setpoint depends was not straightforward. It could seem like it depends on the velocity of the linear motor, wave one is the slowest and has the lowest deviation and wave two is the fastest and has the highest deviation. However this does not explain why wave four, which is nearly as fast as wave two, has lower deviation than wave three. It is logical to assume that deviation from setpoint is related to the acceleration of the wave then, as the acceleration determines how much force the linear motor has to apply to the load in order to compensate for the wave. When plotting the deviation versus the acceleration in figure 8.12 it can be observed that the deviation indeed coincides with the wave acceleration. It is further supported by the fact the deviations are nearly identical in each wave when there is not external load. However when looking at the acceleration of the different waves in figure 8.13 it can be observed that for wave one both the acceleration, and acceleration rate of change, is higher than for wave three and four and still it has the lower deviation. It can therefore be concluded that the deviation during these tests depends on several parameters, but mainly the wave acceleration.

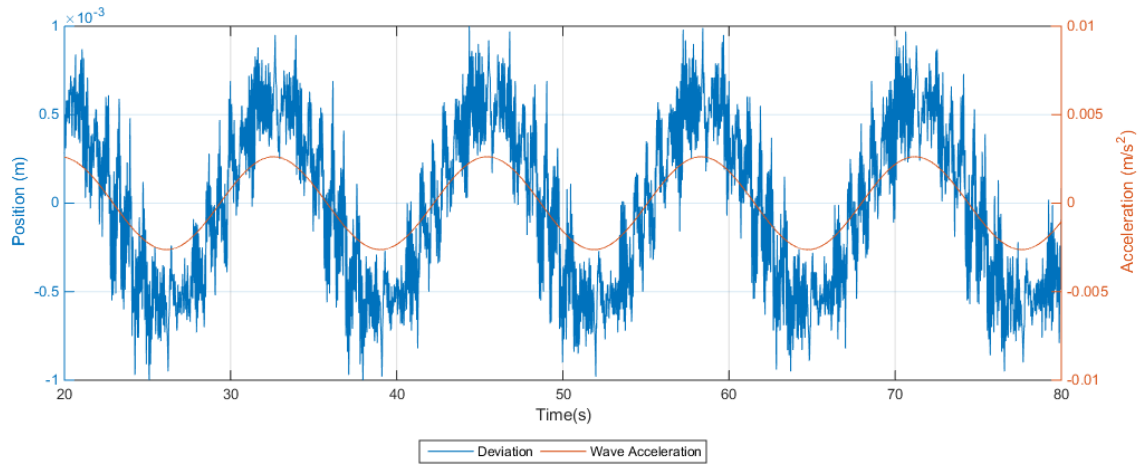


Figure 8.12: Relationship between the deviation and wave acceleration for wave two

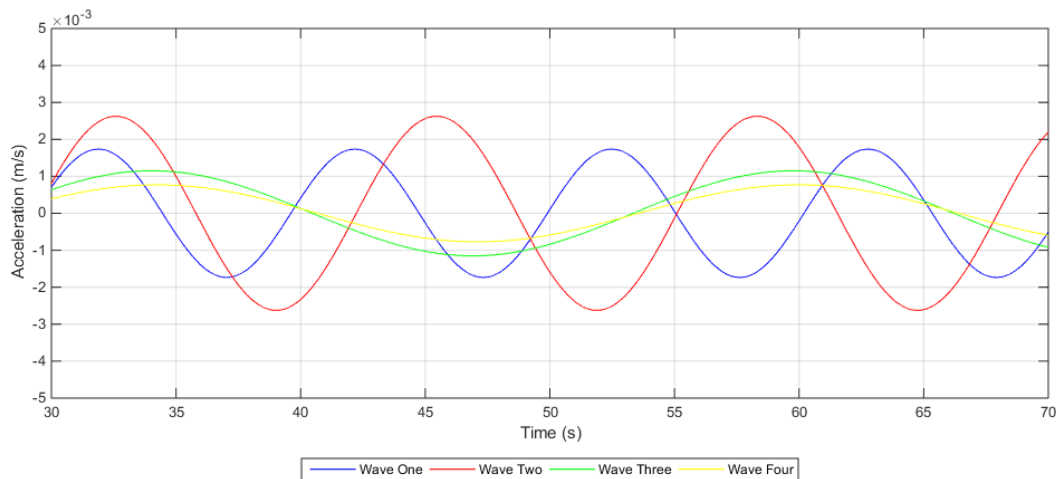


Figure 8.13: Wave acceleration for the four waves

The effect of the function for stopping the integrator while the motor is far away from its setpoint is shown in figure 8.14. The integral part is activated when the deviation is less than 3 mm. This means that when the deviation approaches zero from a positive value the integral term is off until the deviation is 3 mm, while when approaching from a negative value the integral term is always on. This was not intended as described earlier but now serves to show the difference. As seen in the figure the overshoot when approaching zero from a negative value is much larger compared to approaching from a positive value.

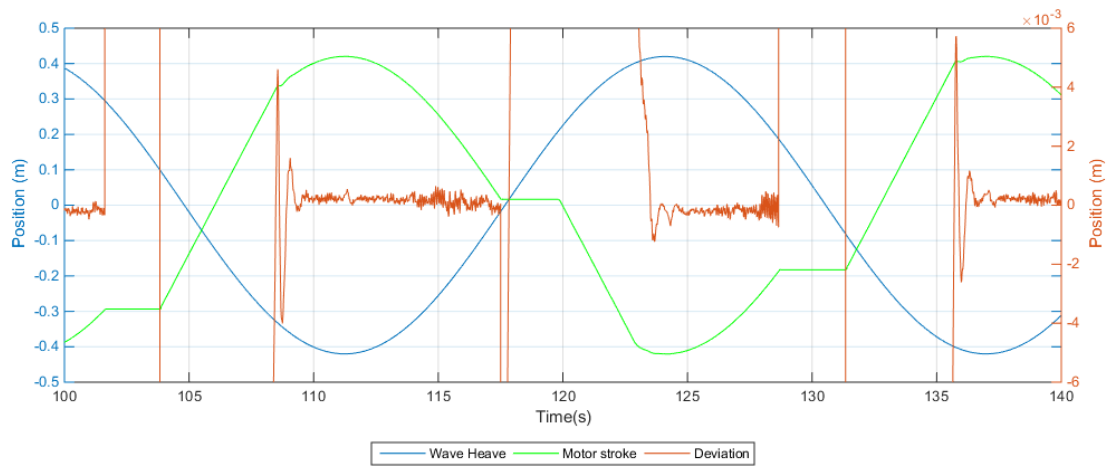


Figure 8.14: Close up of deviation during stop-start of controller

The complete figures from the test results are shown in appendix A.

Chapter 9

Conclusion

As the scale model CMC ended up not being used in the thesis it is not possible to come to a definite conclusion with regards to the linear motor being used in conjunction with the CMC as an active heave compensator (AHC). Also comparing results with the earlier solution will not be directly possible, instead the conclusion to this thesis will focus mostly on the linear motor as an AHC by itself and try to use that information to estimate its compatibility with the CMC.

During testing it very soon became clear that linear motor as it is, without any mechanical additions, is not very suitable as an active heave compensator. The reason is that if the linear motor is accidentally switched off during operation or suddenly loses power, the slider and the load would simply fall to the ground and could potentially cause damage. If planned to be used as an AHC by itself certain mechanical adaptations would have had to be made. However there was no time to investigate this further since the linear motor was originally to be used in conjunction with the scale model CMC and most of the work done in this thesis was done with that in mind. This part is therefore not considered a drawback to the linear motors performance as it was never meant to operate on its own, but in conjunction with the passive CMC.

However when used as an AHC the linear motors performance is excellent. The linear motor manages to reduce the heave impact by 99.4-99.8% of the wave amplitude for a ~ 45 kg load during testing, depending on the characteristics of the wave. It was discovered that the motor exhibited some oscillations when compensating though these will be probably be reduced greatly if used together with a passive system when introducing more damping to the system, and is also likely to be reduced by further work on the control system.

There was no difficulty in incorporating the motor into the scale model CMC however if to be used for the real CMC some things have to be considered. First of all the motor used in this thesis is the second largest motor LinMot® currently makes, no motor of this type is available for the real CMC, although theoretically a motor of that size should be possible to make. As this motor was chosen partly because it was suitable for implementation into the scale model CMC without too much mechanical adaptations, other more powerful motors with different form factors might be more suitable for the real CMC as then the structure can be modified to accommodate these types of linear motor.

Another important aspect is the cost of the linear motor, at a cost of almost 40 000 NOK including cooling flange and cables for the motor used in this thesis, it is considerably more expensive than the system it to replaces. This is an aspect that has to be taken into consideration, if the performance is worth the cost.

One of the surprising drawbacks of the linear motor which was not given much thought before it arrived is the strong magnetic field around the slider which is especially easy to forget about when working near the slider with tools. If the motor and slider was to be scaled up for used with the real

CMC this magnetic field would be extremely strong and could potentially be dangerous if careless, care would therefore have to be made when installing the slider and performing maintenance near it.

All in all it can be concluded that this thesis has proved that a linear motor is indeed suitable as an active heave compensator, though foremost in conjunction with a passive compensation device.

Bibliography

- [1] P. Gu, A. A. Walid, Y. Iskandarani, and H. R. Karimi, “Modeling, simulation and design of a hoisting rig active heave compensation system,” 2012.
- [2] J. Hatleskog and M. W. Dunnigan, “Active heave crown compensation sub-system,” *IEEE*, 2007.
- [3] I.-C. Vese, F. Marignetti, and M. M. Radulescu, “Multiphysics approach to numerical modeling of a permanent-magnet tubular linear motor,” *IEEE Transactions on Industrial Electronics*, vol. 57, pp. 320–326, 2010.
- [4] Z. Yun-fei, S. Bao, and C. Xue-dong, “Position/force control with a lead compensator for pmlsm drive system,” *International Journal of Advanced Manufacturing Technology*, vol. 30, pp. 1084–1092, 2006.
- [5] A. AAlerud and T. Klevmo, “Implementation of active control design for crown mounted compensator to improve drilling performance,” Master’s thesis, University of Agder, 2013.
- [6] “Active heave compensator,” tech. rep., Ocean Drilling Program.
- [7] National Oilwell Varco Norway AS, *User Manual, CMC-E & AHC, Main Schahin 1 Drillship*, 2011. internal document V6605-Z-MA-001 2.rev.
- [8] J. T. Hatleskog and M. W. Dunnigan, “An impedance approach to reduce the contact-instability whilst drilling with active heave compensation,” *Ocean Engineering*, vol. 49, pp. 25–32, 2012.
- [9] J. Haaø, S. Vangen, I. Tyapin, M. Choux, G. Hovland, and M. R. Hansen, “The effect of friction in passive and active heave compensation of crown block mounted compensators,” *Proceedings of the 2012 IFAC Workshop on Automatic Control in Offshore Oil and Gas Production*, 2012.
- [10] Tecsis, *Tension/compression force transducers with thin-film sensor*. data sheet.
- [11] APLISENS, *User’s Manual Pressure Transmitters PCE-28 Differential Pressure Transmitters PRE-28 Hydrostatic Level Probes PCE-28P*, 2014 March.
- [12] FERNSTEUERGÄTE, *Rope Length Transmitters*. catalog.
- [13] Hengstler, *Technical Datasheet EX Heavy Duty Absolute*. data sheet.
- [14] “Linmot linear motor.” <http://www.linmot.com/products/linear-motors/>.
- [15] X. Wang, Z. Zhang, X. Xu, and Y. Cui, “Influence of using conditions on the performance of pm linear synchronous motor for ropeless elevator,” tech. rep., School of Electrical Engineering and Automation, Henan Polytechnic University, China, 2011.
- [16] NTI AG, *Tutorial LinMot Designer 1.9*. manual.
- [17] NTI AG, *Linear Motor Series P10-70 for third party drives*, May 2014. data sheet.
- [18] NTI AG, *LinMot Data Book E-Catalogue*. catalog.

- [19] Y. wu Zhu and Y.-H. Cho, “Thrust ripples suppression of permanent magnet linear synchronous motor,” *IEEE Transactions on Magnetics*, vol. 43, pp. 2537–2539, June 2007.
- [20] N. Bianchi, S. Bolognani, and A. D. F. Cappello, “Back e.m.f imprimprove and force ripple reduction in pm linear motor drives,” *35th Annual IEEE Power Electronics Specialists Conference*, pp. 3372–3377, 2004.
- [21] P. Hor, Z. Zhu, D. Howe, and J. Rees-Jones, “Minimization of cogging force in linear permanent motor,” *IEEE Transactions on Magnetics*, vol. 34, pp. 3544–3547, September 1998.
- [22] L. Lu, Z. Chen, B. Yao, and Q. Wang, “Desired compensation adaptive robust control of a linear-motor-driven precision industrial gantry with improved cogging force compensation,” *IEEE/ASME Transactions on Mechatronics*, vol. 13, pp. 617–624, December 2008.
- [23] M. Choux, I. Tyapin, and G. Hovland, “Extended friction model of a hydraulic actuated system,” tech. rep., University of Agder, 2012.
- [24] L. Harnefors, *Control of Variable-Speed Drives*. 2003.
- [25] Y.-S. Kung, “Design and implementation of a high-performance pmlsm drives using dsp chip,” *IEEE Transactions on Industrial Electronics*, vol. 55, pp. 1341–1351, 2008.
- [26] G. Borghesan and C. Melchiorri, “Model and modeless friction compensation: Application to a defective haptic interface.”
- [27] K. K. Tan, S. Huang, and T. H. Lee, “Robust adaptive numerical compensation for friction and force ripple in permanent-magnet linear motors,” *IEEE Transactions on Magnetics*, vol. 38, pp. 221–228, 2002.
- [28] F. Haugen, “The good gain method for pi(d) controller tuning,” *TechTeach*, 2010.
- [29] NTI AG, *Installation Guide LinMot Linear Motors Motor series: P10-70*, 2014. manual.
- [30] SIEMENS, *SIEMENS SIMATIC Programming with STEP 7*, 05 2010. Manual.

List of Figures

2.1	The passive CMC	5
2.2	CMC location on top of the derrick of the Cerrado drillship	5
2.3	Model of the CMC with platforms removed	7
2.4	Closer look at the main CMC systems [5]	7
2.5	The AHC system	8
2.6	The scaled CMC on top of a stewart platform with a rack and pinion AHC system	9
2.7	The three different waves defined for the project	11
2.8	The response of the CMC with respect to hook load while subjected to wave #3 at 6 bar	12
3.1	Illustrated overview of the instrumentation for the scaled CMC with the rack and pinion system [5]	14
4.1	The force required by the linear motor(s) for the three waves in SimulationX	18
4.2	Waves #2 and #3 in LinMot designer	20
4.3	Stroke of the motor	23
4.4	Testing the linear motor	24
4.5	Friction and cogging forces in the motor	26
4.6	Curve fitting the cogging force	27
5.1	Simple linear motor in SimulationX	28
5.2	Simple linear motor in Simulink	31
6.1	Force PI controller with force feedback	33
6.2	Force PI controller with position feedback	33
6.3	The cascade structure controller	34
6.4	Velocity and friction feed forward without PI controller	34
6.5	Different feed forward strategies	36
6.6	Effect of friction feed forward on position PI controller	37
6.7	PI controller with friction feed forward structure in Simulink	37
6.8	Comparison of the SimulationX s-function and data from the real model	38
6.9	The PI controller with hookload feedback and friction estimator feed forward	39
6.10	Hookload deviation using the PI controller with hookload feedback and friction estimator feed forward	40
6.11	The PI controller with position feedback and friction estimator feed forward	40
6.12	Crownblock deviation using the PI controller with position feedback and friction estimator feed forward	41
6.13	The cascade structure controller with friction estimator feed forward	41
6.14	Crownblock deviation using the cascade structure controller with friction estimator feed forward	42
7.1	The bracket and force transducer assembly with rack and pinion system in place (a) and removed (b)	44
7.2	The top frame of the CMC with the rack and pinion system removed	45

7.3	Stroke and slider connections	45
7.4	Dimensions of the system with lifting cylinders retracted and slider in its lowest position	46
7.5	Suggestions for fastening the stator	47
7.6	The chosen bracket	48
7.7	Forces in the motor and bracket	49
7.8	Stress in the bracket	50
7.9	Deformation of the bracket	51
7.11	The control cabinet	54
7.12	The fabricated linear motor bracket	55
7.13	Draw wire encoder	56
7.14	Scale model CMC fastened to the Stewart platform	57
7.15	58
7.16	The scale model CMC on the stewart platform ready for testing	59
7.17	Illustration of the PLC block hierarchy [30]	60
7.18	Structure of the PLC program before any modifications were made [5]	61
7.19	Screenshot of the HMI screen for the CMC and linear motor system	63
7.20	The GT001 wire encoder measuring the position of the slider	64
7.21	65
7.22	The controller in the drive responsible for regulating the force required	66
7.23	Screenshot of the HMI screen for the linear motor system AHC sytem	67
8.1	70
8.2	71
8.3	72
8.4	Deviations plotted versus the combined wave and motor velocity	73
8.5	Test results for wave three	75
8.6	Force delivered by the linear motor heave compensation during wave three	76
8.7	Close up of the deviation showing the performance when no load is applied	76
8.8	Test results for wave four	77
8.9	Force delivered by the linear motor heave compensation during wave three	78
8.10	Close up of the deviation showing the performance when no load is applied	78
8.11	Oscillations in the deviation	79
8.12	Relationship between the deviation and wave acceleration for wave two	80
8.13	Wave acceleration for the four waves	80
8.14	Close up of deviation during stop-start of controller	81

List of Tables

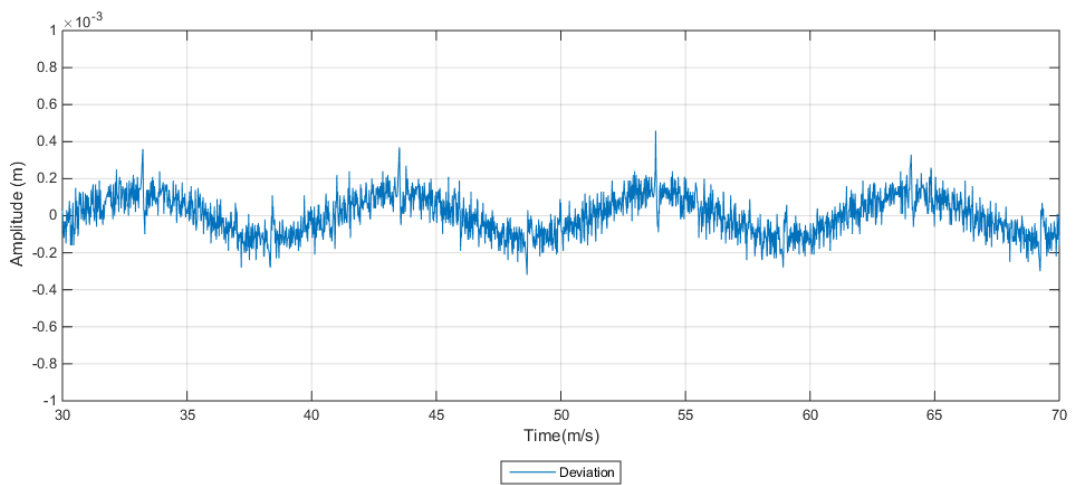
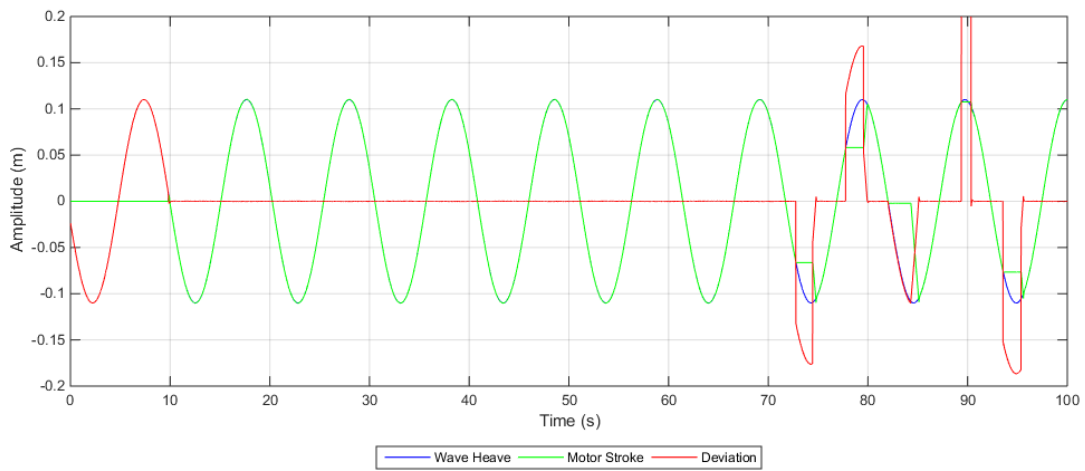
4.1	Linear motor P10-70X320U/1330 [17]	22
4.2	Linear motor P10-70X320U/1330 power supply	22
4.3	Linear motor order information	24
6.1	Friction feed forward parameters	39
8.1	Controller gains	74
8.2	Linear motor deviation in mm (percent of wave amplitude)	79

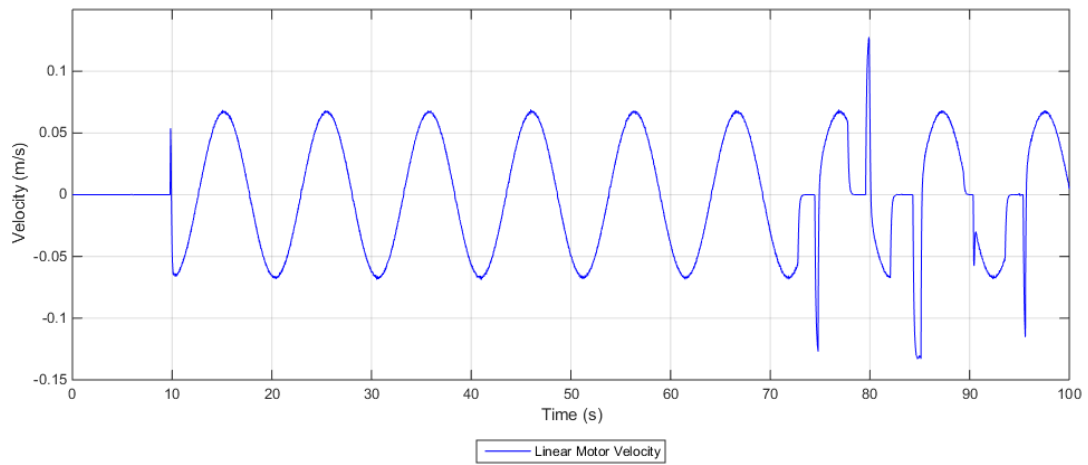
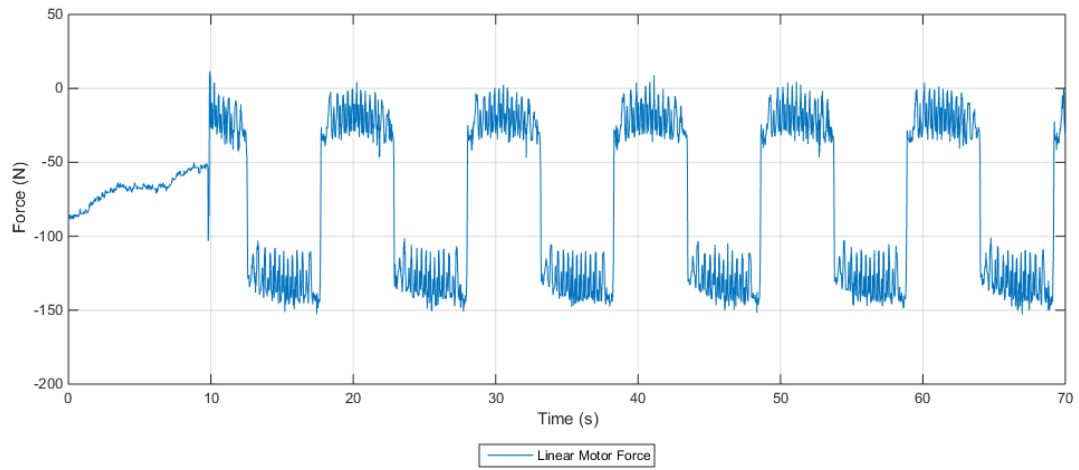
Appendix A

Test Results

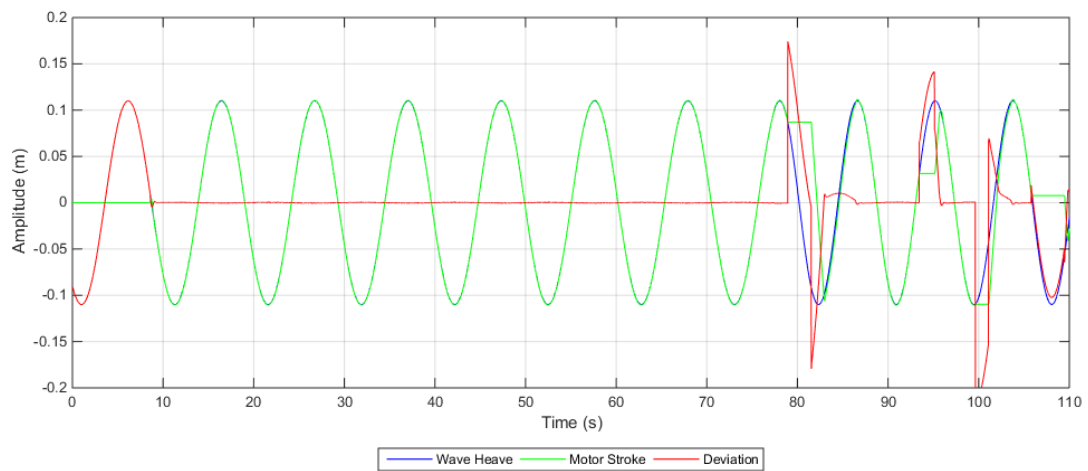
A.1 Wave One

A.1.1 No Load

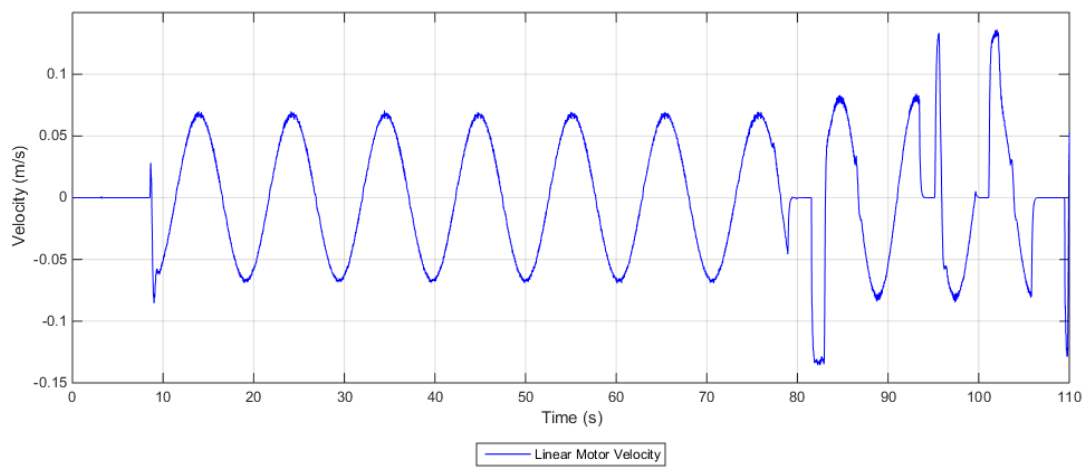
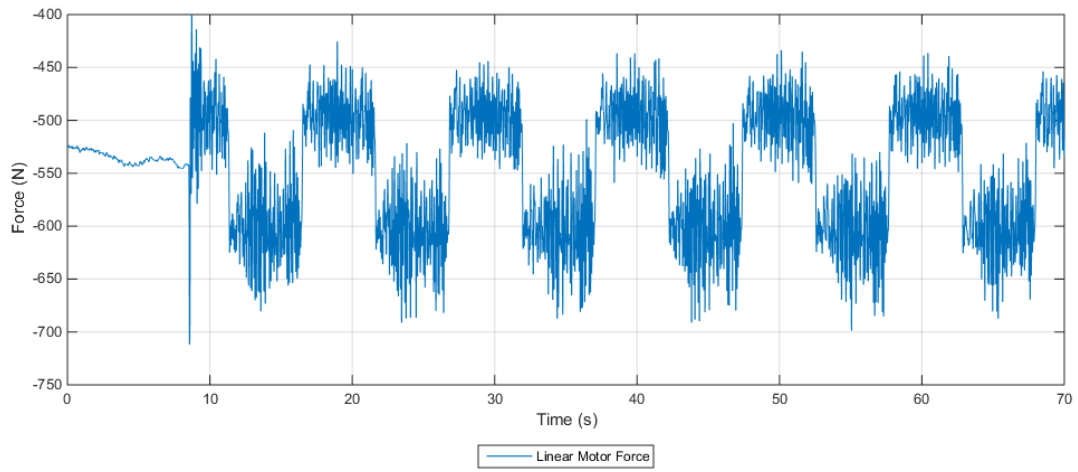
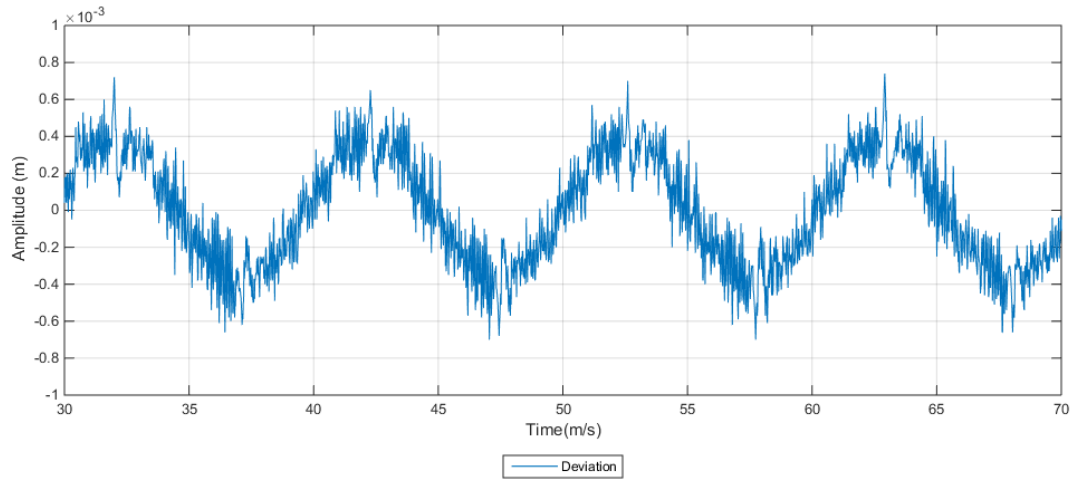




A.1.2 Load

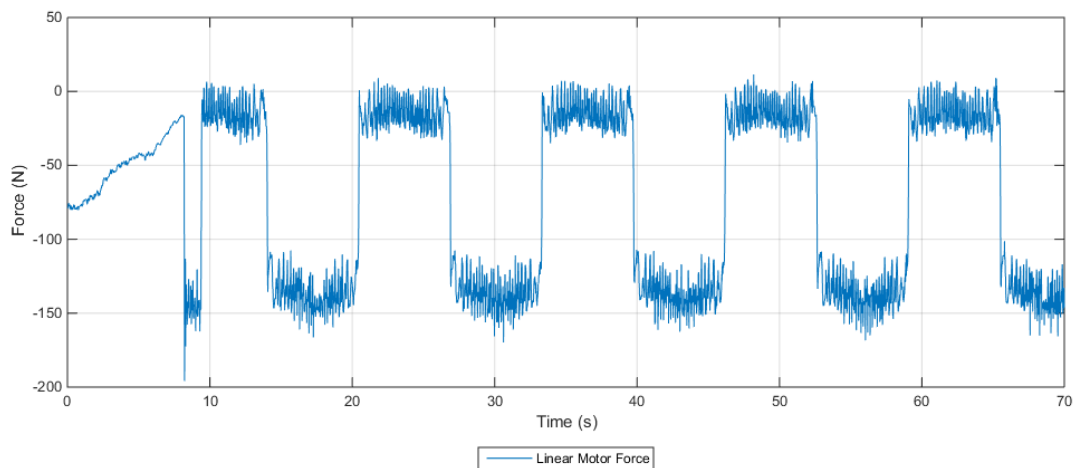
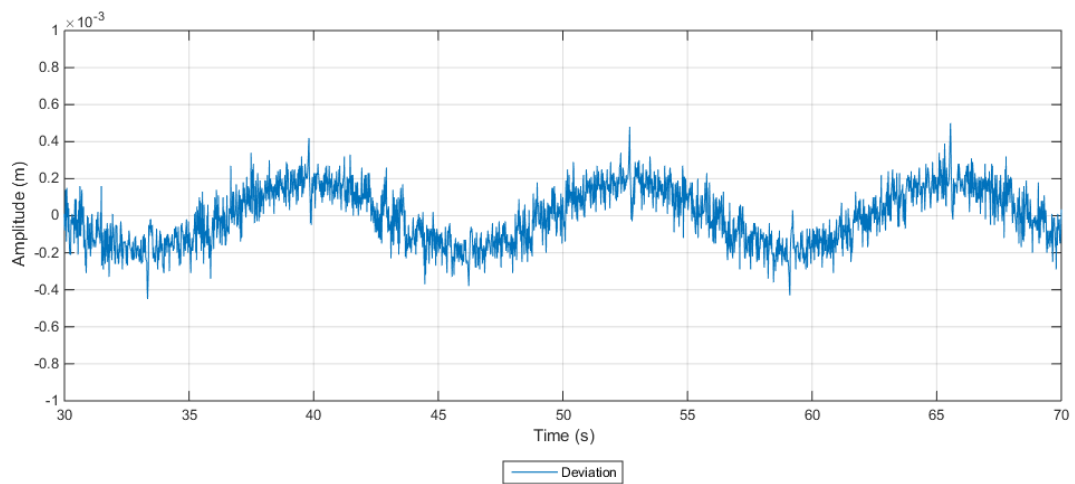
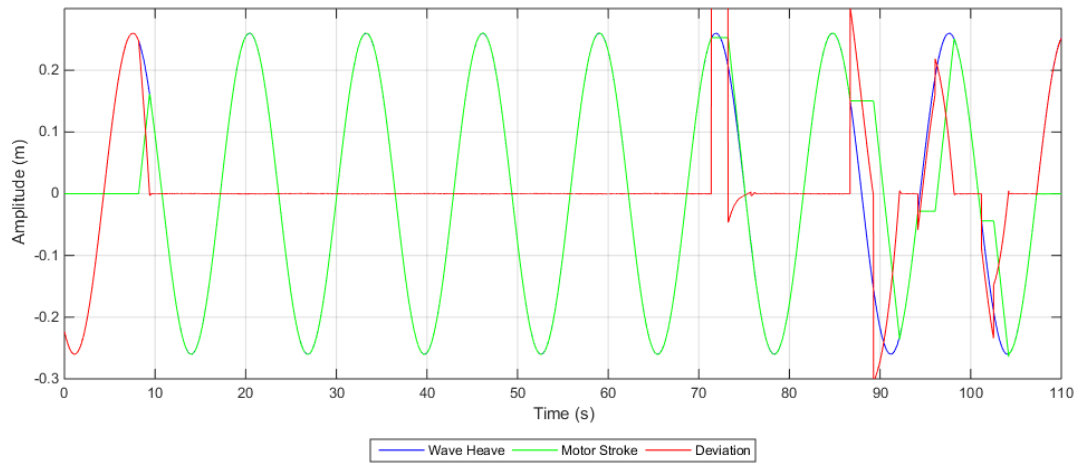


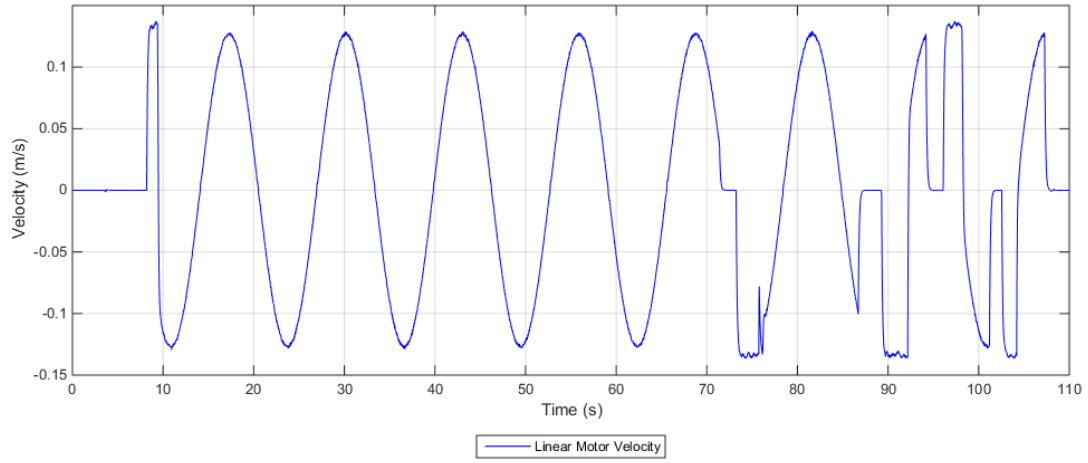
APPENDIX A. TEST RESULTS



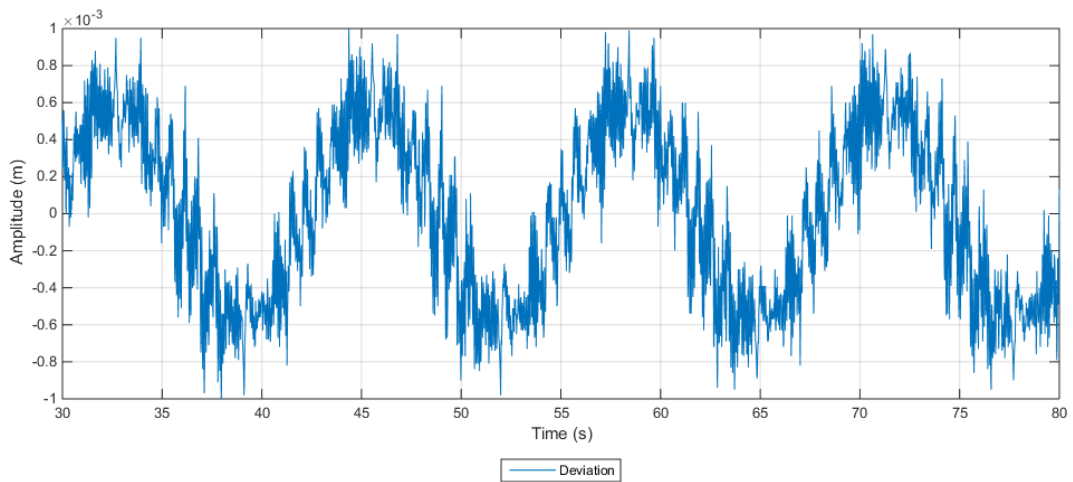
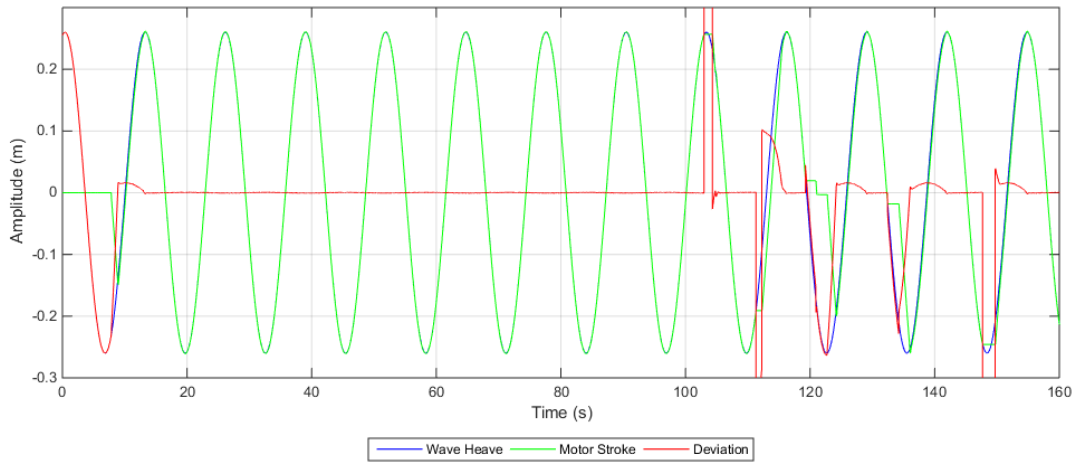
A.2 Wave Two

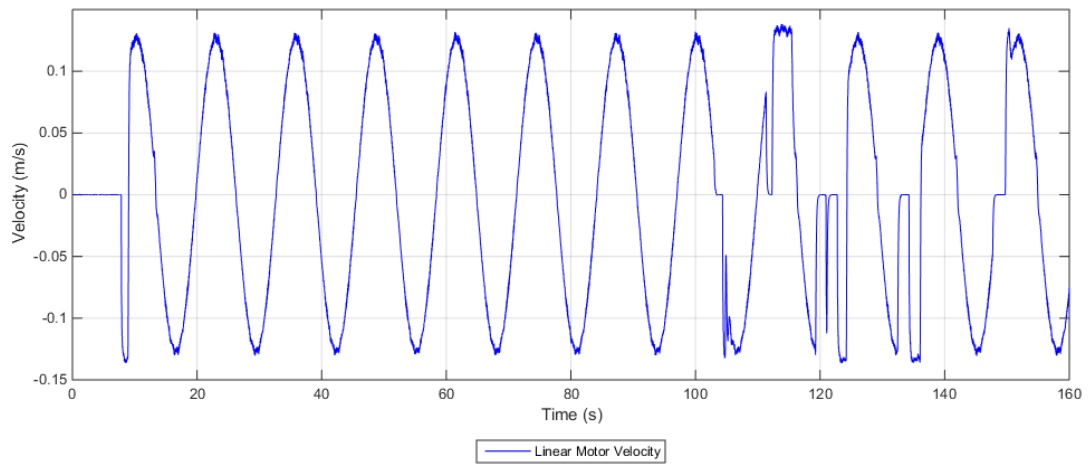
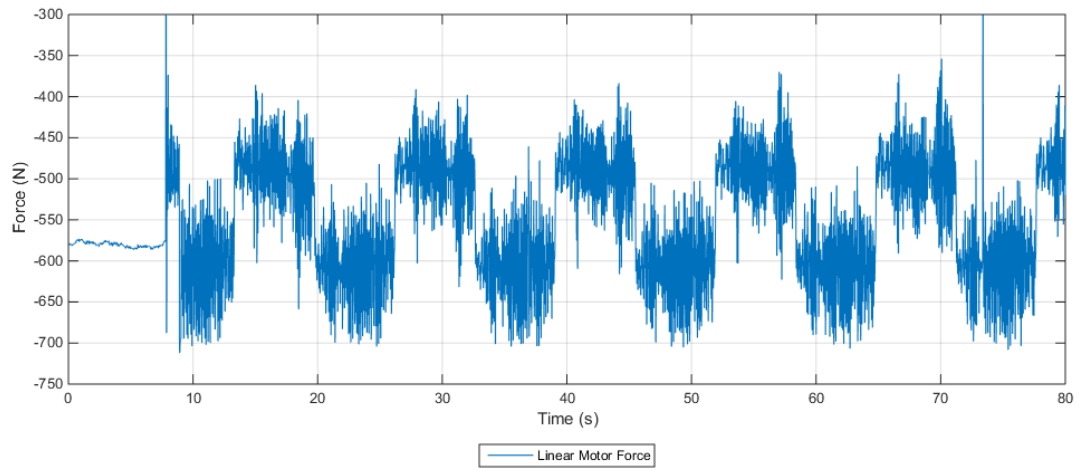
A.2.1 No Load





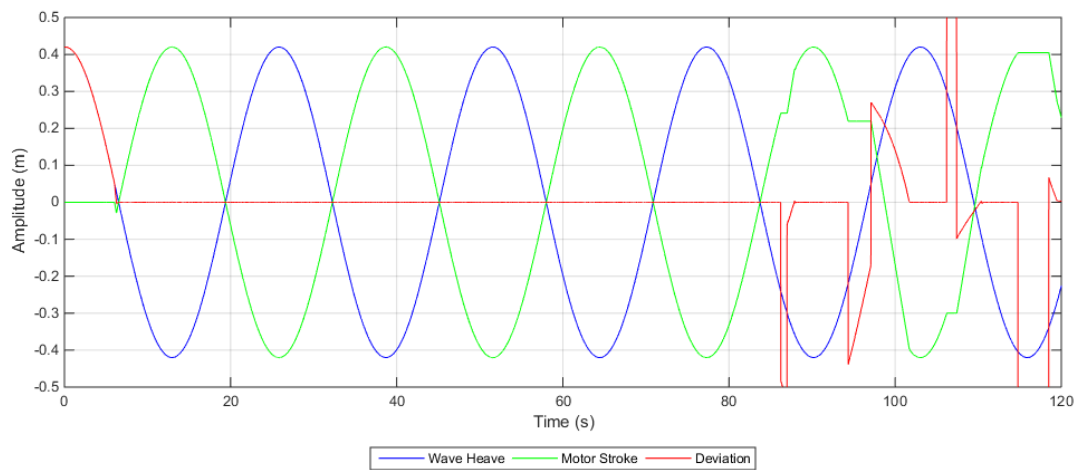
A.2.2 Load



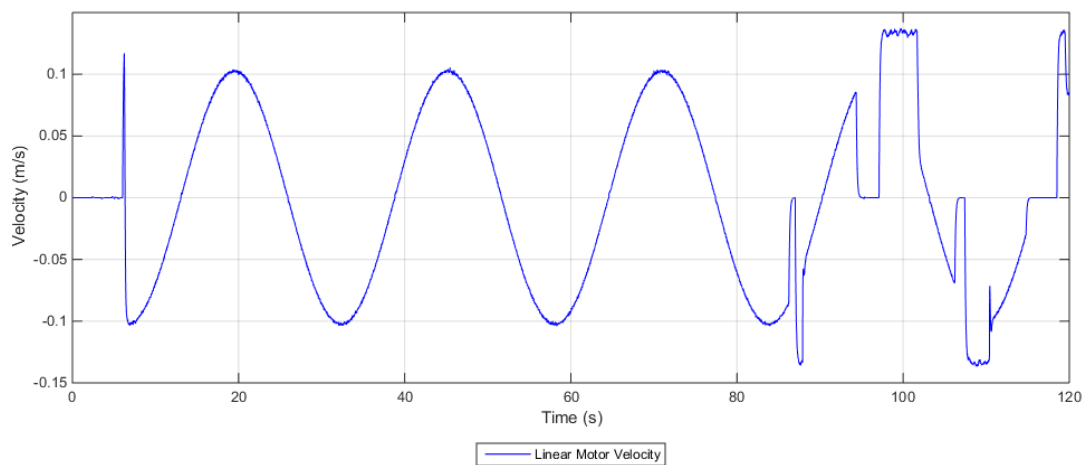
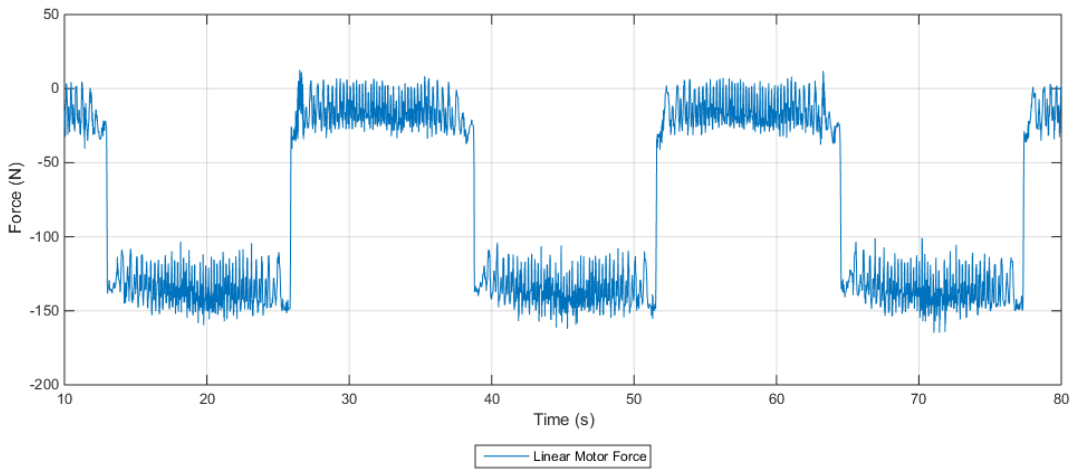
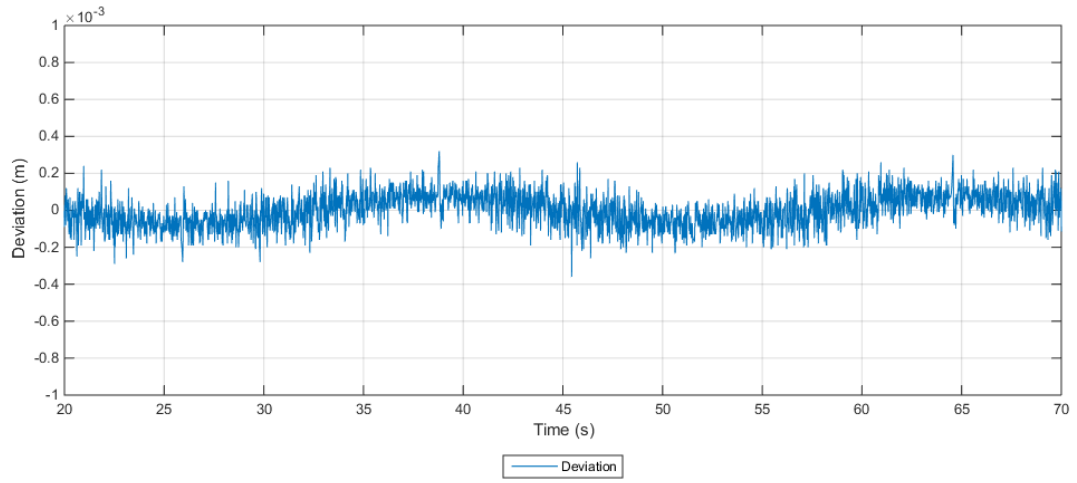


A.3 Wave Three

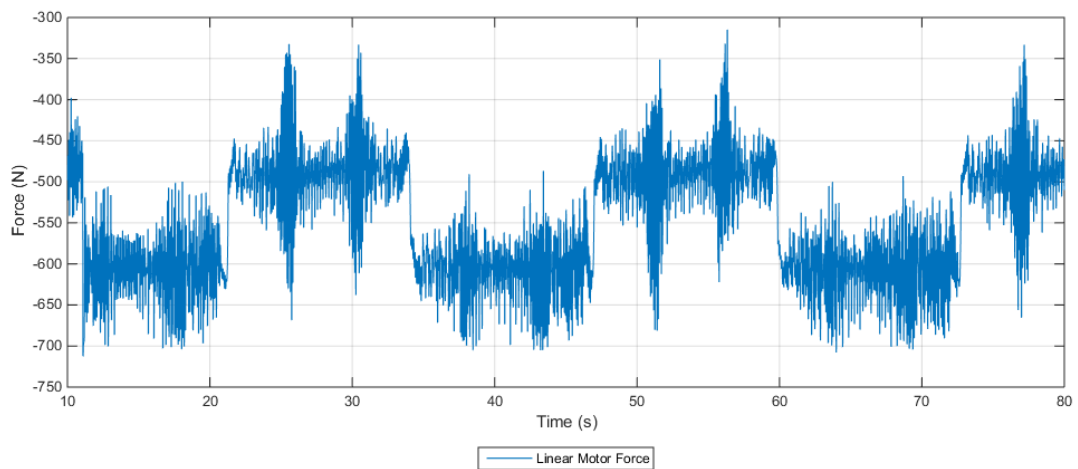
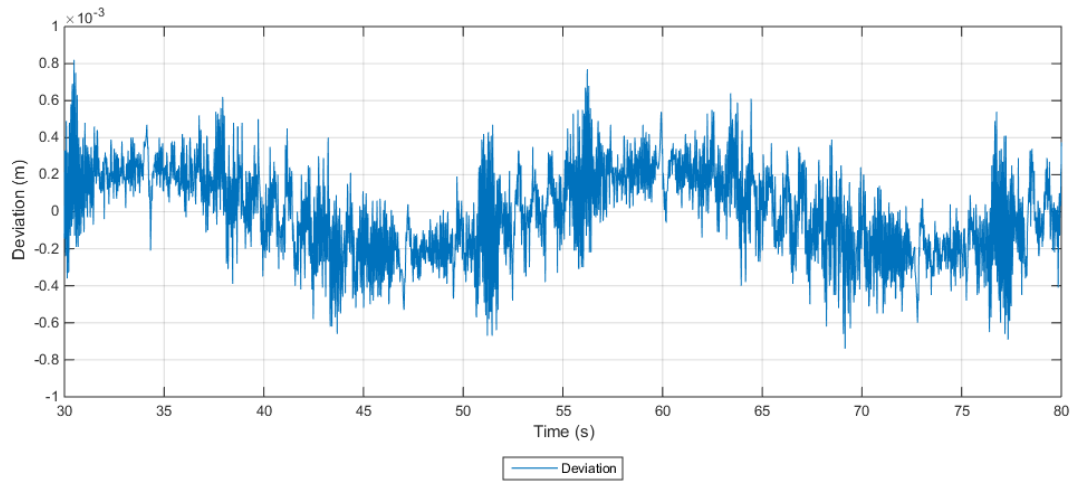
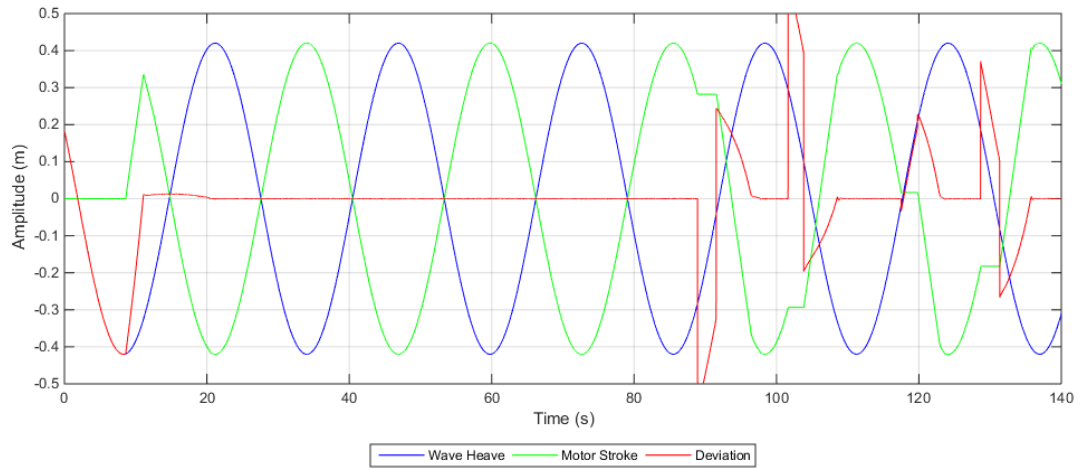
A.3.1 No Load

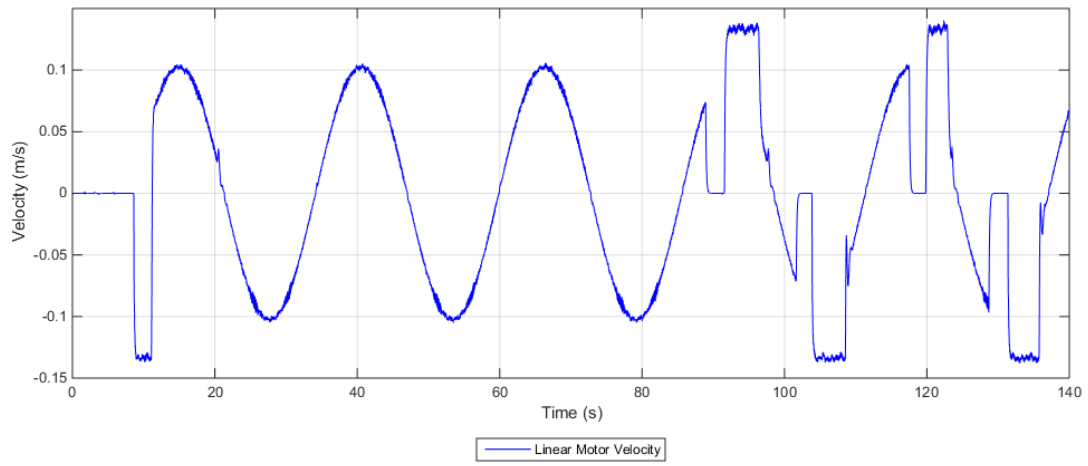


APPENDIX A. TEST RESULTS



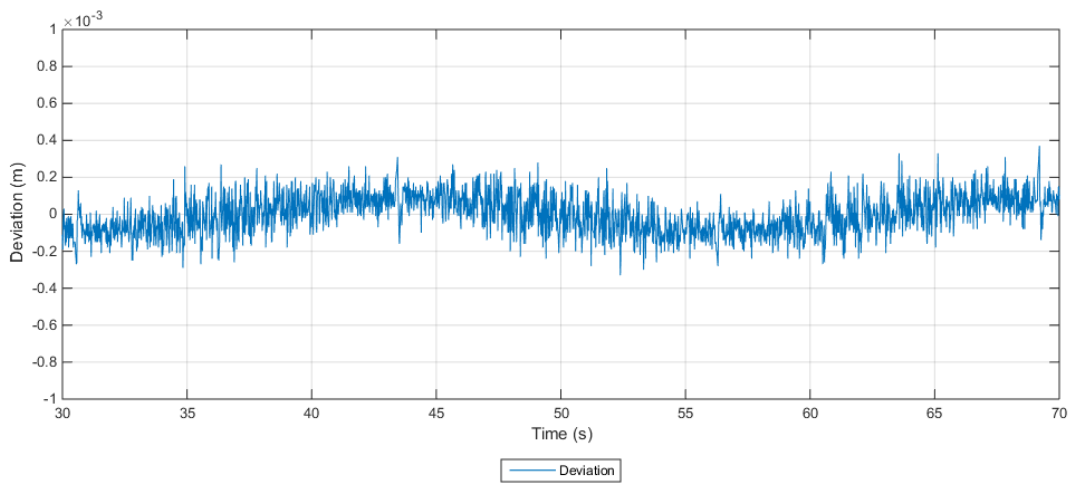
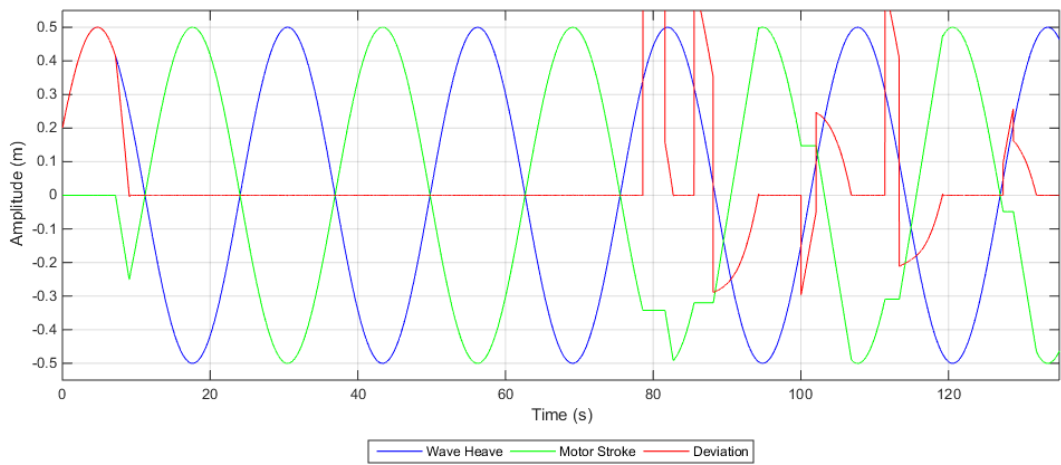
A.3.2 Load

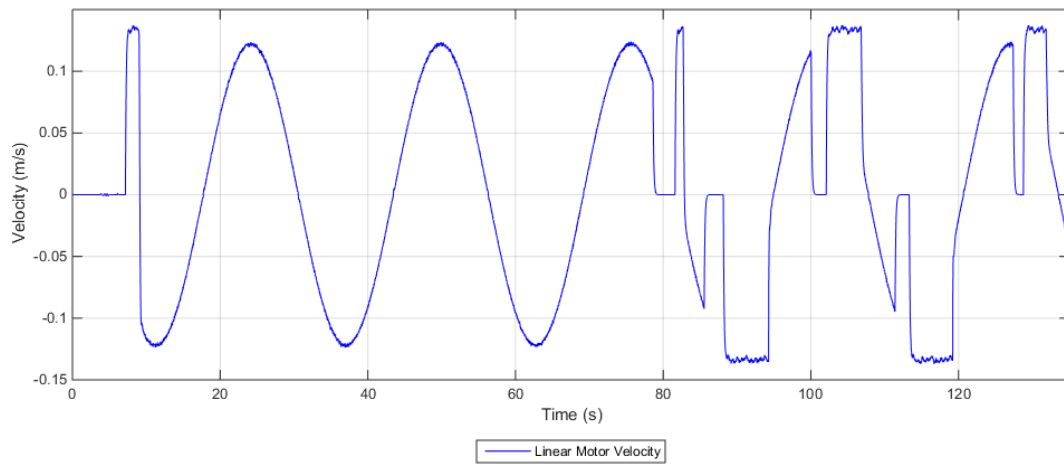
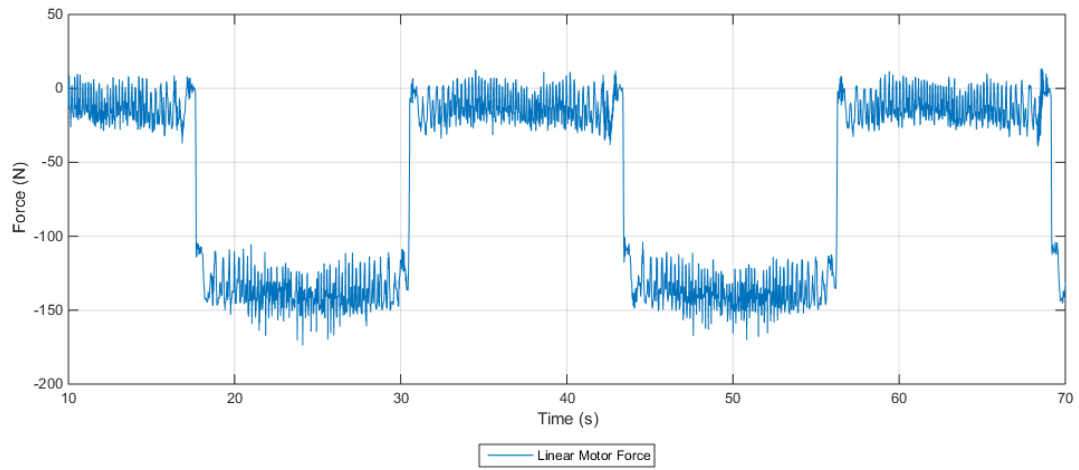




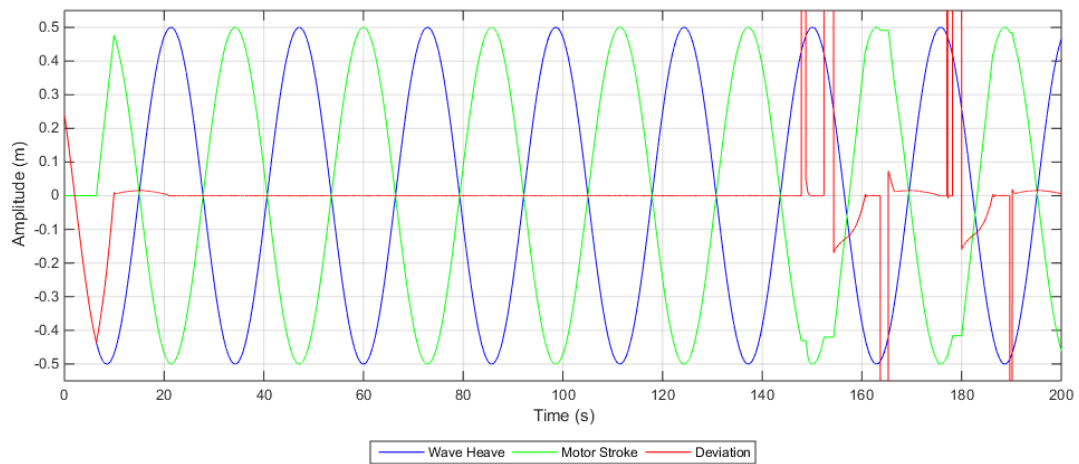
A.4 Wave Four

A.4.1 No Load

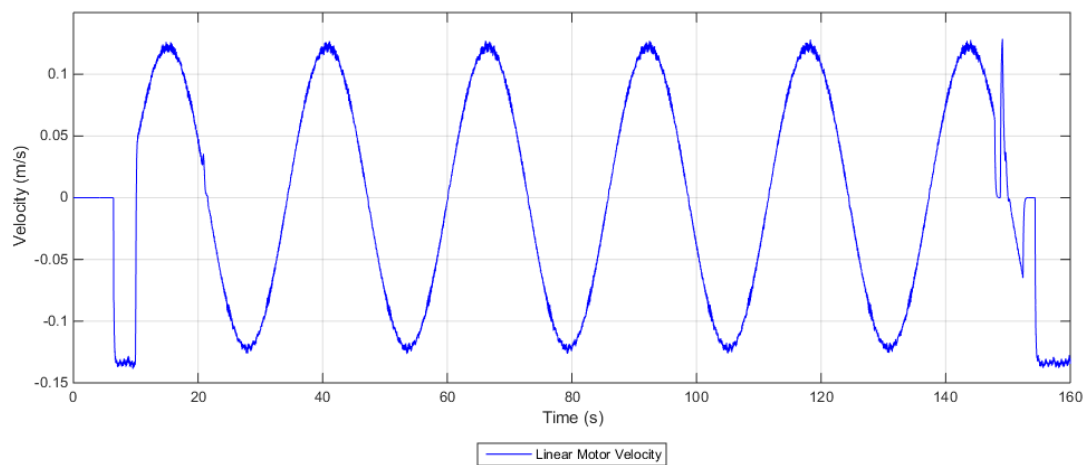
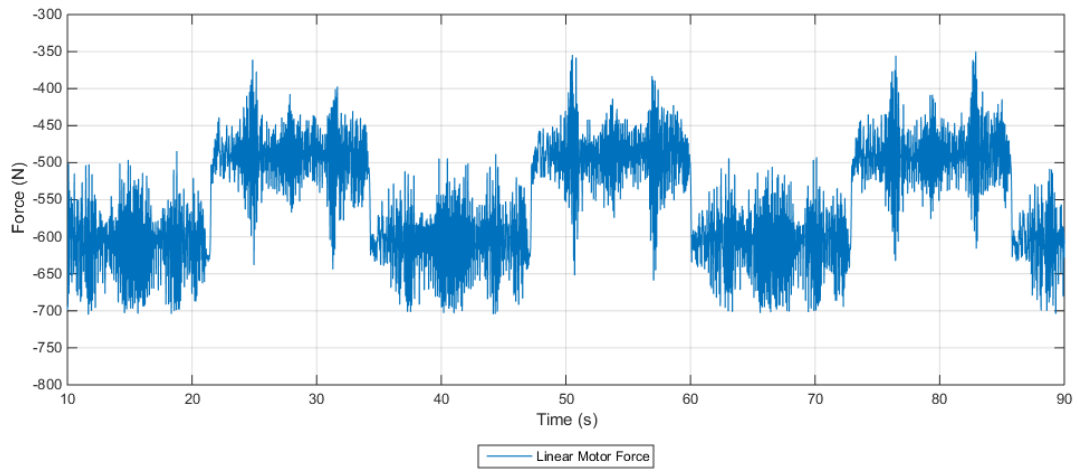
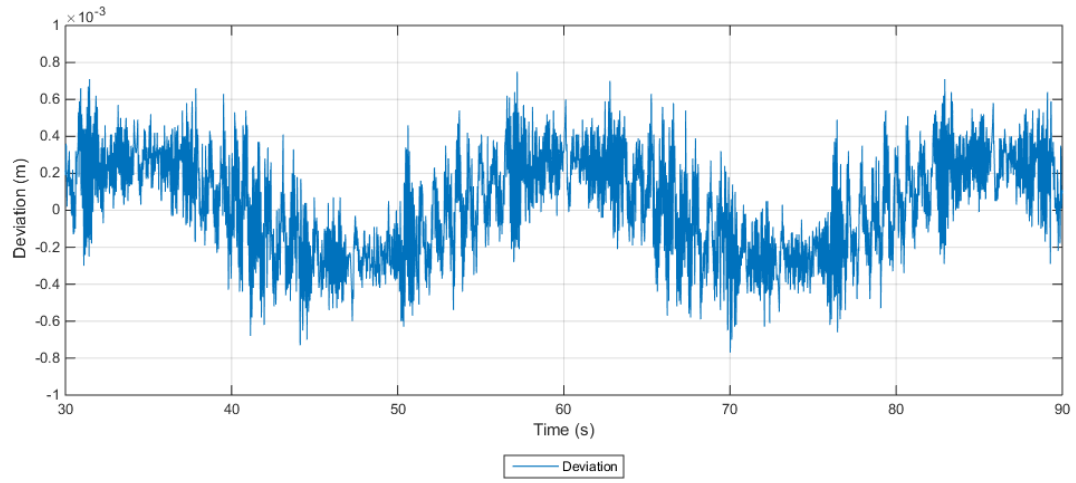




A.4.2 Load



APPENDIX A. TEST RESULTS



Appendix B

PLC Program - Linear Motor AHC

FC3 - <offline>

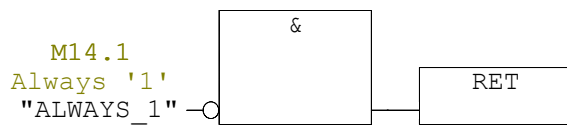
"APP_FAST"

Name: APP**Family:****Author:** STT**Version:** 0.1**Block version:** 2**Time stamp Code:** 05/29/2015 11:58:27 AM**Interface:** 04/14/2004 10:08:55 AM**Lengths (block/logic/data):** 00316 00204 00010

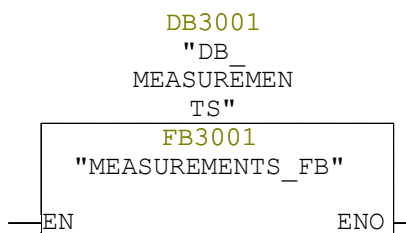
Name	Data Type	Address	Comment
IN		0.0	
OUT		0.0	
IN_OUT		0.0	
TEMP		0.0	
LoadCell_1	Real	0.0	
RETURN		0.0	
RET_VAL		0.0	

Block: FC3 Fast cycle

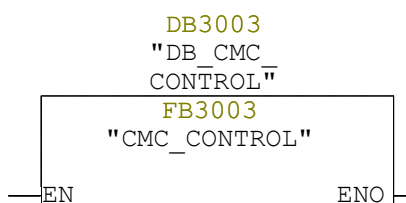
Network: 1 Start program



Network: 2 Analog inputs (ADDED NETWORK FOR MSC-PROJECT)



Network: 3 CMC Control (ADDED NETWORK FOR MSC-PROJECT)



Network: 4 MRU

DB702
GW Analog
measurement
interrupt
"DB_GW_
MRU"

FB702
GW
Analog
measurement
interrupt
"GW_MRU"

M10.0
Always
'0' Test
"ALWAYS_0
TEST"

EN ENO

Network: 5 GW regulation

GW4 Suspended

DB715
GW1 Winch
regulator
functions
"DB_GW1_
REG"

FB715
GW1
Winch
regulator
function
s
"GW1_
REG"

EN ENO

Network: 6 Log FB1000

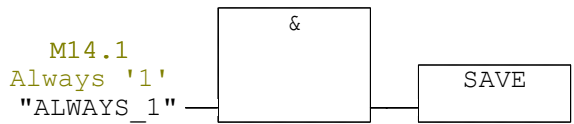
DB1000
"DB LOG"

FB1000
FB used
for
logging
purposes
"LOG_FB"

M14.1
Always '1'
"ALWAYS_1"

EN ENO

Network: 7 Update BR bit



FB3001 - <offline>

"MEASUREMENTS_FB"

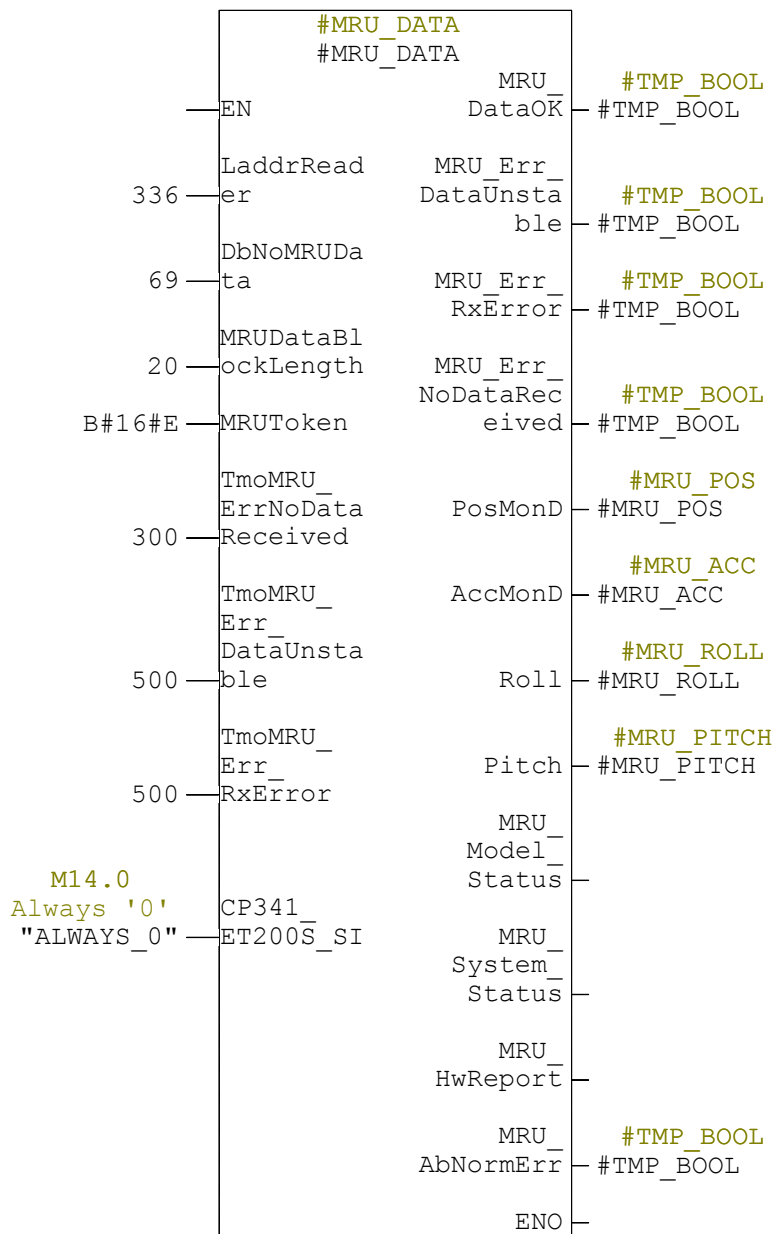
Name: **Family:**
Author: **Version:** 0.1
Block version: 2
Time stamp Code: 05/29/2015 10:33:36 AM
Interface: 05/22/2015 03:11:00 PM
Lengths (block/logic/data): 03268 01804 00048

Name	Data Type	Address	Initial Value	Comment
IN		0.0		
OUT		0.0		
IN_OUT		0.0		
STAT		0.0		
MRU_FILTER_MULTI	MRU_FILTER	0.0		
PT001	Real	122.0	0.000000e+000	
PT002	Real	126.0	0.000000e+000	
WT001	Real	130.0	0.000000e+000	
WT002	Real	134.0	0.000000e+000	
WT003	Real	138.0	0.000000e+000	
WT001_RAW	Real	142.0	0.000000e+000	
WT002_RAW	Real	146.0	0.000000e+000	
WT003_RAW	Real	150.0	0.000000e+000	
GT001	Real	154.0	0.000000e+000	
GT001_SPEED	Real	158.0	0.000000e+000	
WIRE_SPEED_GT001	STD_WINCH_SPEED	162.0		Speed of Slider
PT001_AIR_PRESSURE	ANA_IN	192.0		
PT002_OIL_PRESSURE	ANA_IN	238.0		
WT002_HOOK_LOAD	ANA_IN	284.0		
WT003_WOB	ANA_IN	330.0		
MRU_DATA	MRU_RS232_READ	376.0		
WT001_ACTUATING_FORCE	ANA_IN	840.0		
GT001_WIRE_ENCODER	SM_338_INP	886.0		
WT001_ERROR	Bool	1022.0	FALSE	
WT002_ERROR	Bool	1022.1	FALSE	
GT001_RESET	Bool	1022.2	FALSE	
MRU_SIM	Bool	1022.3	FALSE	MRU Simulator switch
WT001_FILTERED	Real	1024.0	0.000000e+000	
WT002_FILTERED	Real	1028.0	0.000000e+000	
WT003_FILTERED	Real	1032.0	0.000000e+000	
WT001_FILTER	AVERAGEING_FILTER	1036.0		
WT002_FILTER	AVERAGEING_FILTER	1090.0		
WT003_FILTER	AVERAGEING_FILTER	1144.0		
WT002_CHUBBY	Real	1198.0	0.000000e+000	
EST_MRU_HEAVE	Real	1202.0	0.000000e+000	
EST_MRU_SPEED	Real	1206.0	0.000000e+000	
EST_MRU_ACC	Real	1210.0	0.000000e+000	
MEAN_MRU_HEAVE	Real	1214.0	0.000000e+000	
EST_MRU_POS	Real	1218.0	0.000000e+000	
TEMP		0.0		
MRU_POS	Real	0.0		
MRU_ACC	Real	4.0		
MRU_ROLL	Real	8.0		
MRU_PITCH	Real	12.0		
WT_TMP	Real	16.0		
LoadCell_1	Real	20.0		
TMP_DINT	DInt	24.0		
TMP_BOOL	Bool	28.0		

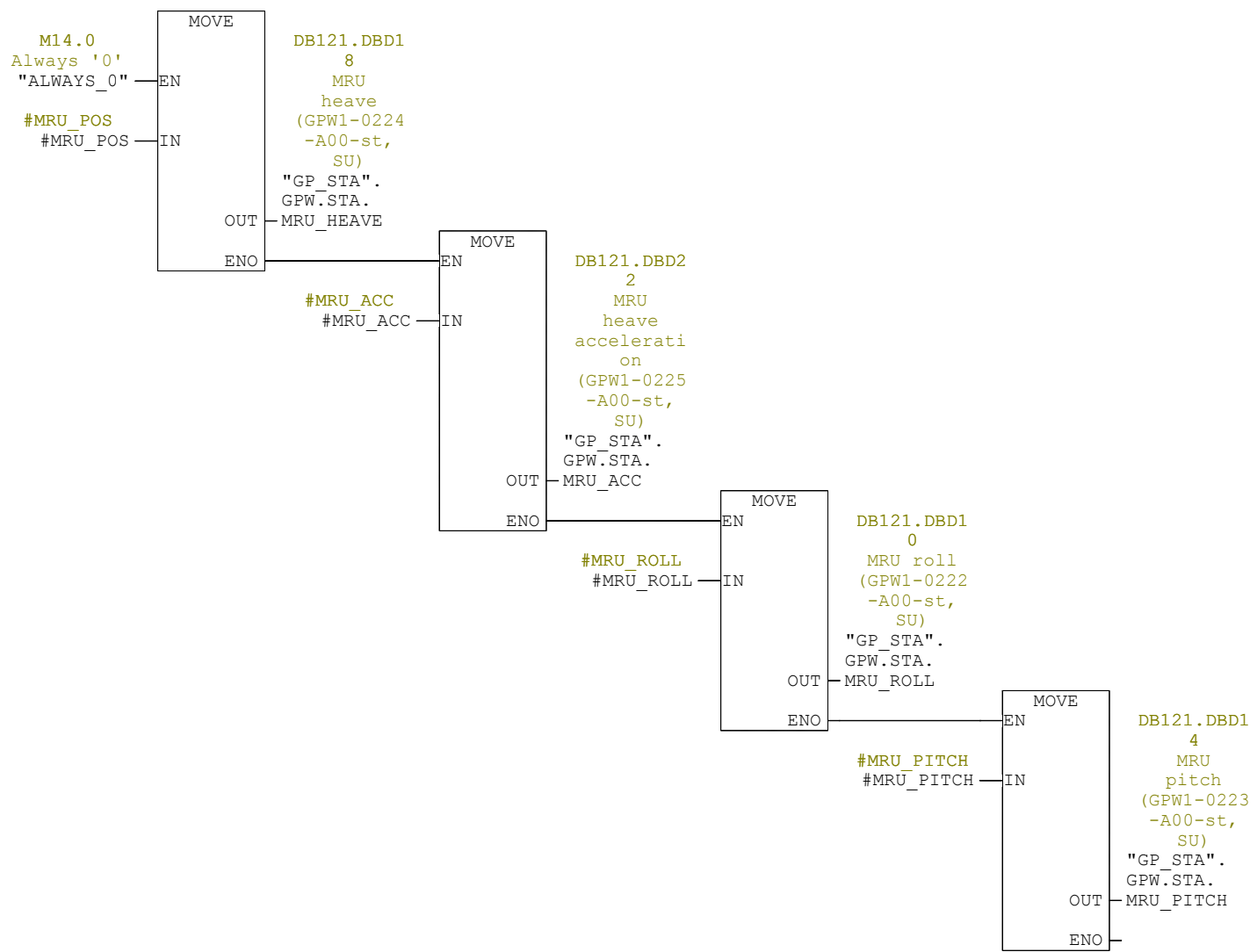
Name	Data Type	Address	Initial Value	Comment
TMP_INT	Int	30.0		
SCALE_VAL	Real	32.0		
TEMP1	Real	36.0		

Block: FB3001

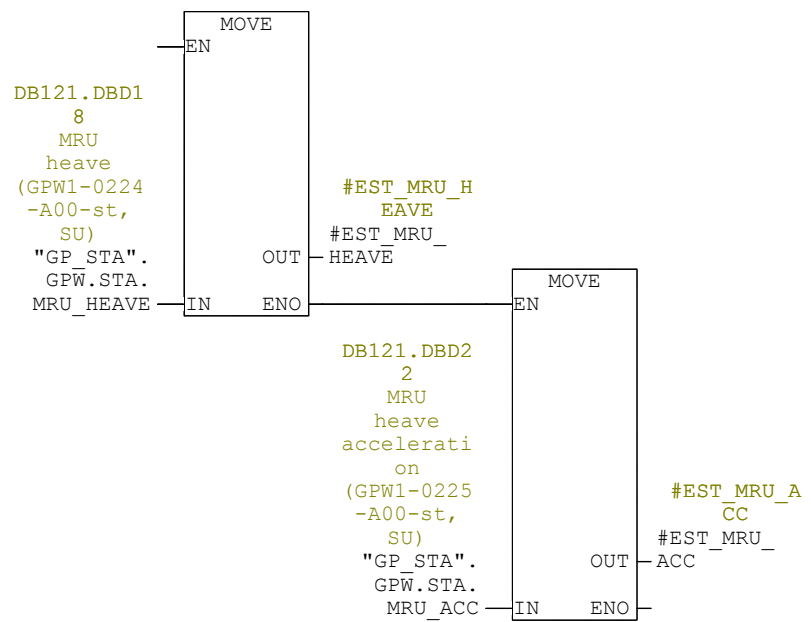
Network: 1 MRU Data interface



Network: 2 MRU interface



Network: 3



Network: 4 MRU filter calculation and AHC flow control

Active heave compensator control (AHC)

Following control system functions are implemented:

- Load compensation (pressure control)
- Position control (MRU estimate control)

This function block must run with the fixed scan rate of 10 ms (fast scan). The block should be connected to the AHC mode control block with the STATE terminal (struct). The AHC mode control block runs with plc scan rate. From STATE terminal, modes and transitions is transferred and used for control and setpoint calculations. The main output from this block is the Q setpoint for controlling AHC flow control valve

```

#MRU_FILTER_MULTI
#MRU_FILTER_MULTI

M14.0
Always '0'
"ALWAYS_0" --- EN

DB121.DBD1
0
MRU roll
(GPW1-0222
-A00-st,
SU)
"GP_STA".
GPW.STA.
MRU_ROLL --- MRUROLL

DB121.DBD1
4
MRU
pitch
(GPW1-0223
-A00-st,
SU)
"GP_STA".
GPW.STA.
MRU_PITCH --- MRUPITCH

DB121.DBD2
2
MRU
heave
accelerati
on
(GPW1-0225
-A00-st,
SU)
"GP_STA".
GPW.STA.
MRU_ACC --- MRUHACC

DB121.DBD1
8
MRU
heave
(GPW1-0224
-A00-st,
SU)
"GP_STA".
GPW.STA.
MRU_HEAVE --- MRUHEAVE

EST_HEAVE --- #EST_MRU_H
EAVE
#EST_MRU_
HEAVE

EST_SPEED --- #EST_MRU_S
PEED
#EST_MRU_
SPEED

EST_ACC --- #EST_MRU_A
CC
#EST_MRU_
ACC

0.000000e+
000 --- DLX
#MEAN_MRU_
HEAVE

MEAN_
HEAVE --- #MEAN_MRU_
HEAVE

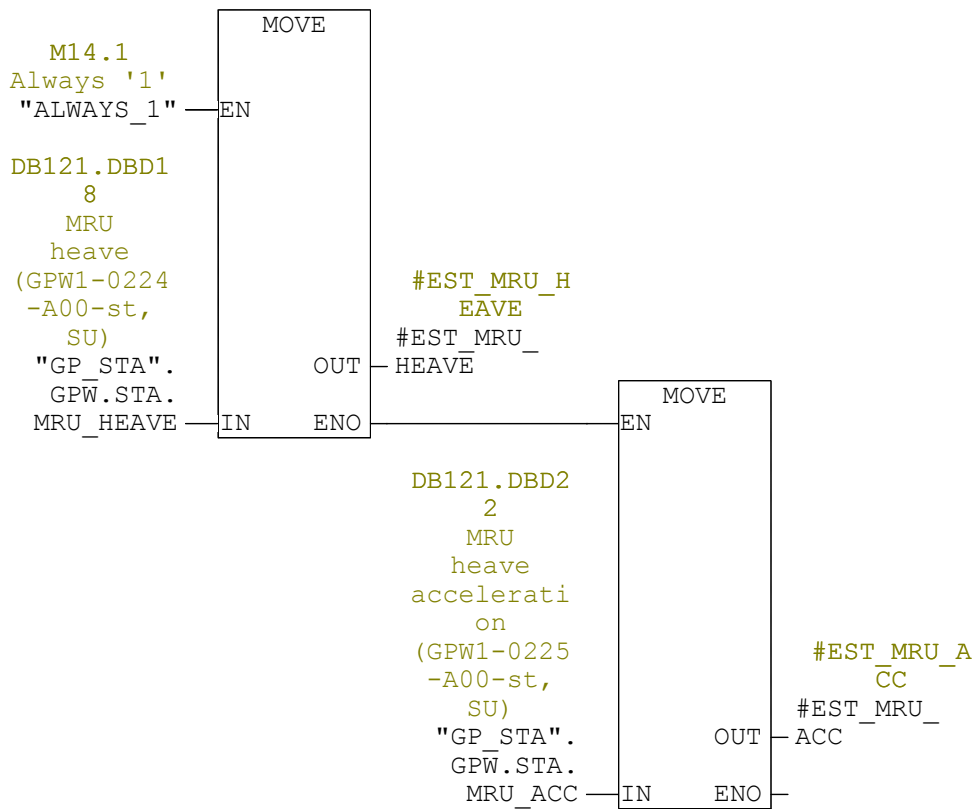
0.000000e+
000 --- DLY

0.000000e+
000 --- DLZ
#EST_MRU_P
OS
#EST_MRU_
POS

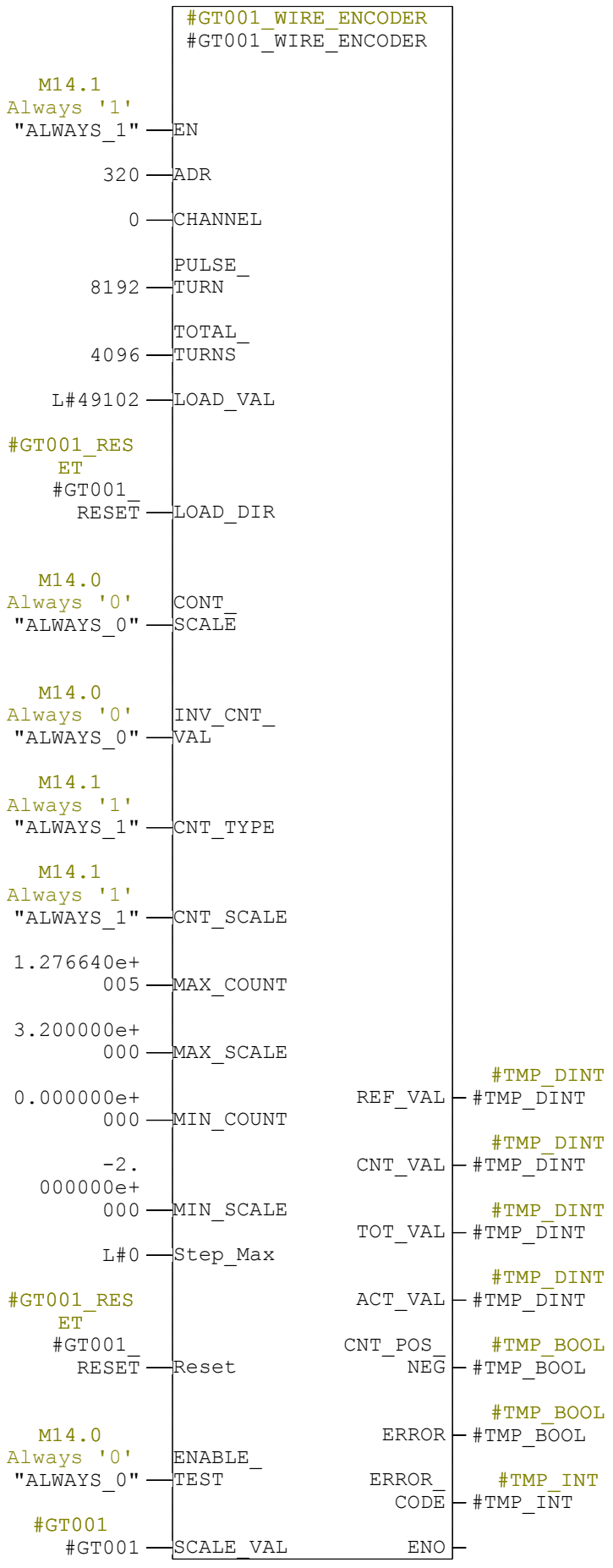
M14.1
Always '1'
"ALWAYS_1" --- DC t200s
ENO

```

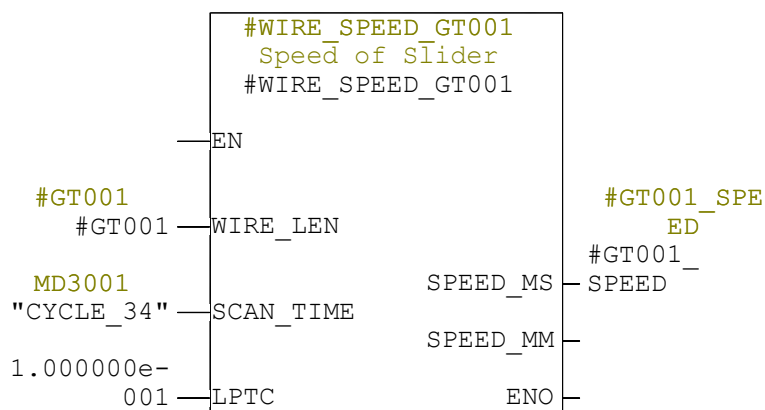
Network: 5



Network: 6 Wire Encoder

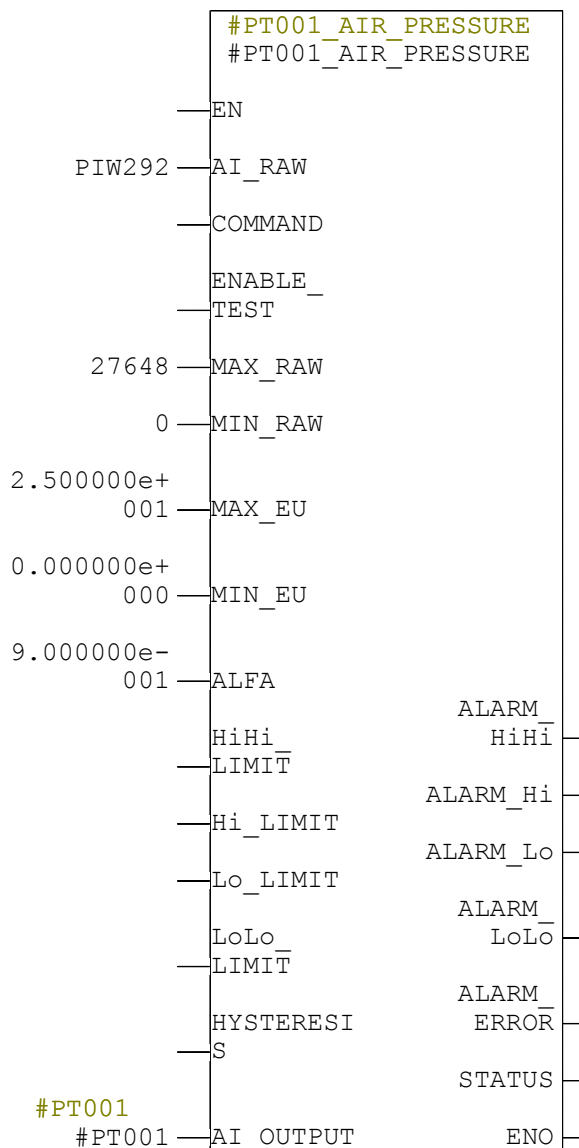


Network: 7 Calculate wire speed m/min

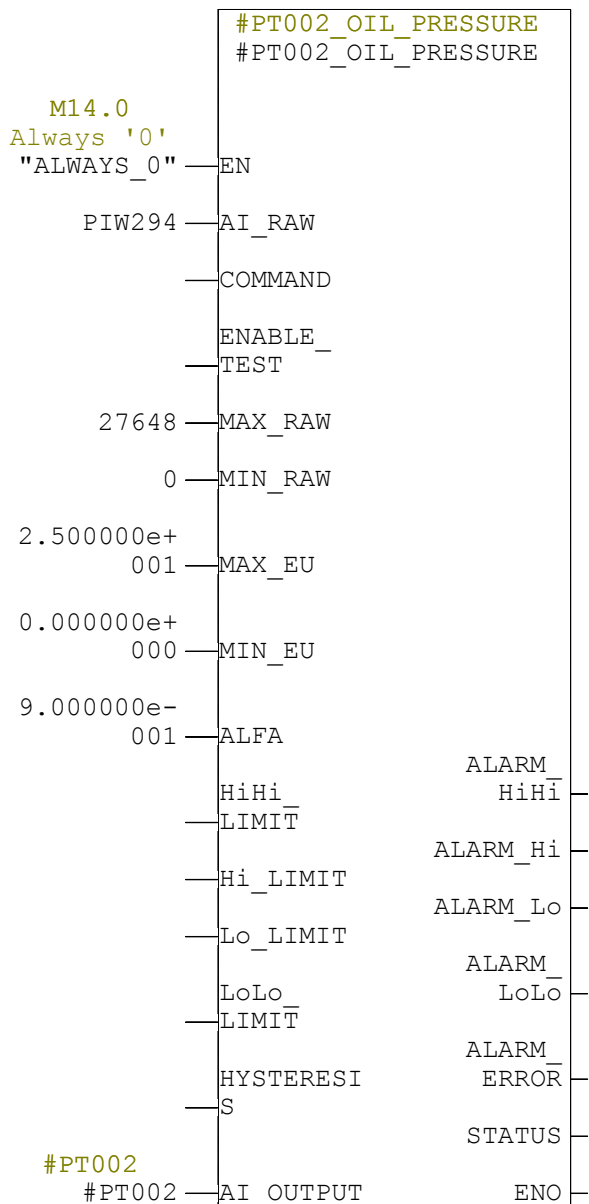


Network: 8 PT001

Pressure transmitter air

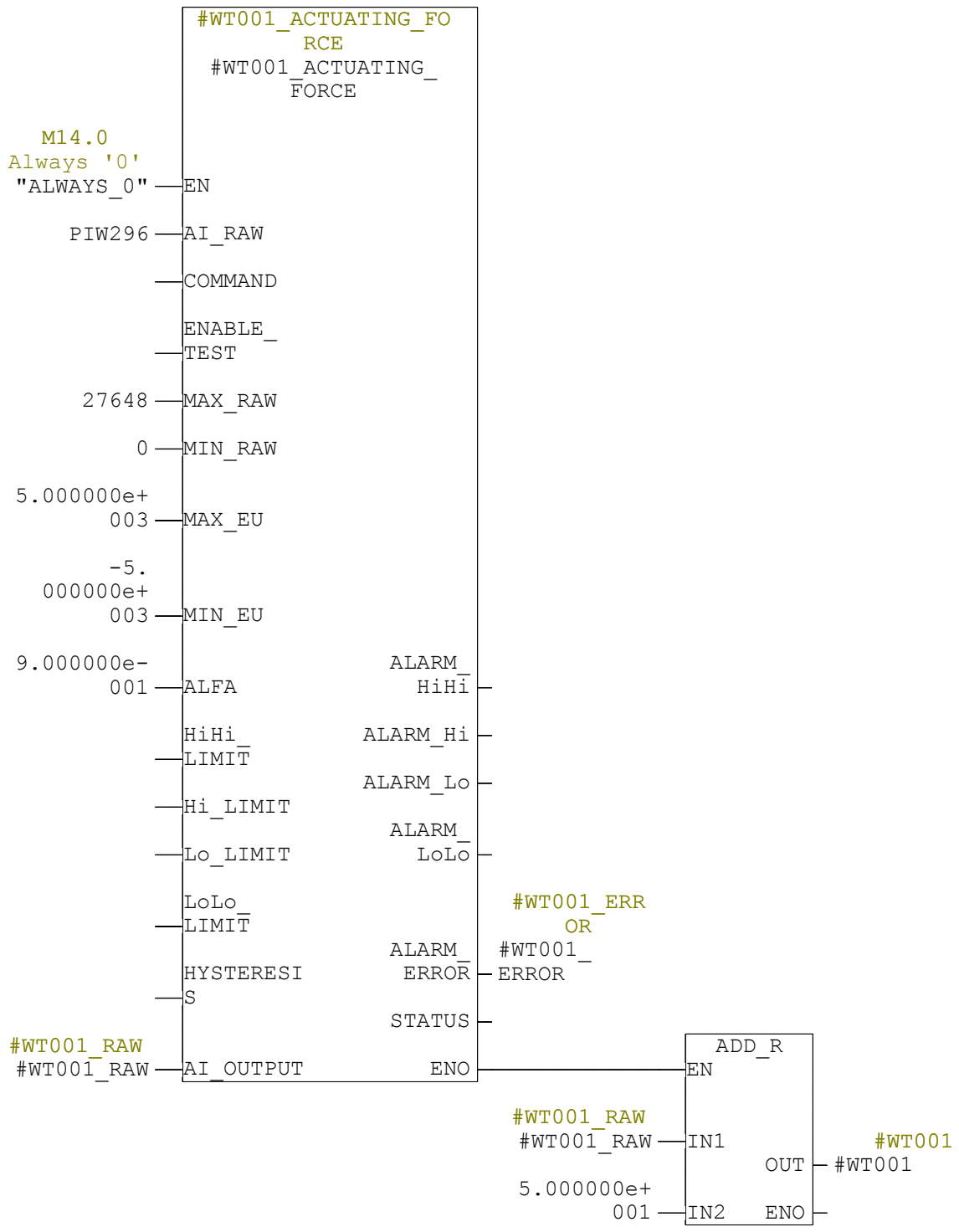


Network: 9	PT002
Pressure transmitter oil (glycol)	



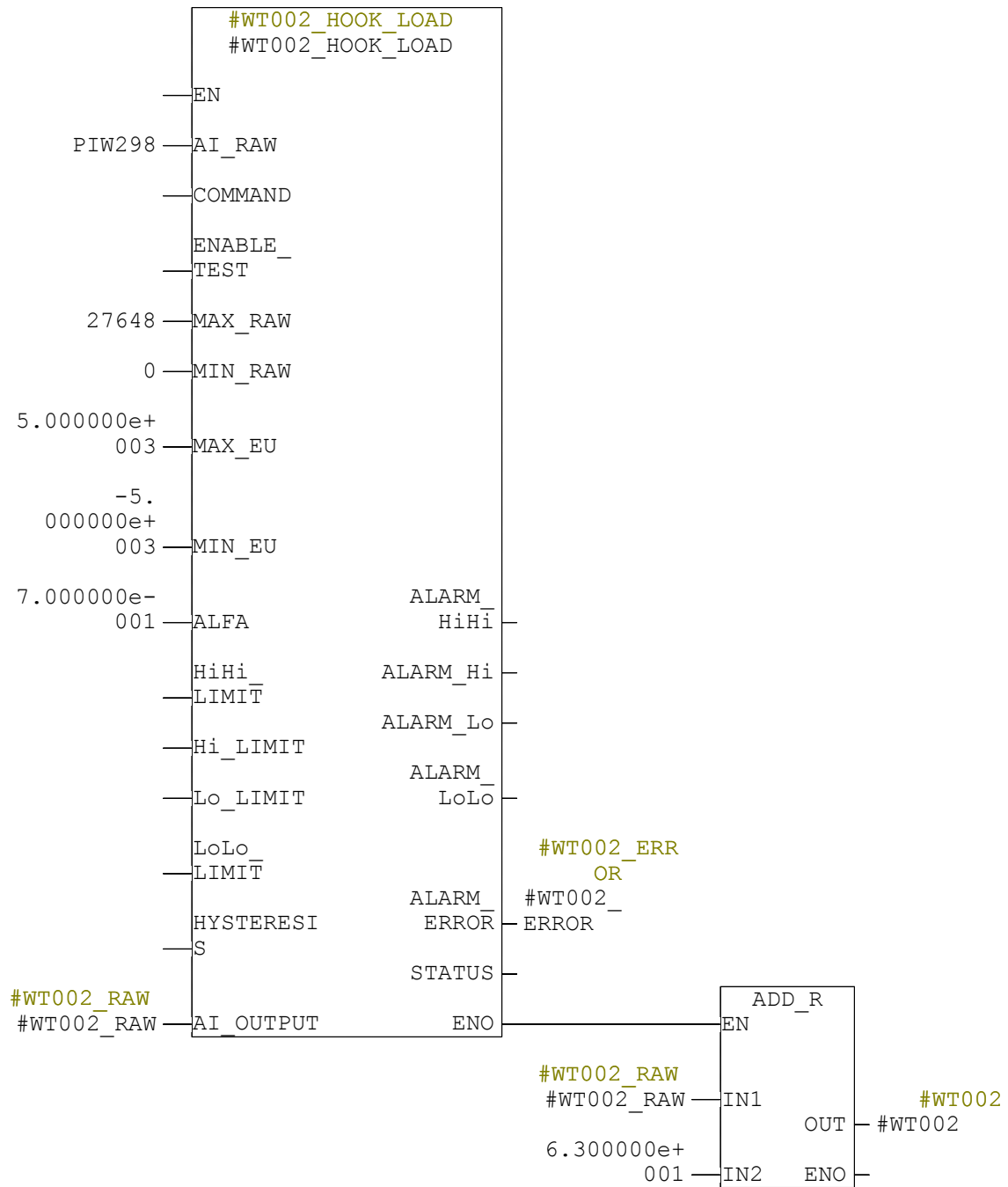
Network: 10 WT001

Loadcell rack actuating force
range 4-20mA = -500 - +500 kg.



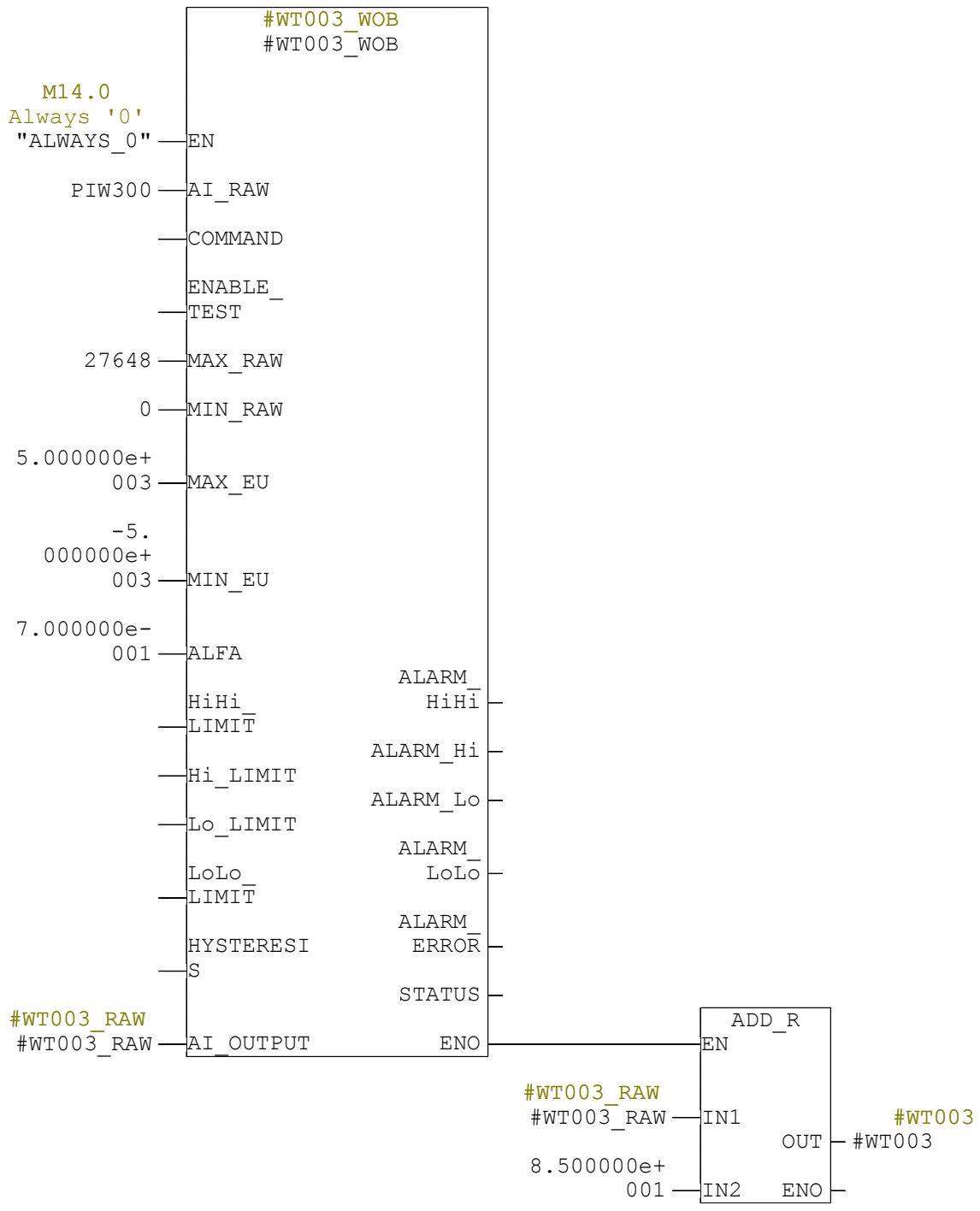
Network: 11 WT002

Loadcell hook load
range 4-20mA = -500 - +500 kg.

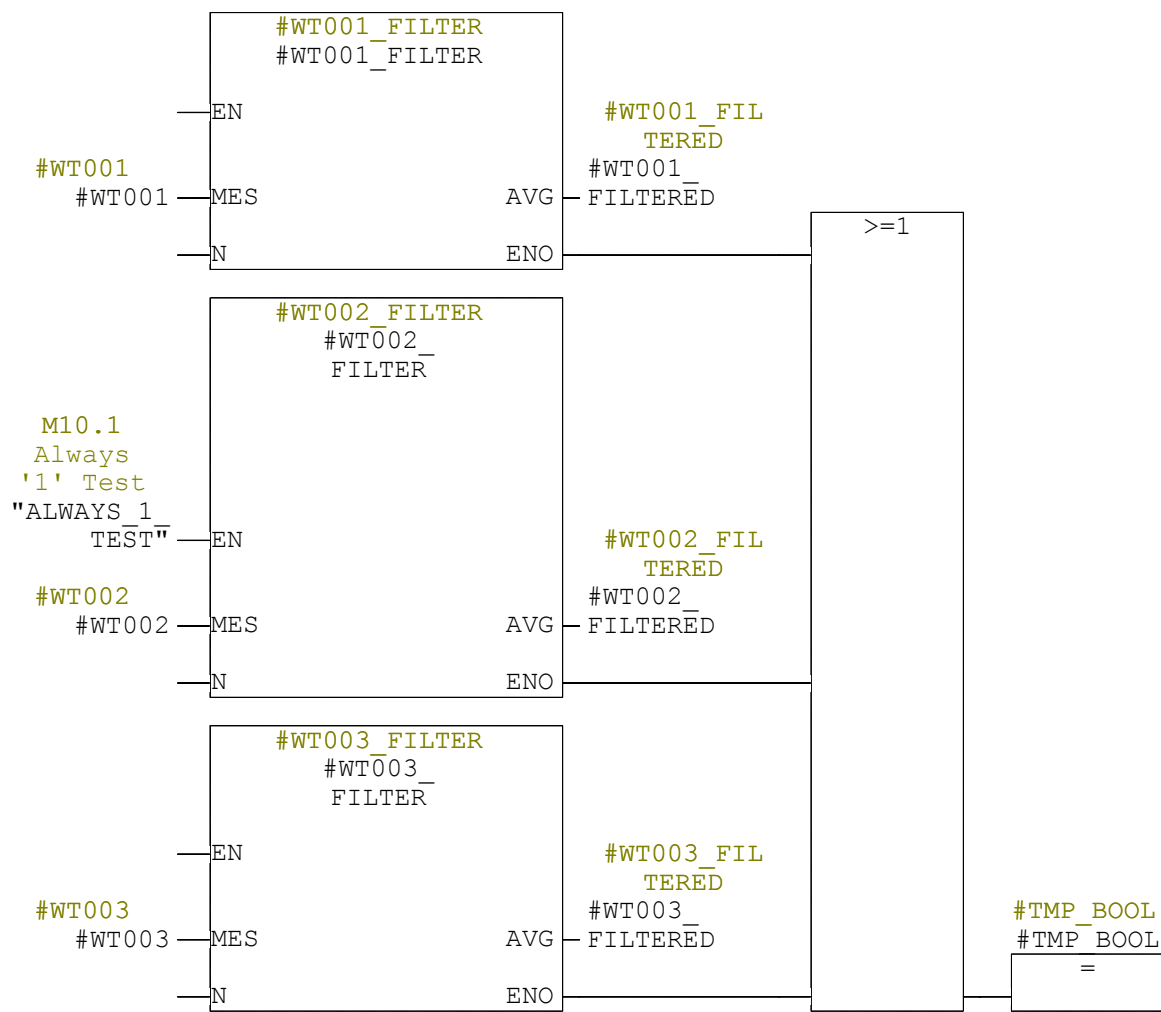


Network: 12 WT003

Loadcell actual weight on bit
range 4-20mA = -500 - +500 kg.



Network: 13 Filtered values



FB3003 - <offline>

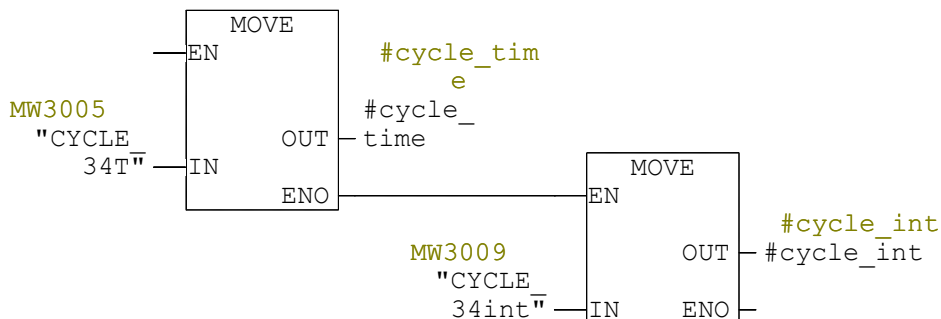
"CMC_CONTROL"

Name: **Family:**
Author: **Version:** 0.1
Time stamp Code: **Block version:** 2
 05/29/2015 10:38:45 PM
 Interface: 05/29/2015 12:43:22 PM
Lengths (block/logic/data): 01734 01438 00072

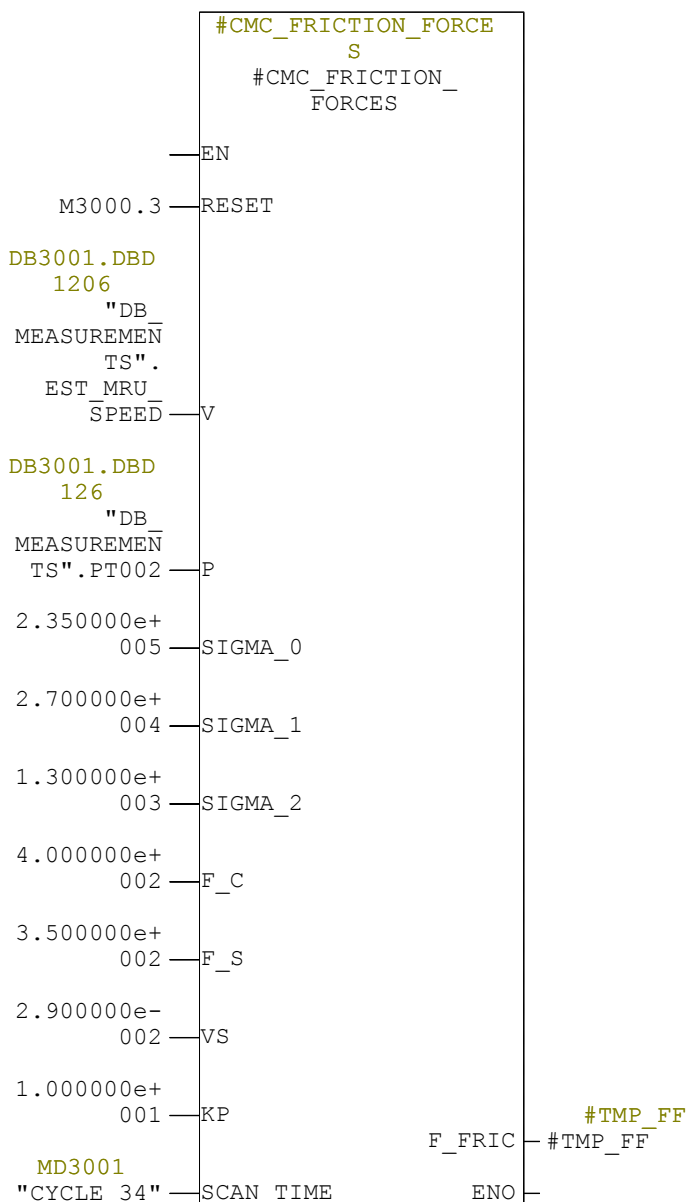
Name	Data Type	Address	Initial Value	Comment
IN		0.0		
OUT		0.0		
IN_OUT		0.0		
STAT		0.0		
CMC_FRICTION_FORCES	LUGRE_FRICTION	0.0		
VEL_LIMIT	Real	54.0	9.000000e+000	
CMC_FRICTION_FORCE	Real	58.0	0.000000e+000	
FF_EN	Bool	62.0	FALSE	
FB_EN	Bool	62.1	FALSE	
TEST_EN	Bool	62.2	FALSE	
FORCE_MODE	Bool	62.3	FALSE	
FORCE_MODE_ACTIVE	Bool	62.4	FALSE	
SET_STARTPOINT	Bool	62.5	FALSE	
I_SELECT	Bool	62.6	FALSE	
FB_P_GAIN	Real	64.0	1.000000e+000	
LM_VEL	Real	68.0	0.000000e+000	
AHC_DEVIATION	Real	72.0	0.000000e+000	
AHC_DEVIATION_MM	Real	76.0	0.000000e+000	
STARTPOINT_POS	Real	80.0	0.000000e+000	
POS_P_GAIN	Real	84.0	0.000000e+000	
VEL_P_GAIN	Real	88.0	0.000000e+000	
POS_I_GAIN	Time	92.0	T#0MS	
POS_FB	Real	96.0	0.000000e+000	
VEL_I_GAIN	Time	100.0	T#0MS	
TEMP		0.0		
TMP_REAL	Real	0.0		
TMP_FF	Real	4.0		
TMP_FB	Real	8.0		
TMP_REAL2	Real	12.0		
TMP_FB_RACK	Real	16.0		
TMP_BOOL	Bool	20.0		
cycle_time	Time	22.0		
cycle_int	Int	26.0		
TMP_POS_SP	Real	28.0		
TMP_FORCE_SP	Real	32.0		
TMP_LM_VEL	Real	36.0		
TMP_POS_FB	Real	40.0		
TMP_VEL_SP	Real	44.0		
TMP_FAST_POS	Bool	48.0		
TMP_FAST_NEG	Bool	48.1		
TMP_VEL_LIMIT_POS	Real	50.0		
TMP_VEL_LIMIT_NEG	Real	54.0		
TMP_VEL_FF	Real	58.0		
TMP_I_ON	Bool	62.0		

Block: FB3003

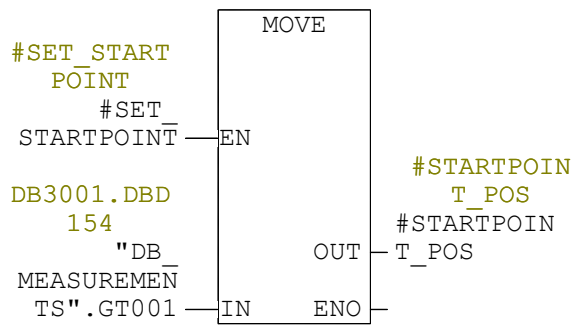
Network: 1



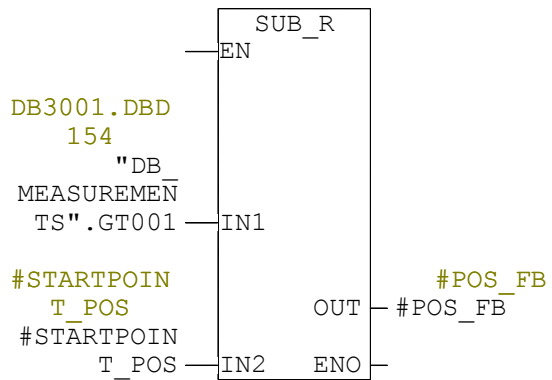
Network: 2 Feed forward (CT) Force



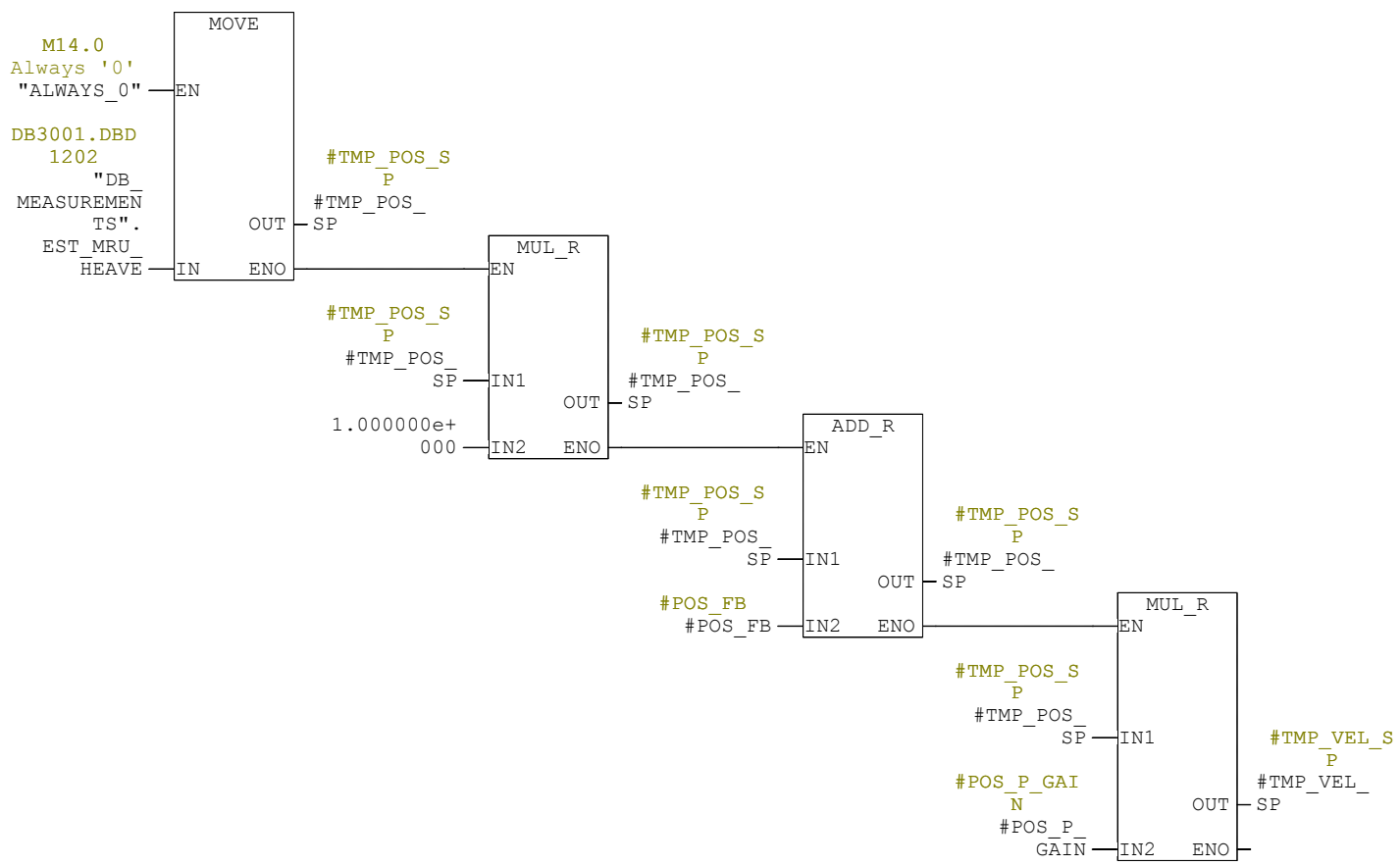
Network: 3 Save starting point



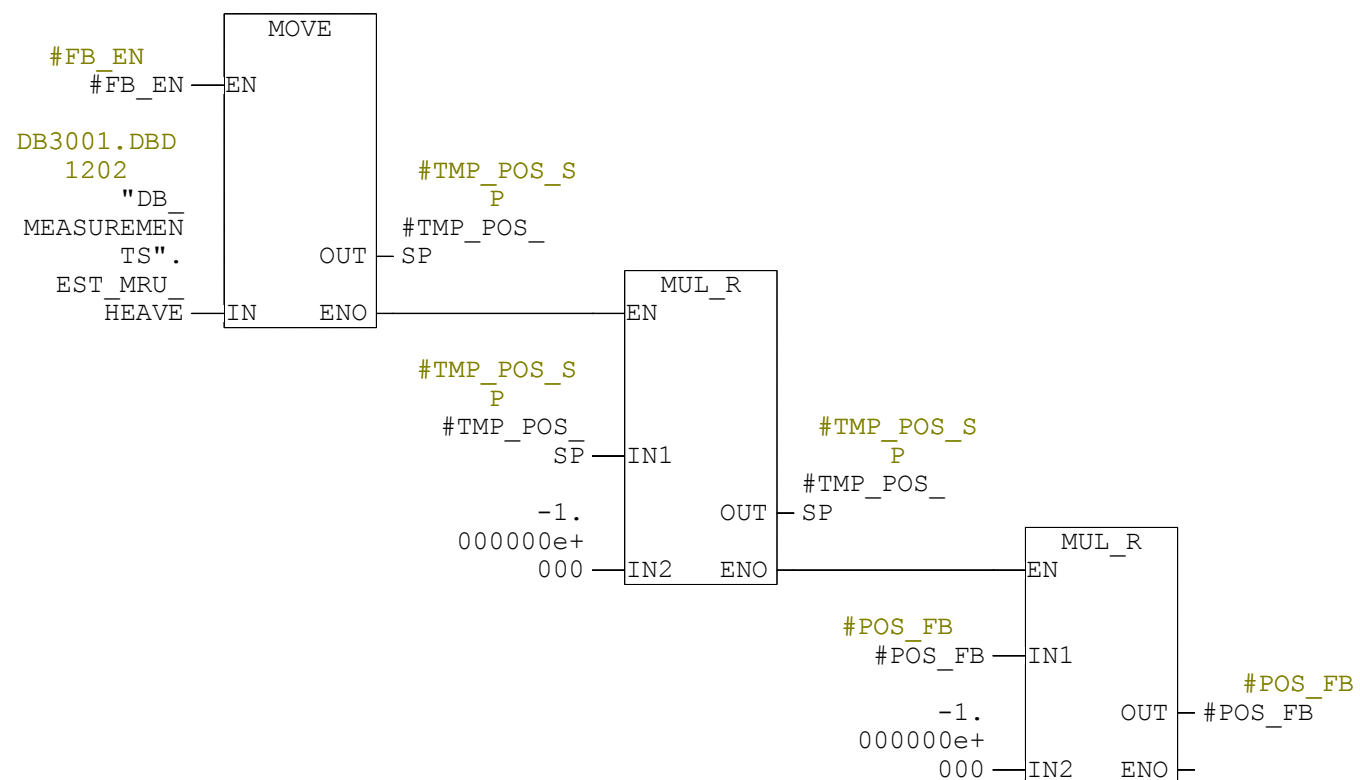
Network: 4 Adjust wire encoder signal according to start position



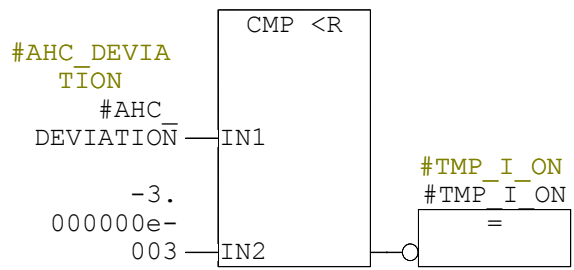
Network: 5 Position setpoint and position P controller



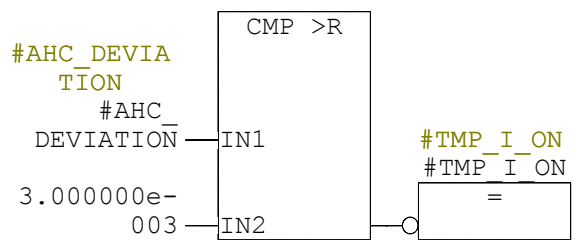
Network: 6 Setpoint and feedback initialization for position controller



Network: 7 Integrator switch 1



Network: 8 Integrator switch 2

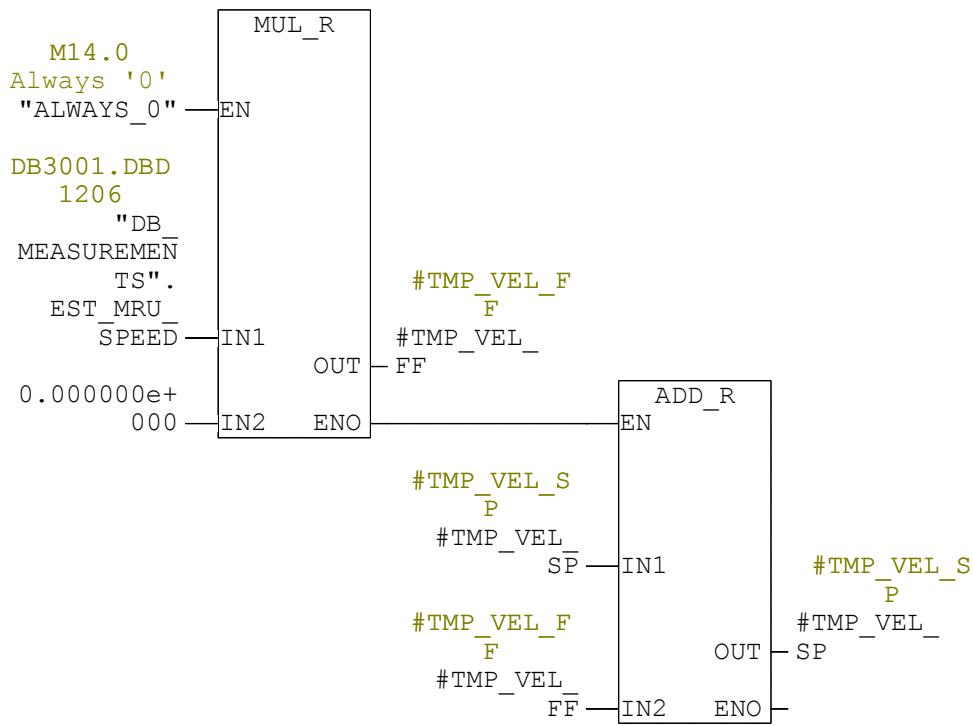


Network: 9	Position PI controller
------------	------------------------

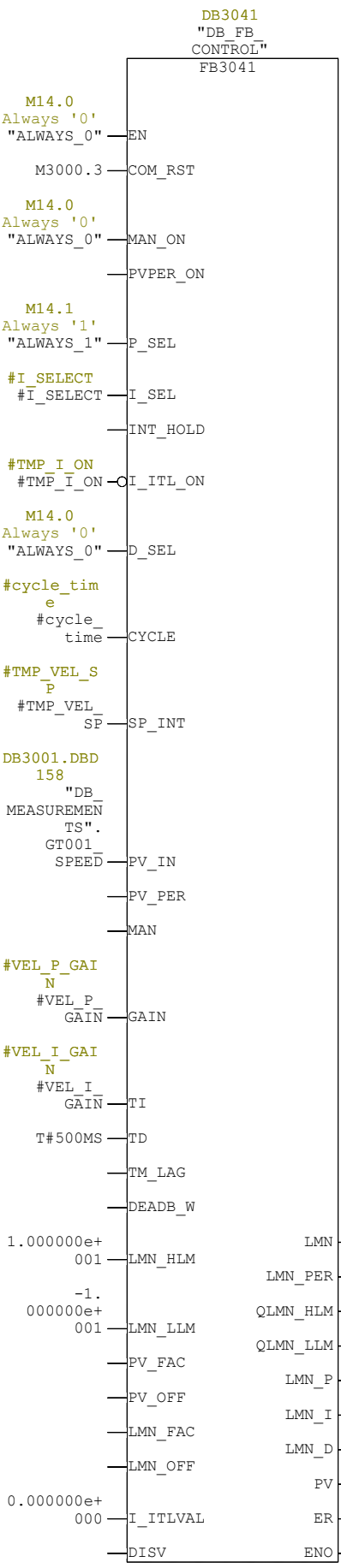
DB3041
"DB_FB
CONTROL"
FB3041

#FB_EN	#FB_EN	EN	
M3000.3	COM_RST		
M14.0			
Always '0'	"ALWAYS_0"	MAN_ON	
		PVPER_ON	
M14.1			
Always '1'	"ALWAYS_1"	P_SEL	
#I_SELECT	#I_SELECT	I_SEL	
		INT_HOLD	
#TMP_I_ON	#TMP_I_ON	OI_ITL_ON	
M14.0			
Always '0'	"ALWAYS_0"	D_SEL	
#cycle_time	#cycle_time	CYCLE	
#TMP_POS_S	#TMP_POS_S	SP_INT	
#POS_FB	#POS_FB	PV_IN	
		PV_PER	
		MAN	
#POS_P_GAIN	#POS_P_GAIN	GAIN	
#POS_I_GAIN	#POS_I_GAIN	TI	
T#500MS		TD	
		TM_LAG	
		DEADB_W	
1.000000e+001		LMN_HLM	#TMP_LM_VE L #TMP_LM_ VEL
		LMN_PER	
-1.000000e+001		LMN_LLM	QLMN_HLM
		PV_FAC	QLMN_LLM
		PV_OFF	LMN_P
		LMN_FAC	LMN_I
		LMN_OFF	LMN_D
0.000000e+000		I_ITLVAL	PV
		DISV	ER
			ENO

Network: 10 Wave Velocity Feed Forward

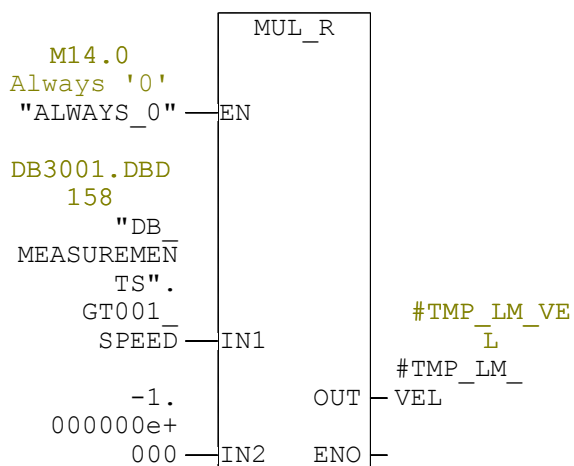


Network: 11 Velocity PI Controller

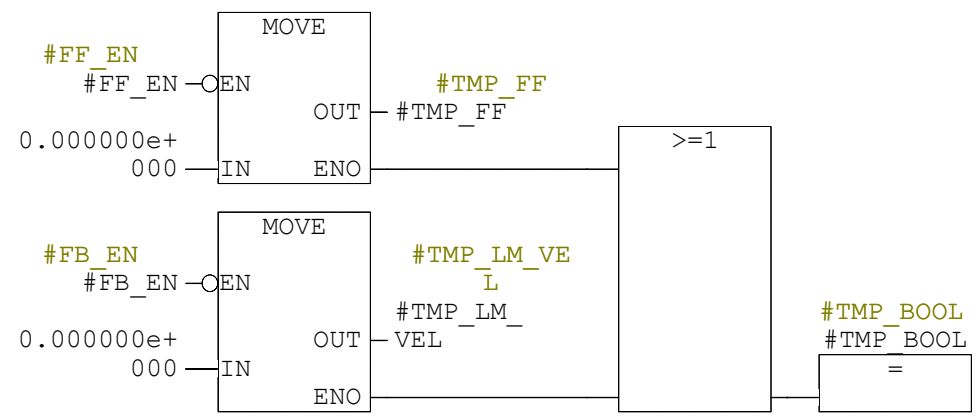


#TMP_LM_VE
L
#TMP_LM_

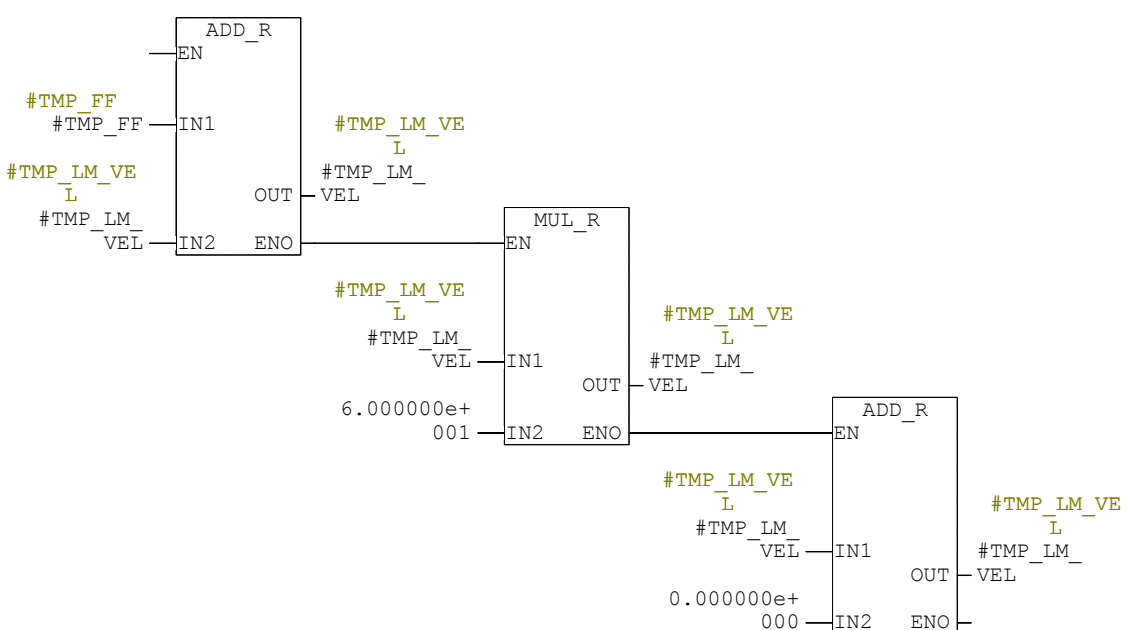
Network: 12 For running on a velocity setpoint with wire encoder to ground



Network: 13 Set velocity to zero when control is not active



Network: 14 Velocity output in m/min



FB1000 - <offline>

"LOG_FB" FB used for logging purposes
Name: **Family:**
Author: **Version:** 0.1
 Block version: 2
Time stamp Code: 05/29/2015 10:36:09 AM
 Interface: 05/26/2015 01:22:41 PM
Lengths (block/logic/data): 00712 00524 00000

Name	Data Type	Address	Initial Value	Comment
IN		0.0		
OUT		0.0		
IN_OUT		0.0		
STAT		0.0		
GW_1_emergency_stop	Bool	0.0	FALSE	
GW1_OVERLOAD_125	Bool	0.1	FALSE	
HOOK_LIMIT_DOWN	Bool	0.2	FALSE	
HOOK_LIMIT_UP	Bool	0.3	FALSE	
NORMAL_MODE	Bool	0.4	FALSE	
AHC_MODE	Bool	0.5	FALSE	
CT_MODE	Bool	0.6	FALSE	
JOYSTICK_CENTER	Bool	0.7	FALSE	
WIRE_SPEED	Real	2.0	0.000000e+000	
WIRE_ON_DRUM	Real	6.0	0.000000e+000	
TIP_POS	Real	10.0	0.000000e+000	
REGULATOR_ERROR	Real	14.0	0.000000e+000	
WIRE_POS_INVERTED	Real	18.0	0.000000e+000	
ACTUAL_LOAD	Real	22.0	0.000000e+000	
SPEED_SP_RPM	Real	26.0	0.000000e+000	
ACTUAL_SPEED	Real	30.0	0.000000e+000	
CT_SP_NM	Real	34.0	0.000000e+000	
ACTUAL_TORQUE	Real	38.0	0.000000e+000	
BRAKE_RELEASED	Bool	42.0	FALSE	
ACCELERATION_TORQUE	Real	44.0	0.000000e+000	
TEMPERATURE	Real	48.0	0.000000e+000	
DC_VOLT	Real	52.0	0.000000e+000	
CONTROL_FB	Real	56.0	0.000000e+000	
MOT_TEMP_C	Real	60.0	0.000000e+000	
MOT_SPEED_RPM	Real	64.0	0.000000e+000	
LuGre_Friction_Force	Real	68.0	0.000000e+000	
GT001	Real	72.0	0.000000e+000	
GT001_SPEED	Real	76.0	0.000000e+000	
PT001	Real	80.0	0.000000e+000	
PT002	Real	84.0	0.000000e+000	
WT001	Real	88.0	0.000000e+000	
WT002	Real	92.0	0.000000e+000	
WT003	Real	96.0	0.000000e+000	
MRU_Filtered_Heave	Real	100.0	0.000000e+000	
MRU_Heave	Real	104.0	0.000000e+000	
EST_MRU_HEAVE	Real	108.0	0.000000e+000	
EST_MRU_SPEED	Real	112.0	0.000000e+000	
EST_MRU_ACC	Real	116.0	0.000000e+000	
MEAN_MRU_HEAVE	Real	120.0	0.000000e+000	
RACK_PAYOUT	Real	124.0	0.000000e+000	
RACK_SPEED	Real	128.0	0.000000e+000	
WT001_FILTERED	Real	132.0	0.000000e+000	
WT002_FILTERED	Real	136.0	0.000000e+000	
WT003_FILTERED	Real	140.0	0.000000e+000	

Name	Data Type	Address	Initial Value	Comment
LM_VEL	Real	144.0	0.000000e+000	
AHC_DEVIATION	Real	148.0	0.000000e+000	
LM_ACTUAL_VEL	Real	152.0	0.000000e+000	
LM_ACTUAL_FORCE	Real	156.0	0.000000e+000	
TEMP		0.0		

Block: FB1000 Plc-Log setupfile...

```
#0;2
@0;192.168.10.99
NORMAL_MODE 121 155 1;1000;0;1;4
AHC_MODE 121 155 2;1000;0;1;5
ACTUAL_TORQUE 121 412;1000;38;2;0
DC_VOLT 121 550;1000;52;2;0
CONTROL_FB 3041 72;1000;56;2;0
MOT_SPEED_RPM 121 396;1000;64;2;0
LuGre Friction Force 3003 40;1000;68;2;0
GT001_3001 154;1000;72;2;0
GT001_SPEED 3001 158;1000;76;2;0
MRU_Filtered Heave 3001 34;1000;100;2;0
MRU_Heave 3001 12;1000;104;2;0
EST_MRU_HEAVE 3001 34;1000;108;2;0
EST_MRU_SPEED 3001 38;1000;112;2;0
EST_MRU_ACC 3001 42;1000;116;2;0
MEAN_MRU_HEAVE 3001 46;1000;120;2;0
LM_VEL 3003 68;1000;144;2;0
AHC_DEVIATION 3003 72;1000;148;2;0
LM_ACTUAL_VEL 121 478;1000;152;2;0
LM_ACTUAL_FORCE 121 498;1000;156;2;0
```

Network: 1 Map data in to DB1000

```
A      "GP_STA".GW1.ALM.EMG_STP          DB121.DBX150.0      -- GW1 Emergency
=      #GW_1_emergency_stop              #GW_1_emergency_stop
A      "GP_STA".GW1.ALM.OVER_LOAD_SWL    DB121.DBX150.2      -- GW1 Overload 1
=      #GW1_OVERLOAD_125                 #GW1_OVERLOAD_125
A      "GP_STA".GW1.ALM.HOOK_DN          DB121.DBX151.1      -- GW1 Hook limit
=      #HOOK_LIMIT_DOWN                  #HOOK_LIMIT_DOWN
A      "GP_STA".GW1.ALM.HOOK_UP          DB121.DBX151.2      -- GW1 Hook limit
=      #HOOK_LIMIT_UP                    #HOOK_LIMIT_UP
A      "GP_STA".GW1.STA.NORM_MODE_STA     DB121.DBX155.1      -- GW1 Normal mod
=      #NORMAL_MODE                      #NORMAL_MODE
A      "GP_STA".GW1.STA.HC_MODE_STA       DB121.DBX155.2      -- GW1 Heave comp
=      #AHC_MODE                          #AHC_MODE
A      "GP_STA".GW1.STA.CT_MODE_STA       DB121.DBX155.3      -- GW1 Constant t
=      #CT_MODE                           #CT_MODE
A      "GP_STA".GW1.STA.JS_0              DB121.DBX158.0      -- GW1 Joystick z
=      #JOYSTICK_CENTER                  #JOYSTICK_CENTER
L      "GP_STA".GW1.STA.WIRE_SPEED        DB121.DBD176        -- GW1 Winch wire
T      #WIRE_SPEED                        #WIRE_SPEED
L      "GP_STA".GW1.STA.ACT_LEN           DB121.DBD216        -- GW1 Winch actu
T      #WIRE_ON_DRUM                      #WIRE_ON_DRUM
L      "GP_STA".GW1.STA.TIP_POS           DB121.DBD272        -- GW1 Tip positi
T      #TIP_POS                           #TIP_POS
```

```

L   "GP_STA".GW1.STA.HC_ERR          DB121.DBD300      -- GW1 Heave cont
T   #REGULATOR_ERROR                #REGULATOR_ERROR
L   "GP_STA".GW1.STA.WIRE_POS_INV    DB121.DBD316      -- GW1 Wire posit
T   #WIRE_POS_INVERTED              #WIRE_POS_INVERTED
L   "GP_STA".GW1.STA.LOAD           DB121.DBD348      -- GW1 Actual loa
T   #ACTUAL_LOAD                    #ACTUAL_LOAD
L   "GP_STA".GW1.STA.MOT_SP_RPM     DB121.DBD392      -- GW1 Motor setp
T   #SPEED_SP_RPM                  #SPEED_SP_RPM
L   "GP_STA".GW1.STA.MOT_SPEED_RPM  DB121.DBD396      -- GW1 Motor spee
T   #ACTUAL_SPEED                  #ACTUAL_SPEED
L   "GP_STA".GW1.STA.MOT_SP_NM      DB121.DBD404      -- GW1 Motor setp
T   #CT_SP_NM                      #CT_SP_NM
L   "GP_STA".GW1.STA.MOT_TORQUE     DB121.DBD412      -- GW1 Motor torq
T   #ACTUAL_TORQUE                 #ACTUAL_TORQUE
A   "GP_STA".GW1.M1.STA.BRAKE_REL    DB121.DBX464.5    -- GW1 Motor 1 br
=   #BRAKE_RELEASED                #BRAKE_RELEASED
L   "GP_STA".GW1.M1.STA.TORQUE_ACC_NM DB121.DBD506      -- GW1 Motor 1 ac
T   #ACCELERATION_TORQUE           #ACCELERATION_TORQUE
L   "GP_STA".GW1.M1.STA.TEMP        DB121.DBD546      -- GW1 Motor 1 te
T   #TEMPERATURE                   #TEMPERATURE
L   "GP_STA".GW1.M1.STA.DC_BUS      DB121.DBD550      -- GW1 Motor 1 DC
T   #DC_VOLT                       #DC_VOLT
L   "DB_FB_CONTROL".LMN            DB3041.DBD72      -- manipulated val
T   #CONTROL_FB                    #CONTROL_FB
L   "GP_STA".GW1.M1.STA.TEMP        DB121.DBD546      -- GW1 Motor 1 te
T   #MOT_TEMP_C                    #MOT_TEMP_C
L   "GP_STA".GW1.STA.MOT_SPEED_RPM  DB121.DBD396      -- GW1 Motor spee
T   #MOT_SPEED_RPM                 #MOT_SPEED_RPM
L   "DB_CMC_CONTROL".CMC_FRICTION_FORCES.F_FRIC DB3003.DBD42      -- Estimated frict
T   #LuGre_Friction_Force          #LuGre_Friction_Force
L   "DB_MEASUREMENTS".GT001        DB3001.DBD154
T   #GT001                          #GT001
L   "DB_MEASUREMENTS".GT001_SPEED   DB3001.DBD158
T   #GT001_SPEED                    #GT001_SPEED
L   "DB_MEASUREMENTS".PT001        DB3001.DBD122
T   #PT001                          #PT001
L   "DB_MEASUREMENTS".PT002        DB3001.DBD126
T   #PT002                          #PT002
L   "DB_MEASUREMENTS".WT001        DB3001.DBD130
T   #WT001                          #WT001
L   "DB_MEASUREMENTS".WT002        DB3001.DBD134
T   #WT002                          #WT002
L   "DB_MEASUREMENTS".WT003        DB3001.DBD138
T   #WT003                          #WT003
L   "DB_MEASUREMENTS".MRU_FILTER_MULTI. EST_HEAVE DB3001.DBD34      -- Estimated heave
T   #MRU_Filtered_Heave            #MRU_Filtered_Heave
L   "DB_MEASUREMENTS".MRU_FILTER_MULTI.MRUHEAVE DB3001.DBD12      -- Heave from MRU
T   #MRU_Heave                     #MRU_Heave
L   "DB_MEASUREMENTS".EST_MRU_HEAVE DB3001.DBD1202
T   #EST_MRU_HEAVE                 #EST_MRU_HEAVE
L   "DB_MEASUREMENTS".MRU_FILTER_MULTI. EST_SPEED DB3001.DBD38      -- Estimated speed

```

```

T      #EST_MRU_SPEED                      #EST_MRU_SPEED
L      "DB_MEASUREMENTS".EST_MRU_ACC      DB3001.DBD1210
T      #EST_MRU_ACC                        #EST_MRU_ACC
L      "DB_MEASUREMENTS".MRU_FILTER_MULT.MEAN_HEAVE DB3001.DBD46      -- Filtered average
                                         e position, 1 minute average
T      #MEAN_MRU_HEAVE                     #MEAN_MRU_HEAVE
L      "GP_STA".GW1.STA.PAYO_LEN          DB121.DBD220      -- GW1 Winch actual
                                         length payed out (GPW1-0407-A00-st
                                         , SU)
T      #RACK_PAYOUT                         #RACK_PAYOUT
L      "DB_GW1_REG".WIRE_SPEED_GW1.SCAN_TIME DB715.DBD652      -- Scan time in se
                                         cond >0
T      #RACK_SPEED                          #RACK_SPEED
L      "DB_MEASUREMENTS".WT001_FILTERED   DB3001.DBD1024
T      #WT001_FILTERED                     #WT001_FILTERED
L      "DB_MEASUREMENTS".WT002_FILTERED   DB3001.DBD1028
T      #WT002_FILTERED                     #WT002_FILTERED
L      "DB_MEASUREMENTS".WT003_FILTERED   DB3001.DBD1032
T      #WT003_FILTERED                     #WT003_FILTERED
L      "DB_CMC_CONTROL".LM_VEL            DB3003.DBD68
T      #LM_VEL                              #LM_VEL
L      "DB_CMC_CONTROL".AHC_DEVIATION     DB3003.DBD72
T      #AHC_DEVIATION                      #AHC_DEVIATION
L      "GP_STA".GW1.M1.STA.SPEED_RPM     DB121.DBD478      -- GW1 Motor 1 ac
                                         tual speed (RPM) (GPW1-0485-A00-st, S
                                         U)
T      #LM_ACTUAL_VEL                      #LM_ACTUAL_VEL
L      "GP_STA".GW1.M1.STA.TORQUE         DB121.DBD498      -- GW1 Motor 1 ac
                                         tual torque (%) (GPW1-0488-A00-st, S
                                         U)
T      #LM_ACTUAL_FORCE                    #LM_ACTUAL_FORCE

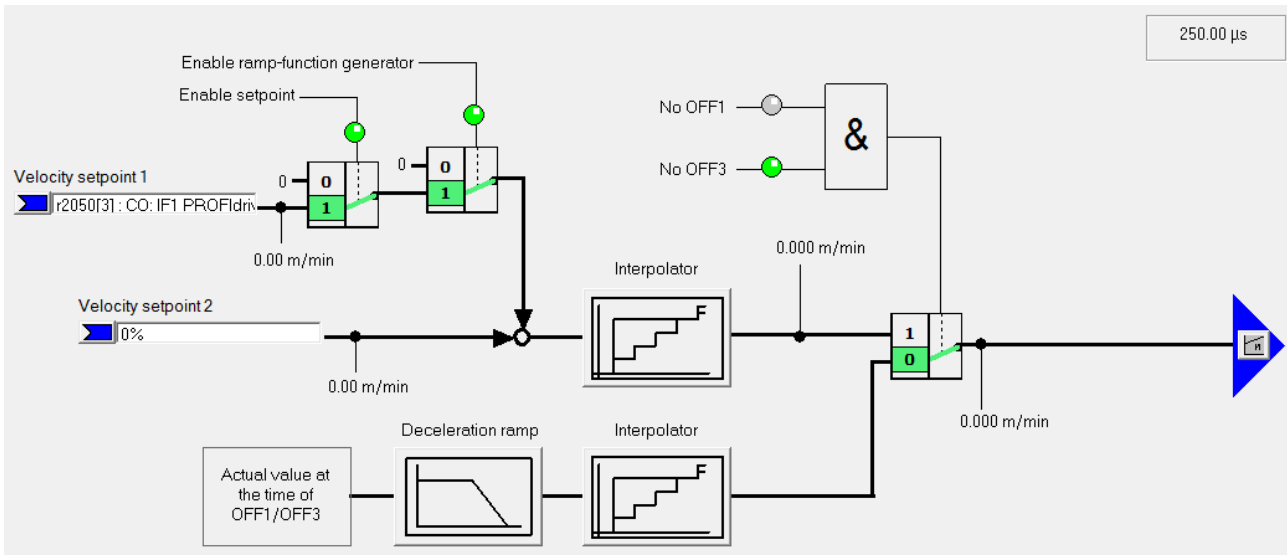
```

Appendix C

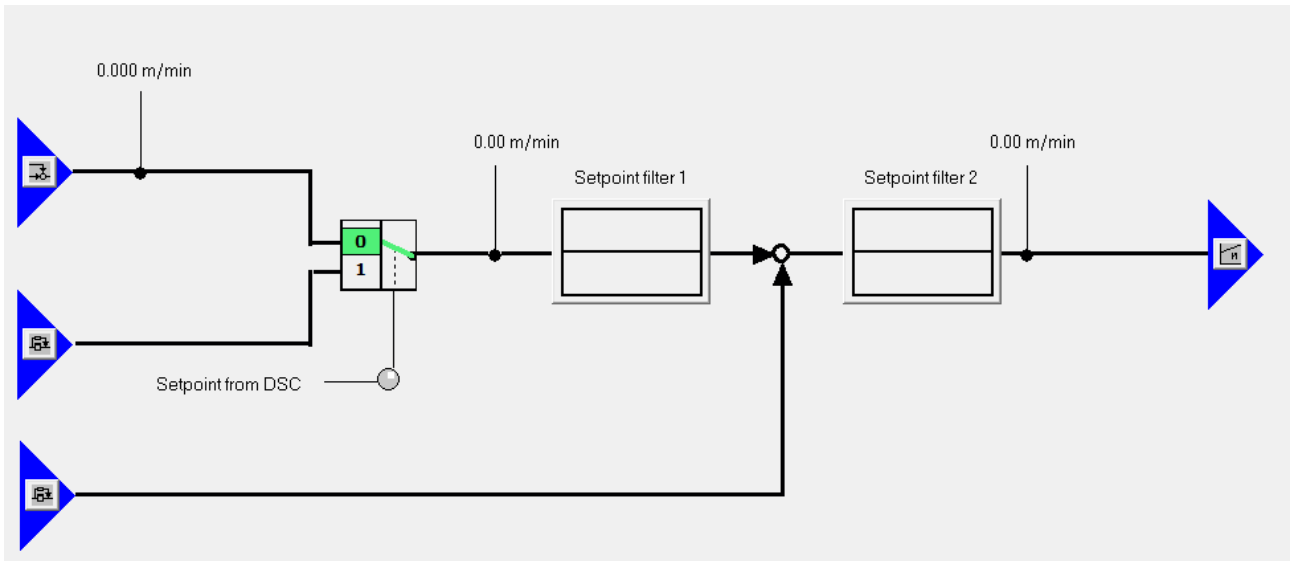
Drive Controller Structure

C.1 Drive System

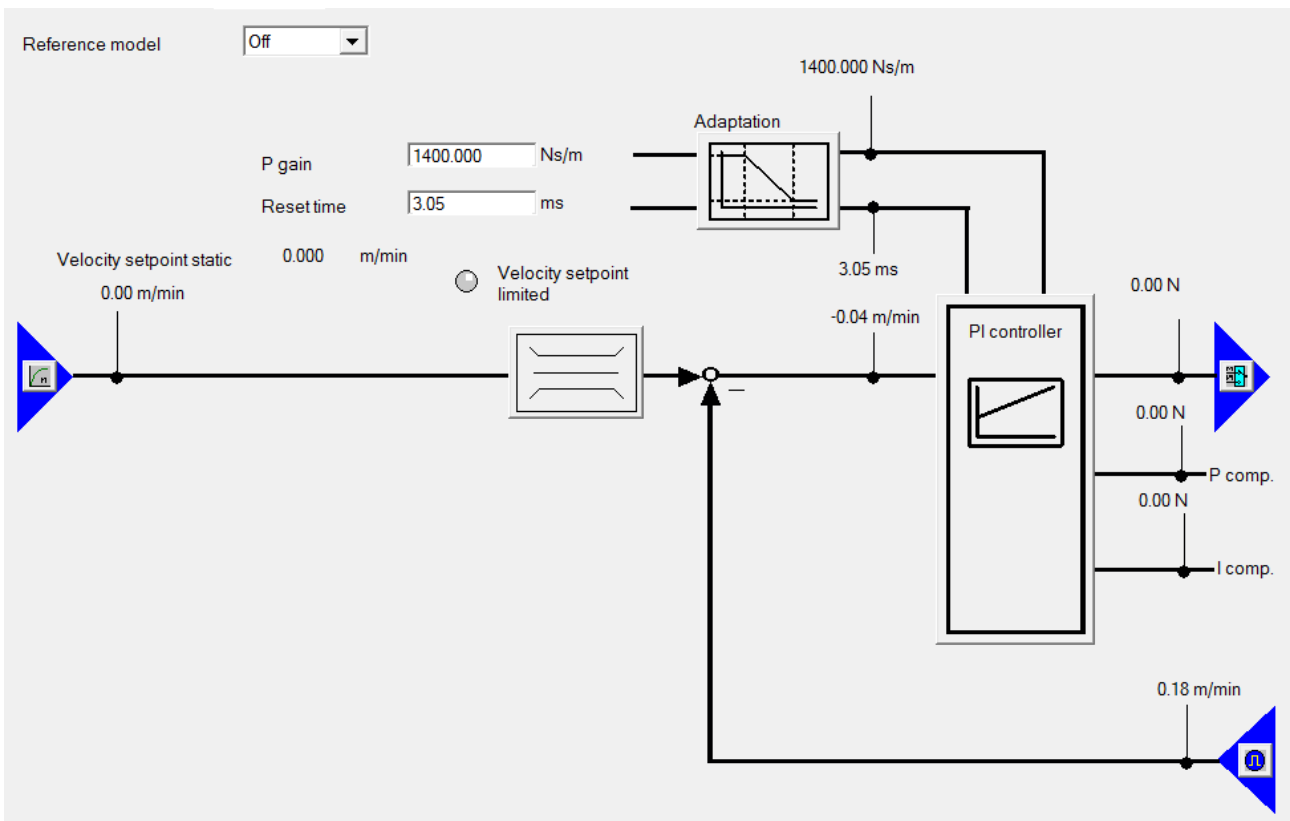
C.2 Drive Velocity Setpoint



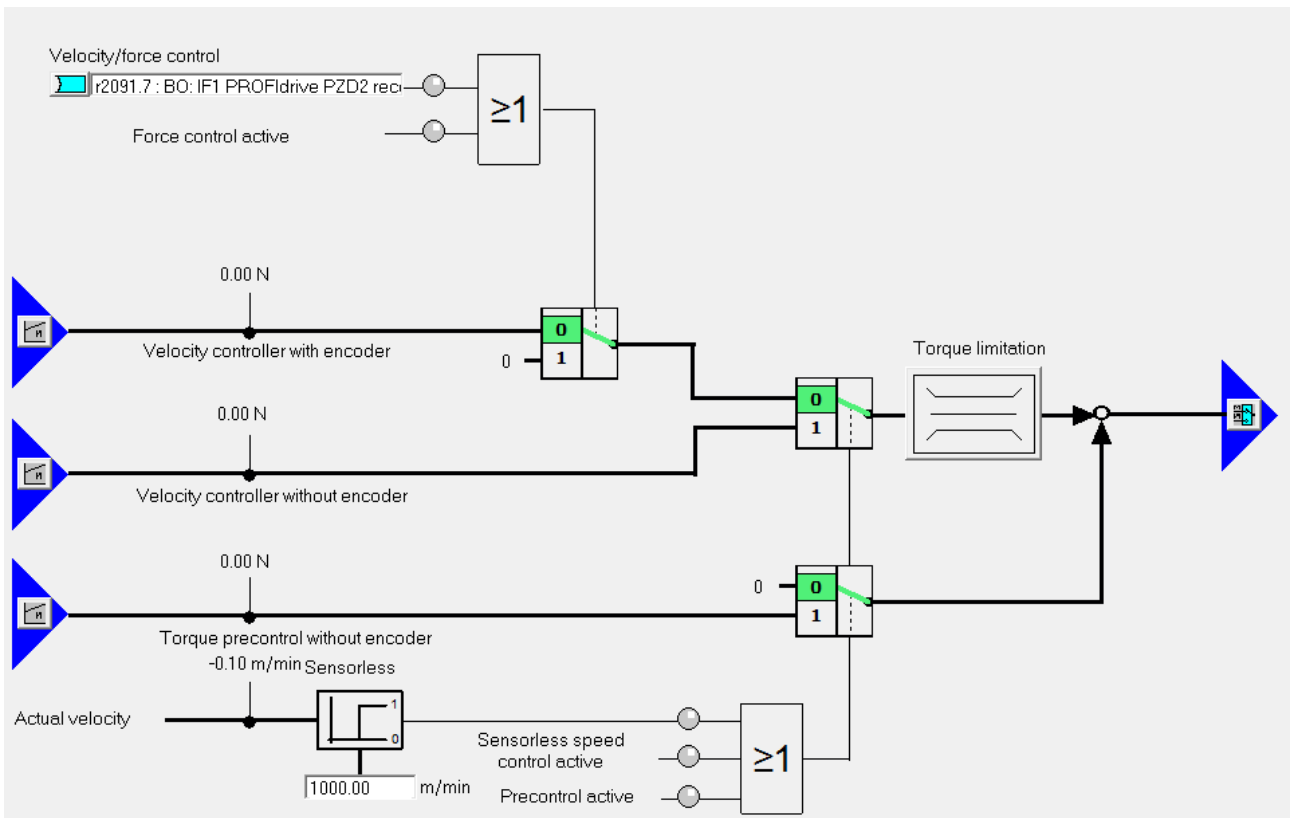
C.3 Drive Velocity Filter



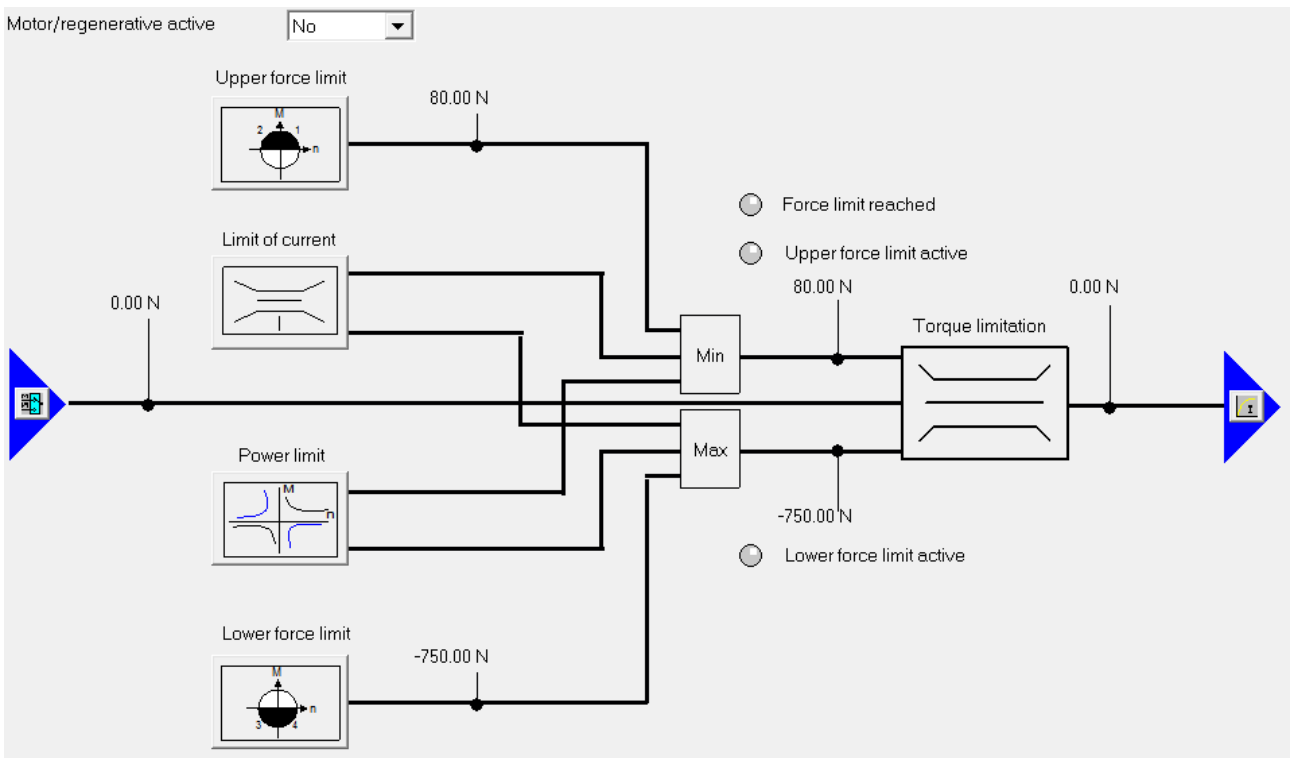
C.4 Drive Velocity Controller



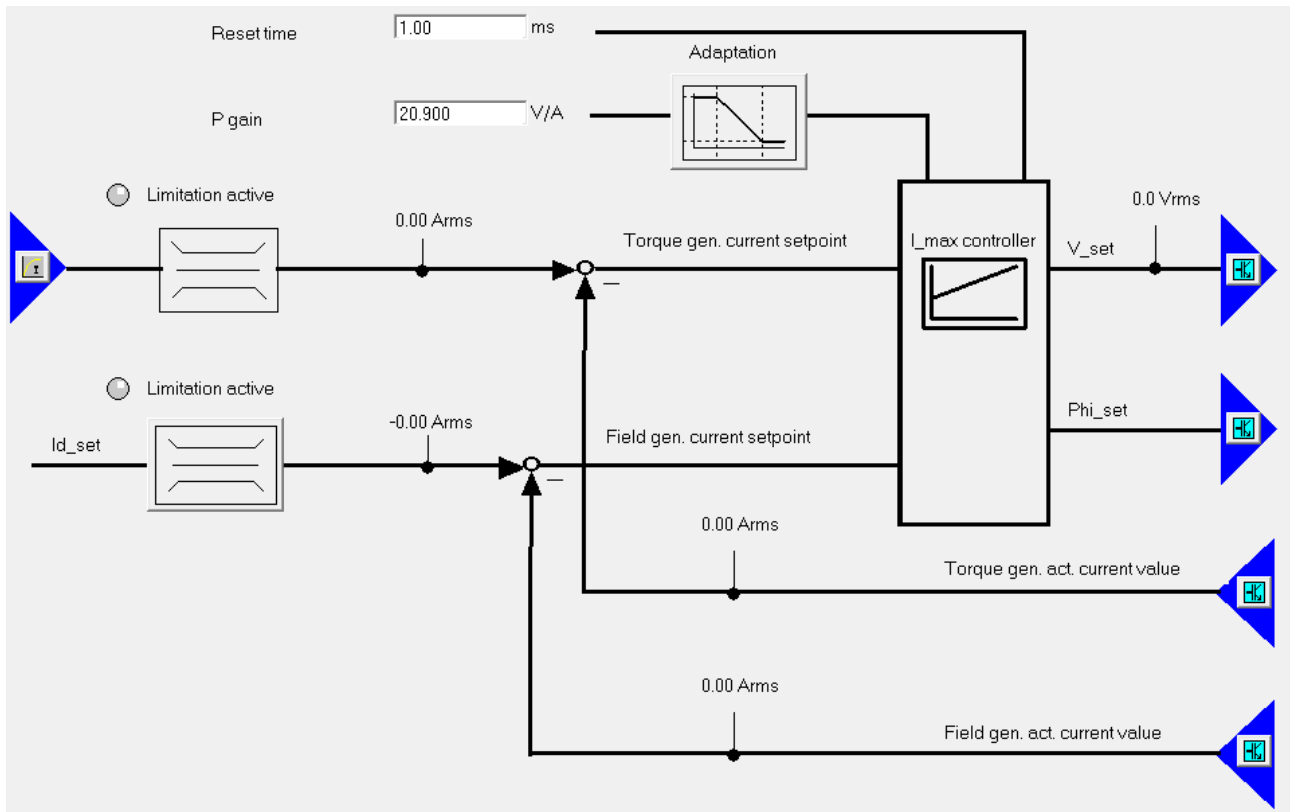
C.5 Drive Force Setpoint



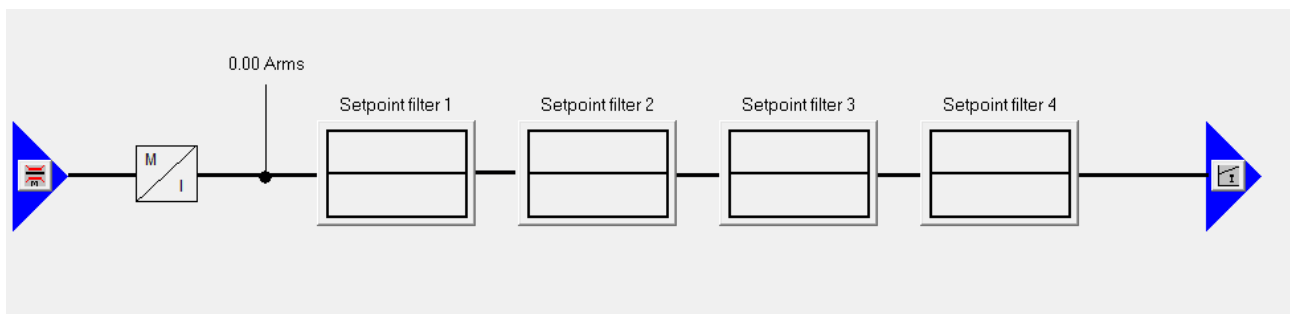
C.6 Drive Force Limit



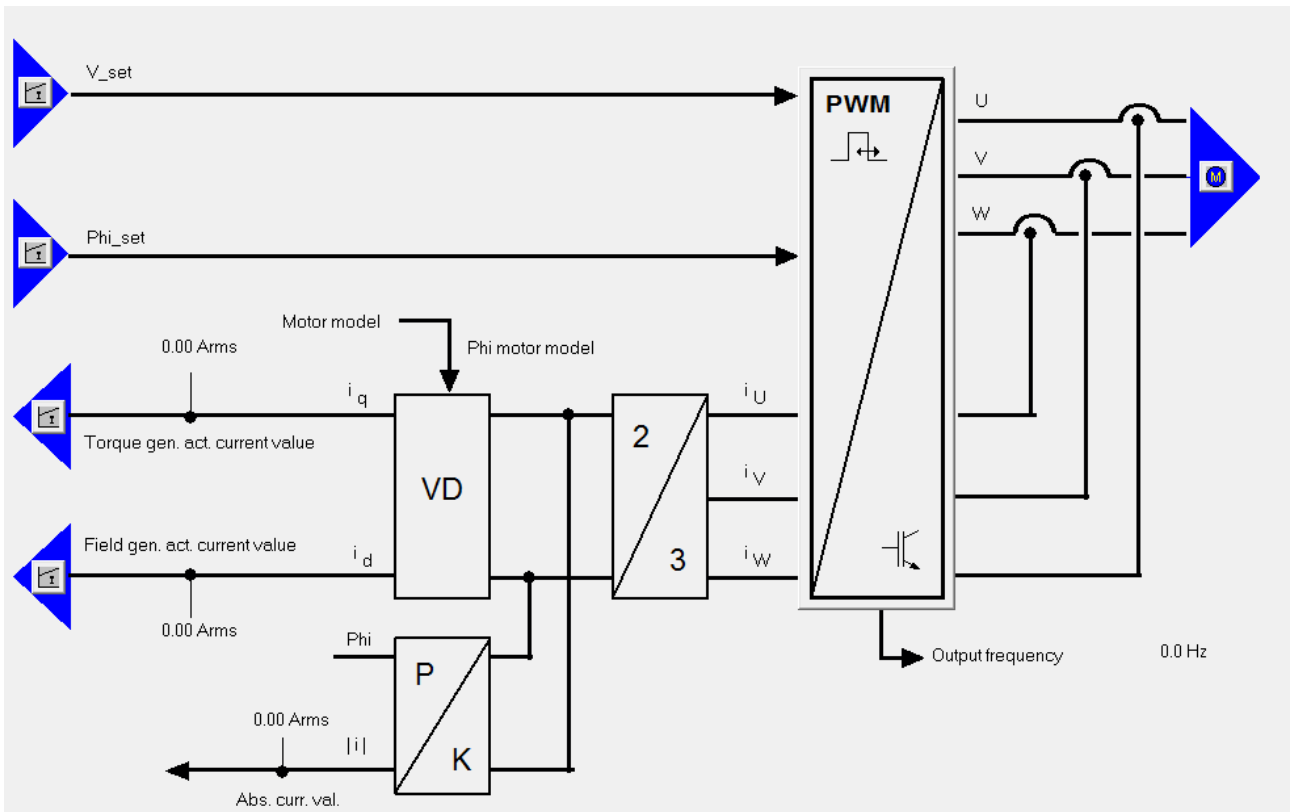
C.7 Drive Current Controller



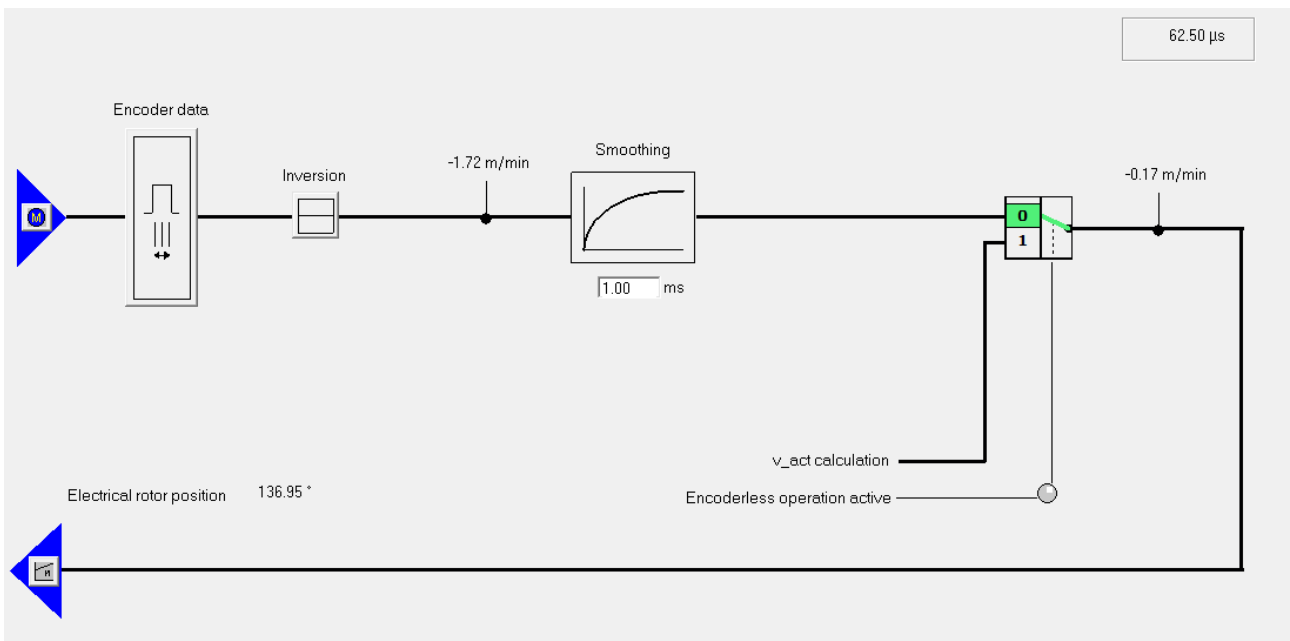
C.8 Drive Current Filter



C.9 Drive Power Unit



C.10 Drive Encoder



Appendix D

SimulationX Model

Diagram View:1

3D-View:2



Volume CAPVs
Parameters

Comment	Name	Current Value	Unit
Volume	V	CAPV_Volume.F	[m ³]
Initial Pressure	p0	pAPV (Fixed)	[Pa]
Initial Temperature	T0	TAtm (Fixed)	[K]
Consider Heat Transfer	condHeatFl	false	

Results

Comment	Name	Current Value	Unit
Pressure	p	0	bar
Temperature	T	-273.15	°C

Sphere Piston1
Parameters

Comment	Name	Current Value	Unit
Reference Frame	frameRef	Predecessor Frame	
Displacement	x0	{-0.2,0,0}	[m]
Calculation of Orientation	rotSelect	Sequence of Angles	
Sequence of Angles	psiSequence	x-y-z (Cardan Angles)	
Rotation Angles	psi0	{0,0,0}	[rad]
Calculation of Moment of Inertia	calcI	Mass and Dimension	
Mass	m	23	[kg]
Radius	rd	10	[mm]
Primary RGB Color	color	{0,1,1}	[-]
Secondary RGB Color	color2	color	[-]
Transparency	alpha	1	[-]

Results

Comment	Name	Current Value	Unit
Displacement	x	{-0.2,0,1.905}	m
Velocity	v	{0,0,0}	m/s
Acceleration	a	{0,0,0}	m/s ²
Orientation	R	{{1,0,0},{0,1,0},{0,0,1}}	-
Angular Velocity	om	{0,0,0}	rad/s
Angular Acceleration	alp	{0,0,0}	rad/s ²
Acceleration Force	Fa	{0,0,0}	N
Acceleration Torque	Ta	{0,0,0}	Nm

Bipolar Force Interface Plunger2
 Parameters

Comment	Name	Current Value	Unit
Reference Frame	frame1Ref	Predecessor Frame	
Displacement	x10	{0.2,0,0}	[m]
Reference Frame	frame2Ref	Predecessor Frame	
Displacement	x20	{0.2,0,0}	[m]
3D Primitive Selection	visSelect	Differential Cylinder	
RGB Color	color	{1.000000,1.000000,0.000000}	[-]
Secondary RGB Color	color2	{0.6,0.6,0.6}	[-]
Transparency	alpha	1	[-]
Length of Cylinder	IC	1270	[mm]
Radius of Cylinder	rC	35	[mm]
Length of Piston Rod	IR	1000	[mm]
Radius of Piston Rod	rR	30	[mm]

Results

Comment	Name	Current Value	Unit
Difference of Displacement	dx	1.905	m
Difference of Velocity	dv	0	m/s
Force at ctr1	F1	0	N
Force at ctr2	F2	0	N

f(x) k

Parameters

Comment	Name	Current Value	Unit
Function f(x)	F	$(-0.4380 * (\text{self.x})^4 + 1.4809 * (\text{self.x})^3 - 2.0204 * (\text{self.x})^2 + 1.3912 * (\text{self.x}) + 0.1385)$	[-]

Results

Comment	Name	Current Value	Unit
Signal Output	y	0	-

f(x) CB_el

Parameters

Comment	Name	Current Value	Unit
Function f(x)	F	$\text{self.x} - \text{PlungerCylinder1.maxStroke} / 2$	[-]

Results

Comment	Name	Current Value	Unit
Signal Output	y	0	-

Differential Cylinder EqCyl2
Parameters

Comment	Name	Current Value	Unit
Maximum Stroke	maxStroke	729	[mm]
Piston Diameter	dPiston	45	[mm]
Rod Diameter	dRod	15	[mm]
Dead Volume Port A	vol0A	0.5	[l]
Dead Volume Port B	vol0B	0.5	[l]
Transfer of Coordinates	dxh	0	[m]
Friction Description	cylFriction	No Friction Losses	
Type of End Stop	cylStop	Elastic End Stop	
Stiffness	cStop	50	[kN/mm]
Damping Coefficient (Critical Damping: $dStop^2 = 4 * m * cStop$)	dStop	$\sqrt{4 * 1 * kg * cStop}$	[Ns/m]
Consider Internal Leakage	intLeakage	false	
Consider External Leakage	extLeakage	false	

Results

Comment	Name	Current Value	Unit
Piston Area Side A	areaA	0	m ²
Piston Area Side B	areaB	0	m ²
Volume Side A	volA	0	dm ³
Volume Side B	volB	0	dm ³
Piston Stroke	xPiston	0	mm
Piston Velocity	vPiston	0	m/s
Cylinder Force	Fcyl	0	N
End Stop Force	Fstop	0	N
Pressure Chamber A	pA	0	bar
Pressure Chamber B	pB	0	bar
Pressure Drop A -> B	pAB	0	bar
Volume Flow Port A	QA	0	l/min
Volume Flow Port B	QB	0	l/min
Mechanical Power	Pmech	0	kW
Hydraulic Power	Phydr	0	kW

Mass mass2
Parameters

Comment	Name	Current Value	Unit
Mass	m	1	[kg]

Results

Comment	Name	Current Value	Unit
Inertia Force	Fa	0	N
Displacement	x	0	m
Velocity	v	0	m/s
Acceleration	a	0	m/s ²
Change of Kinetic Energy	Pk	0	kW

Tank tank2
Parameters

Comment	Name	Current Value	Unit
Tank Pressure	p_Tank	0	[bar]
Volume of Tank considered.	volON	false	

Results

Comment	Name	Current Value	Unit
Pressure	p	0	bar
Volume Flow Balance	Q	0	l/min
Mass Flow Balance	mdot	0	kg/s
External Hydraulic Power Input	Pext	0	kW

Plunger Cylinder PlungerCylinder2
Parameters

Comment	Name	Current Value	Unit
Maximum Stroke	maxStroke	1270	[mm]
Cylinder Diameter	dCyl	70	[mm]
Rod Diameter	dRod	60	[mm]
Transfer of Coordinates	dxh	-self.maxStroke/2	[m]
Dead Volume Port A	vol0A	2	[l]
Friction Description	cylFriction	No Friction Losses	
Type of End Stop	cylStop	Elastic End Stop	
Stiffness	cStop	4*10 ⁹	[N/m]
Damping Coefficient (Critical Damping: $dStop^2 = 4 * m * cStop$)	dStop	sqrt(4*1'kg'*cStop)	[Ns/m]
Consider External Leakage	extLeakage	false	

Results

Comment	Name	Current Value	Unit
Piston Area Side A	areaA	0	m ²
Volume Side A	volA	0	dm ³
Piston Stroke	xPiston	0	mm
Piston Velocity	vPiston	0	m/s
Cylinder Force	Fcyl	0	N
End Stop Force	Fstop	0	N
Pressure Chamber A	pA	0	bar
Volume Flow Port A	QA	0	l/min
Mechanical Power	Pmech	0	kW
Hydraulic Power	Phydr	0	kW

Plunger Cylinder PlungerCylinder1
Parameters

Comment	Name	Current Value	Unit
Maximum Stroke	maxStroke	1270	[mm]
Cylinder Diameter	dCyl	70	[mm]
Rod Diameter	dRod	60	[mm]
Transfer of Coordinates	dxh	-self.maxStroke/2	[m]
Dead Volume Port A	vol0A	2	[l]
Friction Description	cylFriction	Stribeck Curve	
Static Friction Force	Fs	500	[N]
Coulomb Friction Force	Fc	350	[N]
Limit Velocity	vL	0.003	[m/s]
Consider Velocity-Dependency of Friction Force	velDep	true	
Friction Coefficient	kv	500	[Ns/m]
Friction Exponent (0<av<=1)	av	1	[-]
Consider Pressure-Dependency of Friction Force	presDep	true	
Friction Coefficient	kp	10	[N/bar]
Clearance due to Seal Elasticity	stickEI	true	
Clearance	xCl	0.5	[mm]
Damping Coefficient (Critical Damping: $dCl^2 = 4 * m * cCl$)	dCl	$\sqrt{4*1'kg'*cCl}$	[Ns/m]
Type of End Stop	cylStop	Elastic End Stop	
Stiffness	cStop	$4*10^9$	[N/m]
Damping Coefficient (Critical Damping: $dStop^2 = 4 * m * cStop$)	dStop	$\sqrt{4*1'kg'*cStop}$	[Ns/m]
Consider External Leakage	extLeakage	false	

Results

Comment	Name	Current Value	Unit
Piston Area Side A	areaA	0	m ²
Volume Side A	volA	0	dm ³
Piston Stroke	xPiston	0	mm
Piston Velocity	vPiston	0	m/s
Cylinder Force	Fcyl	0	N
Friction Force	Ffr	0	N
Friction State (0=Stick, 1=Slip)	slide	0	-
End Stop Force	Fstop	0	N
Pressure Chamber A	pA	0	bar
Volume Flow Port A	QA	0	l/min
Mechanical Power	Pmech	0	kW
Hydraulic Power	Phydr	0	kW
Frictional Losses	Pfr	0	kW

Constant Throttle Valve Olmsted
Parameters

Comment	Name	Current Value	Unit
Flow Description	flowDescr	a(Re) Characteristics	
Cross Section	crossSec	Circular	
Bore Diameter	NW	15	[mm]
Critical Reynolds Number	ReK	200	[-]
Turb. Flow Coefficient	alphaT	0.62	[-]

Results

Comment	Name	Current Value	Unit
Pressure Drop A -> B	pAB	0	bar
Volume Flow (Meter-In Side)	Q	0	l/min
Mass Flow	mdot	0	kg/s
Reynolds Number	Re	0	-
Cavitation Number	Cav	0	-
Power Dissipation	Pdiss	0	kW

Piston Accumulator (with external connection for piston and gas) Accumulator
Parameters

Comment	Name	Current Value	Unit
Maximum Stroke	maxStroke	1613	[mm]
Piston Diameter	dPiston	90	[mm]
Rod Diameter	dRod	0	[mm]
Dead Volume at Oil-Side	VOil0	2	[l]
Dead Volume at Gas Side	VGas0	2	[l]
Transfer of Coordinates	dxh	-self.maxStroke/2	[m]
Friction Description	cylFriction	Stribeck Curve	
Static Friction Force	Fs	20	[N]
Coulomb Friction Force	Fc	9	[N]
Limit Velocity	vL	0.005	[m/s]
Consider Velocity-Dependency of Friction Force	velDep	true	
Friction Coefficient	kv	12	[Ns/m]
Friction Exponent (0<av<=1)	av	1	[-]
Consider Pressure-Dependency of Friction Force	presDep	false	
Clearance due to Seal Elasticity	stickEl	true	
Clearance	xCl	0.5	[mm]
Damping Coefficient (Critical Damping: $dCl^2 = 4 * m * cCl$)	dCl	$\sqrt{4*1'kg'*Fs/xCl}$	[Ns/m]
Type of End Stop	cylStop	Elastic End Stop	
Stiffness	cStop	500	[kN/mm]
Damping Coefficient (Critical Damping: $dStop^2 = 4 * m * cStop$)	dStop	$\sqrt{4*1'kg'*cStop}$	[Ns/m]
Consider Heat Transfer at Wall	considerHeatTransfer	true	
Ambient Temperature	TEnv	20	[°C]
Heat Transfer Coeff. Oil	alphaOil	800	[W/(m²·K)]
Heat Transfer Coeff. Gas	alphaGas	70	[W/(m²·K)]
Ambient Heat Transfer Coeff.	alphaEnv	70	[W/(m²·K)]
Heat Capacity of Piston	CPiston	1'kg'*450'J/(kg*K)	[J/K]
Heat Capacity of Housing	CHousing	1'kg'*450'J/(kg*K)	[J/K]

Comment	Name	Current Value	Unit
Initial Oil Pressure	pOil0	p0 (Fixed)	[Pa]
Initial Gas Pressure (absolute)	pGas0	pAPV (Fixed)	[Pa]
Initial Gas Temperature	TGas0	TAtm (Fixed)	[K]

Results

Comment	Name	Current Value	Unit
Oil Pressure (relative to pAtm)	pOil	0	bar
Oil Temperature	TOil	-273.15	°C
Oil Volume	VOil	0	dm ³
Volume Flow of Oil into Accumulator	QOil	0	l/min
Gas Pressure (relative to pAtm)	pGas	0	bar
Gas Temperature	TGas	-273.15	°C
Gas Volume	VGas	0	dm ³
Piston Stroke	xPiston	0	mm
Piston Velocity	vPiston	0	m/s
Cylinder Force	FPiston	0	N
Friction Force	Ffriction	0	N
Friction State (0=Stick, 1=Slip)	frictionState	0	-
Frictional Losses	Pfriction	0	kW
Oil Heat Flow	PthOil	0	kW
Gas Heat Flow	PthGas	0	kW
Temperature of Piston	TPiston	-273.15	°C
Temperature of Housing	THousing	-273.15	°C

Mass Piston
Parameters

Comment	Name	Current Value	Unit
Mass	m	4	[kg]
Initial Displacement	x0	0 (Fixed)	[m]
Initial Velocity	v0	0 (Fixed)	[m/s]

Results

Comment	Name	Current Value	Unit
Inertia Force	Fa	0	N
Displacement	x	0	m
Velocity	v	0	m/s
Acceleration	a	0	m/s ²
Change of Kinetic Energy	Pk	0	kW

Constant Throttle Valve MainAirValve
Parameters

Comment	Name	Current Value	Unit
Flow Description	flowDescr	Orifice Geometry	
Meter-In Diameter	d1	14	[mm]
Orifice Diameter	d2	13.92	[mm]
Cross Section	crossSec	Diameter	
Enter Flow Coefficient a	enterFlowCoef	false	
Reference Pressure	pn	1.01325	[bar]
Reference Temperature	Tn	20	[°C]
Change Default Settings for Laminar Range	changeDefault Laminar	false	

Results

Comment	Name	Current Value	Unit
Pressure Drop (A->B)	pAB	0	bar
Pressure Ratio (Meter-Out / Meter-In)	p_ratio	0	-
Mass Flow	mdot	0	kg/s
Flow	Q	0	l/min

Preset preset1
Parameters

Comment	Name	Current Value	Unit
Preset	kind	Fixing	

Results

Comment	Name	Current Value	Unit
Force	F	0	N
External Power	Pe	0	kW
Displacement	xFix	0	m
Velocity	vFix	0	m/s
Acceleration	aFix	0	m/s ²

f(x) Stroke
Parameters

Comment	Name	Current Value	Unit
Function f(x)	F	PlungerCylinder2.xPiston	[m]

Results

Comment	Name	Current Value	Unit
Signal Output	y	0	mm

Differential Cylinder EqCyl1
Parameters

Comment	Name	Current Value	Unit
Maximum Stroke	maxStroke	729	[mm]
Piston Diameter	dPiston	45	[mm]
Rod Diameter	dRod	15	[mm]
Dead Volume Port A	vol0A	0.5	[l]
Dead Volume Port B	vol0B	0.5	[l]
Transfer of Coordinates	dxh	0	[m]
Friction Description	cylFriction	No Friction Losses	
Type of End Stop	cylStop	Elastic End Stop	
Stiffness	cStop	50	[kN/mm]
Damping Coefficient (Critical Damping: $dStop^2 = 4 * m * cStop$)	dStop	$\sqrt{4 * 1 * kg * cStop}$	[Ns/m]
Consider Internal Leakage	intLeakage	false	
Consider External Leakage	extLeakage	false	

Results

Comment	Name	Current Value	Unit
Piston Area Side A	areaA	0	m ²
Piston Area Side B	areaB	0	m ²
Volume Side A	volA	0	dm ³
Volume Side B	volB	0	dm ³
Piston Stroke	xPiston	0	mm
Piston Velocity	vPiston	0	m/s
Cylinder Force	Fcyl	0	N
End Stop Force	Fstop	0	N
Pressure Chamber A	pA	0	bar
Pressure Chamber B	pB	0	bar
Pressure Drop A -> B	pAB	0	bar
Volume Flow Port A	QA	0	l/min
Volume Flow Port B	QB	0	l/min
Mechanical Power	Pmech	0	kW
Hydraulic Power	Phydr	0	kW

Mass mass1

Parameters

Comment	Name	Current Value	Unit
Mass	m	1	[kg]

Results

Comment	Name	Current Value	Unit
Inertia Force	Fa	0	N
Displacement	x	0	m
Velocity	v	0	m/s
Acceleration	a	0	m/s ²
Change of Kinetic Energy	Pk	0	kW

Preset preset2

Parameters

Comment	Name	Current Value	Unit
Preset	kind	Displacement	
Displacement	x	Lstr.F	[m]

Results

Comment	Name	Current Value	Unit
Force	F	0	N
External Power	Pe	0	kW
Displacement	xFix	0	m
Velocity	vFix	0	m/s
Acceleration	aFix	0	m/s ²

Preset preset3

Parameters

Comment	Name	Current Value	Unit
Preset	kind	Fixing	

Results

Comment	Name	Current Value	Unit
Force	F	0	N
External Power	Pe	0	kW
Displacement	xFix	0	m
Velocity	vFix	0	m/s
Acceleration	aFix	0	m/s ²

Tank tank1

Parameters

Comment	Name	Current Value	Unit
Tank Pressure	p_Tank	0	[bar]
Volume of Tank considered.	volON	false	

Results

Comment	Name	Current Value	Unit
Pressure	p	0	bar
Volume Flow Balance	Q	0	l/min
Mass Flow Balance	mdot	0	kg/s
External Hydraulic Power Input	Pext	0	kW

Preset Motion_Centre

Parameters

Comment	Name	Current Value	Unit
Reference Frame	frameRef	Predecessor Frame	
Displacement	x0	{0,0,0}	[m]
Calculation of Orientation	rotSelect	Sequence of Angles	
Sequence of Angles	psiSequence	x-y-z (Cardan Angles)	
Rotation Angles	psi0	{0,0,0}	[rad]
Preset	tKind	Displacement	
Displacement	xPreset	{0,0,Rig_Heave.F}	[m]
Consideration of Rel. Velocity and Acceleration	tCalcDer	true	
Preset	rKind	Fixing	
3D Primitive Selection	visSelect	Cuboid	
Length in X Direction	lx	500	[mm]
Length in Y Direction	ly	500	[mm]
Length in Z Direction	lz	10	[mm]
RGB Color	color	{0,0,1}	[-]
Transparency	alpha	0.5	[-]

Results

Comment	Name	Current Value	Unit
Displacement	x	{0,0,0}	m
Velocity	v	{0,0,0}	m/s
Acceleration	a	{0,0,0}	m/s ²
Orientation	R	{{1,0,0},{0,1,0},{0,0,1}}	-
Angular Velocity	om	{0,0,0}	rad/s
Angular Acceleration	alp	{0,0,0}	rad/s ²
Rel. Displacement	xRel	{0,0,0}	m
Rel. Velocity	vRel	{0,0,0}	m/s
Rel. Acceleration	aRel	{0,0,0}	m/s ²
Rel. Angles	phiRel	{0,0,0}	rad
Rel. Angular Velocity	omRel	{0,0,0}	rad/s
Rel. Angular Acceleration	alpRel	{0,0,0}	rad/s ²
Internal Force	Fi	{0,0,0}	N
Internal Torque	Ti	{0,0,0}	Nm

Bipolar Force Interface Plunger1
Parameters

Comment	Name	Current Value	Unit
Reference Frame	frame1Ref	Predecessor Frame	
Displacement	x10	{-0.2,0,0}	[m]
Reference Frame	frame2Ref	Predecessor Frame	
Displacement	x20	{-0.2,0,0}	[m]
3D Primitive Selection	visSelect	Differential Cylinder	
RGB Color	color	{1.000000,1.000000,0.000000}	[-]
Secondary RGB Color	color2	{0.6,0.6,0.6}	[-]
Transparency	alpha	1	[-]
Length of Cylinder	lC	1270	[mm]
Radius of Cylinder	rC	35	[mm]
Length of Piston Rod	lR	1000	[mm]
Radius of Piston Rod	rR	30	[mm]

Results

Comment	Name	Current Value	Unit
Difference of Displacement	dx	1.905	m
Difference of Velocity	dv	0	m/s
Force at ctr1	F1	0	N
Force at ctr2	F2	0	N

Prismatic Joint Guide
Parameters

Comment	Name	Current Value	Unit
Reference Frame	frameRef	Predecessor Frame	
Displacement	x0	{0,0,0}	[m]
Calculation of Orientation	rotSelect	Sequence of Angles	
Sequence of Angles	psiSequence	x-y-z (Cardan Angles)	
Rotation Angles	psi0	{0,0,0}	[rad]
Axis of Translation	axis	Z-Axis	
Initial Rel. Displacement	xRel0	1.270-PlungerCylinder1.dhx (Fixed)	[m]
Initial Rel. Velocity	vRel0	0 (Fixed)	[m/s]
End Stop	withStop	false	
Consideration of Friction	withFriction	false	
Length in X Direction	lx	50	[mm]
Length in Y Direction	ly	20	[mm]
Length in Z Direction	lz	20	[mm]
RGB Color	color	{0.5,0,0.5}	[-]
Transparency	alpha	1	[-]

Results

Comment	Name	Current Value	Unit
Displacement	x	{0,0,1.905}	m
Velocity	v	{0,0,0}	m/s
Acceleration	a	{0,0,0}	m/s ²
Orientation	R	{{1,0,0},{0,1,0},{0,0,1}}	-
Angular Velocity	om	{0,0,0}	rad/s
Angular Acceleration	alp	{0,0,0}	rad/s ²
Rel. Displacement	xRel	1.905	m
Rel. Velocity	vRel	0	m/s
Rel. Acceleration	aRel	0	m/s ²
Internal Force	Fi	{0,0,0}	N
Internal Torque	Ti	{0,0,0}	Nm
Mass w.r.t. Axis of Translation	m	0	kg
Acceleration Force w.r.t. Axis of Translation	Fa	0	N

Cuboid Crownblock
Parameters

Comment	Name	Current Value	Unit
Reference Frame	frameRef	Predecessor Frame	
Displacement	x0	{0,0,-Guide.xRel0-PlungerCylinder1.dhx}	[m]
Calculation of Orientation	rotSelect	Sequence of Angles	
Sequence of Angles	psiSequence	x-y-z (Cardan Angles)	
Rotation Angles	psi0	{0,0,0}	[rad]
Calculation of Moment of Inertia	calcI	Mass and Dimension	
Mass	m	10	[kg]
Length in X Direction	lx	400	[mm]
Length in Y Direction	ly	160	[mm]
Length in Z Direction	lz	140	[mm]
RGB Color	color	{1.000000,0.407843,0.125490}	[-]
Transparency	alpha	1	[-]

Results

Comment	Name	Current Value	Unit
Displacement	x	{0,0,0.635}	m
Velocity	v	{0,0,0}	m/s
Acceleration	a	{0,0,0}	m/s ²
Orientation	R	{{1,0,0},{0,1,0},{0,0,1}}	-
Angular Velocity	om	{0,0,0}	rad/s
Angular Acceleration	alp	{0,0,0}	rad/s ²
Acceleration Force	Fa	{0,0,0}	N
Acceleration Torque	Ta	{0,0,0}	Nm

Body Force Eq
Parameters

Comment	Name	Current Value	Unit
Reference Frame	frameRef	Predecessor Frame	
Displacement	x0	{0,0,0}	[m]
Calculation of Orientation	rotSelect	Sequence of Angles	
Sequence of Angles	psiSequence	x-y-z (Cardan Angles)	
Rotation Angles	psi0	{0,0,0}	[rad]
Force	F	{0,0,-2*EqCyl1.Fcyl*k.F}	[N]
Shaft Radius	rd	5	[mm]
Length of Arrowhead	l	20	[mm]
Scale Factor	scale	0.000001	[-]
RGB Color	color	{1,0,0}	[-]
Transparency	alpha	1	[-]

Results

Comment	Name	Current Value	Unit
Internal Force	Fi	{0,0,0}	N

Sphere Hook
Parameters

Comment	Name	Current Value	Unit
Reference Frame	frameRef	Predecessor Frame	
Displacement	x0	{0,0,-Crownblock.lz/2-Sheaves.ro}	[m]
Calculation of Orientation	rotSelect	Sequence of Angles	
Sequence of Angles	psiSequence	x-y-z (Cardan Angles)	
Rotation Angles	psi0	{0,0,0}	[deg]
Calculation of Moment of Inertia	calcI	Mass and Dimension	
Mass	m	155	[kg]
Radius	rd	50	[mm]
Primary RGB Color	color	{1,1,0}	[-]
Secondary RGB Color	color2	color	[-]
Transparency	alpha	1	[-]

Results

Comment	Name	Current Value	Unit
Displacement	x	{0,0,0.435}	m
Velocity	v	{0,0,0}	m/s
Acceleration	a	{0,0,0}	m/s ²
Orientation	R	{{1,0,0},{0,1,0},{0,0,1}}	-
Angular Velocity	om	{0,0,0}	rad/s
Angular Acceleration	alp	{0,0,0}	rad/s ²
Acceleration Force	Fa	{0,0,0}	N
Acceleration Torque	Ta	{0,0,0}	Nm

f(x) Lstr

Parameters

Comment	Name	Current Value	Unit
Function f(x)	F	-	[-]
		$0.0472*(self.x)^4+0.1292*(self.x)^3+0.1846*(self.x)^2+0.1988*(self.x)+0.0005$	

Results

Comment	Name	Current Value	Unit
Signal Output	y	0	-

Cylinder Sheaves

Parameters

Comment	Name	Current Value	Unit
Reference Frame	frameRef	Predecessor Frame	
Displacement	x0	{0,0,-Crownblock.lz/2}	[m]
Calculation of Orientation	rotSelect	Sequence of Angles	
Sequence of Angles	psiSequence	x-y-z (Cardan Angles)	
Rotation Angles	psi0	{0,0,90}	[deg]
Calculation of Moment of Inertia	calcI	Mass and Dimension	
Mass	m	30	[kg]
Inner Radius	ri	0	[mm]
Outer Radius	ro	130	[mm]
Height	h	160	[mm]
Primary RGB Color	color	{1.000000,0.407843,0.125490}	[-]
Secondary RGB Color	color2	color	[-]
Transparency	alpha	1	[-]

Results

Comment	Name	Current Value	Unit
Displacement	x	{0,0,0.565}	m
Velocity	v	{0,0,0}	m/s
Acceleration	a	{0,0,0}	m/s ²
Orientation	R	{{6.12323399573677e-017,1,0},{-1,6.12323399573677e-017,0},{0,0,1}}	-
Angular Velocity	om	{0,0,0}	rad/s
Angular Acceleration	alp	{0,0,0}	rad/s ²
Acceleration Force	Fa	{0,0,0}	N
Acceleration Torque	Ta	{0,0,0}	Nm

Sphere Piston2
Parameters

Comment	Name	Current Value	Unit
Reference Frame	frameRef	Predecessor Frame	
Displacement	x0	{0.2,0,0}	[m]
Calculation of Orientation	rotSelect	Sequence of Angles	
Sequence of Angles	psiSequence	x-y-z (Cardan Angles)	
Rotation Angles	psi0	{0,0,0}	[rad]
Calculation of Moment of Inertia	calcI	Mass and Dimension	
Mass	m	23	[kg]
Radius	rd	10	[mm]
Primary RGB Color	color	{0,1,1}	[-]
Secondary RGB Color	color2	color	[-]
Transparency	alpha	1	[-]

Results

Comment	Name	Current Value	Unit
Displacement	x	{0.2,0,1.905}	m
Velocity	v	{0,0,0}	m/s
Acceleration	a	{0,0,0}	m/s ²
Orientation	R	{{1,0,0},{0,1,0},{0,0,1}}	-
Angular Velocity	om	{0,0,0}	rad/s
Angular Acceleration	alp	{0,0,0}	rad/s ²
Acceleration Force	Fa	{0,0,0}	N
Acceleration Torque	Ta	{0,0,0}	Nm

f(x) Pmain
Parameters

Comment	Name	Current Value	Unit
Function f(x)	F	PlungerCylinder1.vPiston*Eq.Fi	[m]

Results

Comment	Name	Current Value	Unit
Signal Output	y	0	mm

f(x) Peq
Parameters

Comment	Name	Current Value	Unit
Function f(x)	F	-2*EqCyl1.vPiston*EqCyl1.Fcyl	[m]

Results

Comment	Name	Current Value	Unit
Signal Output	y	0	mm

Volume Pipes
Parameters

Comment	Name	Current Value	Unit
Volume	V	10	[dm ³]
Wall Capacity	Cw	0	[cm ³ /bar]
Initial Pressure	p0	0 (Fixed)	[bar]
Consider Local Air Volume	locGas	false	

Results

Comment	Name	Current Value	Unit
Pressure	p	0	bar

f(x) CAPV_Volume
Parameters

Comment	Name	Current Value	Unit
Function f(x)	F	0.048	[-]

Results

Comment	Name	Current Value	Unit
Signal Output	y	0	-

f(x) SetPoint
Parameters

Comment	Name	Current Value	Unit
Function f(x)	F	-Rig_Heave.y	[-]

Results

Comment	Name	Current Value	Unit
Signal Output	y	0	-

Summing Junction sum2
Parameters

Comment	Name	Current Value	Unit
x1	X1Var	+	
x2	X2Var	-	
x3	X3Var	-	

Results

Comment	Name	Current Value	Unit
Signal Output	y	0	-

f(x) FeedBack
Parameters

Comment	Name	Current Value	Unit
Function f(x)	F	Crownblock_Displacement_CMC.y	[-]

Results

Comment	Name	Current Value	Unit
Signal Output	y	0	-

Limitation Function limit1
Parameters

Comment	Name	Current Value	Unit
Lower Range Limit	x_min	-700	[-]
Upper Range Limit	x_max	700	[-]
Gain	G	1	[-]

Results

Comment	Name	Current Value	Unit
Signal Output	y	0	-
State	state	0	-

Bipolar Force Interface LinearMot
Parameters

Comment	Name	Current Value	Unit
Reference Frame	frame1Ref	Predecessor Frame	
Displacement	x10	{0,0,1.35}	[m]
Reference Frame	frame2Ref	Predecessor Frame	
Displacement	x20	{0,0,0.5}	[m]
3D Primitive Selection	visSelect	Differential Cylinder	
RGB Color	color	{0.04,0.82,1}	[-]
Secondary RGB Color	color2	{0.6,0.6,0.6}	[-]
Transparency	alpha	1	[-]
Length of Cylinder	IC	409.5	[mm]
Radius of Cylinder	rC	35	[mm]
Length of Piston Rod	IR	1790	[mm]
Radius of Piston Rod	rR	14	[mm]

Results

Comment	Name	Current Value	Unit
Difference of Displacement	dx	1.055	m
Difference of Velocity	dv	0	m/s
Force at ctr1	F1	0	N
Force at ctr2	F2	0	N

Sphere Slider
Parameters

Comment	Name	Current Value	Unit
Reference Frame	frameRef	Predecessor Frame	
Displacement	x0	{0.2,0,0}	[m]
Calculation of Orientation	rotSelect	Sequence of Angles	
Sequence of Angles	psiSequence	x-y-z (Cardan Angles)	
Rotation Angles	psi0	{0,0,0}	[rad]
Calculation of Moment of Inertia	calcI	Mass and Dimension	
Mass	m	8410	[g]
Radius	rd	10	[mm]
Primary RGB Color	color	{0,1,1}	[-]
Secondary RGB Color	color2	color	[-]
Transparency	alpha	1	[-]

Results

Comment	Name	Current Value	Unit
Displacement	x	{0.2,0,1.905}	m
Velocity	v	{0,0,0}	m/s
Acceleration	a	{0,0,0}	m/s ²
Orientation	R	{{1,0,0},{0,1,0},{0,0,1}}	-
Angular Velocity	om	{0,0,0}	rad/s
Angular Acceleration	alp	{0,0,0}	rad/s ²
Acceleration Force	Fa	{0,0,0}	N
Acceleration Torque	Ta	{0,0,0}	Nm

External Force LinearMotorForce
Parameters

Comment	Name	Current Value	Unit
Force	F	self.in1	[N]

Results

Comment	Name	Current Value	Unit
Internal Force	Fi	0	N
Displacement Difference	dx	0	m
Velocity Difference	dv	0	m/s
External Power	Pe	0	kW

Proportional Gain (P Gain) P_Controller
Parameters

Comment	Name	Current Value	Unit
Gain	G	1000000	[-]

Results

Comment	Name	Current Value	Unit
Signal Output	y	0	-

Sphere Weight
Parameters

Comment	Name	Current Value	Unit
Reference Frame	frameRef	Predecessor Frame	
Displacement	x0	{0,0,-1}	[m]
Calculation of Orientation	rotSelect	Sequence of Angles	
Sequence of Angles	psiSequence	x-y-z (Cardan Angles)	
Rotation Angles	psi0	{0,0,0}	[deg]
Calculation of Moment of Inertia	calcI	Mass and Dimension	
Mass	m	200	[kg]
Radius	rd	100	[mm]
Primary RGB Color	color	{0,1,1}	[-]
Secondary RGB Color	color2	color	[-]
Transparency	alpha	1	[-]

Results

Comment	Name	Current Value	Unit
Displacement	x	{0,0,-0.565}	m
Velocity	v	{0,0,0}	m/s
Acceleration	a	{0,0,0}	m/s ²
Orientation	R	{{1,0,0},{0,1,0},{0,0,1}}	-
Angular Velocity	om	{0,0,0}	rad/s
Angular Acceleration	alp	{0,0,0}	rad/s ²
Acceleration Force	Fa	{0,0,0}	N
Acceleration Torque	Ta	{0,0,0}	Nm

f(x) Crownblock_Deviation
Parameters

Comment	Name	Current Value	Unit
Function f(x)	F	Crownblock_Displacement_CMC.y+Rig_H eave.y	[-]

Results

Comment	Name	Current Value	Unit
Signal Output	y	0	-



f(x) ControlPoint
 Parameters

Comment	Name	Current Value	Unit
Function f(x)	F	0.627927	[-]

Results

Comment	Name	Current Value	Unit
Signal Output	y	0	-

f(x) Crownblock_Displacement_CMC
 Parameters

Comment	Name	Current Value	Unit
Function f(x)	F	Crownblock.x[3]-self.x- Motion_Centre.x[3]	[-]

Results

Comment	Name	Current Value	Unit
Signal Output	y	0	-

f(x) Rig_Heave
 Parameters

Comment	Name	Current Value	Unit
Function f(x)	F	self.x	[-]

Results

Comment	Name	Current Value	Unit
Signal Output	y	0	-

Curve RampUp
 Parameters

Comment	Name	Current Value	Unit
Reference Value	RefVar	Simulation Time t [s]	
No Handling of Discontinuities	noDiscont	no	

Curve curve

Results

Comment	Name	Current Value	Unit
Signal Output	y	0	m
Signal Output	ydot	0	-

Single Pass Switch singlePass1
Parameters

Comment	Name	Current Value	Unit
Threshold	th	0	[-]

Results

Comment	Name	Current Value	Unit
Signal Output	y	0	-
State (0 - open, 1 - closed)	state	0	-

Single Pass Switch singlePass2
Parameters

Comment	Name	Current Value	Unit
Threshold	th	0	[-]

Results

Comment	Name	Current Value	Unit
Signal Output	y	0	-
State (0 - open, 1 - closed)	state	0	-

Single Pass Switch singlePass3
Parameters

Comment	Name	Current Value	Unit
Threshold	th	0	[-]

Results

Comment	Name	Current Value	Unit
Signal Output	y	0	-
State (0 - open, 1 - closed)	state	0	-

Summing Junction sum1
Parameters

Comment	Name	Current Value	Unit
x1	X1Var	+	
x2	X2Var	+	
x3	X3Var	+	

Results

Comment	Name	Current Value	Unit
Signal Output	y	0	-

f(x) CMC3
Parameters

Comment	Name	Current Value	Unit
Function f(x)	F	$\sin(2\pi \cdot (1/600) \cdot t) \cdot (-0.15 \cdot \sin(2\pi \cdot 0.08 \cdot t) - 0.1 \cdot \sin(2\pi \cdot 0.11 \cdot t))$	[m]

Results

Comment	Name	Current Value	Unit
Signal Output	y	0	mm

Signal Generator CMC2
Parameters

Comment	Name	Current Value	Unit
Reference Value	RefVar	Simulation Time t [s]	
Curve Shape	CurveTyp	Sine	
Frequency	f	0.08	[Hz]
Amplitude	y_a	-0.26*self.x	[-]
Offset	y0	0	[-]
Phase Shift	phi0	-5.301	[deg]

Results

Comment	Name	Current Value	Unit
Signal Output	y	0	-
Phase	phi	0	rad

Signal Generator CMC1
Parameters

Comment	Name	Current Value	Unit
Reference Value	RefVar	Simulation Time t [s]	
Curve Shape	CurveTyp	Sine	
Frequency	f	0.1	[Hz]
Amplitude	y_a	-0.1*self.x	[-]
Offset	y0	0	[-]
Phase Shift	phi0	-5.301	[deg]

Results

Comment	Name	Current Value	Unit
Signal Output	y	0	-
Phase	phi	0	rad

f(x) Wave

Parameters

Comment	Name	Current Value	Unit
Function f(x)	F	1	[m]

Results

Comment	Name	Current Value	Unit
Signal Output	y	0	mm

Internal Force and Torque Sensor WT002

Parameters

Comment	Name	Current Value	Unit
Reference Frame	frameRef	Predecessor Frame	
Displacement	x0	{0,0,0}	[m]
Calculation of Orientation	rotSelect	Sequence of Angles	
Sequence of Angles	psiSequence	x-y-z (Cardan Angles)	
Rotation Angles	psi0	{0,0,0}	[rad]
RGB Color	color	{0.2,0.2,1}	[-]
Transparency	alpha	1	[-]

Results

Comment	Name	Current Value	Unit
Displacement	x	{0,0,0.435}	m
Velocity	v	{0,0,0}	m/s
Acceleration	a	{0,0,0}	m/s ²
Orientation	R	{{1,0,0},{0,1,0},{0,0,1}}	-
Angular Velocity	om	{0,0,0}	rad/s
Angular Acceleration	alp	{0,0,0}	rad/s ²
Internal Force	Fi	{0,0,0}	N
Internal Torque	Ti	{0,0,0}	Nm
Internal Force, resolved in Origin	FO	{0,0,0}	N
Internal Torque, resolved in Origin	TO	{0,0,0}	Nm

Mechanical Connection (linear) connection42

Results

Comment	Name	Current Value	Unit
Displacement	x	0	m
Velocity	v	0	m/s
Acceleration	a	0	m/s ²

Hydraulic Connection connection53

Parameters

Comment	Name	Current Value	Unit
Temperature Calculation	heatMode	Constant Temperature	
Temperature Setting	T1	TAtm	[K]
Calculation of Gas Fraction	aerationMode	Gas Fraction according to Static Pressure Level	
Gas Fraction (Normal State)	alphaURef	0.2	[%]
Constant Gas Fraction	alphaUconst	0	[%]

Results

Comment	Name	Current Value	Unit
Pressure (Relative to Atmosphere Pressure)	p	0	bar
Absolute Pressure	pAbs	0	bar
Pressure Change Rate	pdot	0	bar/s
Temperature	T	-273.15	°C
Volume Fraction of Undissolved Air	alphaU	0	%
Total Volume	V	0	cm ³
Volume Change	Vdot	0	l/min
Hydraulic Capacity	Ch	0	cm ³ /bar
Equivalent Bulk Modulus	Ee	0	bar
Density	rho	0	g/cm ³
Kinematic Viscosity	ny	0	mm ² /s
Coefficient of Compressibility	beta	0	1/bar
Bulk Modulus	E	0	bar
Heat Expansion Coefficient	gamma	0	1/K
Bunsen Coefficient	alphaV	0	-
Vapour Pressure (absolute)	pv	0	bar
Change of Potential Energy	Pp	0	kW

Mechanical Connection (linear) connection5
Parameters

Comment	Name	Current Value	Unit
Initial Displacement	x0	0 (Fixed)	[m]
Initial Velocity	v0	0 (Fixed)	[m/s]

Results

Comment	Name	Current Value	Unit
Displacement	x	0	m
Velocity	v	0	m/s
Acceleration	a	0	m/s ²

Pneumatic Connection connection6
Parameters

Comment	Name	Current Value	Unit
Use Real-Gas Equations of State	realGas	no	
Initial Pressure	p0	pAPV (Fixed)	[Pa]
Initial Temperature	T0	TAtm (Fixed)	[K]

Results

Comment	Name	Current Value	Unit
Absolute Pressure	p	0	bar
Temperature	T	-273.15	°C
Specific Enthalpy	h	0	J/kg
Specific Volume	v	0	cm ³ /g
Mass	m	0	kg
Total Mass Flow	mdot	0	kg/s
Total Volume	Vol	0	cm ³
Density	rho	0	kg/m ³
Specific Heat at Const. Pressure	cp	0	J/(kg·K)
Specific Heat at Const. Vol.	cv	0	J/(kg·K)
Adiabatic Exponent	kappa	0	-
Specific Gas Constant	R	0	J/(kg·K)
Kinematic Viscosity	ny	0	mm ² /s
Thermal Conductivity	lambda	0	W/(m·K)
Enthalpy Change Rate	Hdot	0	W
Conductive Heat Transport	Qdot	0	W

Mechanical Connection (linear) connection2
Results

Comment	Name	Current Value	Unit
Displacement	x	0	m
Velocity	v	0	m/s
Acceleration	a	0	m/s ²

Mechanical Connection (linear) connection30
Results

Comment	Name	Current Value	Unit
Displacement	x	0	m
Velocity	v	0	m/s
Acceleration	a	0	m/s ²

Hydraulic Connection connection32
Parameters

Comment	Name	Current Value	Unit
Temperature Calculation	heatMode	Constant Temperature	
Temperature Setting	T1	TAtm	[K]
Calculation of Gas Fraction	aerationMode	Gas Fraction according to Static Pressure Level	
Gas Fraction (Normal State)	alphaURef	0.2	[%]
Constant Gas Fraction	alphaUconst	0	[%]

Results

Comment	Name	Current Value	Unit
Pressure (Relative to Atmosphere Pressure)	p	0	bar
Absolute Pressure	pAbs	0	bar
Pressure Change Rate	pdot	0	bar/s
Temperature	T	-273.15	°C
Volume Fraction of Undissolved Air	alphaU	0	%
Total Volume	V	0	cm ³
Volume Change	Vdot	0	l/min
Hydraulic Capacity	Ch	0	cm ³ /bar
Equivalent Bulk Modulus	Ee	0	bar
Density	rho	0	g/cm ³
Kinematic Viscosity	ny	0	mm ² /s
Coefficient of Compressibility	beta	0	1/bar
Bulk Modulus	E	0	bar
Heat Expansion Coefficient	gamma	0	1/K
Bunsen Coefficient	alphaV	0	-
Vapour Pressure (absolute)	pv	0	bar
Change of Potential Energy	Pp	0	kW

Mechanical Connection (linear) connection31
Parameters

Comment	Name	Current Value	Unit
Initial Displacement	x0		[m]
Initial Velocity	v0		[m/s]

Results

Comment	Name	Current Value	Unit
Displacement	x	0	m
Velocity	v	0	m/s
Acceleration	a	0	m/s ²

Mechanical Connection (linear) connection35
Parameters

Comment	Name	Current Value	Unit
Initial Displacement	x0	0 (Fixed)	[m]
Initial Velocity	v0	0 (Fixed)	[m/s]

Results

Comment	Name	Current Value	Unit
Displacement	x	0	m
Velocity	v	0	m/s
Acceleration	a	0	m/s ²

Mechanical Connection (linear) connection36

Parameters

Comment	Name	Current Value	Unit
Initial Displacement	x0	0 (Fixed)	[m]
Initial Velocity	v0	0 (Fixed)	[m/s]

Results

Comment	Name	Current Value	Unit
Displacement	x	0	m
Velocity	v	0	m/s
Acceleration	a	0	m/s ²

Mechanical Connection (linear) connection41

Parameters

Comment	Name	Current Value	Unit
Initial Displacement	x0	0 (Fixed)	[m]
Initial Velocity	v0	0 (Fixed)	[m/s]

Results

Comment	Name	Current Value	Unit
Displacement	x	0	m
Velocity	v	0	m/s
Acceleration	a	0	m/s ²

Hydraulic Connection connection3

Parameters

Comment	Name	Current Value	Unit
Initial Pressure (relative to pAtm)	p0	p0 (Fixed)	[Pa]
Temperature Calculation	heatMode	Constant Temperature	
Temperature Setting	T1	TAtm	[K]
Calculation of Gas Fraction	aerationMode	Gas Fraction according to Static Pressure Level	
Gas Fraction (Normal State)	alphaUref	0.2	[%]
Constant Gas Fraction	alphaUconst	0	[%]

Results

Comment	Name	Current Value	Unit
Pressure (Relative to Atmosphere Pressure)	p	0	bar
Absolute Pressure	pAbs	0	bar
Pressure Change Rate	pdot	0	bar/s
Temperature	T	-273.15	°C
Volume Fraction of Undissolved Air	alphaU	0	%
Total Volume	V	0	cm ³
Volume Change	Vdot	0	l/min
Hydraulic Capacity	Ch	0	cm ³ /bar
Equivalent Bulk Modulus	Ee	0	bar
Density	rho	0	g/cm ³
Kinematic Viscosity	ny	0	mm ² /s
Coefficient of Compressibility	beta	0	1/bar
Bulk Modulus	E	0	bar
Heat Expansion Coefficient	gamma	0	1/K
Bunsen Coefficient	alphaV	0	-
Vapour Pressure (absolute)	pv	0	bar
Change of Potential Energy	Pp	0	kW

Pneumatic Connection connection4 Parameters

Comment	Name	Current Value	Unit
Use Real-Gas Equations of State	realGas	no	
Initial Pressure	p0	pAPV (Fixed)	[Pa]
Initial Temperature	T0	TAtm (Fixed)	[K]

Results

Comment	Name	Current Value	Unit
Absolute Pressure	p	0	bar
Temperature	T	-273.15	°C
Specific Enthalpy	h	0	J/kg
Specific Volume	v	0	cm ³ /g
Mass	m	0	kg
Total Mass Flow	mdot	0	kg/s
Total Volume	Vol	0	cm ³
Density	rho	0	kg/m ³
Specific Heat at Const. Pressure	cp	0	J/(kg·K)
Specific Heat at Const. Vol.	cv	0	J/(kg·K)
Adiabatic Exponent	kappa	0	-
Specific Gas Constant	R	0	J/(kg·K)
Kinematic Viscosity	ny	0	mm ² /s
Thermal Conductivity	lambda	0	W/(m·K)
Enthalpy Change Rate	Hdot	0	W
Conductive Heat Transport	Qdot	0	W

Hydraulic Connection connection1
Parameters

Comment	Name	Current Value	Unit
Initial Pressure (relative to pAtm)	p0	0 (Fixed)	[bar]
Temperature Calculation	heatMode	Constant Temperature	
Temperature Setting	T1	TAtm	[K]
Calculation of Gas Fraction	aerationMode	Gas Fraction according to Static Pressure Level	
Gas Fraction (Normal State)	alphaURef	0.2	[%]
Constant Gas Fraction	alphaUconst	0	[%]

Results

Comment	Name	Current Value	Unit
Pressure (Relative to Atmosphere Pressure)	p	0	bar
Absolute Pressure	pAbs	0	bar
Pressure Change Rate	pdot	0	bar/s
Temperature	T	-273.15	°C
Volume Fraction of Undissolved Air	alphaU	0	%
Total Volume	V	0	cm ³
Volume Change	Vdot	0	l/min
Hydraulic Capacity	Ch	0	cm ³ /bar
Equivalent Bulk Modulus	Ee	0	bar
Density	rho	0	g/cm ³
Kinematic Viscosity	ny	0	mm ² /s
Coefficient of Compressibility	beta	0	1/bar
Bulk Modulus	E	0	bar
Heat Expansion Coefficient	gamma	0	1/K
Bunsen Coefficient	alphaV	0	-
Vapour Pressure (absolute)	pv	0	bar
Change of Potential Energy	Pp	0	kW

Mechanical Connection (linear) connection14
Parameters

Comment	Name	Current Value	Unit
Initial Displacement	x0		[m]
Initial Velocity	v0		[m/s]

Results

Comment	Name	Current Value	Unit
Displacement	x	0	m
Velocity	v	0	m/s
Acceleration	a	0	m/s ²

Mechanical Connection (linear) connection15
Parameters

Comment	Name	Current Value	Unit
Initial Displacement	x0		[m]
Initial Velocity	v0		[m/s]

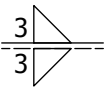


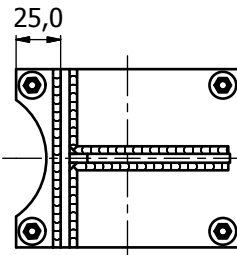
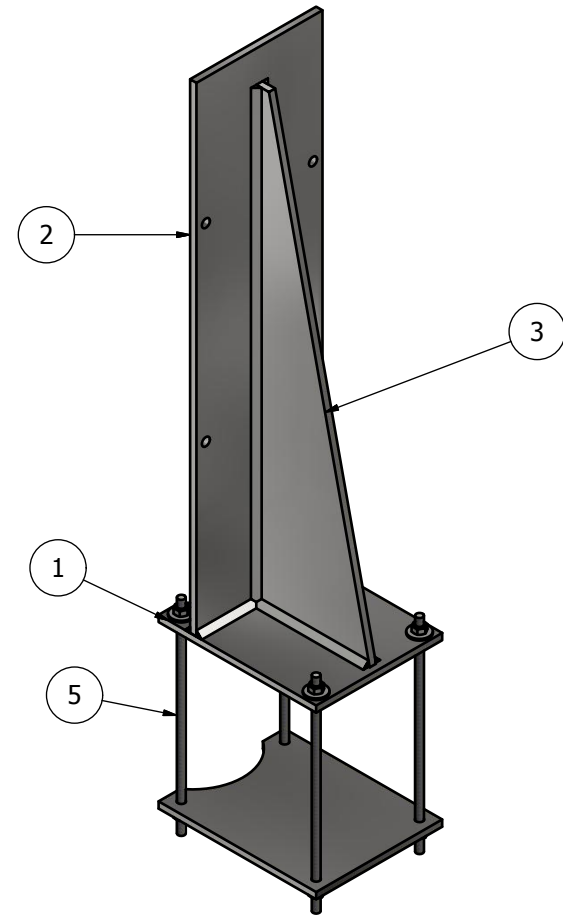
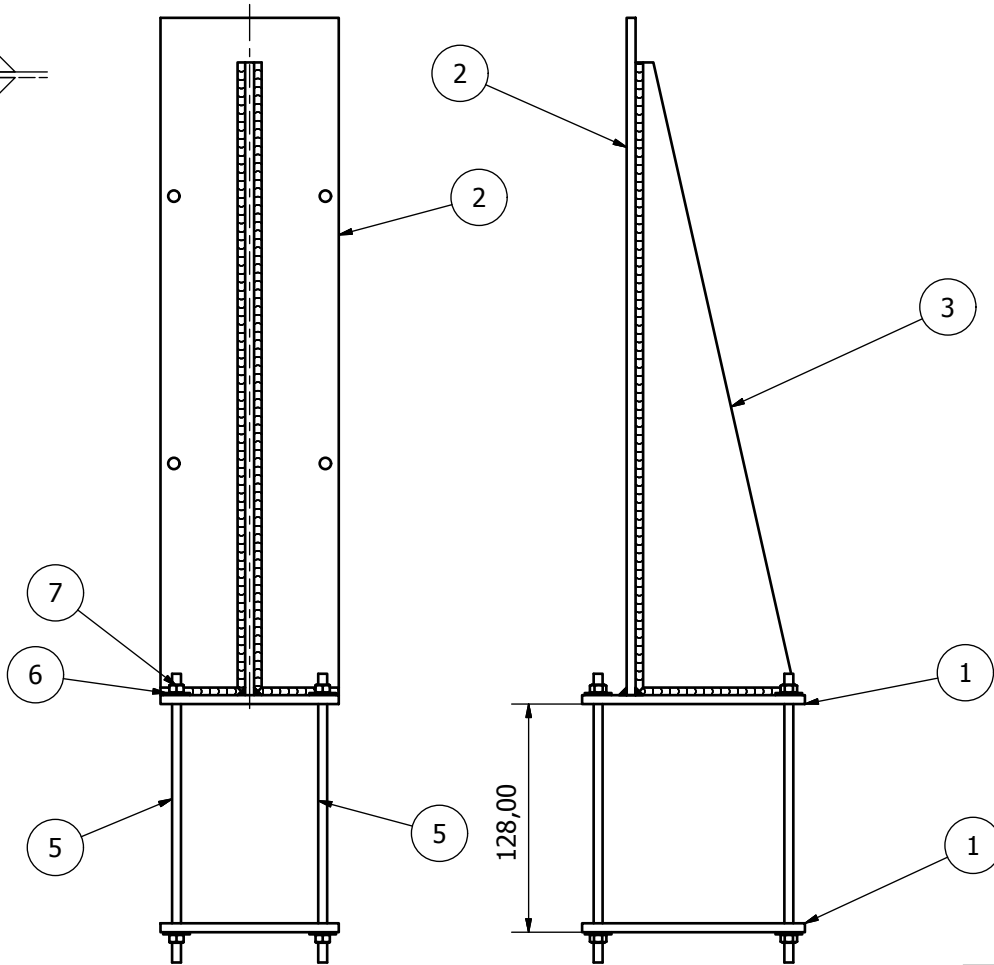
Results

Comment	Name	Current Value	Unit
Displacement	x	0	m
Velocity	v	0	m/s
Acceleration	a	0	m/s ²

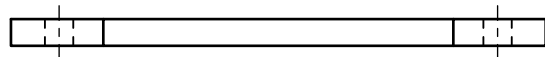
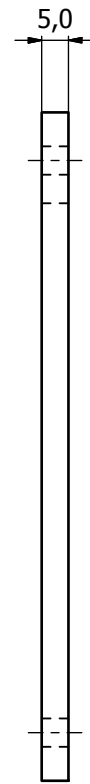
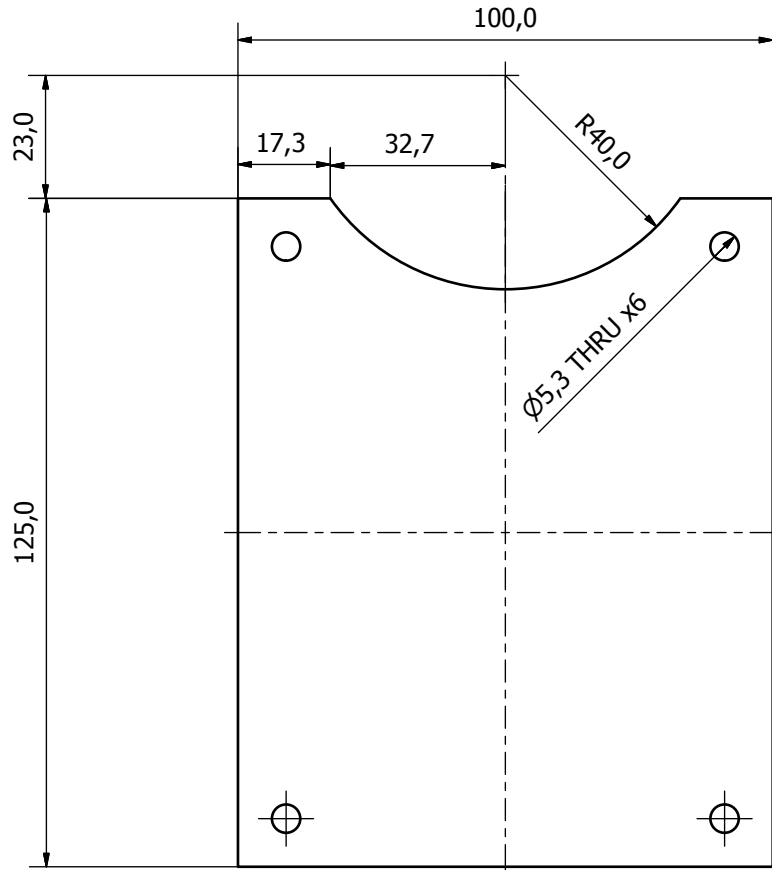
Appendix E

CAD Drawings

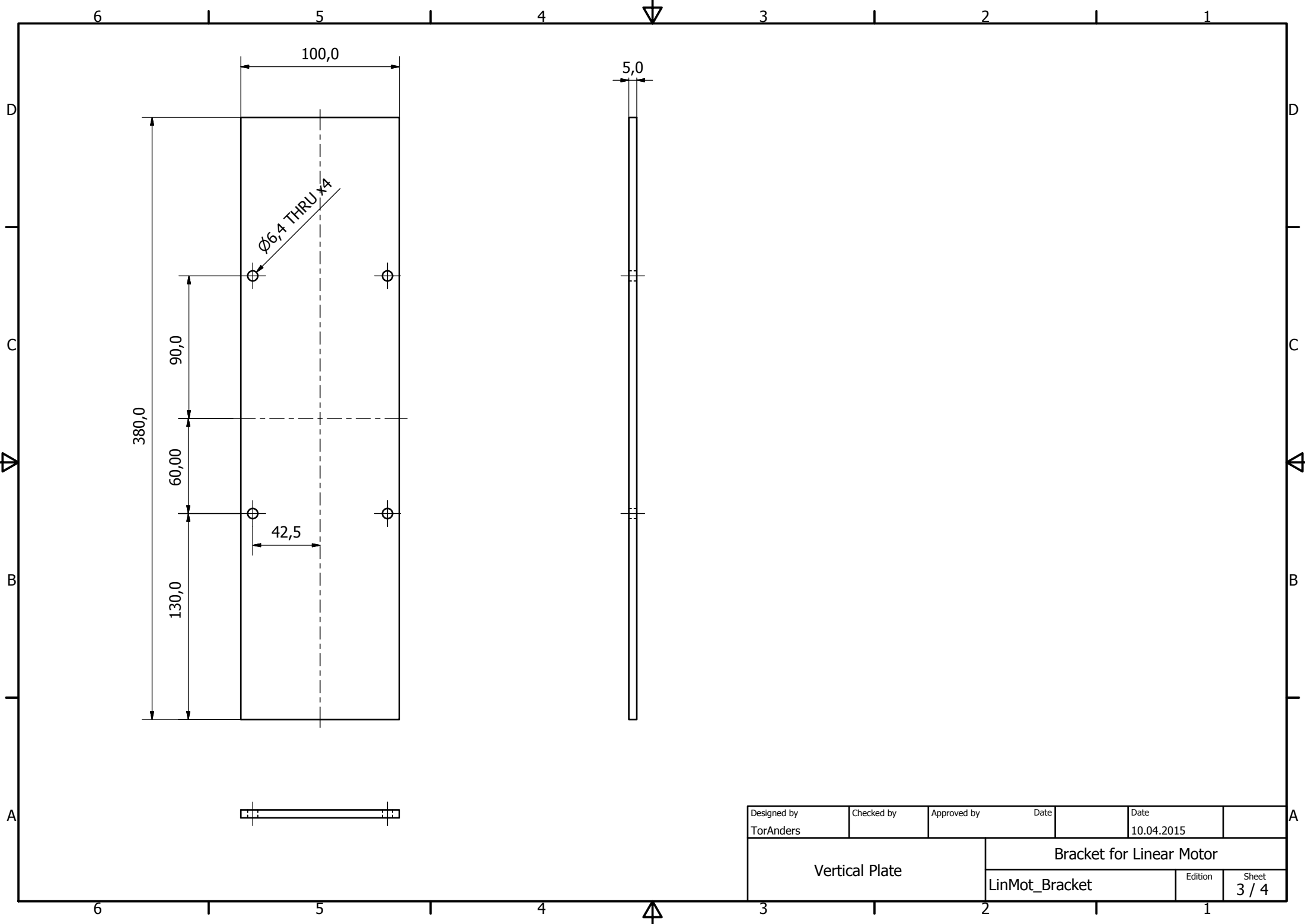
All welds to be 

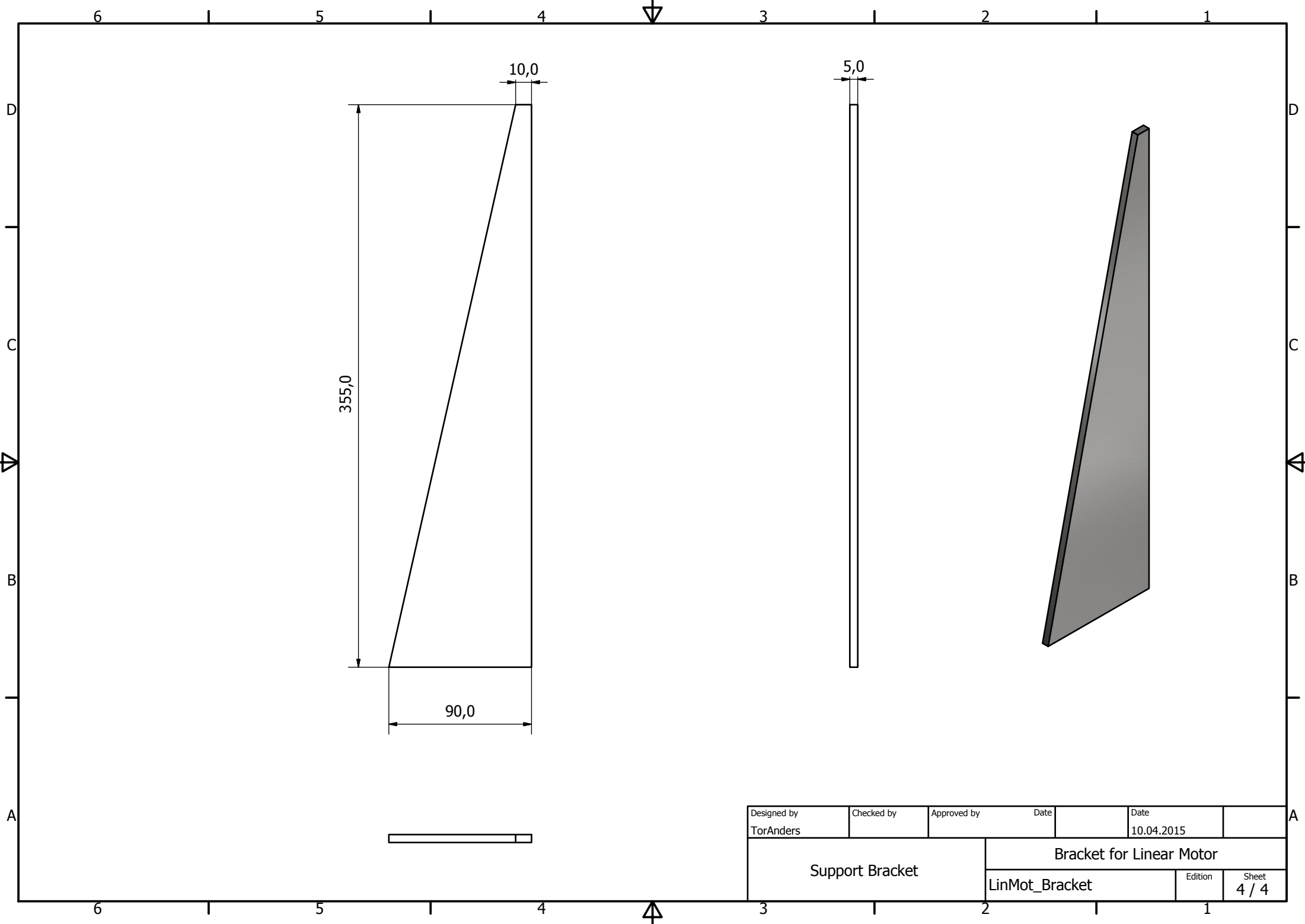


PARTS LIST			
ITEM	QTY	PART NUMBER	DESCRIPTION
1	2	Top/Bottom Plate	
2	1	Vertical Plate	
3	1	Support Plate	
5	4	Threaded Rod	M5 - 170mm
6	8	Washer	M5
7	8	Hex Nut	M5
Designed by TorAnders		Checked by	Approved by
		Date 10.04.2015	Date
Bracket for Linear Motor			
LinMot_Bracket		Edition	Sheet 1 / 4



Designed by TorAnders	Checked by	Approved by	Date	Date 10.04.2015	
Top/Bottom Plate			Bracket for Linear Motor		
			LinMot_Bracket	Edition	Sheet 2 / 4





Designed by TorAnders	Checked by	Approved by	Date	Date 10.04.2015
Support Bracket		Bracket for Linear Motor		
		LinMot_Bracket	Edition	Sheet 4 / 4